Sodium Coolant Properties and Experience

Contents

Tables

Figures

Abbreviations

ACRR	Annular Core Research Reactor
AEC	Atomic Energy Commission
CEA	Commissariat à l'Énergie Atomique
CRBR	Clinch River Breeder Reactor
DOE	United States Department of Energy
DRACS	direct reactor auxiliary cooling system
EBR	Experimental Breeder Reactor
FBR	Fast Breeder Reactor
FBTR	Fast Breeder Test Reactor
FFTF	Fast Flux Test Facility
GE	General Electric
HEDL	Hanford Engineering Development Laboratory
HFEF	Hot Fuel Examination Facility
HTS	heat transport system
IFR	Integral Fast Reactor
IHTS	intermediate heat transport system
IHX	intermediate heat exchanger
INL	Idaho National Laboratory
LMFBR	Liquid Metal-Cooled Fast Breeder Reactor
LOCA	loss of coolant accident
LWR	light water reactor
MOX	mixed oxide fuel
PAC	Protection Action Criteria
PFBR	Prototype Fast Breeder Reactor
PFR	Prototype Fast Reactor
PPE	personal protection equipment
PRISM	Power Reactor Innovative Small Module
RACS	reactor air cooling system
SAFR	Sodium Advanced Fast Reactor
SASS	self-actuated shutdown system
SFPS	sodium fire protection system
SFR	Sodium-cooled Fast Reactor
SHTS	secondary heat transport system
SID	Sodium Ionization Detector
SIMP	Surface Ionization Monitor for Particulates
SNAPL	Sandia Sodium Purification Loop

SNL	Sandia National Laboratory
SRE	Sodium Reactor Experiment
TREAT	Transient Reactor Test Facility
ZPPR	Zero Power Physics Reactor

1 Introduction

Sodium cooled reactors fill a need in the advanced nuclear reactor development community. Accelerated nuclear testing of fuels and materials is needed to allow designs to proceed. To accomplish this, a fast neutron spectrum is needed. To have a fast neutron spectrum, the reactor coolant needs to not only have excellent heat transfer properties to sufficiently cool the reactor core, but also not significantly slow neutrons down following their birth in the fission process. Sodium is an excellent choice that can fulfill these needs and many others. Sodium is the sixth most abundant element in the Earth's crust and can be acquired easily through simple chemical separation methods. Sodium, however, does react when in contact with water and air, but with proper precautions, these scenarios can be avoided. Therefore, a comprehensive understanding of sodium properties is needed. This document provides fundamental sodium knowledge along with discussion of its applications, historical information, and industrial uses.

2 What Is Sodium?

Sodium metal (Figure 1) is soft, malleable, and silvery white in color until it oxidizes to a dull gray in air. Sodium combines with oxygen to form sodium oxide, another highly reactive material. Traditional extinguishing agents, such as carbon dioxide, dry chemical foam, and carbon tetrachloride, can cause explosions and fire when interacting with sodium.

Like other metals, sodium conducts electricity and heat efficiently; it is approximately 100 times more effective at transferring heat than water, which allows it to be considered for use within nuclear reactors as a coolant [1]. Being so effective at heat transfer, this allows for the reactor core to be smaller and more compact. Sodium as a liquid is opaque, meaning that during a leak, liquid sodium should be visible and is typically accompanied by dense white smoke, thus making emergency responses easy when proper training has occurred.

Figure 1. Sodium metal [2].

2.1 Discovery, History, and Applications

Sodium, in the form of sodium chloride (table salt), has been known by man for centuries. Indeed, man's use of salt to season food was the basis for one of the earliest examples of international trade—the journeying of caravans centuries ago to obtain this valuable commodity from the Romans who controlled the salt deposits near the Dead Sea (Figure 2) [3].

Figure 2. The Dead Sea [4].

The isolation and identification of elemental sodium was accomplished in the same year as was elemental potassium, 1807. Sir Humphry Davy (Figure 3) first produced metallic potassium in the autumn of that year by electrolysis of potassium hydroxide, and shortly thereafter produced sodium metal by the same route. Both discoveries were announced by Sir Davy at the same time before the Royal Society in London on November 19, 1807. The following year, Thenard and Gay-Lussac prepared sodium by reducing caustic soda with iron at high temperatures. Today, a Downs cell is used to mass produce metallic sodium from a mixture of sodium chloride and calcium chloride. This technique was first used in 1921 by the chemist James Cloyd Downs [3].

Figure 3. Humphry Davy [5].

2.1.1 Occurrence and Distribution

Sodium metal is highly reactive; hence it is not found in nature in its elemental form. Sodium is one of the most abundant elements and alkali metals on Earth, making up 2.83% of its crust (Figure 4 [6]) [7].

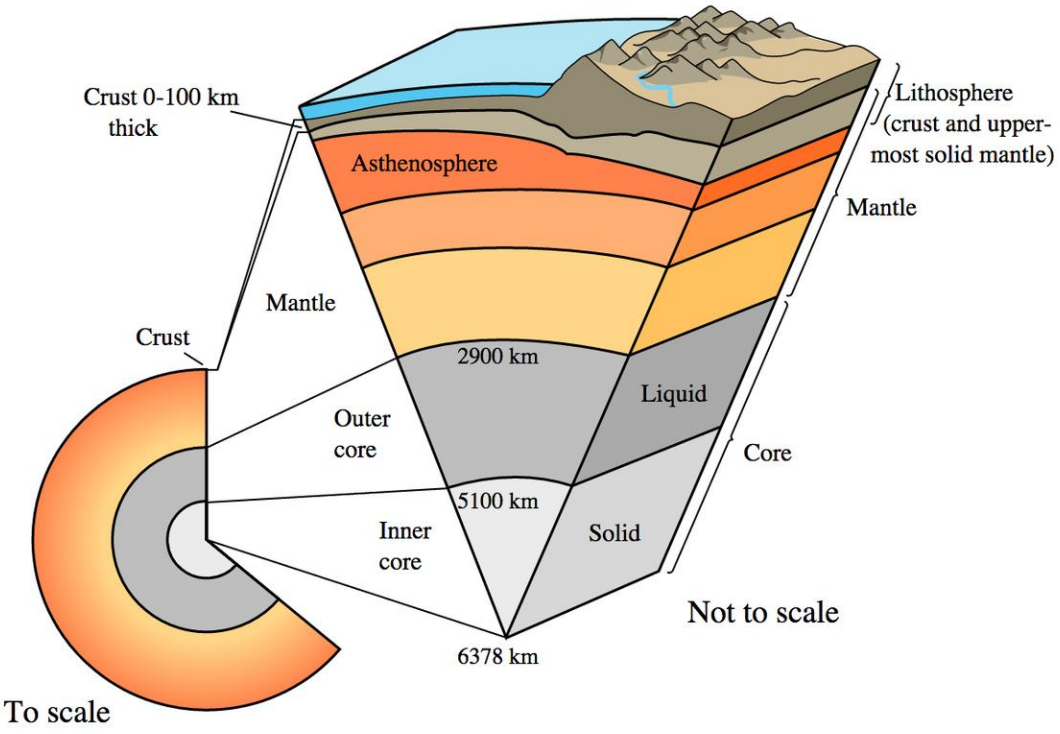

Figure 4. Cutaway view of the Earth's crust.

Sodium, in compound form, is relatively easy to find in extensive deposits of chloride, sulfate and other salts. It is largely found in vast underground deposits of sodium chloride or dissolved in sea water. These sodium deposits can be attributed to crystallization and/or evaporation of the ancient seas that once covered much of the Earth during prehistoric times. Although sodium chloride is by far the most common natural source of sodium, as rock salt or halite, other important sodium salts found extensively in nature are sodium borate (borax), sodium carbonate (soda or trona), sodium nitrate (Chile saltpetre), and sodium sulphate (thenardite or mirabilite). Generally, all of these minerals, except rock salt, are mined primarily for their anion values rather than for their sodium content [3].

2.1.2 Production and Industrial Use

In many cases, the production of sodium metal starts via the electrolysis of fused sodium chloride in a Downs cell (Figure 5). The electrolyte is a eutectic mixture of roughly 40% sodium

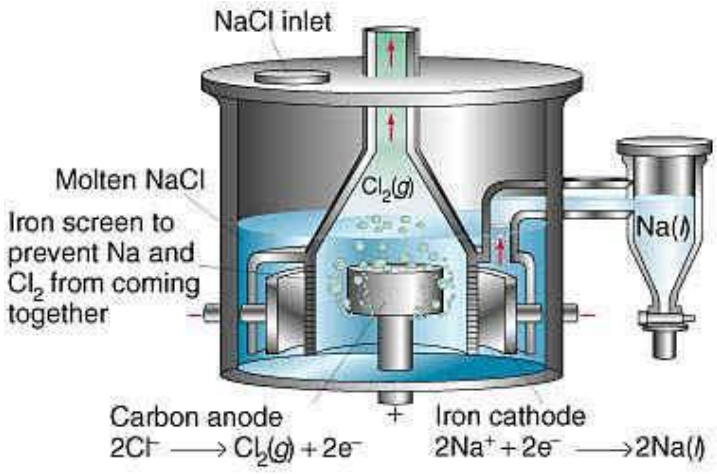

Figure 5. Downs Cell.

chloride (NaCl) and 60% calcium chloride ($CaCl_2$), chosen so that the melting point of the mixed salt system is considerably lower (about 580°C) than each of its constituents; this also serves as the operating temperature of the cell. The applied voltage drop across the cell is about 7 V, and the current efficiency is roughly 85%. As current flows through the molten salt mixture, chlorine is liberated at the anode, and both sodium metal and calcium metal are formed at the cathode; an iron gauze diaphragm between the electrodes prevents recombination [3].

Industrial uses of sodium metal are based primarily on its strong reducing properties. Approximately 80% of worldwide production of sodium in the 20th century was to produce tetraethyllead and tetramethyl lead for use as a gasoline anti-knock compound; sodium is alloyed with metallic lead, and the resultant alloy is reacted with the appropriate alkyl chloride in an autoclave to form the tetraethyl lead compound.

Most of the current production of sodium is now used to manufacture sodium alkyl sulfates, which are utilized in detergent production. Nearly 10% of the annual sodium production is now used to produce titanium metal through the reduction of titanium tetrachloride. The remaining 10%

is used to produce compounds, such as sodium hydride, sodium alkoxides and sodium peroxide; as a coolant in fast nuclear reactors; as an electrical conductor in sodium-filled transmission lines; and for a variety of other, smaller uses [3].

2.2 Sodium Physical Properties

All alkali metals – including sodium – are silvery, low-temperature melting, soft, ductile materials. Their densities are relatively low, and their thermal and electrical conductivities are among the highest of all known materials.

Sodium is approximately 100 times more efficient at transferring heat than water.

Sodium vapor in heavy layers appears bluish. At higher temperatures, this color turns to yellow. In the saturated-vapor state, sodium monomer and dimer are in equilibrium, the dimer being favored by increasing temperature [7]. The proportion of dimer in the superheated vapor decreases with temperature. Table 1 synthesizes the physical properties of sodium.

Table 1. Physical Properties of Sodium

Physical Properties of Sodium	
Atomic weight	22.9898 g/mol
Crystal form	BCC
Atomic radius	1.896Å
Ionic radius	0.95Å
Atomic volume	23.7 c.c./g-atom
Lattice constant	4.24 (A-173°C)
Ionization potential	5.12 V
Electron work function	2.28 eV
Electrode potential	2.714 V
Electron emission wavelength	0.6m
Thermal conductivity (cal/sec °C cm.), m.p.	
200°C	0.193
400°C	0.17
Specific heat (cal/°C g), 0°C	
20-25°C	0.092
50-100°C	0.33

2.3 Chemical Properties

The elemental symbol for sodium is Na, which comes from the Latin word for sodium, *natrium*. Elemental sodium is most often found within the Earth's crust in the form of sodium chloride. Sodium is also found as the silicate in igneous rocks and natural compounds that include sodium nitrate, sodium sulfate, sodium carbonate, sodium bicarbonate, and sodium tetraborate. In its natural form it can be found in soils, waters, and the bodies of plants and animals. In the case of sodium metal, it is rarely found isolated in nature and is chiefly produced from the compounds by first preparing the chloride form and then electrolytically fusing it with sodium carbonate.

Sodium metal is a malleable metal having a density of 0.97$\frac{g}{cm^3}$ and a melting point of 97°C. It oxidizes within a few seconds when it is contacted by air. It can also burn when in contact with humid air, and presents with a characteristic yellow flame; additional, metallic sodium can react violently with water, releasing a considerable amount of hydrogen gas as part of the rapid oxidation

process [8]. A more detailed overview of sodium reactions and fires can be found in Section 3 below.

Table 2 contains a summary of important chemical properties of solid and molten sodium. Note that at atmospheric pressure, the density of sodium is roughly the same as the density of water at standard atmospheric pressure. Sodium coolant systems can also operate near atmospheric pressures due to its high boiling point. The use of sodium within nuclear reactors requires less pressure than light water reactors, meaning that the reactor is inherently safer to perform maintenance on.

Table 2. Chemical and Physical Properties of Sodium [9]

Chemical Properties of Sodium	
Atomic number	11
Atomic mass	22.98977 $g.mol^{-1}$
Electronegativity (Pauling)	0.9
Density	0.97 g.cm -3 at 20 °C
Melting point	97.5 °C
Boiling point	883 °C
Vander Waals radius	0.196 nm
Ionic radius	0.095 (+1) nm
Isotopes	21 [only Na-23 is stable]
Electronic shell	[Ne] 3s1
Energy of first ionization	495.7 $kJ.mol^{-1}$
Standard potential	- 2.71 V

2.3.1 Atomic Structure

An atom is composed of a nucleus containing a certain number of protons and neutrons and an electron cloud containing electrons equal to the number of protons. Figure 6 shows a Bohr model of Na-23's atomic structure. The Bohr model selected shows, in a simplistic manner, the locations of the subatomic particles are divided between the nucleus and electronic cloud. The structure shows an electrically neutral Na-23 atom that contains 11 protons, 11 electrons, and 12 neutrons and is radioactively stable. The model shown in Figure 6 does not represent an ion, which is an atom with an unequal proton-electron ratio that results in a charged nucleus. Each element

has its own atomic number, also known as a "Z" number, equal to the number of protons in its nucleus. The most basic of atoms is hydrogen with an atomic number of 1. A sample of these numbers is shown in Figure 7. Elements also possess an "A" number, representing the total number of nucleons – protons and neutrons added together – within the atomic nucleus.

An isotope is an atom of the same element, same Z number, but a different A number. Hydrogen, for example, has two stable isotopes: Hydrogen-1 does not have neutrons in its nucleus while hydrogen-2 does. Na-23 is the only stable isotope of sodium, making it a monoisotopic element. Inside the reactor core, the primary sodium will be irradiated, and radioactive Na-24 will be created when Na-23 absorbs a neutron. Na-24 will then decay into Mg-24 by beta decay with 14.95 hour half-life. For more information on the sodium decay process, see Section 4.

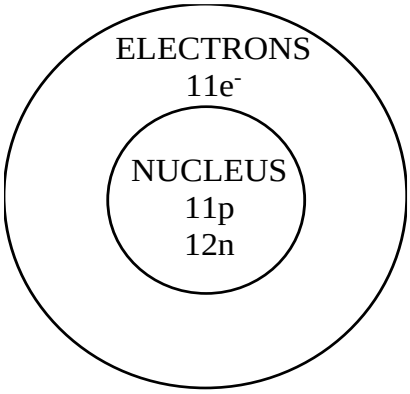

Figure 6. Bohr model of the atomic structure of Na-23.

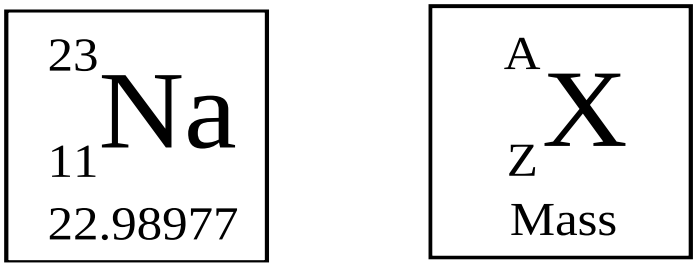

Figure 7. Na-23 isotopic information (left) compared to a generic placeholder (right).

3 Sodium Chemical Reactions

3.1 Sodium-Water Reactions

Sodium is an alkali metal because of its single valence electron. This unpaired electron is readily available to react with other molecules around it to stabilize sodium with a full outer shell. Water, on the other hand, is made of one oxygen atom that is polar covalently bonded to two hydrogen atoms. Oxygen has two unpaired electrons, which are available to react with the valence electron of sodium. This reaction between sodium and water follows two primary schemes with the formation of three different products and can be seen in Eq. (1). Sodium hydroxide and hydrogen gas are found to be the major products [10].

$$\begin{aligned} \mathrm{Na} \quad + \ H_2O &\rightarrow NaOH + \tfrac{1}{2}H_2 \\ 2\mathrm{Na} + H_2O \ &\rightarrow Na_2O \ + \ H_2 \end{aligned} \tag{1}$$

The Japan Nuclear Cycle Development Institute studied two types of sodium water interactions: a liquid sodium to water vapor reaction and a gas-to-gas reaction. In the liquid sodium to water vapor reaction, the reaction rate is "sufficiently higher" than the diffusion rate, resulting in most interactions staying at the liquid sodium surface. The water molecules react with a sodium molecule and remove it from the sodium pool. In a gas-to-gas reaction, a water-sodium complex is first formed, and then subsequently forms sodium hydroxide and hydrogen gas as the major products [10].

When liquid water contacts sodium instead of water vapor, hydrogen gas is rapidly emitted and can ignite if oxygen is present. Before hydrogen plays a role, however, within just several picoseconds (10^{-12} s) the sodium loses its valence electron to the surrounding water molecules and causes the sodium atom to ionize. After ionization occurs, the positively charged sodium ions can repel each other with such force that it may cause them to rip apart [11]. This event, along with the possibility of hydrogen gas burning, can lead to an explosion. As this reaction is endothermic in nature, the sodium will heat up and begin to melt if it is in solid form.

If sodium and water come in contact within a closed area, such as a pipe, “the hydrogen gas covers up the liquid gas interface” between the sodium and water vapor. With this hydrogen interference, it can moderate the sodium-water reaction [10]. With the introduction of hydrogen gas comes a possible rise in pressure, which could burst the pipe if not properly designed to handle such incidents.

3.2 Sodium Fires

Two types of sodium combustion will be discussed in this section: pool fires and jet spray fires. Table 3 shows physical properties of sodium at different temperatures.

Table 3. Sodium Temperature Characteristics

Sodium State	**Temperature (°C)**
Boiling	881
Monoxide Evaporation	1350
Flame	1350

Sodium’s flame temperature is equal to the monoxide evaporation temperature as shown in Table 3, which means if there are flames present, then monoxide is also present and should be considered. As a comparison temperature, lava from the Kilauea Volcano in Hawaii is about 1,170°C, meaning that sodium burns hotter than lava. A sodium fire leaves two types of residues: aerosols and a crust layer. The aerosols are composed of sodium peroxide, which could be transformed at first into hydroxide and then into carbonate when in contact with air. The crust is a mixture of sodium monoxide, sodium peroxide, and sodium-carbonate [12].

3.2.1 Sodium Pool Fire

Pool fires refer to a leakage of some sort, such as in a pipe or a vessel. Due to their nature, these are a localized phenomenon. In this type of fire, sodium burns either in a vapor phase with the formation of sodium oxide (Na_2O) in the flame area, or on the surface with the formation of peroxide. Sodium pool fires usually occur in a gaseous mixture of air, with the sodium temperature between 200°C and 500°C. The gas mixture occurring between sodium and air causes fire

propagation. Initial temperature of sodium has little to no effect on the combustion rate because the sodium stabilizes during combustion at a value varying between 570°C and 750°C.

It is possible to predict the amount of sodium burned during a fire using Eq. (2), where K = 527 kg/m^3 for fires burning in a variable atmosphere, S = surface area in m^2, and d = thickness of the sodium pool in m.

$$m_b = \mathrm{K} * \mathrm{S} * \mathrm{d} \tag{2}$$

Eq(2) holds until d = 26.5 cm, at which point the burned mass is only dependent on the surface of combustion. If the fire is not extinguished and left to burn out naturally, it is estimated that 52% of the initial amount of sodium will burn.

The humidity of the pool ambient air is another factor that influences sodium fires. It has been reported by the ESMERALDA program that humidity inhibits combustion up to a relative humidity of 30% at 20°C. This is due to the formation of a film of sodium-carbonate on the surface of the metal [12].

3.2.2 Sodium Jet Spray Fire

A jet spray fire refers to a fast-flowing spray of sodium that is ejected from a pipe or vessel. The direction of the jet spray is the most important factor when considering the thermodynamic consequences of this type of fire. Consider also that the combustion is limited by the diffusion of oxygen towards the jet temperature at 550°C. Furthermore, when the sodium flowrate increases, the ratio of the mass of sodium burnt and the mass of sodium ejected reaches a limit of 10%. This means that segregating the rooms into smaller, separate units is efficient at reducing the thermodynamic consequences of a sodium jet fire.

3.3 Sodium-Concrete Reactions

When concrete undergoes its hydration process, it ends up containing large amounts of water, up to 20% of total volume. Sodium-concrete interactions play a critical role in the design of sodium cooled reactors due to concretes widespread use in infrastructure. As explained earlier in the sodium chemistry section, sodium’s interaction with the environment tends to be violent.

Hanford Engineering Development Laboratory (HEDL) performed several experiments on this premise in 1979.

Two of the major safety concerns associated with sodium-concrete reactions are hydrogen gas generation and chemical energy release. The general behavior of sodium-concrete reactions was analyzed by HEDL with the parameters of temperature, penetration, and general observation. The experiments at HEDL considered three types of concrete: Basalt, magnetite and limestone aggregate. All specimens were first cast into hollow cylinders and then had 24 kg of hot sodium (510 – 870°C) poured into their centers. The bulk of the penetration occurred during the initial eight hours with little additional penetration afterwards. Hydrogen was released in significant quantities and had a 3 – 4% increase per hour. 80% of the concrete moisture was released after eight hours. The initial reaction of sodium with concrete occurs with water being thermally released from the concrete. Most of this water originates at a substantial distance from the reaction interface. Both energy release and hydrogen gas generation are dominated by the reaction of sodium with the thermally-released water to form NaOH [13].

4 Radiological Properties

Nuclear properties of the lighter alkali metals have been investigated at considerable length, primarily due to the use of sodium or a sodium-potassium alloy as a coolant in fast reactors. Neutron capture produces Na-24 from Na-23. In addition to this simple neutron capture, Na-23 also undergoes (n, 2n), (n, p) and (n, α) reactions. These interactions are expressed in Table 4.

Table 4 . Sodium Nuclear Reactions

Neutron capture	$Na^{23} + n_0^1 \rightarrow Na^{24}$
(n, 2n)	$Na^{23} + n_0^1 \rightarrow Na^{22} + 2n_0^1$
(n, p)	$Na^{23} + n_0^1 \rightarrow Ne^{23} + H^1$
(n, α)	$Na^{23} + n_0^1 \rightarrow F^{20} + He^4$

The primary sodium pool will be the main location where neutron capture will occur, but some activation will occur in the intermediate loop as well. The neutron capture cross-section of sodium at thermal energies (0.025 eV) is 0.53 barns and a total cross section value (at 0.025 eV) of 3.9 barns. The total cross-section is relatively constant at about 3 barns until 2.85 keV, where a large resonance increases the value to about 370 barns.

4.1 Decay Types

4.1.1 Beta Decay

Beta decay occurs in two modes: beta minus decay (negatron decay) and beta positive decay (positron decay). Beta decay also releases another subatomic particle called a neutrino or an antineutrino; both antineutrinos and neutrinos are chargeless particles [14]. The nucleus ejects an electron, referred to as a beta particle denoted by β^- [14]. The general decay of Na-24 shown below in Eq. (3) depicts beta minus decay.

$$ {}^{24}_{11}Na \rightarrow [{}^{24}_{12}Mg]^+ + {}^{0}_{-1}\beta + \bar{\nu}_e \tag{3} $$

Beta minus decay occurs when an isotope is neutron rich, meaning the isotope has more neutrons than protons. Sodium isotopes that decay via a beta positive reaction possess less neutrons

than Na-23 and are thusly very unlikely to occur in a fast reactor. Beta minus decay of sodium occurs in isotopes Na-24 and Na-24m [15].

4.1.2 Isomeric Transition

Na-24 has the potential to exist at excited states also referred to as metastable nuclei or isomers [14]. The atom would release the "excitation energy in the form of a gamma ray" [14]. Below is the general decay of Na-24 via isomeric transition (4).

$$^{24m}_{11}Na \rightarrow ^{24}_{11}Na + ^{0}_{0}\gamma \tag{4}$$

Gamma rays emit from sodium in the activation and subsequent decay of the isotope Na-24 and the decay of Na-24m. Gamma rays are electromagnetic waves or photons within the "200 keV to 200 MeV energy range" of the electromagnetic spectrum [16]. Na-24m decays through isomeric transition with a 472.3 keV gamma ray as it releases energy to reach the ground state of Na-24.

4.2 Atmospheric Dispersion

Dispersion models are important tools for dealing with hazardous material releases into the atmosphere [17]. The typical model used for dispersions is the Gaussian dispersion model. The Gaussian model is used for predicting how much of the pollutant is spreading out once it enters the air and how quickly the plume is expanding (diffusing). Diffusion describes a high concentration of solute in one location transporting to a different area of lower concentration (entropy) [18].

4.2.1 Atmospheric Diffusion

Sodium is a naturally toxic chemical with toxic reaction products, and under a release of molten sodium, a plume of aerosol sodium can be released. The concentrations of aerosol sodium, gaseous sodium or sodium dust, and reaction products disperse in a Gaussian model for plume diffusion. The model best matches experimental data and is consistent with the randomness of turbulence models for fluid dynamics [19].

Figure 8 shows a diagram of a plume highlighting the aspects within the model [19]. Notable aspects shown are that the height in the image is not the same as the height at the source. A cross section of the plume released is also provided and shows the standard deviations of the wind direction is in the vertical z and the cross horizontal y directions.

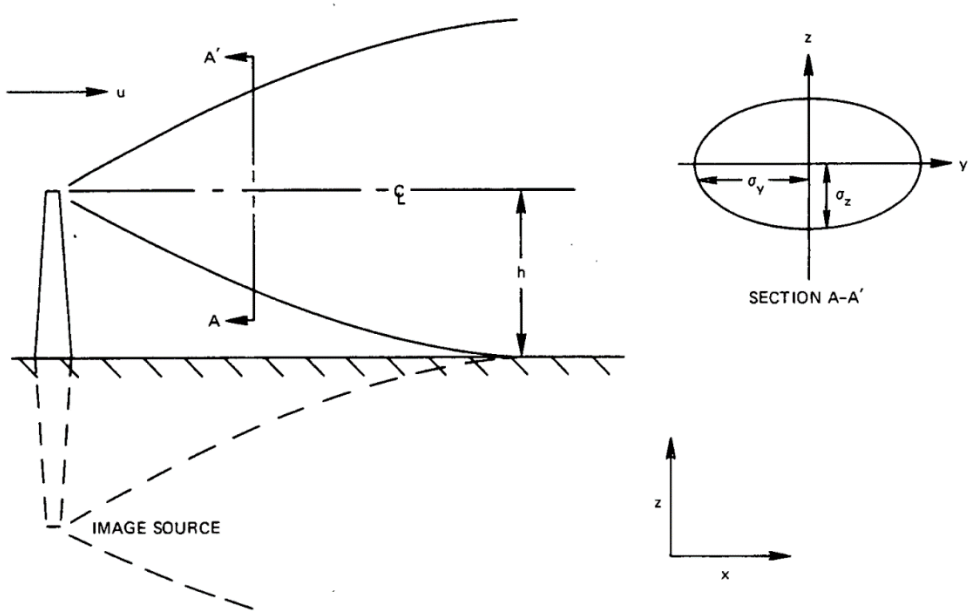

Figure 8. Example plume model for atmospheric dispersion [19].

4.2.2 Gaussian Plume Model

A Gaussian plume model displays the spread of a concentration of gaseous materials or dust particles into the atmosphere. The Gaussian model is used because it has a simple mathematical procedure and has consistency with the random nature of the turbulence. The Gaussian model characteristics have been used by the Environmental Protection Agency since 1978 for describing atmospheric releases [19].

4.2.2.1 Fundamental Principles

The resultant concentration source material formula of the Gaussian model is found below in Eq. (5) where C is the concentration of the source material, x is the distance from the source, Q is the continuous source strength, σ_y is the standard deviation in the horizontal direction, σ_z is

the standard deviation in the vertical direction, u is the wind speed, y is the horizontal direction, z is the height above ground, and h is the effective height above the ground [19].

$$C = \frac{Q}{2\pi\sigma_y\sigma_z u} e^{-\frac{y^2}{2\sigma_y^2}} \left(e^{-\frac{(z-h)^2}{2\sigma_z^2}} + e^{-\frac{(z+h)^2}{2\sigma_z^2}} \right) \quad (5)$$

The Gaussian model above is time independent, meaning to improve the model the equation must be adjusted to account for time. To make the adjustment, the source mass flow rate, Q, is modified. The equation below (6) breaks the mass flow rate into a time dependent model.

$$Q = \frac{m}{t} \quad (6)$$

Substituting Eq. (6) into Eq. (5) and then simplifying yields Eq.(7).

$$C = \frac{\frac{m}{t}}{2\pi\sigma_y\sigma_z u} e^{-\frac{y^2}{2\sigma_y^2}} \left(e^{-\frac{(z-h)^2}{2\sigma_z^2}} + e^{-\frac{(z+h)^2}{2\sigma_z^2}} \right) \quad (7)$$

4.2.2.2 Stability Classifications

Sodium and its reaction products with potential to release due to an emergency event is dependent upon the stability of the local weather during an emergency scenario. The various levels of stability are ranked from *A* to *F*, with *A* being very unstable and *F* being moderately stable. Each letter stands for the Pasquill's turbulence type. Figure 9 shows a graphical representation of Pasquill's turbulence types as a function of Monin-Obukhov stability length and aerodynamic roughness [19]. The stability is related to whether the location is urban or rural.

Table 5 provides a mathematical equation representing the standard deviations of wind in their respective direction. Most notably, it shows the impact stability has on the standard deviation coefficients in rural areas, as well as a power factor adjustment for wind speed as a relationship to the Pasquill Turbulence type.

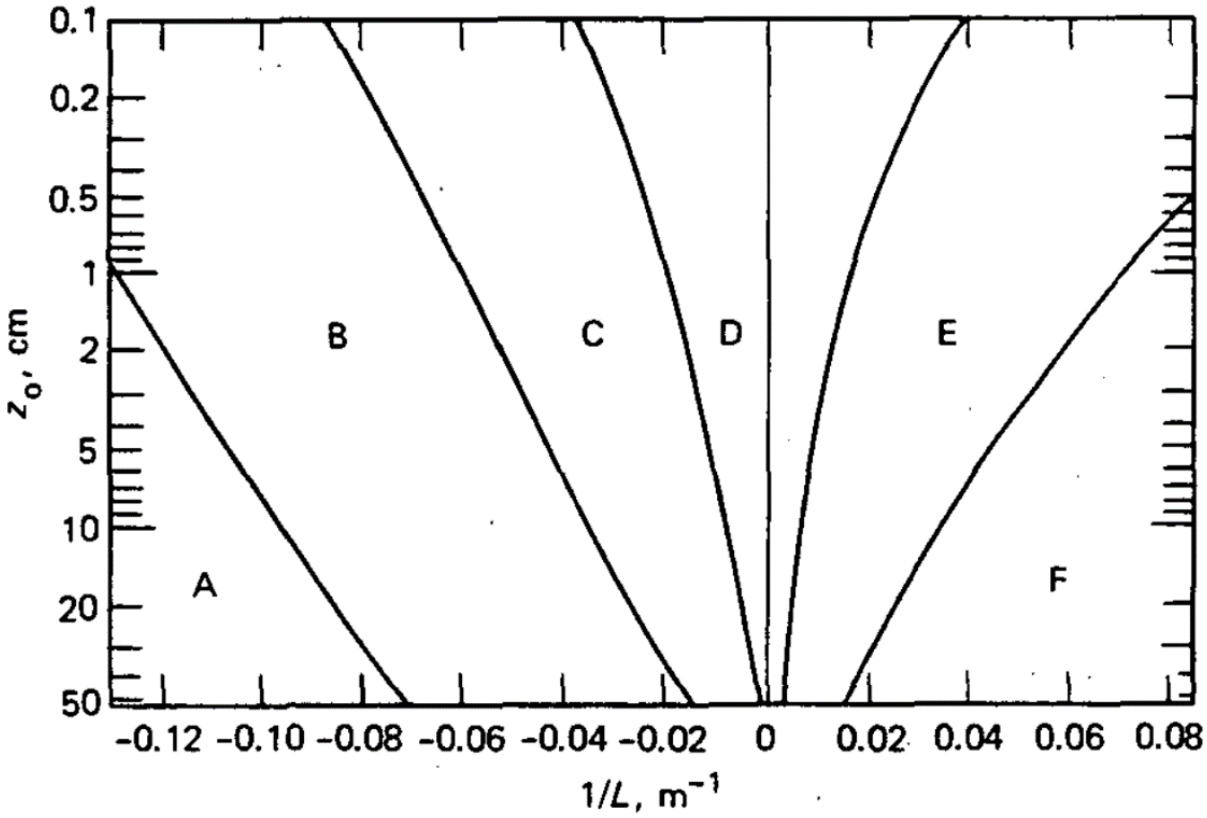

Figure 9. Pasquill's turbulence model as a function of stability length [19].

Table 5. Designations of Stability & Standard Deviation Factors [19]

Stability Description	Type	σ_y [m]	σ_z [m]	p
Very Unstable	A	$0.22x(1+0.0001x)^{-\frac{1}{2}}$	$0.20x$	0.07
Moderately Unstable	B	$0.16x(1+0.0001x)^{-\frac{1}{2}}$	$0.12x$	0.07
Slightly Unstable	C	$0.11x(1+0.0001x)^{-\frac{1}{2}}$	$0.08x(1+0.0002x)^{-\frac{1}{2}}$	0.10
Neutral	D	$0.08x(1+0.0001x)^{-\frac{1}{2}}$	$0.06x(1+0.0015x)^{-\frac{1}{2}}$	0.15
Slightly Stable	E	$0.06x(1+0.0001x)^{-\frac{1}{2}}$	$0.03x(1+0.0003x)^{-1}$	0.35
Moderately Stable	F	$0.04x(1+0.0001x)^{-\frac{1}{2}}$	$0.016x(1+0.0003x)^{-1}$	0.55

4.2.2.3 Assumptions

The assumptions made to the original concentration equation to fit a nuclear facility were used to determine the coefficients of σ_y, σ_z, u, p, z, and h. The most conservative stability factor would be to assume the weather would be designated as a moderately stable day, meaning the equations for standard deviations σ_y and σ_z and power factor p from Table 5 will reflect such in calculations.

The standard deviation in the y direction account for a 60-minute averaging time and a 10-minute sampling time for yielding the below equations, (8) and (9), where *x* is the distance from the source of the material release. The concentrations calculated are at a reference distance of 100 m away from the release.

$$\sigma_y = 0.04x(1 + 0.0001x)^{-\frac{1}{2}}\left(\frac{60}{10}\right)^{0.2} \tag{8}$$

$$\sigma_z = 0.016x(1 + 0.0003x)^{-1} \tag{9}$$

Figure 10 shows a visual representation of the standard deviation with respect to the distance from the point of origin. The wind speed used in the calculations must average the wind speed of the area of the implementation of this model. The use of wind speed averages at a 10 m height are adjusted using the equation below (10), where p is determined from the stability of the atmosphere as shown in Table 5 and z is the height above ground.

$$u_{adj} = u_{10}\left(\frac{z}{10}\right)^{p} \tag{10}$$

The height above ground is 2 m, as 2 m is sufficiently high to cover approximate height differences of the source to people. The deposition velocity is 0.003 m/s, a value more conservative than the values recommended by DOE-STD-1189-2008 [20]. The effective height is 0 m as the effective height of a rupture. After applying assumptions into the final calculations, Eq. (11) shows the final result for the atmospheric dispersion.

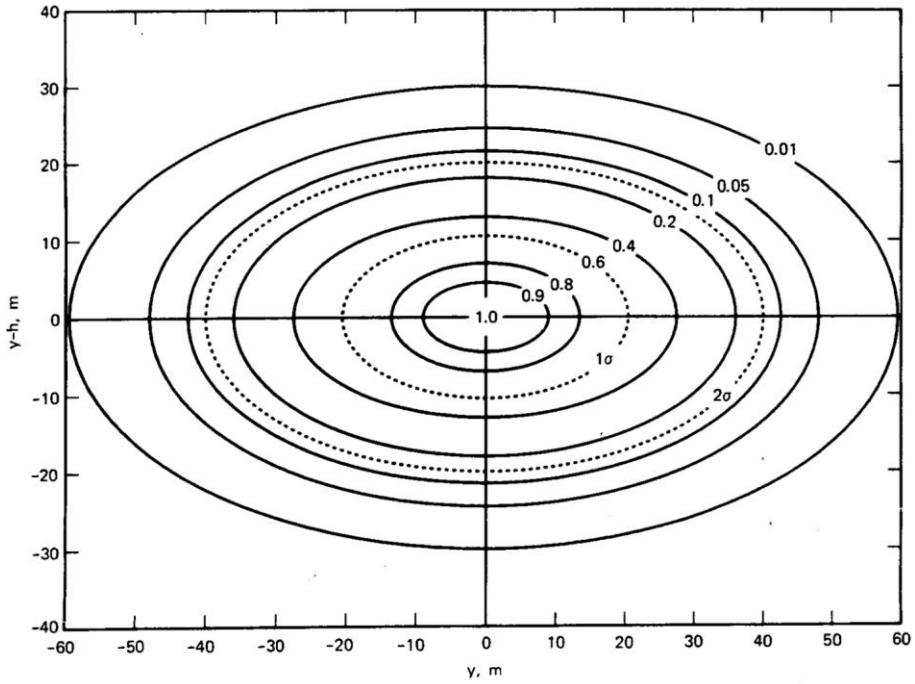

Figure 10. Visualization of wind direction standard deviation [19].

$$C(m,x,t) = \frac{m}{t\pi\sigma_y\sigma_z u}\left(e^{\frac{x}{\sigma_z}}\right)^{\left(-\frac{2}{\pi}\right)^{\frac{1}{2}}\left(\frac{v_d}{u}\right)} \tag{11}$$

4.2.3 Chemical Dose

Sodium toxicity is comparable to some more commonly known materials using the Protective Action Criteria (PAC) Revision-29 concentration levels [21]. PAC levels function as limits to define the concentration of airborne chemicals at which protective actions are required [20]. Table 6 shows the assessment of each PAC level and the qualitative assessment of each of level [22].

Table 7 compares six different particles with their respective Chemical Abstracts Service Numbers (CASRNs) and PAC threshold values. The escaping particles related to Sodium-cooled Fast Reactors (SFRs) are elemental sodium and its reaction products with air (sodium oxide) and water (sodium hydroxide). These sodium particles are compared with an equivalently toxic amount of carbon monoxide, cyanide, and formaldehyde. Carbon monoxide, cyanide, and formaldehyde

are well known as toxic compounds. Most notably, Table 7 shows the most hazardous of the six items are the inhalation of sodium oxide and sodium hydroxide at PAC level 1.

Table 6. PAC Assessment Levels

PAC Level	Qualitative Assessment
PAC-1	Mild, Transient Health effects
PAC-2	Irreversible or serious health effects
PAC-3	Life-threatening health effects

Table 7. Protective Action Criteria for Select Chemicals [21]

Particle	CASRNs	Symbol	PAC Threshold [mg/m^3]		
			PAC-1	PAC-2	PAC-3
Sodium Oxide	1313-59-3	Na_2O	0.5	5	50
Sodium Hydroxide	1310-73-2	$NaOH$	0.5	5	50
Sodium	7440-23-5	Na	13	140	870
Carbon Monoxide	630-08-0	CO	86	95	380
Cyanide	57-12-5	CN	6	8.3	50
Formaldehyde	50-00-0	CH_20	1.1	17	69

Sample calculations of a plume at 100 m away from the excursion event yielded the concentrations in Table 8. Each of the sodium products along with an equivalent amount were found using calculations shown in Appendix E: Atmospheric Dispersion Sample Calculation. The resulting equivalencies are shown in the table and it is seen that in the event of a release, 885.16 g of sodium is equivalent to only 74.90 g of formaldehyde or 408.53 g of cyanide to surpass the first level of protective action criteria (PAC-1). While a particulate release of sodium can be shown to

be relatively safe, sodium reaction products with air and water are much more hazardous, both only needing 34.04 g to exceed the PAC-1 limit.

Table 8. Resulting PAC Value Mass Equivilancies

Particle	Symbol	Mass to Exceed PAC Value [g]		
		PAC-1	PAC-2	PAC-3
Sodium	Na	885.16	9532.46	59237.41
Sodium Hydroxide	NaOH	34.04	340.44	3404.45
Sodium monoxide	Na_2O	34.04	340.44	3404.45
Carbon Monoxide	CO	5855.65	6468.45	25873.81
Cyanide	CN^-	408.53	565.14	3404.45
Formaldehyde	CH_20	74.90	1157.51	4698.14

4.2.4 Radiological Dose

4.2.4.1 Activated Pipe Example

The primary loop of sodium will be directly contacting the core and will be activated during operation. The secondary loop however will not be in contact with the core and will be significantly less activated than the primary loop sodium. A model representing the activation of sodium within a pipe provides a basis behind the activation of sodium and can lead to the derivation of maintenance limitations to ensure safety of faculty.

A conservative activation approximation assumes that the loop experiences 4×10^{15} n/cm^2 s. The sodium activation and subsequent exponential decay occurs within the primary loop within a 1-inch diameter pipe segment with a diameter to length ratio of 1:10. The resultant dose from sodium during activation and decay addressed with a point kernel shielding method, approximating the dose received from one meter away attenuating a beta particle and gamma ray.

4.2.4.2 Activation

The irradiation of the sodium, referred to as activation, will result in varying amounts of sodium isotopes. The most prominent isotope will be Na-24 as all isotopes beyond Na-24 have half-lives less than one minute [23]. Due to the exceptionally large disparity between Na-24 and

all other sodium isotopes, all other sodium isotopes are negligible for activation. As an example, the next largest sodium isotope produced is Na-22 with a half-life of 2.6 years. This might seem like a big contributor of radiation; however, Na-22 is produced at a rate of roughly 0.005% as that of Na-24 [24]. The reaction rate equation can be found in (12) where Φ is the neutron flux, σ_γ is the microscopic cross section for radiative capture, ρ_{Na} is sodium density, and M_{Na} is the molar mass of sodium.

$$RR = \frac{\phi \sigma_\gamma \rho_{Na} \frac{0.6220141 \; at \; cm^2}{mol \; b}}{M_{Na}} \tag{12}$$

The activation model requires a knowledge of the core volume and the amount of sodium atoms within the core. Using a core volume estimate of 500 cm^3 and assuming the core volume is 50% sodium, the activity of the sodium can be estimated. The Na-24 activity of the primary sodium is plotted against time in Figure 11 where it is seen that after approximately 120 hours, the sodium activation reaches an equilibrium.

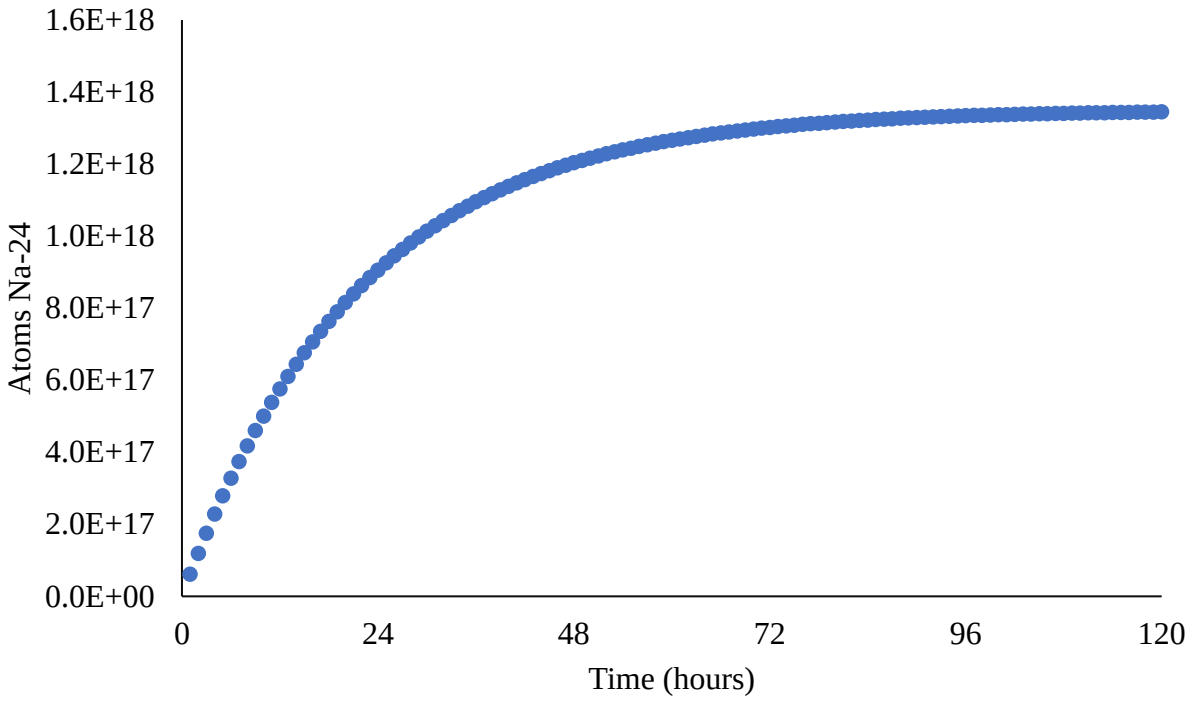

Figure 11. Activation of sodium-23 into Na-24.

4.2.5 Cross Section Information

Sodium has several cross sections involved with its activation and decay. Table 9 contains cross sections for a 16 multigroup diffusion model including the transport cross section (σ_{tr}), radiative capture cross section ($\sigma_{n,\gamma}$), elastic removal cross section (σ_{er}), and the inelastic scattering cross section $\sigma_{n,n'}$) for each of the 16 energy groups. Sodium activation has the potential to activate at any energy level. However, the higher energy cross sections will dominate within a fast reactor.

Table 9. Sodium Multigroup Constants [25]

j	E_L	σ_{tr}	$\sigma_{n,\gamma}$	σ_{er}	$\sigma_{n,n',j\rightarrow j+k}$							
					$\sigma_{n,n'}$	k=0	1	2	3	4	5	6
1	3.668	1.30	0.0005	0.137	0.633	0.158	0.166	0.141	0.084	0.046	0.027	0.011
2	2.225	1.47	0.0001	0.164	0.57	0.238	0.228	0.029	0.038	0.016	0.014	0.007
3	1.35	1.96	0.0001	0.215	0.541	0.27	0.271	0	0	0	0	0
4	0.825	2.89	0.0002	0.374	0.480	0.061	0.284	0.135	0	0	0	0
5	0.5	3.93	0.0003	0.594	0.236	0	0.127	0.056	0.030	0.012	.011	0
6	0.3	3.22	0.0005	0.5	--	--	--	--	--	--	--	--
7	0.18	3.49	0.0007	0.518	--	--	--	--	--	--	--	--
8	0.11	3.10	0	0.458	--	--	--	--	--	--	--	--
9	0.067	3.46	0	0.468	--	--	--	--	--	--	--	--
10	0.0407	4.77	0.003	0.619	--	--	--	--	--	--	--	--
11	0.025	3.88	0	0.518	--	--	--	--	--	--	--	--
12	0.015	4.10	0	0.515	--	--	--	--	--	--	--	--
13	0.0091	5.01	0	0629	--	--	--	--	--	--	--	--
14	0.0055	7.23	0	0.907	--	--	--	--	--	--	--	--
15	0.0021	22.81	0.377	0.969	--	--	--	--	--	--	--	--
16	0.0005	5.93	0	--	--	--	--	--	--	--	--	--

4.2.5.1 Radiative Capture

Radiative capture is a nuclear reaction between a neutron and a nucleus where the nucleus absorbs or captures the neutron, increasing the atom's A number by 1, and emitting extra energy as a gamma ray. When natural sodium undergoes radiative capture, the Na-23 becomes Na-24 or metastable Na-24m. The Na-24m is an isomer of Na-24; isomers are atoms with the same A and Z numbers but at different energy states. Equation (13) describes the neutron capture of Na-23.

$$n + {}^{23}_{11}Na \rightarrow {}^{24m}_{11}Na \rightarrow {}^{24}_{11}Na + \gamma \quad (13)$$

4.2.5.2 Elastic Scattering

Elastic scattering is the process by which a neutron-nucleus interaction produces a neutron where conservation of kinetic energy applies. Energy transfers to the recoiling nucleus from the neutron where the resultant neutron has an associated angle of scattering and a lower energy than the original neutron [14]. The equation below (14) is an example of the elastic scattering of Na-23.

$$n + {}^{23}_{11}Na \rightarrow {}^{23}_{11}Na + n \quad (14)$$

4.2.5.3 Inelastic Scattering

Inelastic scattering occurs when conservation of momentum applies but kinetic energy is not conserved in a neutron-nucleus reaction. The nucleus releases a neutron and one or more gamma rays to move back to ground state [14]. The equation below (15) is an example of the inelastic scattering of Na-23.

$$n + {}^{23}_{11}Na \rightarrow n + {}^{23}_{11}Na + \gamma \quad (15)$$

4.2.6 Decay

Once the reactor shuts down, the sodium activation process ceases. The neutron-activated sodium then begins the process of radioactive decay to achieve a stable state. Sodium decays in a manner displayed in the decay diagram in Figure 12. The figure highlights that there is only one decay mode that applies to Na-24: beta decay; however, the decay of Na-24 will decay to Mg-24 at three different energy levels. Na-23 activation may also activate into an isomer of Na-24; however, the isomer of Na-24 will most frequently decay by isometric transition [23]. The daughter Mg-24 atoms will decay by isomeric transition. Figure 12 shows the most frequent isomer of

Mg-24, with an energy of 4122.9 keV, and subsequently releases a 2754 keV energy photon to a lesser isomer with energy of 1368.7 keV. The final isomer will then release a 1368.7 keV photon to a stable state.

Once sodium is irradiated to become Na-24, it will decay down to a more stable state through a stochastic process of radioactive decay. The process is surmised by the fundamental law of radioactive decay shown in Eq. (16).

$$\frac{dN}{dt} = -\lambda N \tag{16}$$

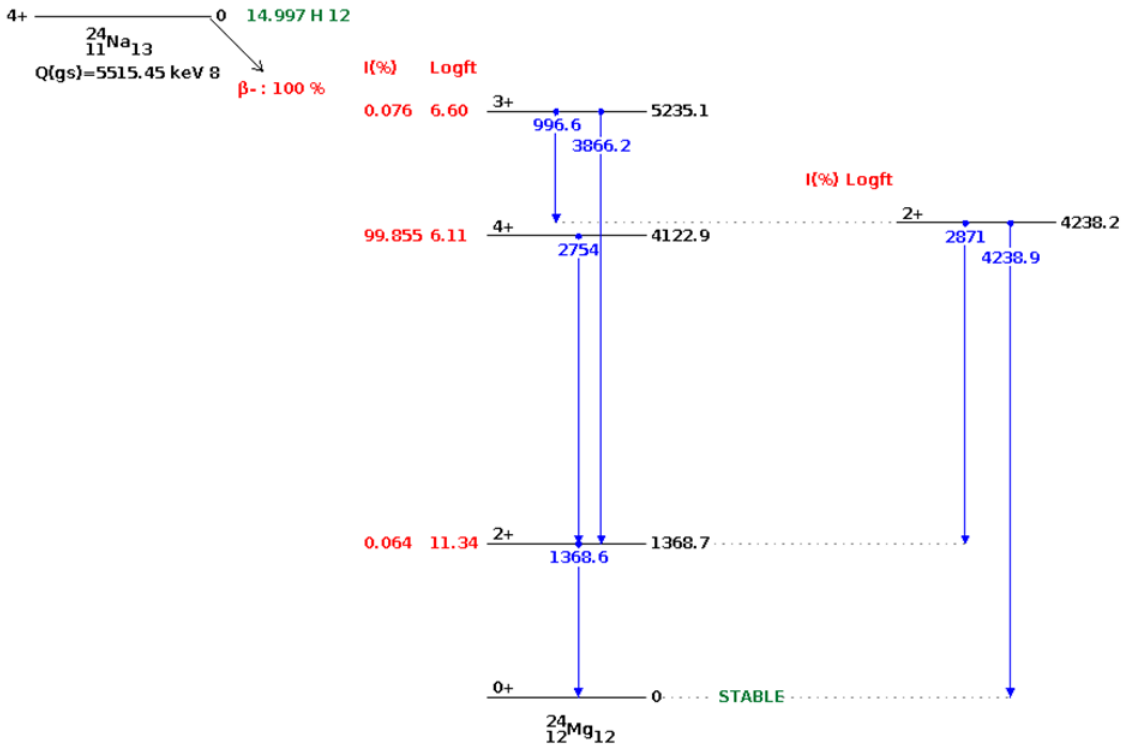

Figure 12. Na-24 decay diagram [26].

The integration of the equation yields a useable form of the law below (17), where the initial amount of activated material is n_0, the decay constant is λ, and the time after reactor shutdown, *t*.

$$n(t) = n_0 e^{-\lambda t} \tag{17}$$

A model for the decay of Na-24 is a simple exponential decay and is shown in Figure 13. The exponential decay depicts sodium within the primary loop of a 1-inch diameter pipe segment with a diameter to length ratio of 1:10. The figure also describes the absorbed dose rate from beta minus decay of Na-24. Estimation of dose rate allows for the determination of proper maintenance controls and posting requirements to mitigate undesired dose to maintenance personnel.

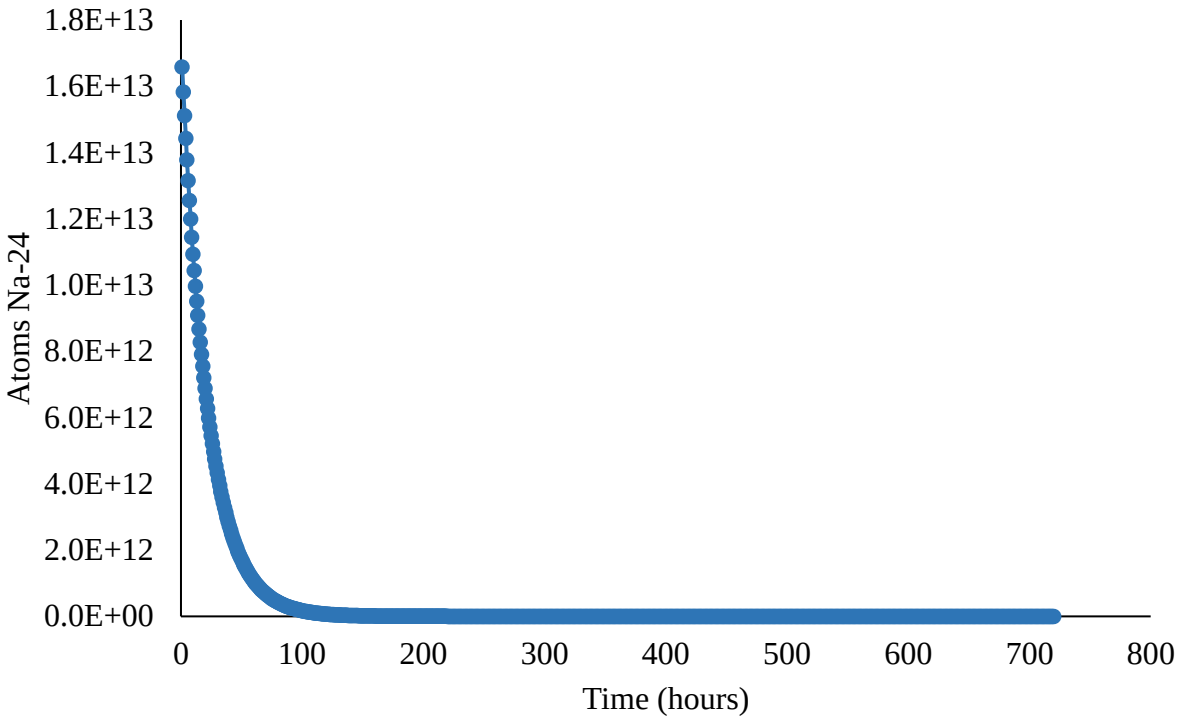

Figure 13. Decay rate of Na-24.

4.2.7 Dose Assessment

The dose assessment is calculated using the point kernel method utilizing a source in the shape of a linear pipe. Point-kernel calculations use the systems fluence, and due to the shape of the source being a linear pipe, Eq. (18) applies for the fluence calculation where ϕ is the fluence rate of the source, S is the source strength, x is the tangential distance from the source, and L_1/L_2 are the length of the pipe from the midpoint. The activation calculation performed uses the point-

kernel shielding technique as it accounts for attenuation through a material, source of the activation, and buildup of secondary particles at various energies.

$$\phi = \frac{S}{4\pi x}\left[\tan^{-1}\frac{L_2}{x} + \tan^{-1}\frac{L_1}{x}\right] \tag{18}$$

Figure 14 shows the activation and decay of Na-24 immediately after one another. The figure combines the plot from Figure 11 and Figure 13 to show a theoretical 60-day period, with a 30-day operational period followed by a 30-day shutdown period. The equation below (19) is used to determine the dose of individuals exposed to the pipe.

$$\dot{D} = 0.0576\frac{S}{2\pi x}E\left(\frac{\mu_a}{\rho}\right)\tan^{-1}\frac{L}{x} \tag{19}$$

To generate Figure 14, the sodium within the pipe was activated with an average flux of 4×10^{15} n/cm^{2}s for one month and then allowed to decay for a month without the reactor's flux. The figure shows Na-24 approaches its maximum population in five days and shows the sodium activation occurs shortly after a reactor startup. Five days following a reactor shutdown, Na-24 will experience eight half-lives and drop to less than 0.4% of its maximum population. A source is commonly assumed to be dead after six to ten half-lives, so maintenance performed on the primary coolant loop should occur 4-6 days after shutdown to prevent undue radiation risk to workers.

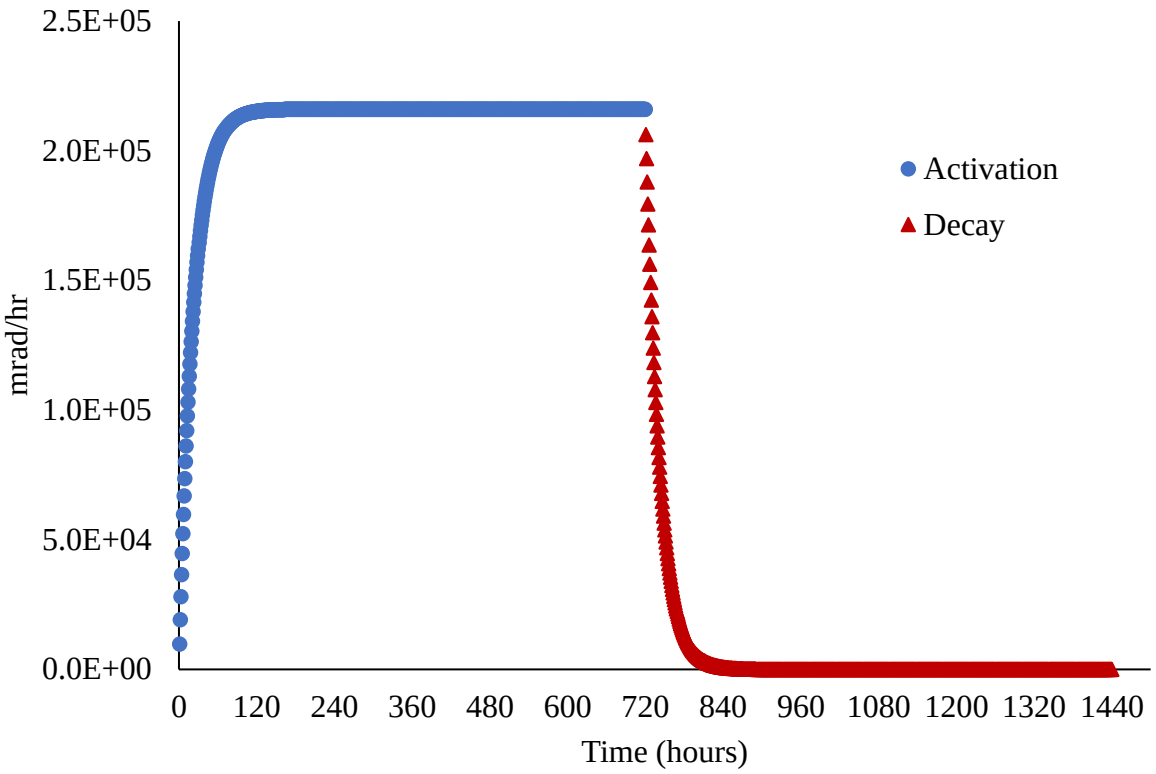

Figure 14. Activation and decay dose of primary Na-24 at 30 cm.

5 Engineering and Designing Sodium Systems

When designing sodium systems, several important features must be considered including heat transfer, material compatibility, instrumentation, and mechanical equipment selection.

This section will go into a general overview of the various systems that are included in the function of most SFRs. Each subsection will discuss a specific system and is accompanied by various examples from different SFRs and the process that led to a successful system design. Refer to the Appendix B: History of Different SFRs for an in-depth review of the engineering and design of each SFR discussed.

5.1 Pumps

There are many different types of pumps that have been utilized over the years to circulate sodium through the reactor and heat exchanger system. Examples include electromagnetic pumps, centrifugal pumps, and others. Provided below are a few examples of pumps used in sodium systems, including their advantages and drawbacks.

5.1.1 Centrifugal Pumps

Whatever type of application is desired, centrifugal pumps can output varying degrees of head and flow depending on the impeller used. Radial impellers offer a high head but a low flow, while axial impellers offer a low head with high flow. Mixed impellers also are available that offer a mix of head and flow. The impeller can either be welded or threaded to the fastener, although threaded attachment can introduce galling [27].

The Sodium Reactor Experiment (SRE) in California was a pioneer sodium reactor. The primary sodium loop utilized impeller pumps, with seals made of frozen sodium. An organic coolant (tetralin) kept the sodium seals frozen. In July 1959, it was found that the tetralin had leaked into the primary sodium over the course of many days and caused blockages in random channels in the core. 13 out of its 43 fuel elements were partially melted or ruptured. This incident helped understanding of pump design flaws and how to avoid such incidents in the future. [56]

Cavitation is an issue that should be dealt with when working with

centrifugal pumps. Due to the high operating temperature that the liquid sodium will be at, mechanical components inside the pump may deteriorate at a faster rate when compared to ambient water cavitation. Parts should be routinely checked for cavitation damage, which requires pump disassembly.

Centrifugal pumps offer a large range of uses but are often difficult to seal. One solution to this problem has been to implement vertical shaft pumps, which elevates the motor casing above the sodium operating level, as seen in Figure 15.

The FBTR in India was able to run its original four pumps for more than 125,000 hours without failure or incident. This helps prove the feasibility of sodium equipment with proper design and scheduled maintenance.

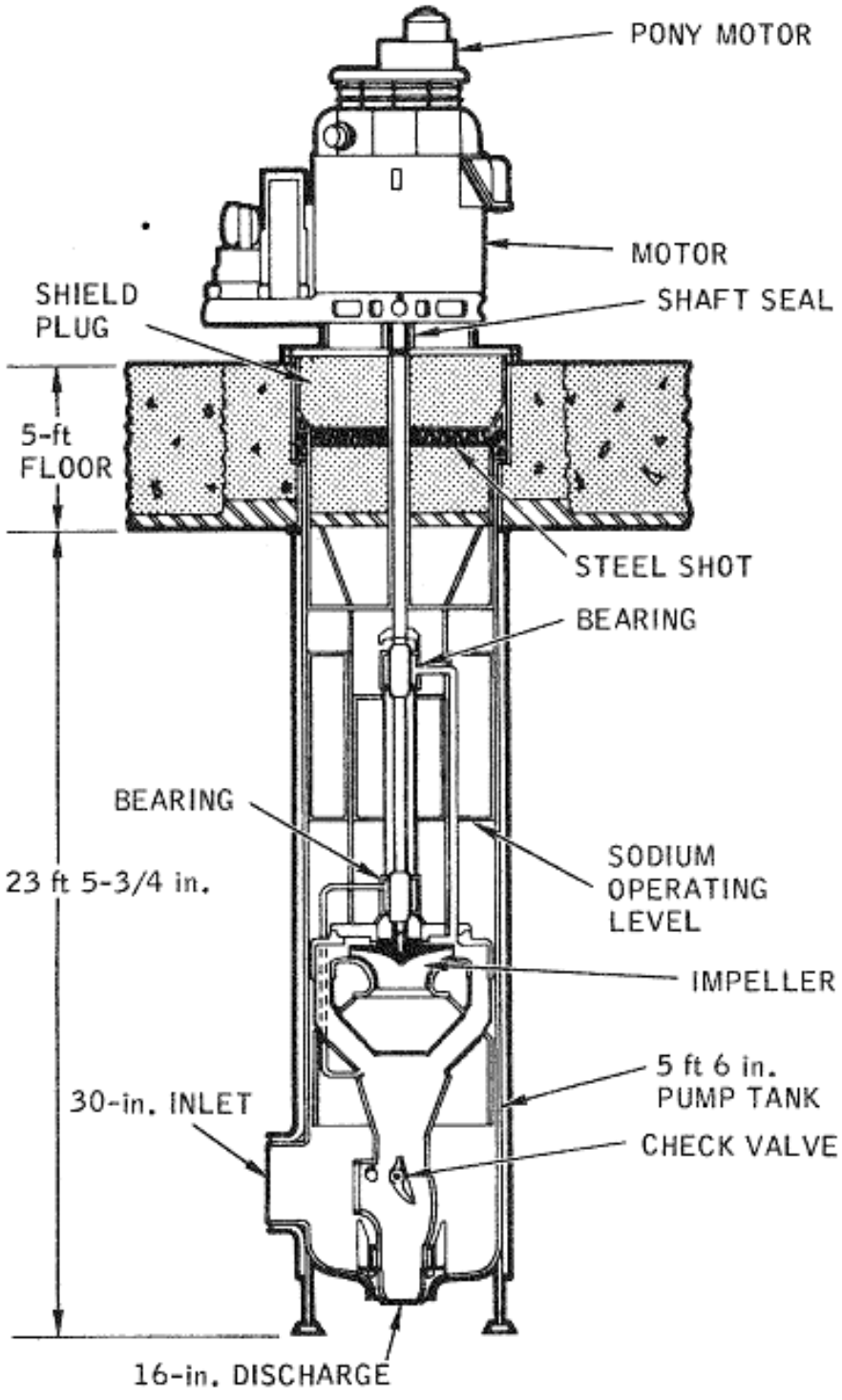

Figure 15. Vertical shaft pump used in the Fermi reactor power plant. [27]

5.1.2 Electromagnetic Pumps

Due to liquid sodium metal being paramagnetic, electromagnetic pumps are able to circulate liquid sodium through a system using either conduction or induction. The metal moves as it interacts with the current and magnetic field produced. Electromagnetic pumps possess some qualities that are not achievable with mechanical pumps. They are relatively simple and very reliable. Some of the top advantages to electromagnetic pumps are explained by Foust as follows;

1. No moving parts are in contact with liquid metal.
2. No seals are required.
3. The piping system carrying the pumped fluid is not rigidly anchored by the pump.
4. The piping system does not have to be opened when pump maintenance is required.
5. An electromagnetic pump can operate in any position.
6. No free surface between cover gas and liquid metal exists in an electromagnetic pump. This is of importance in primary coolant systems for nuclear reactors where gas bubbles in the liquid-metal stream create a potential hazard. The change in reactivity as bubbles pass through a reactor core is a potential cause of meltdown.
7. An electromagnetic pump installed in a primary coolant system can convert quickly from pumping the coolant to retarding coolant flow immediately following “scram”, thereby minimizing stresses in the reactor core. [27]

Electromagnetic pumps contain many benefits, but they also have their drawbacks. If any void is present in the liquid metal, it can cause a large increase in temperature of the duct and its walls and can lead to pump failure. Overtemperature of the liquid metal or pressure fluctuations inside the duct can also lead to reduced performance of electromagnetic pumps.

5.1.2.1 Sandia Sodium Purification Loop (SNAPL)

Sandia National Laboratory (SNL) created SNAPL to further the research and development of sodium safety and activated sodium for fast breeder reactors. One component in SNAPL was the implementation of an electromagnetic pump, which circulated “sodium through both the loop but also through the Experimental Apparatus” when a specific voltage input is supplied [28]. The

pump used is shown in Figure 16, which shows the direction of the current and flux of the magnetic field that moves the sodium through the pump.

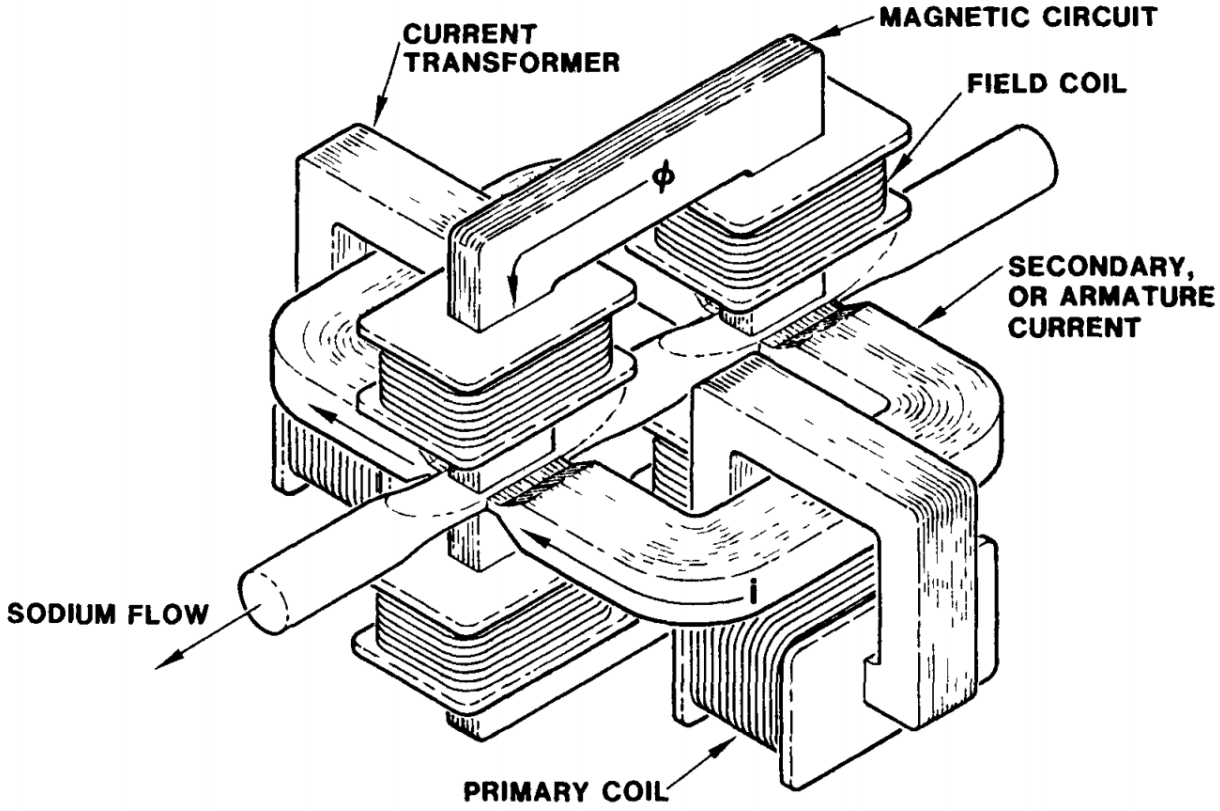

Figure 16. Two-stage electromagnetic pump [28].

5.2 Piping and Valves

Piping in a sodium system is different than a water system in that sodium is not as corrosive to pipe wall materials (generally stainless steel) as water and steam. Since sodium has such a high boiling point its systems can provide excellent heat transfer properties while operating at near-atmospheric pressure. This can prove advantageous when designing piping and valve systems, whereas light water reactors (LWRs) operate under very high pressures, in the range of 1,500 (BWRs) to 2,500 (PWRs) psia.

Even though sodium possesses low corrosion characteristics towards stainless steel, a monitoring system should still be used to detect any debris or particulate that could affect the performance of coolant flow. A filtration system should be present that can catch any particulates in the coolant that may come from corrosion, a reaction with air, or other impurities. This is important because particulates can clog different parts of the heat transfer system and could cause damage to piping, valves, pumps, the reactor core, etc.

Pipes and valves should be made from materials with high hot hardness and good corrosion resistance. This is especially important because the sodium will be working in the temperature range of 600°C. Piping systems should possess some method for preheating prior to hot sodium introduction, as the large temperature gradient between the sodium and piping could cause premature cracking or fissures. This is often done through electric cables or trace heaters.

> The Russian BN-10 reactor operated for 44 years without any significant corrosion in any sodium system. This was accomplished through sodium purification systems and proved the feasibility of 60-year life spans of sodium piping and equipment. [55]

A very common spot for cracking to occur in piping are welds. Over constraint can occur during heat transients if welds are excessively welded which can cause cracking of welds and result in a coolant leak. Great care should be taken when welding pipes, valves, and other components of the reactor system.

Another aspect that needs to be considered is the cover gas system. Since sodium is reactive when it comes in contact with water and air, an inert atmosphere is maintained above the sodium pool to prevent such interaction. This means the piping and valves should have a gas tight barrier. The inert gases used could be nitrogen, helium, argon, or another gas depending on the design. Cover gas systems are discussed in more detail in section 5.3.

The Prototype Fast Reactor (PFR) in Dounreay experienced many weld cracks throughout its lifetime with all cracks originating in welds that were reworked during fabrication. Cracks appeared to initially be non-penetrating, but subsequently grew due to the residual stress field present. Repair procedures for weld cracks should be carefully planned in SFRs as the repair could possibly do more damage than fixing the issue. [55]

Piping oftentimes is built with a double walled system to contain any leaks that may occur. If there is a breach in the main pipeline, sodium will still be retained without leaking into the atmosphere and reacting. This double walled system has proven effective on multiple occasions--for instance, the Experimental Breeder Reactor-II (EBR-II) reactor system did not have a single unwanted sodium exposure due to pipe failure during its lifetime.

Valves serve several purposes inside the primary and secondary sodium coolant loops. Isolation valves allow operators to isolate certain loops for maintenance or other reasons while still allowing the operation of other loops to continue. Anti-flow-reversal valves permit the flow of sodium in only one direction which permits loops to still operate if other loops lose pumping power. Flow control valves help regulate sodium flow along with pumps to optimize heat removal and dissipation either in a shutdown situation or other scenarios, such as for research purposes. An example sodium loop system with valve placement can be seen in Figure 17 [27].

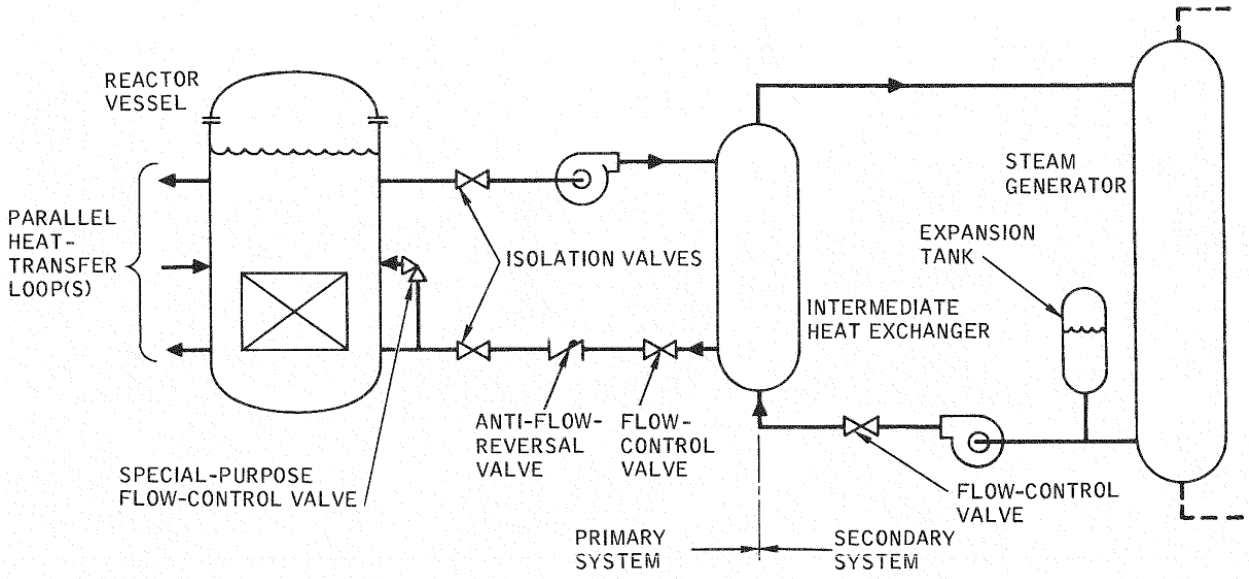

Figure 17. Valve placement in a typical heat transport system.

5.2.1 SNAPL

All piping used for the loop is stainless steel 304L for its “corrosion resistance” and “welding characteristics” [28]. A sample valve shown in Figure 18 could expect use within the sodium loop. This valve type is a “bellows valve” because the valves’ stems “do not rotate” and provides a “positive barrier against leakage” [28]. One possible drawback from bellows valves would be misuse that could lead to failure, as bellows valves will likely rupture if an individual attempts operating the valves while “the sodium is still frozen” within the piping system [28].

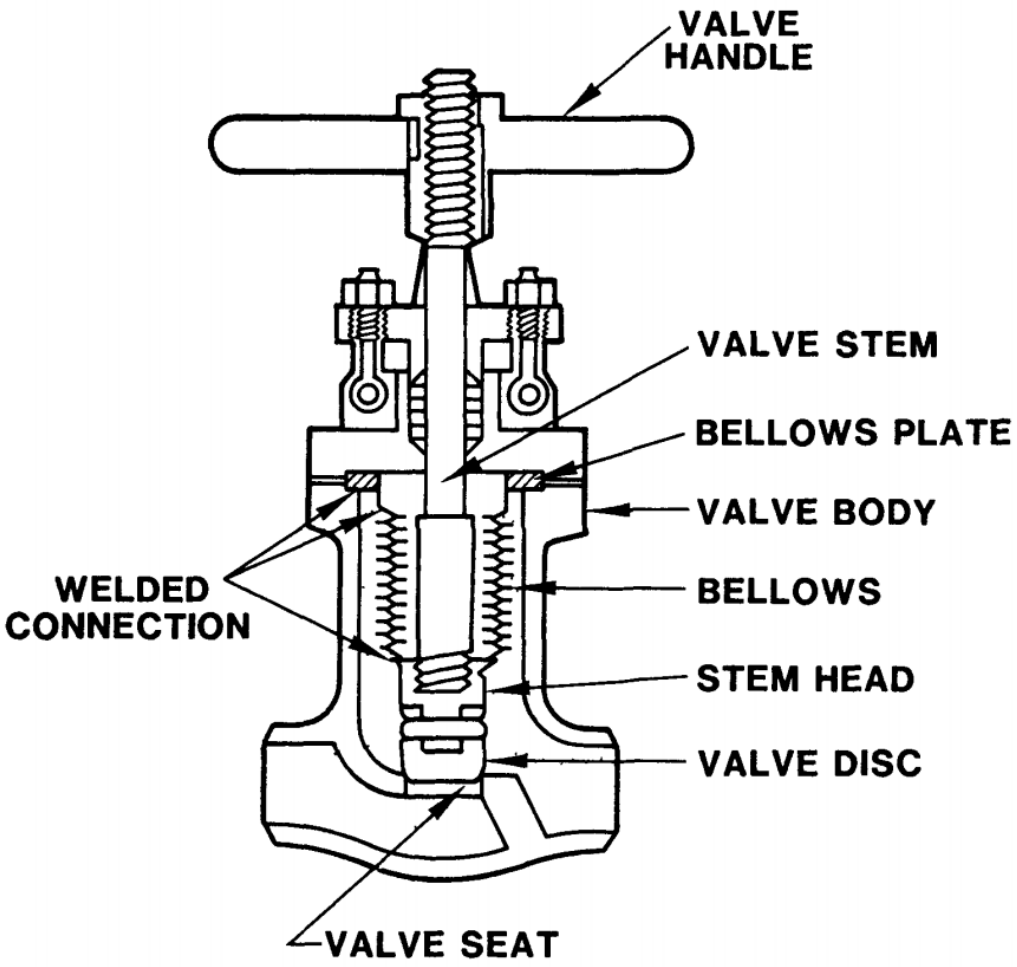

Figure 18. Bellows valve [28].

In 2002, India's Fast Breeder Test Reactor (FBTR) experienced a sodium leak in one of its purification cabins. The leak was caused by a manufacturing defect in the bellows of a sodium service valve. It is important to inspect components before installation, as this can mitigate a costly accident in the future. [55]

5.3 Sodium Leak Detection and Containment

Containing the sodium within its respective working area is of the upmost importance because of its reactivity potential with air and water. Leak detection in all areas of sodium systems is important, not just in valves and piping.

5.3.1 PRISM Reactor

The Power Reactor Innovative Small Module (PRISM) reactor was developed by General Electric based on SFR designs that were first investigated at the Argonne National Laboratory-West site (now, Idaho National Laboratory [INL]). This reactor was one of the first SFR designed for commercial production within the U.S. fleet of nuclear reactors. The reactor module enclosure consists of the reactor vessel, the containment vessel, and the reactor closure head. The reactor vessel is a 5.08 cm (2 in.) thick stainless-steel vessel, 5.74 m (18.83 ft) in diameter and 16.9 m (55 ft 7 in.) high. The reactor containment vessel is a 2.5 cm (l in.) thick stainless-steel vessel and approximately 6.04 m (19.83 ft) in diameter as shown in Figure 19. The reactor closure head is common to both vessels. A 15.2 cm (6 in.) diametral gap filled with argon gas exists between the reactor vessel and the containment vessel. The vessels are designed to allow in service visual inspection of each vessel, while the gap between the two vessels is also intended to contain a primary coolant leak without resulting in uncovering the core.

The closure head is a 0.3-m (1 ft) thick steel plate with a rotatable plug (Figure 20) for refueling, and contains penetrations for the primary coolant pumps, the intermediate heat exchanger system, and instrumentation and hardware. The system is designed so that all of the reactor containment penetrations only penetrate through the closure head. This allows for easier monitoring as all systems penetrate in one location.

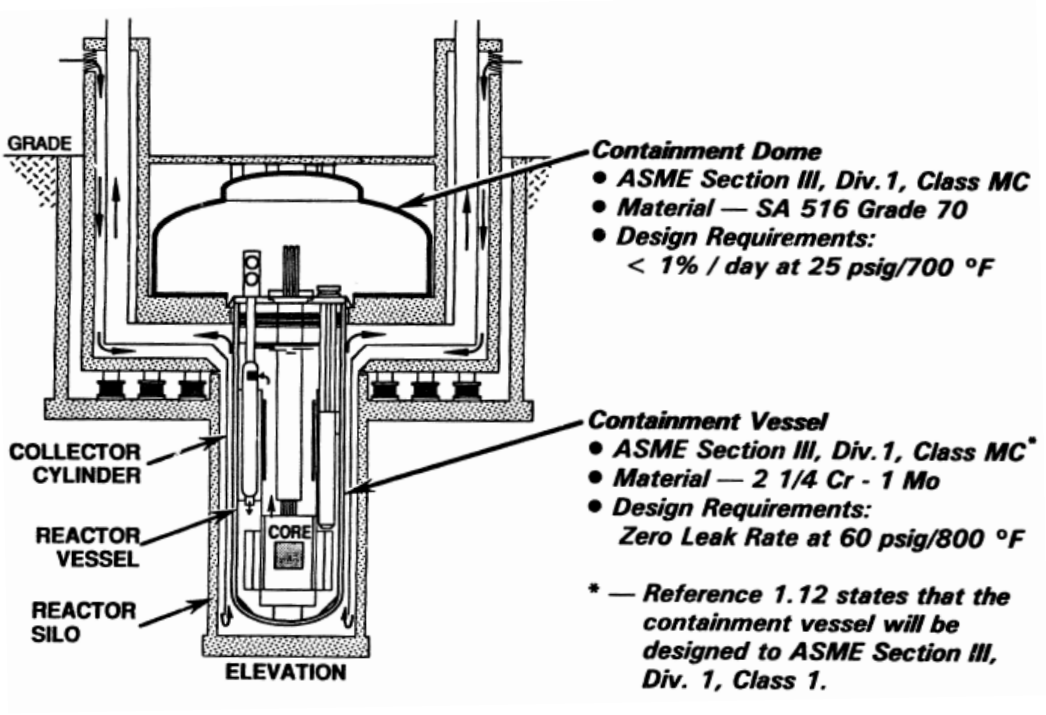

Figure 19. PRISM reactor containment dome and vessel information.

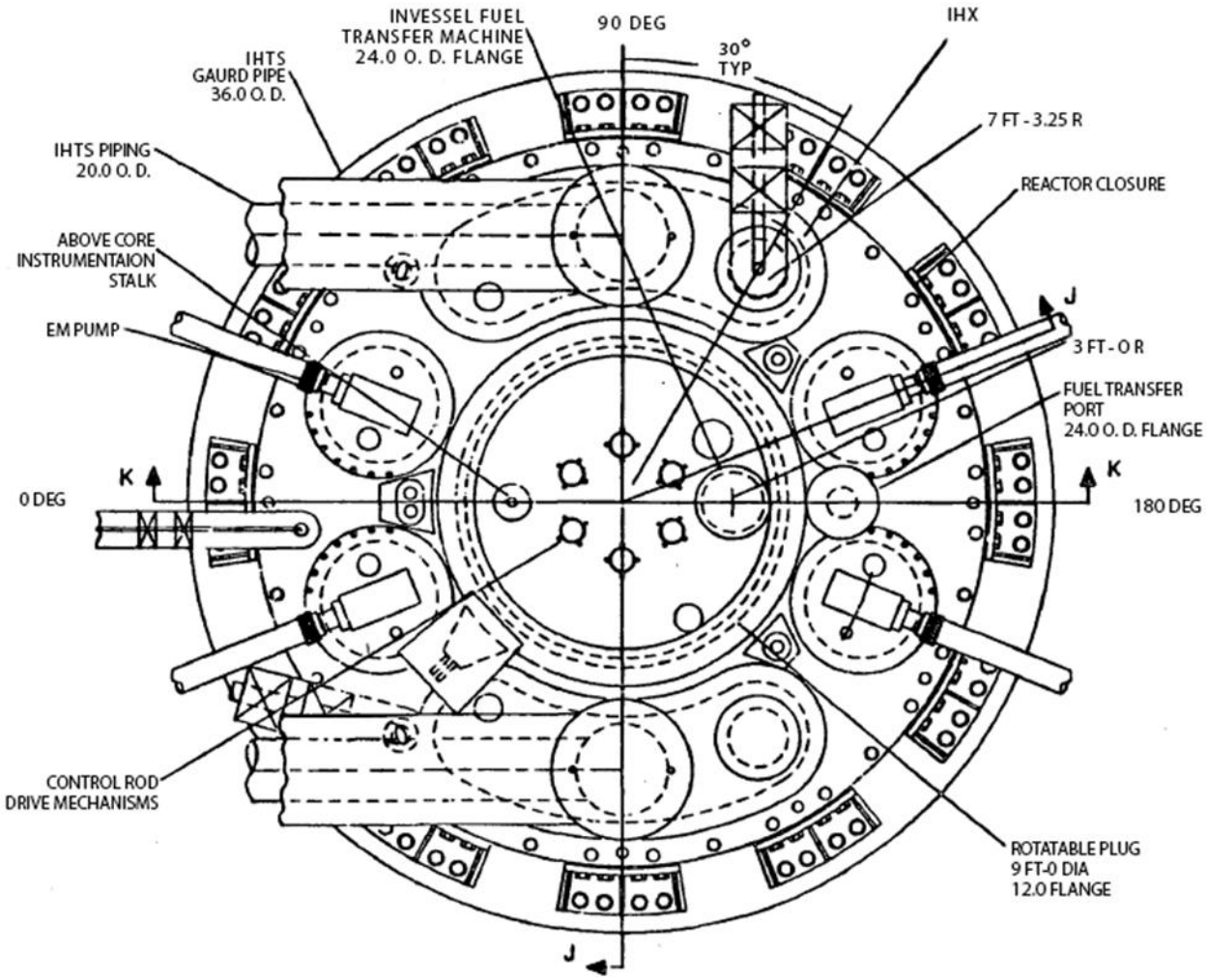

Figure 20. PRISM reactor closure head.

5.3.2 Sodium Advanced Fast Reactor (SAFR)

The Sodium Advanced Fast Reactor (SAFR) was designed to be an alternative to the PRISM reactor. The SAFR was designed to have inherent passive safety features and have a scalable electric capacity. All components within the reactor that contain sodium have multiple insulation layers. The first will be a gas annular space of about a 1-inch thickness. This space will not only enclose electric heaters that will preheat the sodium, but also allows a special atmosphere that will be sampled to detect any sodium leakage. The second layer of insulation will be physical insulation (fiberglass or similar), that will have an inner stainless-steel sheath that can withstand a

jet impingement should a moderate energy fluid system leak occur. Piping will also be present inside the annular gas gap that will allow sodium leaks to drain through gravity and collect in the leak collection header. The collection header will drain the sodium to a drainage vault. This system of sodium detection and draining can be seen in Figure 21 [29].

The drainage tank will have vent lines attached to it to allow for pressure relief in the event that sodium leaks and drains into the tank. The vent lines will be equipped with check valves that will allow pressure relief but at the same time prevent atmospheric air from entering the vault. The vault will be large enough to contain all of the possible sodium that could be leaked into it. The philosophy behind the system consists of three principal features: an insulation confinement and collection system, a system of piping to carry away sodium leakage, and catch-pans to safely collect accumulated leakage [30].

During its 30 years of operation, EBR-II experienced no unwanted reactions between water and sodium. This was attributed to the facility using double walled tubes in the steam generators, the tubes being either concentric or swaged together. This success is a great example of sodium handling for the rest of the SFR industry. [55]

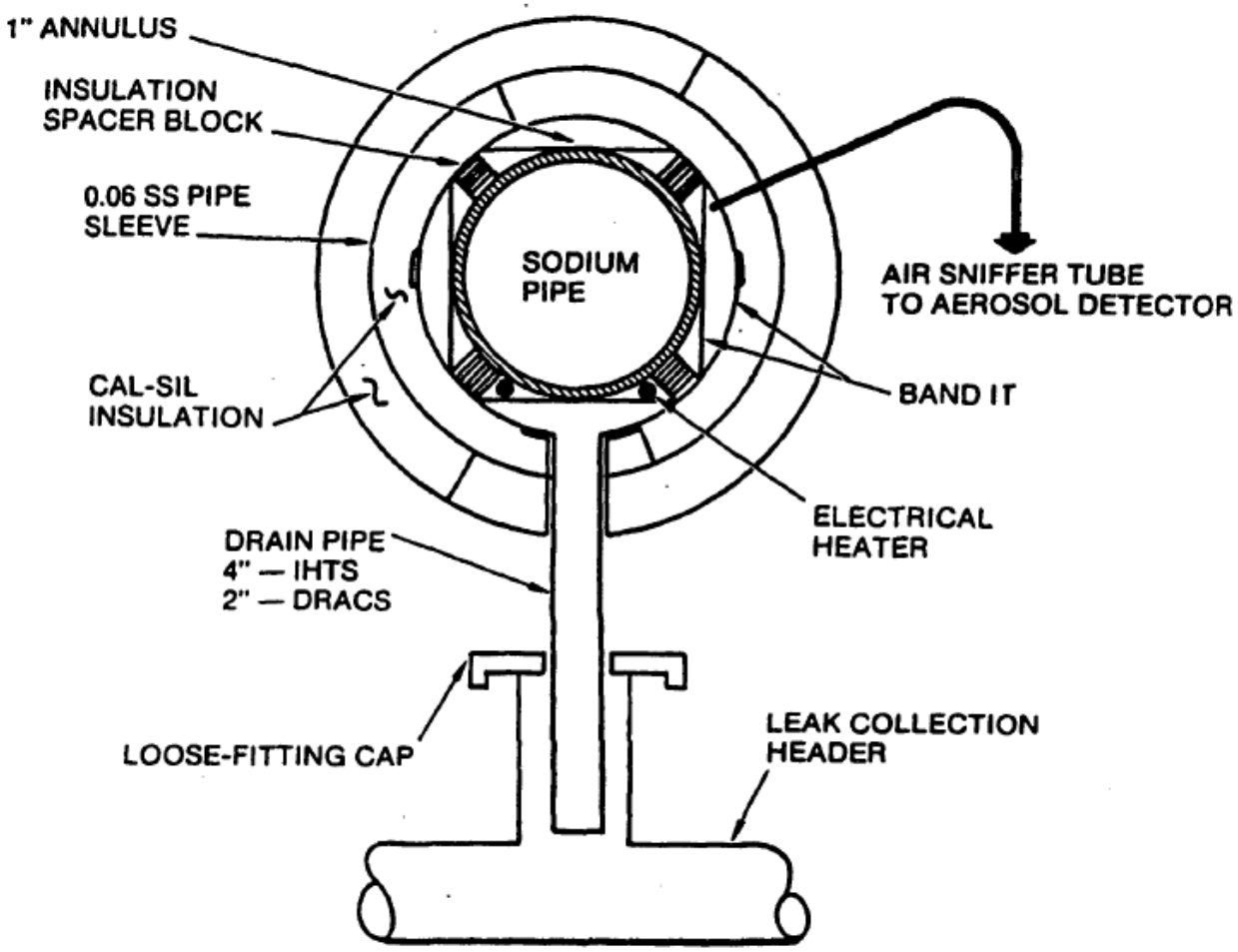

Figure 21. Sodium leak detection and leak drainage.

5.3.3 Clinch River Breeder Reactor (CRBR)

The Clinch River Breeder Reactor was another reactor that was designed but never built. CRBR had an in-depth design for leak detection and was part of the Department of Energy's (DOE) reactor development program in Oakridge, Tennessee. The Clinch River Breeder Reactor possesses three engineered safety features: the containment system, the containment isolation system, and the control room habitability system. The containment functional design is described, and the containment design basis accident is identified as a barrier against a failure of the primary sodium tank. A negative pressure differential will be maintained in the annulus, thus ensuring any leaks are directed into that location and can be monitored [31].

The sodium to atmosphere detection systems proposed for CRBR are as follows: sodium ionization detection, a hydro detector, surface ionization monitor for particulates, and liquid sodium detection.

Sodium to atmosphere leaks occur due to a positive pressure differential between sodium and the surrounding gaseous environment. The escaping sodium can react with the environment, producing numerous by-products including aerosols or vapors. In some reactions, hydrogen gas can be released. In addition, sodium can react exothermically, possibly producing heat, smoke, or fire.

The sodium ionization detector (SID) monitors for sodium aerosol /vapor leaks from the primary and intermediate heat transport systems to the surrounding atmosphere. The SID is activated by passing a gas sample through an ionization chamber operating via a hot filament technique. The hot filament ionizes sodium and sodium species, generating a recordable signal. When the sample gas contains no sodium vapor or aerosols, the ionization current is low, 0.01 to 0.2 nanoampere (nA). However, as the sodium aerosol concentration increases, the SID ionization current increases. This increase is proportional to the concentration of sodium vapor/aerosol in the gas passing through the SID chamber at any given time; the increase is not a function of sodium aerosol collection over time. The SID schematic is shown in Figure 22.

The smoke detector (Figure 23) proposed for CRBR is a commercially available unit and monitors the cell atmosphere for sodium aerosols. The smoke detector operates on an ionization principle; combustion products entering the detector's outer chamber disturb the balance between it and the inner reference chamber. This unbalance causes the gas discharge tube to ignite, generating a signal indicating the presence of combustion products.

The hydrogen detector (Figure 24) proposed for CRBR is a commercially available, laboratory-grade gas chromatograph. This device separates and analyzes sample gas' from the test cell environment. In the presence of moisture, a sodium leak will generate hydrogen gas that can be monitored by the detector and used as an indicator of a reaction.

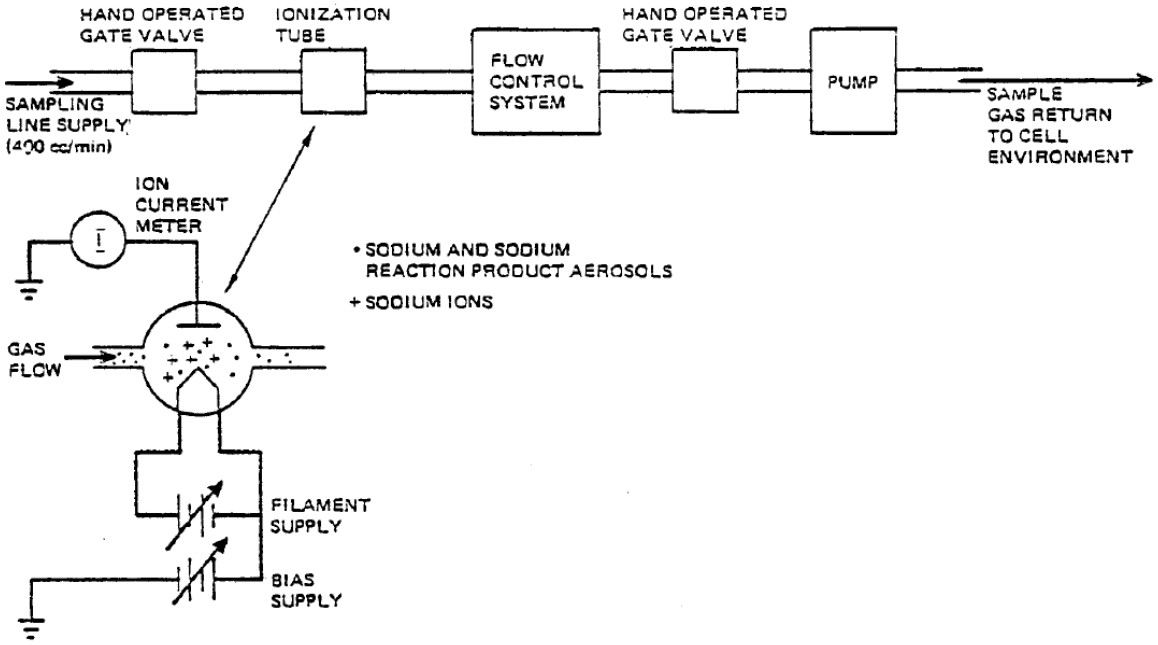

Figure 22. Sodium ionization detection schematic.

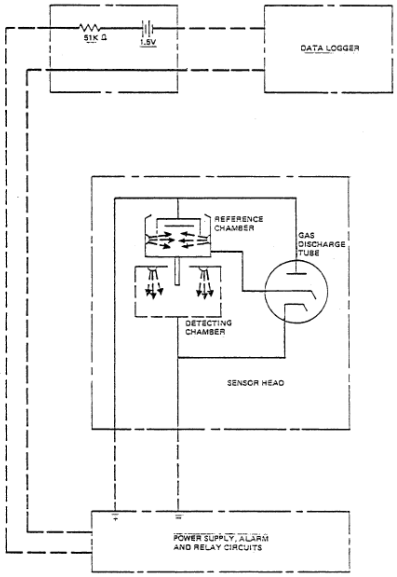

Figure 23. Sodium aerosol smoke detector.

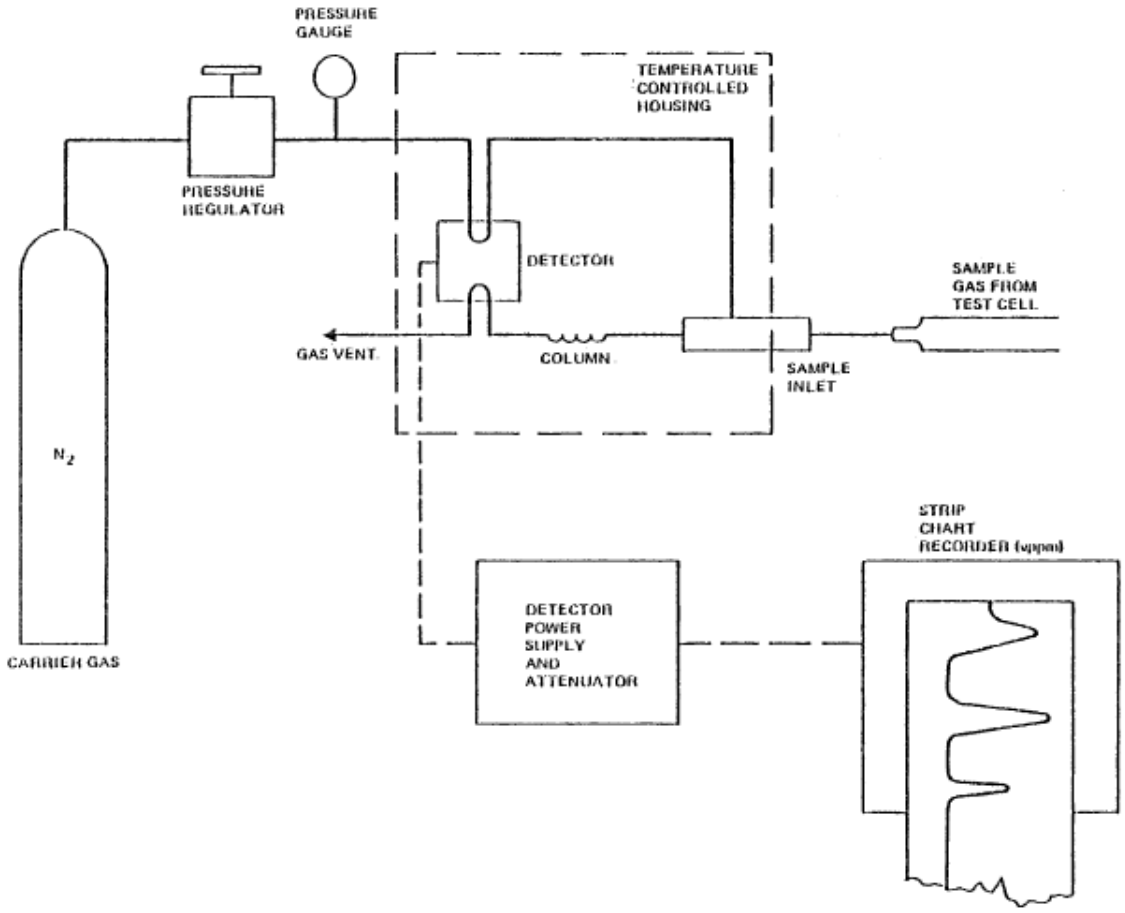

Figure 24. Hydrogen detection schematic.

A surface ionization monitor for particulates (SIMP) is proposed to monitor the cell environment for sodium and sodium reaction products in the form of aerosols. A schematic of this monitor can be found in Figure 25. The SIMP detector responds to sodium aerosol presence in two ways: to measure the average ion current and measure the "counts" of particulates. When particulate "counts" are measured, they can be displayed via a digital count meter through a signal processed within the SIMP, or a strip chart recorder signal, which is the integrated output of a sawtooth signal originating within a triggering unit synchronized to the detector's ionization current.

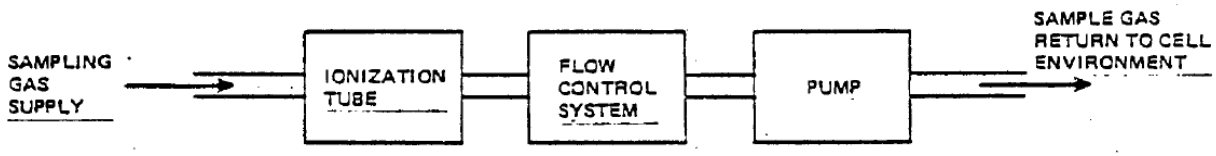

Figure 25. Surface ionization monitor for particulates (SIMP) diagram.

A liquid sodium leak can be detected through a cable detector or a contact detector. The cable detector consists of a thin, stainless steel-sheathed, mineral insulated (magnesium oxide) coaxia1 cable, with perforations in the outer (grounded) sheath. This detector can be seen in Figure 26. Liquid sodium penetrating the perforated sheath causes a low resistance path to ground, which then produces an increased voltage drop and activates an alarm. The response to liquid sodium is indicated on a strip recorder and data logger.

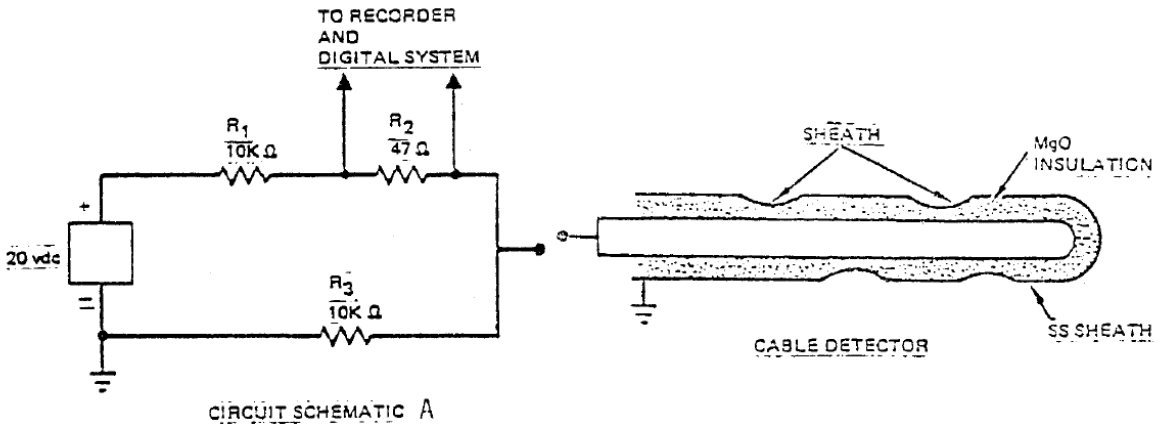

Figure 26. Cable detector.

The contact detector (spark plug) consists of a stainless steel-sheathed, mineral -insulated (MgO) coaxial cable, joined as an exposed junction within a bonnet at the end. Liquid sodium flowing into the gap between the electrodes provides an electrical short circuit between the exposed junction and the stainless-steel sheath [32]. The contact detector can be seen in Figure 27.

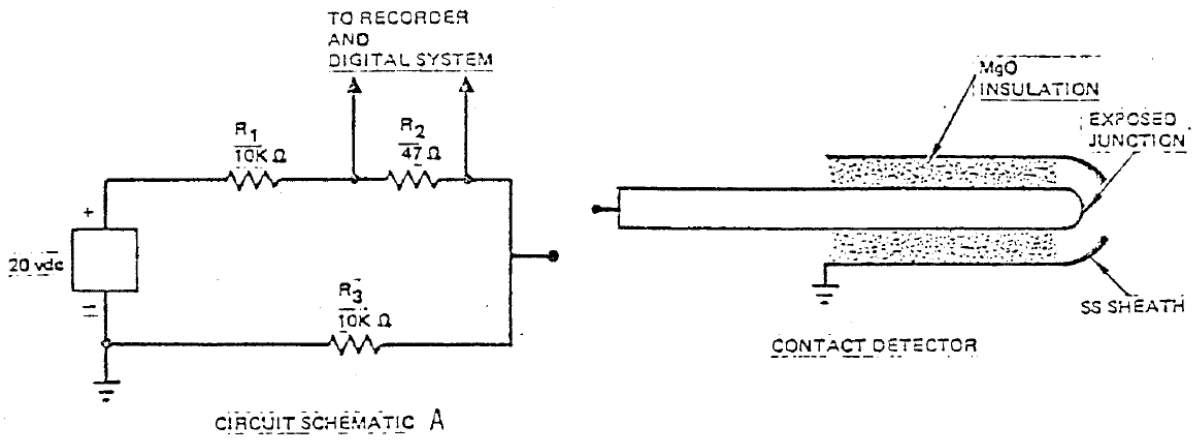

Figure 27. Sodium contact detector.

5.3.4 Sodium to Water Leak Detection

It is important to identify locations where sodium to water interactions may occur. These locations are primarily at the steam generators in other SFRs since the only localized place in the plant where sodium and water meet are in the process of transferring heat from the sodium to the water for the turbine.

5.3.4.1 CRBR

The steam generator leak detection system is designed in such a way that it can detect the presence of hydrogen or oxygen gas. Leak detection is based on the measurement of the hydrogen concentration in both the sodium and in the cover gas spaces. Oxygen concentration measurements are found in the sodium only and are complementary to the hydrogen detectors, thus providing a diverse method to ensure early detection.

The measurement of hydrogen in the sodium is performed by allowing the hydrogen to diffuse through a thin-walled nickel membrane and then detecting the hydrogen with an ion gauge and an ion pump. The monitor may operate in a static mode using the ion gauge to monitor steady state hydrogen concentration, since hydrogen content is directly related to the pressure measured in the chamber. The monitor may also operate in a dynamic mode, using the ion pump to constantly pump the chamber since the hydrogen concentration is directly related to the ion-pump current.

The hydrogen detection in the expansion tank cover gas utilizes a gas chromatograph. A continuously monitoring hydrogen detector similar to the in-sodium detectors is also provided for the cover gas. The hydrogen detector proposed for CRBR water to sodium leak detection is shown in Figure 28. The nickel membrane is inserted into the liquid sodium. On the other side of the nickel membrane is a vacuum created by an ion pumping system. Hydrogen resulting from a leak diffuses through the nickel membrane into the vacuum, where it can be detected through several means; measuring the pressure rise, employing a mass spectrometer, or monitoring the ion pump current [32].

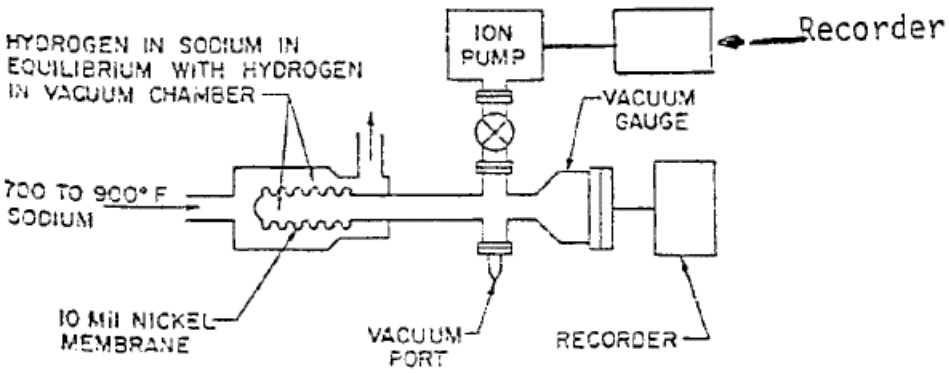

Figure 28. Hydrogen Detector Schematic.

Oxygen detectors are electrochemical cells immersed in sodium that continuously monitor in-sodium concentration and consist of a reference oxygen electrode separated from the sodium by a $ThO_2 - Y_2O_3$ solid electrolyte (see Figure 29). The electrical potential difference between the reference electrode and the sodium is a measure of the oxygen content in the sodium [32].

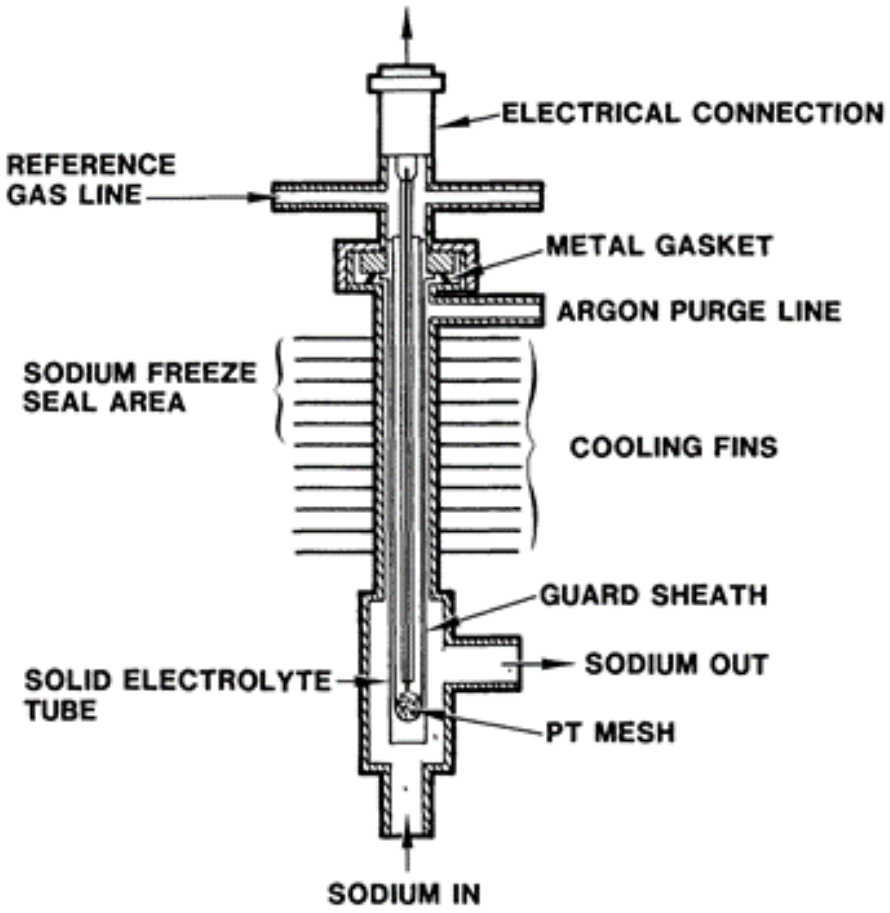

Figure 29. Oxygen detector schematic.

5.3.5 Cladding Failure Detection

Fuel pin failure has been a common occurrence in reactors. Detecting these failures early is very important because a release of fissile materials and fission products. Traps and detectors should be put into place to mitigate any adverse effects that fuel pin failure could cause. Fuel pin failure can be caused by several factors. Temperature transients can cause the cladding to swell and crack, irradiation can embrittle the cladding, or simply abnormal corrosion.

When a cladding failure does occur, fuel and sodium will come in contact and can create reaction products. These products should be monitored and trapped alongside fission products that could be released into the primary sodium.

The Fast Flux Test Facility (FFTF) experienced several fuel pin failures alongside its many successes. The cladding breaches released cesium into the primary sodium loop and cover gas system. This radioactive release lead to system complications at the time. However, a cesium trap was installed in 1987, and all subsequent cesium releases were contained and mitigated any contamination of the sodium loop. This illustrates the need for passive safety and planning for fuel pin failure. [55]

5.4 Fire Suppression

5.4.1 SAFR

The SAFR design approach for fire suppression was a modified form of the CRBR [30]. Figure 30 shows the design of the fire suppression system for the steam generator building. The image shows the drain line entering the header "where the sodium is conducted to the sodium water reaction protection system (SWRPS) vault" [30]. In the event of a leak within the SAFR plant, the leak collects in the leak collection header as shown on the left of Figure 30. The SAFR plant required the use of "sensitive, reliable leak detectors," the implementation of leak detection resulted in testing various methods [30]. Five different detection method evaluations: "two conductivity-types and three aerosol-type," were investigated [30].

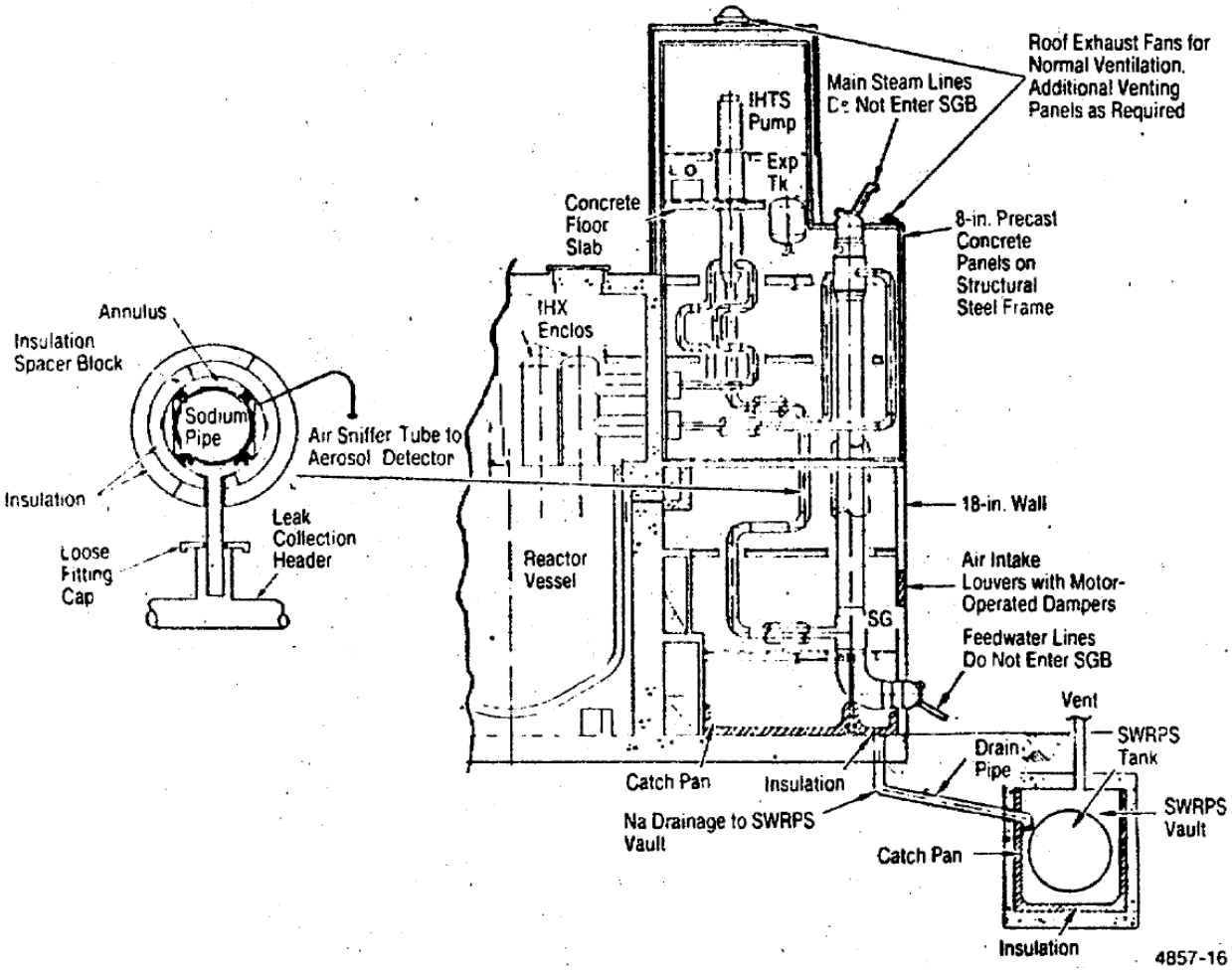

Figure 30. Passive sodium fire mitigation provided by SAFR steam generator building [30].

The overall fire protection system has two types of systems: a non-sodium fire-protection system (NSFPS) and a sodium-fire-protection system (SFPS) [30]. The non-sodium fire-protection system will be equipped with 300,000-gallon redundant storage tanks, with a series of sprinklers, pumps, and a water spray [30]. For rooms with water sensitive equipment, such as computers and electronics, pressurized storage cylinders located outside the rooms and cable ways will be equipped with a flooding system filled with Halon 1301 (Bromotrifluoromethane) [30]. The sodium-fire-protection system is equipped with fire-detection and alarm instrumentation, aerosol release-limiting instrumentation, a leak-collection and catch-pan system, and transportable fire extinguishers coupled with protective clothing to mitigate the risk of sodium leaks and fires. [30].

These components all work to prevent the uncontrolled release of a moderate energy fluid system (MEFS)-size leak by design. The philosophy behind the system consists of three principal features: an insulation confinement and collection system, a system of piping to carry away sodium leakage, and catch-pans to safely collect accumulated leakage [30].

5.5 Heat Transport Systems

The purpose of the heat transport systems (HTRs) is to remove heat from the reactor core and transport it to either be used in steam generators, dump it as waste heat, store it for later use such as in a molten salt, or other applications as seen fit.

The sodium that is in direct contact with the reactor core will be bombarded with neutrons. Sodium is relatively transparent to neutrons, but some activation of the sodium will still occur. Radioactive elements outside of the containment vessel is not desired, so most sodium systems utilize a primary sodium loop which is in direct contact with the reactor core, and a secondary or intermediate sodium loop, which transports heat away from the primary loop. This is especially important if the sodium will be used in steam generators as the sodium could react and release into the atmosphere.

There are two different types of sodium systems that have generally been used, the pool or loop system. Pool-type reactors use a large pool of sodium that completely engulfs the reactor core and transports heat away from the core. Loop-type reactors utilize a smaller pool and rely more heavily on pumping sodium to cool the reactor. Pool reactors are generally safer because in a loss of coolant accident (LOCA) heat can still be removed through conduction.

A general schematic showing the similarities and differences between pool and loop type reactors is shown in Figure 31.

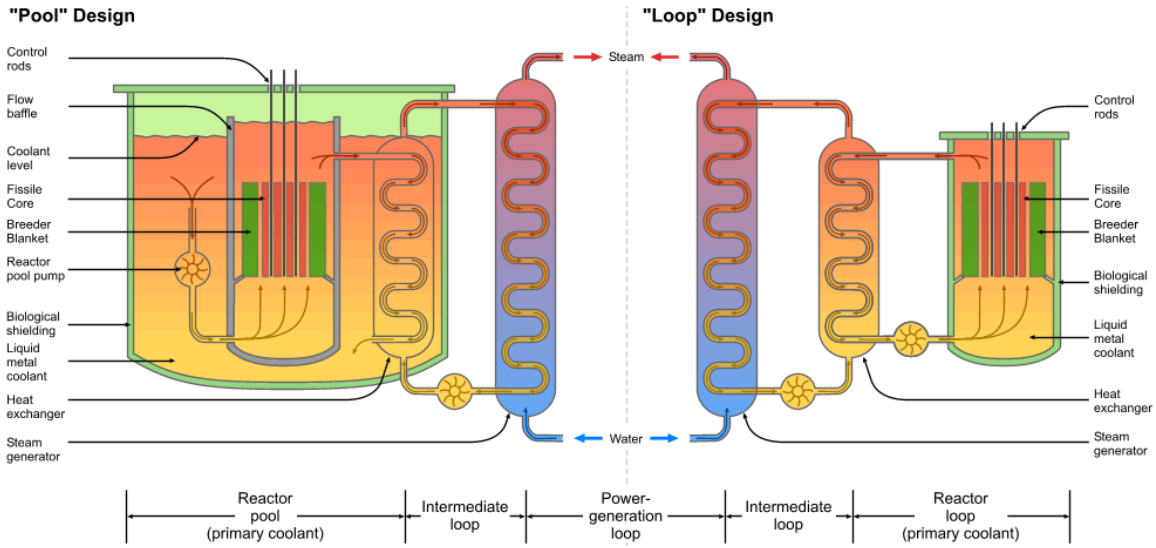

Figure 31. Similarities and differences between pool and loop type reactors. [33]

During its 35 years of operation, the Phénix Reactor experienced one significant leak within its secondary heat exchanger. During its design, the effects were not fully considered from the different thermal expansion loads between the inner and outer shells. An improved design allowed more flexibility between the top closure head and the inner shell, as well as improved mixing between the outlet and bundle sodium. It's important to consider whether or not thermal expansion plays a role in the system.

FFTF

The Fast Flux Test Facility (FFTF) reactor is positioned in a heavily shielded cell at the center of a domed containment building. Heat is removed from the reactor by liquid sodium circulating under low pressure through three primary cooling loops. Intermediate heat exchangers separate the radioactive sodium in these primary loops from the nonradioactive sodium in the secondary system. Three secondary sodium loops transport the heat from the intermediate heat

exchangers to twelve dump heat exchangers, which are cooled by air. Figure 32 depicts the main heat transport system utilized by FFTF [34].

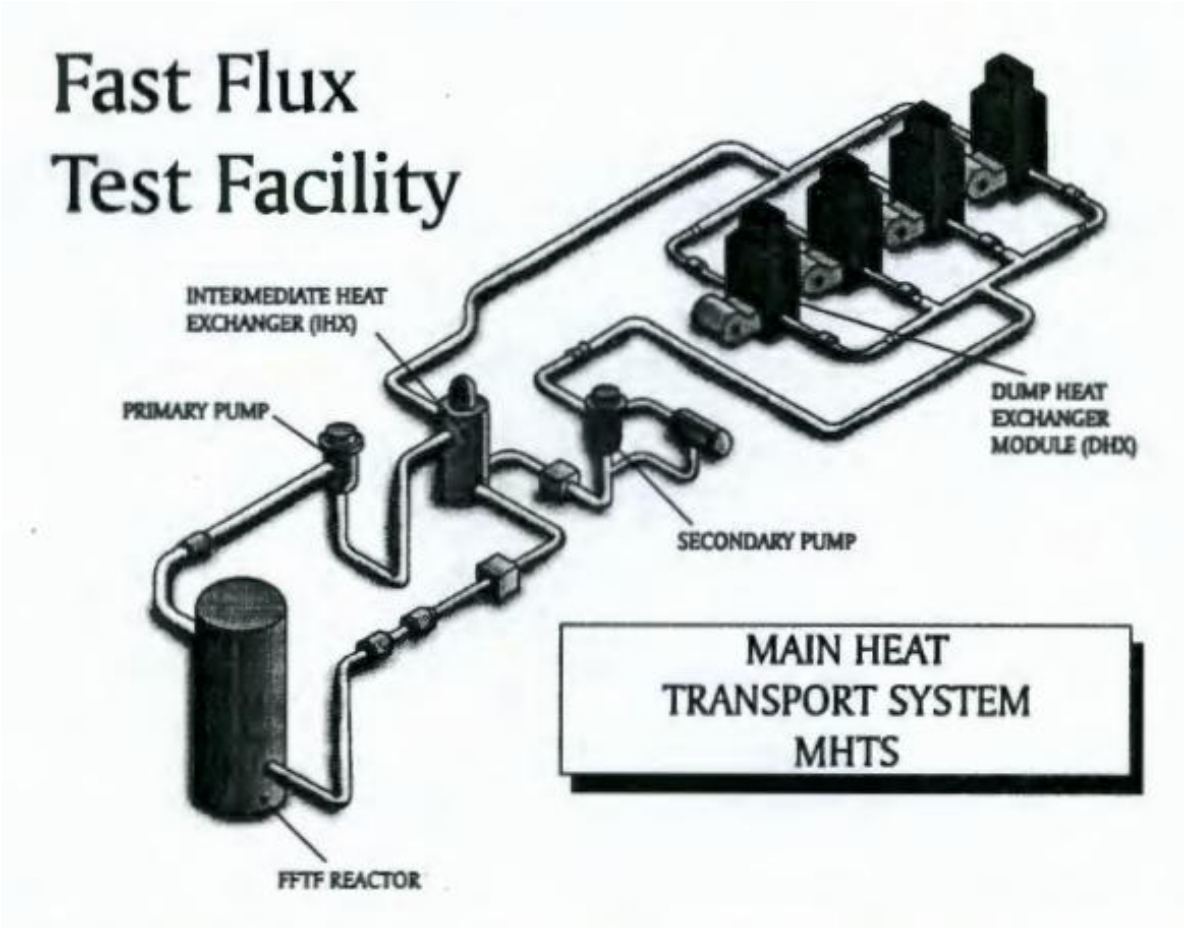

Figure 32. Main heat transport system in FFTF.

EBR-II

EBR-II works by generating heat in the core, and then transferring that heat into the primary sodium coolant that is pumped through the core. The grid plenum assembly, as depicted in **Error! R eference source not found.**, is responsible for directing sodium flow through the core and consists of upper and lower grid plates that are interconnected through a system of stainless-steel tubes. The plates are then surrounded by a cylindrical stainless-steel structure that also seal the pumped sodium flow.

After the primary sodium leaves the core, a primary-to secondary heat exchanger is used, which is then discharged directly to the sodium-filled primary tank. The heated secondary coolant is then pumped from the heat exchanger to the sodium-boiler building where steam is produced and superheated. From this point the steam rotates a turbine which converts the kinetic energy of the rotation into electricity. With this design the EBR-II was capable of producing 62.5 MWt and 20 MWe.

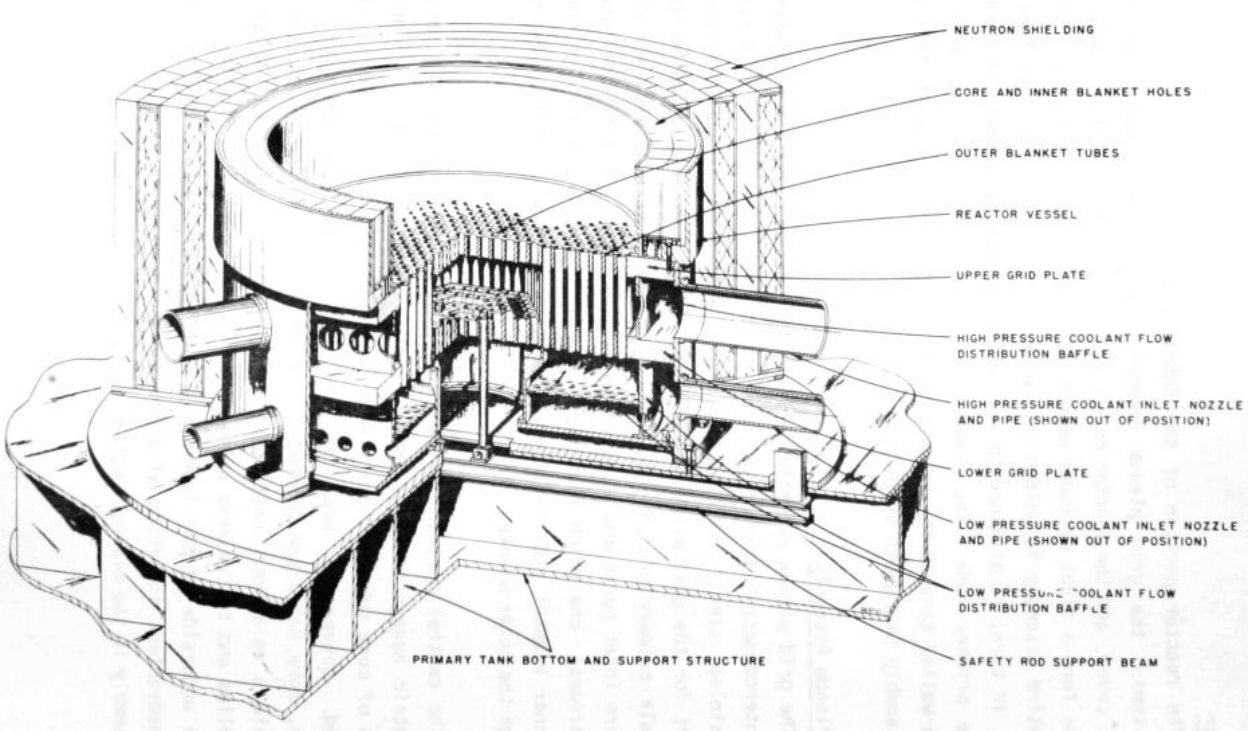

Figure 33. EBR-II grid plenum assembly [35].

EBR-I

After leaving the outlet plenum, the coolant flowed via gravity to a primary-secondary (NaK to NaK) heat exchanger, then into a receiving tank in the basement. A pump, operated at a capacity slightly higher than the main coolant flow, returned the coolant to the gravity supply tank. An overflow system connecting the supply tank to the receiving tank guaranteed a constant delivery rate of coolant to the core and blanket. Heat from the secondary NaK was removed in a steam generator which consisted of a water heater, boiler, and superheater. Water, in the form of a film, traveled downward through the heat exchanger tubes. Heat transferred from the counter-flowing secondary NaK and in turn generated steam which, after superheating, was used to drive a conventional turbine-generator. Approximately 200 kW of electricity was generated – enough to satisfy the needs of the EBR-I facilities. A schematic layout of the plant is given in Figure 34.

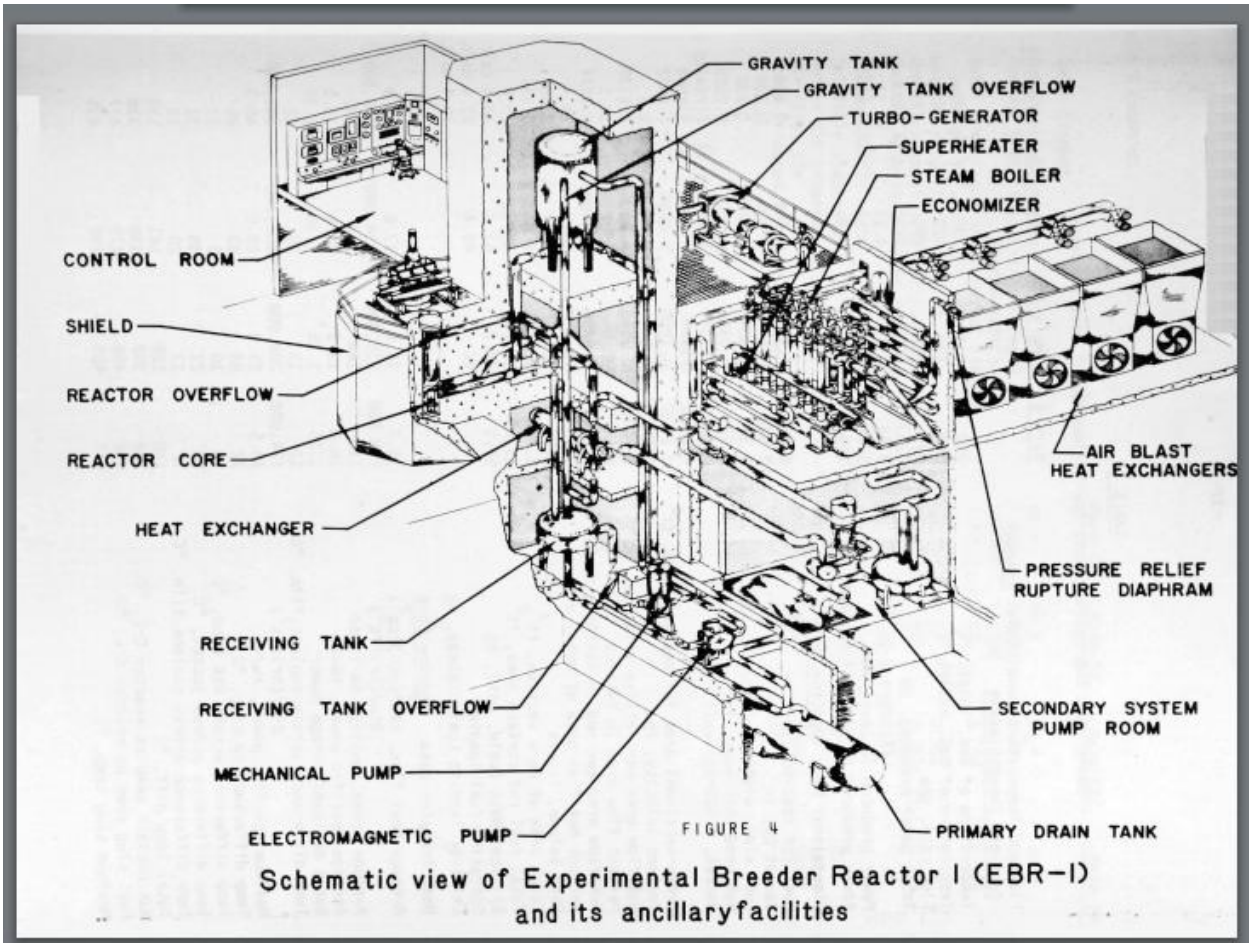

Figure 34. EBR-I schematic.

5.5.1 Heating Methods

Several different heating methods exist when it comes to controlling pipe temperature in the sodium loop system. Temperature control is very important is it maintains pipe integrity by helping to prevent thermal shock, cycling, or large temperature gradients which could degrade the pipes. Several criteria should be considered when thinking about what heating method to use and is summarized below by C. F. Braun & Co.;

1. The system must preheat the empty piping evenly to the range of 350 to 400 F. The system must also heat full piping to a maximum of 800 F for pipes up to about 8-inch size.

2. Heater reliability must be retained through a reasonable lifetime during which pipewall temperatures could reach 1200 F.

3. Control must be adequate to prevent uneven heating and permit melting away from a free surface in the event solidification occurs.

4. Materials must not be damaged by contact with liquid sodium and must be compatible with other piping components.

5. The system must be designed to permit surveillance of the piping and to have negligible effect on instrumentation.

6. The system must be designed to withstand any mechanical damage likely to occur, including pipe movement and vibration.

7. Ease of assembly and disassembly is desirable to minimize installation defects and facilitate maintenance or repair.

8. The system must withstand nuclear radiation, if such is present.

9. Installation of the system should not contribute materially to pipe stresses [36].

The most important aspect is evenly heating the piping to prevent any unwanted temperature gradients. Temperature gradients can take a heavy toll on piping materials and can lead to breaks and leaks if not properly handled. Tapered pipes or differing wall thickness need to also be considered when designing a heating system.

5.5.1.1 Pipe Insulation

Retaining heat is a key factor when it comes to heat transport and a big role is carried out by insulation. Some general guidelines for insulation are, “good resistance to heat loss, sufficiently high maximum service temperature, compatibility with piping and piped fluid, adequate personnel protection, and maintenance of a satisfactory thermal environment in areas adjacent to the piping” [36].

In addition to these general guidelines, sodium piping is often coupled with heaters which means the insulation must withstand highly concentrated heat loads. The insulation should also not prematurely breakdown over successive applications of concentrated heat loads as this could hurt the integrity of the insulation system. Since sodium also reacts with water, insulating materials should be non-hygroscopic and chemically inert when in contact with sodium.

Despite precautions, sodium leaks can still occur in piping due to a various number of reasons. As an extra layer of protection, there is often an annular stainless steel sheath accompanying piping insulation to prevent the sodium from permeating the insulation escaping to the outside environment. The metal sheath also helps prevent the pipe heater from burning out and reflects the heat into the pipe instead of outward.

When installing insulation, it is much easier and safer to have the insulation prefabricated to fit your system. This will help ensure that the insulation fits properly and leaves the right amount of clearance for other pipe systems like heaters, instrumentation, support structures, etc. When attaching the insulation to the piping straps or similar methods should be used. Welds and studs should be avoided to prevent additional stresses to the pipe. Different types of insulation material can be found in Table 10 [36].

Table 10. Different Types of Insulation Material Used in SFR's

Material	Maximum Service Temperature, F	Density LB/CU FT
Amosite asbestos	1500	16
Mineral wool	1900	17
Diatomaceous silica	1900	24
Ceramic wools	2300	3 - 24
Calcium silicate	1200	11
Unbonded fiberglass	1000	9 - 11
Reflective insulation	1500	--

When choosing an insulating material, it is important to look at the material properties such as max service temperature and thermal conductivities. It is also common to use a multilayered insulation scheme made of different materials to achieve certain insulating properties. It is also seen from the table that insulation for SFR's is still under investigation because amosite asbestos is recommended, which we know to be a toxic substance. This table was published in 1969, and insulation materials have changed since then and need more review and testing.

5.5.2 Filling/Draining Sodium into HTS

Filling

Sodium primarily arrives to a plant in the form of solid metal stored in drums or tank cars. Two techniques to liquify the sodium and prepare it for loading is through "wrap around electric heaters" or through a circulating hot oil system [37]. Once the sodium has been melted, an inert gas (usually nitrogen) is used to pressurize the transport tanks and force the sodium through a filter and subsequently into the reactor fill tanks. The filter traps any particulates that may arise from sodium oxidation during transport. Before the sodium is loaded into the reactor's primary and secondary loops; however, the loops are first purged of oxygen and moisture using nitrogen.

The reactor piping system/fill tanks should be equipped with trace heaters that pre-heat the system to mitigate any freezing that may occur while the sodium is being transported into the heat exchange system [38]. Once the fill tanks are full, gravity should first be used to fill the primary sodium loop until the pump suction is covered, at which point the pump can be utilized at a low setting to finish the filling process. The secondary heat exchange system can be filled in a similar

manner, or through pressurized nitrogen gas. An inert atmosphere inside the heat exchange system should be present during the duration of the filling process.

Draining

The heat exchange system is drained in a similar manner as it is filled. The fill tanks are pre-heated using trace heaters, and then pumps or pressurized nitrogen are utilized to remove sodium from the heat exchange system into their proper fill tanks.

5.5.3 Sodium Levels Inside HTS

Sodium levels inside the heat transport systems is monitored at all times.

5.5.3.1 SNAPL

The sodium loop uses two separate tanks to detect the level of the sodium and thus the volume of sodium within the loop. Figure 35 shows the schematic of tank T2 and depicts the rods are used to determine the level within the tank. Different LED lights will turn on depending on which probes are in contact with the sodium.

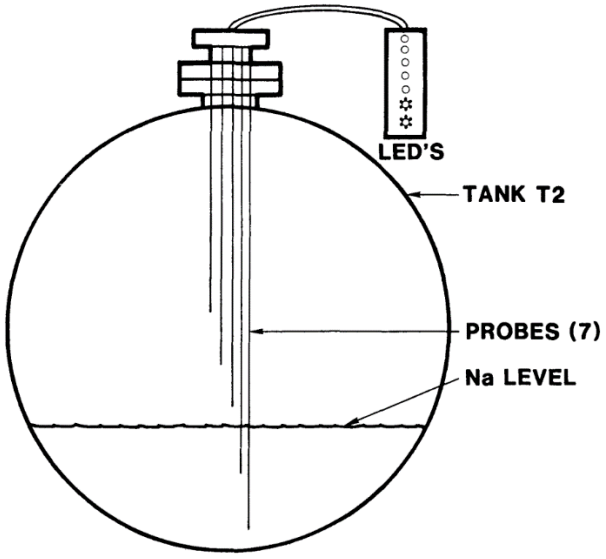

Figure 35. Probe level detector schematic [28].

5.5.4 Power and Control of HTS

The purpose of the heat transport system (HTS) job is to transport heat. The amount of heat that is being transported needs to be monitored and controlled at all times. This is mainly done through measuring the rates of heat gain or loss, and coolant flow through the system. The monitoring system should have several aspects, and some monitoring systems for different reactors are described in this section.

5.5.4.1 SNAPL

The sodium loop control uses a dedicated computer system [28]. The computer system issues commands or alarms after reading the various instruments. The computer system is comprised of divisions, and each division operates independently. A typical control circuit used by the computer system can be seen in Figure 36. The computer has five control functions: heater on-off, cold trap fan on-off, E. M. pump on-off, drain valve open-close, and entire system on-off [28].

The loop can also be manually controlled using a very simple control system [28]. The manual control's function is to ensure the computer control program is operating and ensuring the loop is operating properly [28]. The manual system can also isolate operational problems that may arise.

Another important aspect to the controls system is the function and location of thermocouples. The thermocouples used within the sodium loop were specially designed to negate the requirement of welding it to the piping directly. The loop used 123 type J (iron-constantan) thermocouples to monitor the temperature of the loops. 58 of them were connected to the computer, 42 connected to the manual control system, and 23 acted as backups [28]. The loop also had 14 thermocouples located at the exit legs of the loop [28].

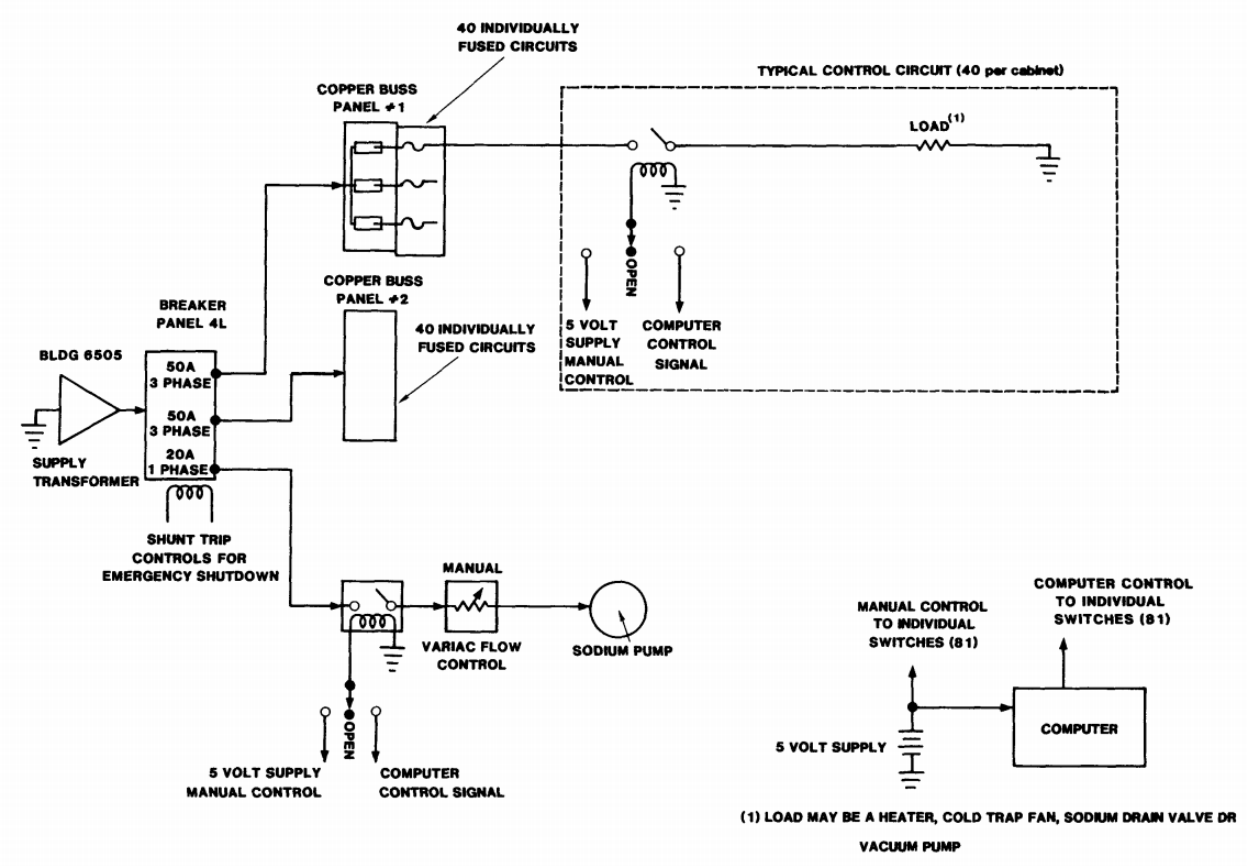

Figure 36. Typical control circuit [28].

5.5.5 Flow Meters

Flow meters give real time data on how much sodium is physically being pumped through the heat transport system. Flow values can be used to determine a variety of things: the amount of heat that is being produced and subsequently removed from the reactor core, possible blockages or leaks occurring due to reduced or diverted coolant flow, and others.

5.5.5.1 SNAPL

Magnetic flowmeters measure the flow of the sodium as it moves through a section of pipe in the loop [28]. Effectively these flowmeters operate in the opposite of the electromagnetic pump by generating an output voltage as the sodium moves through the device. A schematic of an electromagnetic flowmeter is shown in Figure 37.

For the devices utilized by SNAPL, the electromagnetic field (emf) generated comes from Eq. (20). In the equation, Q is the sodium flow rate in gpm, d is the inside pipe diameter in inches, B is the flux density in gauss, $K1$ is the pipe wall shunting factor, $K2$ is the end effect factor, $K3$ is the magnet temperature factor, and $K4$ is the pipe expansion factor.

$$emf(mv) = \frac{QB(K1)(K2)(K3)}{3162d(K4)} \tag{20}$$

For more information on how to get the specific constants for Eq. (20), go to the SNAPL section in Appendix B: History of Different SFRs.

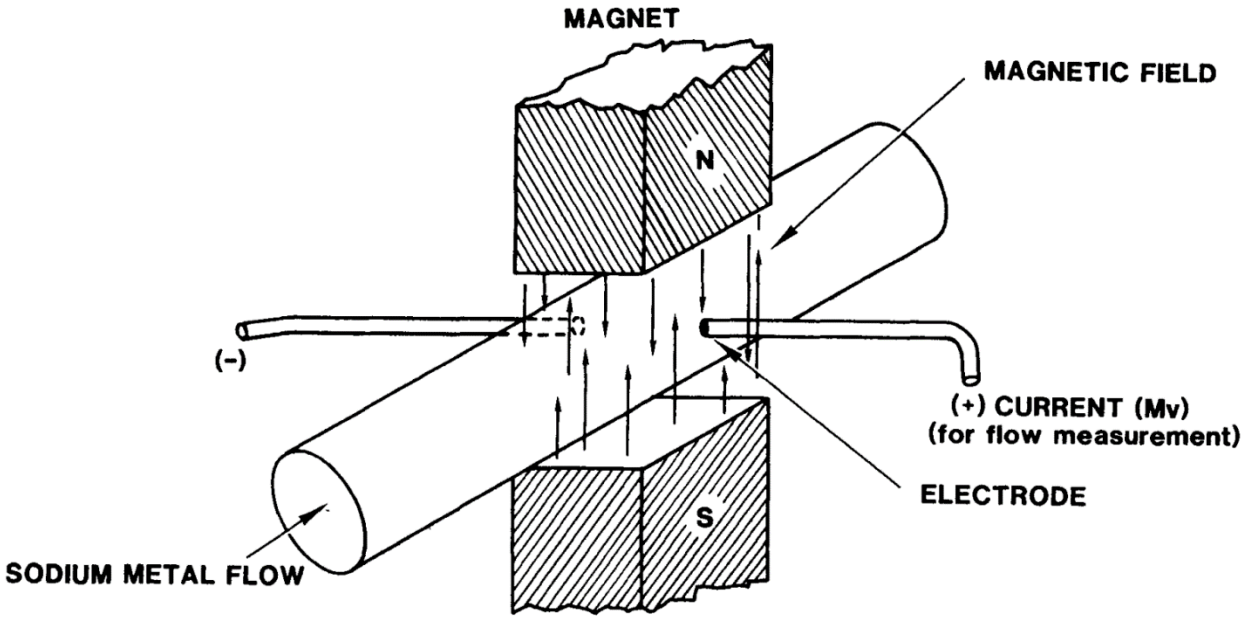

Figure 37. Schematic of electromagnetic flowmeter [28].

Both the Monju and Phenix reactors had leaks involving thermocouples. Sodium flow had caused increase vibrations in the thermocouples that led to weld cracks. The thermocouples were welded to the pipes, which allowed the cracks to arise in the first place. [55]

5.6 Decommissioning and Neutralizing Sodium Systems

5.6.1 Carbonation of EBR-II

After EBR-II was shut down in 1994, sodium in the primary and secondary loops needed to be drained and stored. This posed a challenge, however, because even after draining the bulk of the sodium, residual sodium would still remain inside both the primary and secondary loops. This residual sodium needed to be neutralized to mitigate future risk involving the decommissioned plant. Before the decommissioning of EBR-II, the accepted process to neutralize residual sodium was a technique that used a gaseous mixture of nitrogen and water vapor. For EBR-II, a process was developed that involved humidified carbon dioxide verses nitrogen. This helped create a more stable and predictable reaction sequence to safely get rid of the sodium.

5.6.1.1 Humidified Carbon Dioxide

The two main reasons that scientists and engineers decided to not use humidified nitrogen to decommission EBR-II were:

1. Due to system geometry, it can be difficult to remove sodium hydroxide at the same rate that it is formed. This can cause pockets or pools of hydroxide to form, which then can lead to a sudden mixture of sodium and water in an uncontrolled reaction. Unforeseen increases in pressure and heat can pose threats to personnel and system integrity.

2. Humidified nitrogen reacting with sodium causes large amounts of concentrated sodium hydroxide which is corrosive to system materials and hazardous to operators. This hydroxide solution also has to be treated after the decommissioning process which adds additional costs to the entire operation [39].

Because of these disadvantages, scientists decided to investigate and use humidified carbon dioxide as the sodium neutralizer. The water vapor first reacts with the sodium to first form sodium hydroxide which is then quickly reacted with carbon dioxide to form sodium carbonate or sodium bicarbonate. These products are solid, brittle, and porous and do not allow the build-up of sodium hydroxide in the system.

To first test the effectiveness of humidified carbon dioxide, a test chamber was constructed and different sodium test samples were created. The chamber consisted of an air-tight vessel that allowed for the steady flow of humidified carbon dioxide. The carbon dioxide was bubbled through a water column to humidify it before entering the test chamber. A schematic showing the layout of the test loop can be seen in Figure 38, and a physical depiction of the loop can be seen in Figure 39. Many test samples were made by melting sodium and filling clear glass graduated cylinders of different sizes (Figure 40). Other samples were made by pouring molten sodium into various sized slits between stainless steel plates (Figure 41).

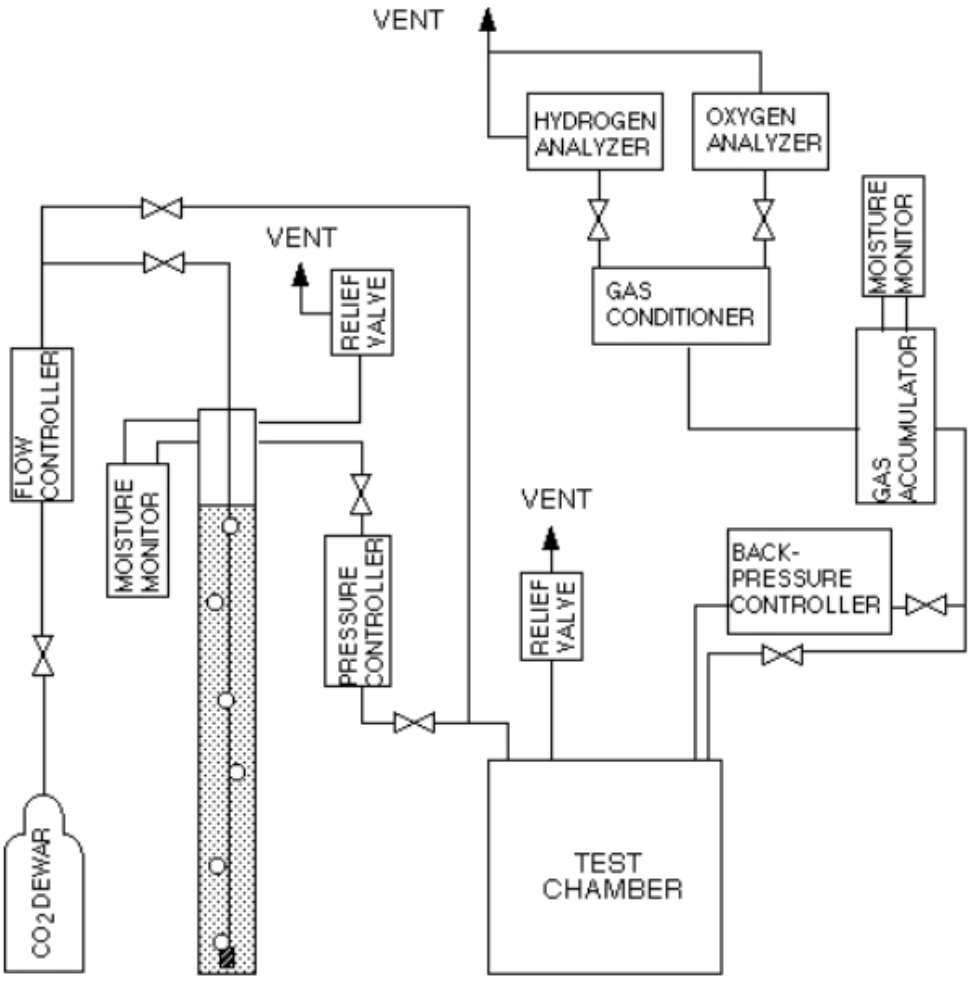

Figure 38. Schematic showing the layout of the sodium test loop [39].

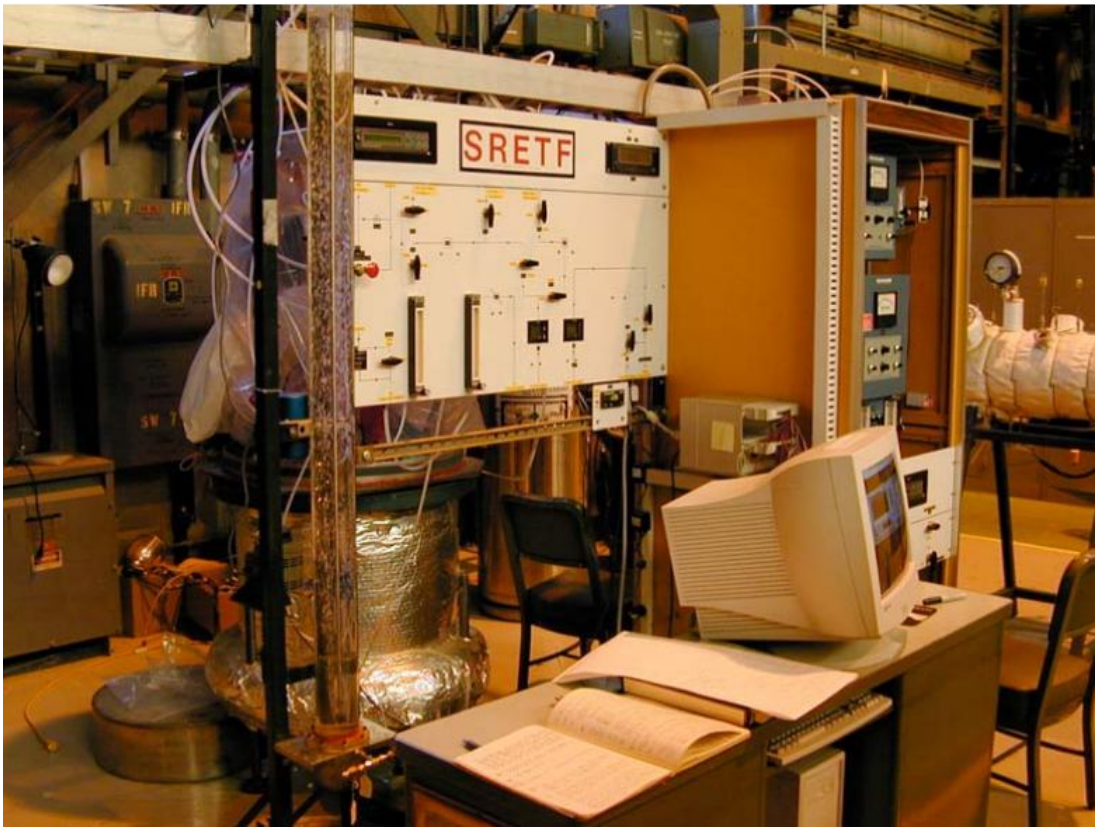

Figure 39. Physical depiction of the sodium test loop [39].

Figure 40. Clear glass graduated cylinders filled with sodium used for testing [39].

Figure 41. Slits between stainless steel plates used for sodium testing [39].

The different configurations of test samples were chosen due to the fact that during the process of draining the sodium, different points of the primary and secondary loop will have local minima that will cause the sodium to not completely drain. Having different samples allowed a broad spectrum of possibilities during carbonation to be tested.

All samples were inside the testing chamber for a period between 29 and 219 days. The samples were periodically checked and measured. The sodium would react with the water and carbon dioxide to form sodium bicarbonate or sodium carbonate. As more and more sodium would react throughout the testing process, the sodium carbonates would build up in the sample containers, and often overflow their containers. Sodium carbonates are a white powdery substance and are less dense than sodium. Due to some of the geometry of the sample containers, the sodium carbonates would build up and expand in such a way that would cause the graduated cylinders to crack during the test. This would then allow the humidified carbon dioxide to reach the center of the sodium and cause more carbonate build up. A visual of the cracked graduated cylinder and the overflowing sodium bicarbonate products can be seen in Figure 42.

Figure 42. Cracked test vessel [39].

Results of the test showed that for every centimeter of solid sodium that reacted, approximately 5 cm of reaction products would be produced. The results also showed that reacting sodium beyond a depth of 5 cm is very difficult due to limited mass transfer between the humidified carbon dioxide and the sodium as the reaction products start to build.

5.6.1.2 Secondary Sodium Loop Decommissioning

After testing was complete, the secondary loop was the first to be decommissioned. This was to prove the effectiveness of humidified carbon dioxide in a full-scale operation. The secondary loop was used as the proving ground because the primary loop once contained irradiated sodium and had a more complicated geometry. Before the loop was drained it contained around 130 m^3 of sodium. Once the loop was drained, it was approximated to have 400 L of residual sodium left in it. The loop was prepped for carbonation by dismantling unnecessary electric systems and modified to create 14 gaseous flow paths.

Vent lines, hydrogen monitors, oxygen monitors, and gas-conditioning units were all installed, and the argon cover gas that was present was purged by forcing dry carbon dioxide through the system. The system was then presented with carbon dioxide that was humidified between 65% and 75%. Different humidification levels were produced by controlling the

temperature of the carbon dioxide. The amount of residual sodium that had reacted was calculated by keeping a log of how much hydrogen was being produced.

During the first and second phase of treatment approximately 92 kg and 90 kg, respectively, of sodium was reacted leaving around 220 kg of unreacted sodium in the secondary loop. It was determined safe enough to stop, but further treatment is needed to react all of the sodium. During the second phase a blockage occurred in one of the pipe elbows. It was determined that reaction products had built up and caused the blockage. Instead of clearing the blockage, an alternate gas path was identified and the decommissioning process continued. Once the process was complete, the loose carbonate layer was left in place to act as a covering for long term storage.

After the process was over, certain parts of the secondary loop were drilled and tapped to verify the levels of residual sodium and carbonate products. It was determined that over the 84 days that it took to complete phase one and phase two of the process, only 2.5 inches of sodium had reacted. Much more time would be needed react all the residual sodium left in the secondary loop, especially in the deeper parts of the loop. The loop was then placed under a stagnant carbon dioxide cover gas with a small positive pressure [39].

5.6.1.3 Primary Sodium Loop Decommissioning

The primary sodium loop was decommissioned in a very similar manner as the secondary sodium loop. The primary sodium was kept at a steady 200°C while it was drained from the system. After all the sodium that could feasibly be removed was drained, it took several months for the sodium to cool to 50°C before carbonation could start. After the primary loop was drained, it was estimated to have 1,116 L of residual sodium left inside. This approximation was found by analyzing engineering drawings and locating hydraulic low points and their respective volumes.

The main primary tank contained the largest portion of residual sodium, which was around 473 L. The primary tank contained 58 nozzles and penetrations which were utilized for instruments and devices and as the gas outlet for the carbonation process. A gas pressure regulator was also installed to prevent atmospheric air inside the exhaust gases from going back into the system. During the carbonation process, a safety level of 0.5 % for oxygen and 4.0 % for hydrogen was

not exceeded. If these levels were breached, humified carbon dioxide was stopped and dry carbon dioxide was used to purge the system until gas concentrations returned to acceptable levels.

The argon cover gas that was used during operation of EBR-II was purged for 11 days with dry carbon dioxide. Humidified carbon dioxide was then introduced and caused to react with the sodium. The primary tank was carbonated first, with hydrogen concentrations constantly being monitored for sodium reaction rates. A hydrogen concentration of 1 vol% meant that 100% of the introduced humidity was reacting with the sodium [40].

Twenty days into the primary tank carbonation process, the carbon dioxide supplies ran out and the process had to be unexpectedly stopped. After the carbon dioxide gas tanks were refilled, the hydrogen concentration in the primary tank had a consistent reading of 1.5 vol%, which meant that either extra moisture was seeping into the system or the hydrogen detector was incorrect, with the latter being the more probable cause. Carbonation proceeded without recalibration of the detector because it would require the process to shut down completely.

Other systems in the primary loop were purged in the same way, such as the intermediate heat exchanger, over the course of several hundred days. The total amount of residual sodium that reacted in the primary loop was approximately 775 L, which was about 70% of the initial sodium content. At this point, the sodium carbonate layers were becoming too thick to effectively react any more of the sodium lying underneath, as the carbonates were rate determining in the sodium/moisture reaction. Figure 43 depicts how the buildup of the carbonate layer limited the amount of sodium that could be further reacted. The sodium layer was reacted to a depth of 2.5 cm and the sodium carbonate layer was 11.5 cm at its deepest. The primary system is kept in a static state with a cover gas of stagnant carbon dioxide [40].

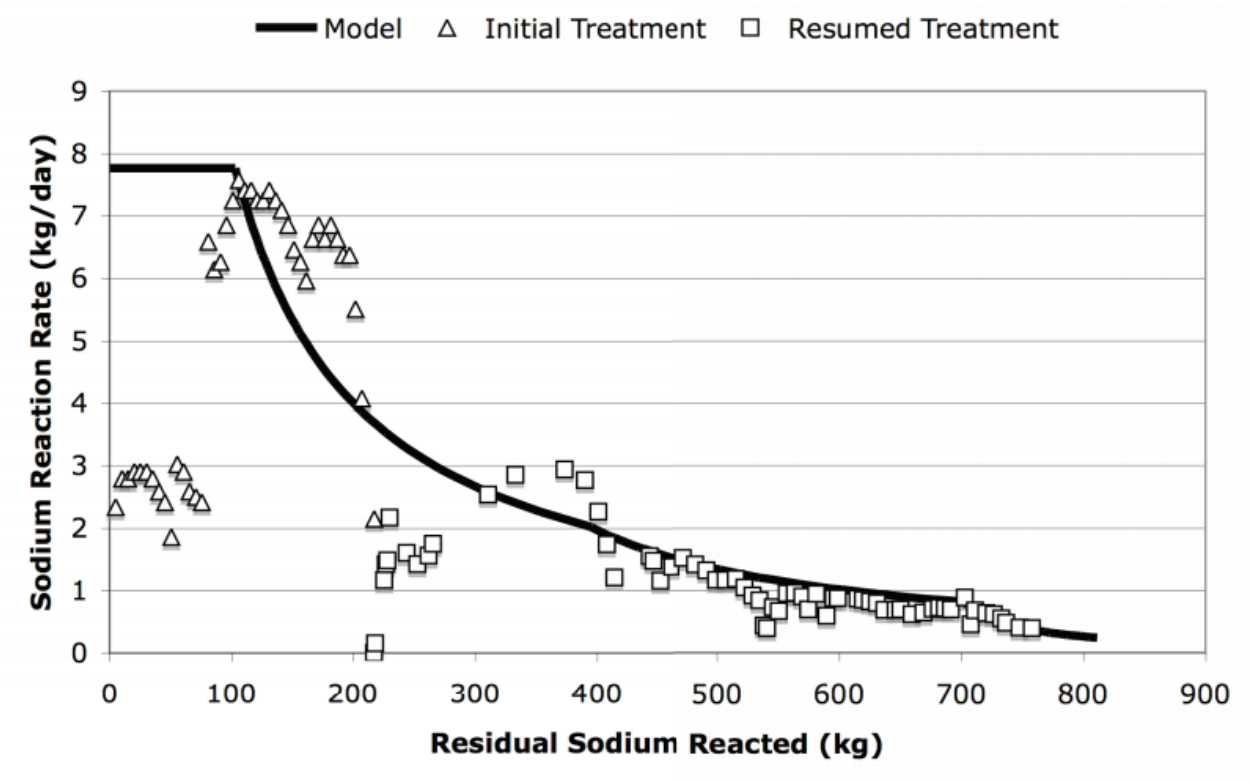

Figure 43. The build-up of reaction products negatively effects the further reaction rate of additional sodium.

6 Sodium Safety in Industry

6.1 Commissariat à l'Énergie Atomique

The French Alternative Energies and Atomic Energy Commission (CEA) is actively involved with defense and security, low carbon energies (nuclear and renewable energies), technological research for industry, and fundamental research in the physical and life sciences. CEA works at providing public authorities and the industry with the expertise and innovation needed to develop improved nuclear power generation systems. It has also been involved in renewable energies for around thirty years and is now focusing on solar energy (thermal and photovoltaic) and its integration in the home.

Figure 44. CEA scientists.

Regarding CEA contributions on sodium cooled fast reactors, they are working on the development of a new reactor core concept with optimized safety features, the elimination of sodium interaction possibilities with air or water (risk of chemical reactions) and the development of a corium core catcher. In terms of their business model, they offer partnerships to work in areas of research and they are based in 9 areas of France [41].

The objective of CEA regarding sodium training is to train operators working with Sodium Fast Reactors, to train design engineers involved in SFR projects, and to train fire brigades. CEA's approach to training regarding sodium coolant consists of lectures, discussions, and training on a

sodium loop (Figure 45). The topics addressed are the physical and chemical properties of sodium coolant, purification, corrosion, contamination, cleaning and decontamination, sodium technology, description and operation of components, instrumentation, visualization, inspection, and repair. Regarding sodium safety, the specific hazards induced by the chemical properties of sodium are described as sodium-water reaction and hydrogen risk assessment, sodium fires, safety rules, prevention, intervention, and exercise on a real sodium fire. In support of the processes used for decommissioning SFRs, lecturers present and address the following items: specific risks, dismantling techniques, sodium treatment, sodium waste storage, and decommissioning of Na-K facilities [42].

Figure 45. Sodium loop used for training.

6.2 Creative Engineers Inc.

Creative Engineers Inc. (CEI) is a company with an emphasis on working with alkali metals and have facilities located in New Freedom, PA and Greenville, SC (Figure 39). They base their products on designing, building, and operating research projects to meet customers' needs and expectations.

Figure 46. Creative Engineering Inc. facilities.

As experts on alkali metal engineering, CEI works on equipment such as electromagnetic pumps, electromagnetic flow meters, high temperature pressure transmitters, pump, and flow meter testing. Regarding services they offer, among them are clean ups, building code, fire code, and regulation consulting, as well as research and automatization.

Regarding sodium safety training, CEI provides both standard and custom training courses at its facility in New Freedom. Courses typically offer a mix of classroom and hands-on training and demonstrations. It's typical classroom work includes properties and hazards of alkali metals, fire, spill, emergency response, buildings, equipment, systems, storage, and transportation. In terms of hands-on work, it includes: demonstration of a sodium-water reaction, proper extinguishing technique, and small spill cleanup. This course is tailored for engineers, managers, safety professionals, operators, and fabricators who design or operate systems that contain or use alkali metals. No technical background is needed to attend this course (Figure 40).

The course lasts for two days. On day one students learn: properties and hazards of alkali metals, personal protection equipment (PPE) and first aid, fire, spill, and emergency response, buildings, equipment, systems, storage and transportation of alkali metals. On day two, hands-on work develops the following: demonstration of water reaction, sodium fire with proper

extinguishing technique, small spill cleanup, and cleanup of components used for alkali metals [43].

6.3 Industrial Accidents

The ALMERIA solar plant was located in the southeast part of Spain. An incident occurred in 1986 and consisted of 12 tons of sodium spilling into the central receiver system room floor over a period of 30 minutes. The sodium part of the plant was mainly housed in a steel framework building that was built on concrete with a walled basement and a roof made of corrugated sheet. The building itself had access to ventilation by several roof fans as it was designed to be a conventional industrial building with regular specifications. In terms of fire protection/prevention, the sodium building had sodium leakage collection-pans on each bottom floor, local leak detection systems in collecting pans, smoke detection systems, several mobile sodium catch pans, 470 kg of graphex powder, and several mobile fire extinguishers filled with 6 kg of graphex each.

The plant was shut down due to a small leak in a valve that occurred several days before the accident. The section of the valve was “cold” meaning that sodium was not being pumped or heated. During the first instance of repair, the valve was being ground down. During grinding, the seal weld was maintained by the auxiliary helicoflex seal until about 2/3 of the valve was ground, at which point the helicoflex seal gave away. The flange was suddenly lifted up and gas with sodium aerosols were released, followed soon after by a strong sodium jet that began a violent sodium spray fire. After two hours the fire was stopped by graphex powder. The damaged materials were as follows:

- Ferritic steel - failure of thin support structures, local ductile deformations of support structures and collecting pans.
- Austenitic steel - pipe ruptures as consequence of support failure.
- Galvanized iron - cladding of thermal insulation, gratings, stairs
- Aluminum alloy - casings of valve driving motors.
- Electrical systems and I&C [44]

The ILONA Laboratories incident consisted of the release of 4.5 tons of sodium from a filled vessel. The accident took place in 1992 in Ebensburg, Germany. The accident occurred due to a failure of a pressure relief valve [44]. ILONA was a large sodium test facility for natural convection in decay heat removal loops with down scaled components (1/3) and full-size elevation. The origin of the accident was not caused by ILONA itself, but a provisional installation in the basement of the ILONA plant. Due to a failure of the pressure regulation valves, the cover gas control became unavailable during the heating procedure. The increasing gas pressure lifted the gland in the dip pipe and released sodium. About 6 hours after the start of the heating procedure, the fire alarm from the ILONA basement was sounded through the central fire alarm system. Sodium leakage came in contact with the concrete floor and walls, which started a sodium concrete reaction.

Extensive damage was done by the fire, including the destruction of 50 m^2 of concrete wall that was destroyed by the thermal effect. The concrete of the floor was lifted through sodium reacting with bound water and the thermal expansion of reinforcement steel. As found by post-accident investigations, the sodium leakage flowed along the vessel surface downwards and dropped on the concrete floor. There was no protection through the use of steel cladding or a sodium catch pan. Consequently, the behavior was that of a pool fire coupled with a sodium-concrete reaction with the floor and wall surfaces. No propagation occurred [44].

7 Conclusion

To have a fast neutron spectrum, a reactor coolant needs to not only have excellent heat transfer properties to sufficiently cool the reactor core, but also not significantly slow neutrons down following their birth in the fission process. Sodium is an excellent choice that can fulfill these needs and many others. Sodium, however, does react when in contact with water and air. Therefore, a comprehensive understanding of sodium properties is needed by all personnel involved in the design, construction, operation, and experiment planning and execution.

8 References

[1] "Nuclear Power - Thermal Conductivity of Sodium," Nuclear Power.net, 2020. [Online]. Available: https://www.nuclear-power.net/nuclear-engineering/heat-transfer/thermal-conduction/thermal-conductivity/thermal-conductivity-of-sodium/. [Accessed 31 March 2020].

[2] S. Jojn, "Sodium Metal Market Sluggish," Communal News, 20 March 2020. [Online]. Available: https://communalnews.com/sodium-metal-market-sluggish/. [Accessed 8 July 2021].

[3] T. P. Whaley, "The Chemistry of Lithium, Sodium, Potassium,Rubidium, Cesium, And Francium," UK, Pergamon Press, 1973.

[4] DEADSEA.com, "What is the Dead Sea? Where is the Dead Sea Located?," [Online]. Available: https://www.deadsea.com/articles-tips/interesting-facts/why-is-the-dead-sea-called-the-dead-sea/. [Accessed 8 7 2021].

[5] S. Dumais, "A Chemist's Dreams and Visions," UNH Today, 16 May 2016. [Online]. Available: https://www.unh.edu/unhtoday/2016/05/chemists-dreams-and-visions. [Accessed 8 July 2021].

[6] U. D. o. t. Interior, 5 May 1999. [Online]. Available: https://www.usgs.gov/media/images/cutaway-views-showing-internal-structure-earth-left. [Accessed 22 September 2021].

[7] O. J. Foust, Sodium-NaK Engineering Handbook, New York: Science Publishers, Inc., 1973.

[8] U.S. Atomic Energy Commission, The Radiochemestry of Sodium, National Academy of Sciences-National Reseach Council.

[9] Lennitech, "Water Treatment Solutions," [Online]. Available: https://www.lenntech.com/periodic/elements/na.htm#:~:text=It's%20a%20soft%20metal

%2C%20reactive,produce%20sodium%20hydroxide%20and%20hydrogen.. [Accessed 04 June 2020].

[10] A. Y. Takashi Takata, "Numerical Thermal-Hydraulics Study on Sodium-Water Reaction," Japan Nuclear Cycle Development Institute, Japan, 2003.

[11] D. M. N. Ryan M. Young, "Dynamics of Solvated Electrons in Clusters," American Chemical Society, 2012.

[12] J. MALET, "Ignition and Combustion of Sodium-Fire Consequences-Extinguishment and Prevention," Institut de Protection et de Surete Nucleaire, 13108 St-Paul-Lez-Durance Cedex.

[13] P. Colburn, "Sodium Concrete Reactions," American Nuclear Society, Seattle, Washington, August 19-23, 1979.

[14] K. J. Schultis and R. E. Faw, Fundamentals of Nuclear Science and Engineering Third Edition, Boca Raton: Taylor & Francis Group, 2017.

[15] Brookhaven National Laboratory, "Nudat 2.8," Brookhaven National Laboratory, [Online]. Available: https://www.nndc.bnl.gov/nudat2/reCenter.jsp?z=11&n=13. [Accessed 1 july 2020].

[16] National Aeronautics and Space Administration, "Gamma Rays," NASA, 10 August 2010. [Online]. Available: https://science.nasa.gov/ems/12_gammarays. [Accessed 25 March 2020].

[17] Committee on the Atmospheric Dispersion of Hazardous Material Releases, Tracking and Predicting the Atmospheric Dispersion of Hazardous Material Releases, Washington, DC: The National Academies Press, 203.

[18] I. Wait, Director, *VE 351 - Class 34 (Atmospheric Dispersion and Gaussian Model).* [Film]. You Tube, 30 Nov 2015.

[19] S. R. Hanna, G. A. Briggs and J. R. P. Hosker, Handbook on Atmospheric Diffusion, Springfield: Tchnical Information Center, 1982.

[20] U.S. Department of Energy, "Integration of Safety into the Design Process," March 2008. [Online]. Available: https://www.standards.doe.gov/standards-documents/1100/1189-AStd-2008/@@images/file. [Accessed 17 February 2020].

[21] United States Department of Energy, "edms.energy.gov," [Online]. Available: https://edms.energy.gov/pac/TeelDocs. [Accessed 15 January 2020].

[22] Public Health and Compliance, "Protective Action Criteria Review Summary," January 2017. [Online]. Available: https://open.alberta.ca/dataset/a2902063-2264-4363-afe2-20cef61c02c4/resource/cdea6e50-b298-4c28-9914-dafce9ab1ca4/download/Protective-Action-Criteria-Review-Summary-2017.pdf. [Accessed 15 February 2020].

[23] E. M. Baum, M. C. Ernesti, H. D. Knox, T. R. Miller and A. M. Waston, Nuclides and Isotopes: Chart of the Nuclides 17th Edition, Bechtel, 2009.

[24] D. Grabaskas, A. Brunett and e. al, "Regulatory Technology Development Plan," Argonne National Laboratory, Chicago, 2015.

[25] Argonne National Laboratory, Reactor Physics Constants ANL-5800 Second Edition, Chicago: United States Atomic Energy Commission, 1963.

[26] B. Shu, "NuDat 2.8," NNDC, [Online]. Available: https://www.nndc.bnl.gov/nudat2/getdecayscheme.jsp?nucleus=24MG&dsid=24na bM decay (14.997 h)&unc=nds. [Accessed 15 April 2020].

[27] O. J. Foust, Sodium--NaK engineering handbook. Volume IV. Sodium pumps, valves, piping, and auxiliary equipment, USDOE, 1978.

[28] R. U. Acton, R. L. Weatherbee, L. A. Smith, F. L. Mastin and K. E. Nowotny, "Sandia Sodium Purification Loop (SNAPL) description and operations manual," Sandia National Laboratory, Albuquerque, 1985.

[29] R. King, "Preapplication Safety Evaluation Report for the Sodium Advanced Fast Reactor (SAFR) Liquid-Metal Reactor," U.S. Nuclear Regulatory Commission, 1991.

[30] R. T. Lancet, R. T. Johnson, E. Matlin, D. E. Fields, E. Gluekler, J. D. McCormack, C. W. Miller and D. R. Pedersen, "United States Position Paper on Sodium Fires Design Basis and testing," 1989.

[31] Project Managment Corporation, "Clinch River Breeder Reactor Project," NRC.

[32] C. J. M. a. S. R. Doctor, "An Evaluation of Liquid Metal Leak Detection Methods for the Clinch River Breeder Reactor Plant," U.S. Nuclear Regulatory, December 1977.

[33] Emoscopes, "File:LMFBR schematics.png," Wikipedia , 6 Feb 2006. [Online]. Available: https://en.wikipedia.org/wiki/File:LMFBR_schematics.png. [Accessed 11 November 2020].

[34] D. Dr. Terry Lash, "Fast Flux Test Facility (FFTF)," U.S. Department of Energy, Hanford Site, December 1997.

[35] Argonne National Laboratory, "EBR-II Sixteen Years of Operation," Idaho Falls, Argonne National Laboratory, 1980, pp. 15 - 101.

[36] C F Braun & Co, "A Study of Heating and Insulation Methods for LMFBR Sodium Piping," US Atomic Energy Commission, Alhambra, California, 1969.

[37] Atomics International, "100-MW Nuclear Power Plant Utilizing a Sodium Cooled, Graphite Moderated Reactor," 1958.

[38] NRC, "Clinch River Breeder Reactor Tutorial," NRC, 1982.

[39] S. R. Sherman, "Summary Report Part 1: Laboratory Experiments and Application to EBR-II," INL, 2005.

[40] Steven R. Sherman, "Summary Report Part 2: Application to EBR-II Primary Sodium System and," Idaho National Laboratory, Idaho Falls, 2006.

[41] CEA, "De la recherche à l'industrie," [Online]. Available: http://www.cea.fr/.

[42] F. C. Latgé, "TeachingSodiumFastReactorsinCEA," HAL Id:cea-02328976, Paris,France., 2018.

[43] Creative Engineers, "Creative Engineers," 1 April 2020. [Online]. Available: https://creativeengineers.com/.

[44] K. Luster, "Feedback from Practical Experience with Large sodium Fire Accidents," (Siemens AG KWU), 1996.

[45] Office of Nuclear Reactor Regulation, "Preapplication Safety Evaluation Report for the Power Reactor Innovative Small Module (PRISM)," in *NUREG-1368*, Washington,, 1994.

[46] R. T. Lancet and J. F. Marchaterre, "Proceedings of the international Topical Meeting on Fast Reactor Safety Vol. I," ANS/Nuclear Reactor Safety Division Atomic Energy of Japan, Knoxville, 1985.

[47] N. E. Division, "Advanced Burner Reactor 1000MWth Reference Concept," Argonne National Laboratory, 2007.

[48] Breeder Reactor Corporation, Oak Ridge, TN (United States), "Breeder Basics," OSTI, Oak Ridge, 1980-09-01.

[49] W. Davis, "ANSNUCLREARCAFE," 29 November 2012 . [Online]. Available: http://ansnuclearcafe.org/2012/11/29/clinch-river-site-will-once-again-lead-nuclear-development/#sthash.Gg3q58nY.dpbs. [Accessed August 2020].

[50] U.S. DEPARTMENT QF ENERGY, "Report to the Congress on Alternative Financing of the Clinch River Breeder Reactor Plant Project," Assitant Secretary for Nuclear Energy, Washington, D.C. 20545, MARCH 1983.

[51] Argonne National Laboratory, "Fast Reactor Technology," *Nuclear Engineering Division.*

[52] W. E. Unbehum, "AECD-3712," in *History and Status Of EBR*, Lemont, illinois, April 15, 1953.

[53] S. LASKOW. [Online]. Available: https://www.atlasobscura.com/articles/ebri-reactor-meltdown-1955-nuclear-power .

[54] J. I. Sackett, "EBR-II Test and Operating Experience," US Nuclear Regulatory Commission, 2008.

[55] D. Turk, "Advanced Non-Light-Water Reactors Materials and Operational Experience," U.S. Nuclear Regulatory Commission, NRC-HQ-60-17-T-0002, 2019.

[56] R. C. Gerber, "Safety Evaluation of Sodium Graphite Reactors," Atomics International, 1956.

[57] Wikipedia, "Sodium Reactor Experiment," [Online]. Available: https://en.wikipedia.org/wiki/Sodium_Reactor_Experiment. [Accessed 27 November 2020].

[58] R. L. Ashley, R. J. Beeley, F. L. Fillmore, W. J. Hallett and A. A. Jarrett, "SRE Fuel Element Damage Final Report," Atomics International, 1961.

[59] United States Nuclear Regulatory Commission, "Fermi -- Unit 1," 19 November 2019. [Online]. Available: https://www.nrc.gov/info-finder/decommissioning/power-reactor/enrico-fermi-atomic-power-plant-unit-1.html. [Accessed 20 May 2020].

[60] International Atomic Energy Agency, "IAEA Power Reactor Information System," International Atomic Energy Agency, 21 May 2020. [Online]. Available: https://pris.iaea.org/pris/CountryStatistics/ReactorDetails.aspx?current=602. [Accessed 20 May 2020].

[61] R. E. Mueller, C. E. Branyan and J. B. Nims, "Initial Loading to Criticlaity of the Enrico Fermi Reactor," Atomic Power Development Associates, Inc., Detroit, Detroit, 1964.

[62] H. O. Monson, F. A. Smith, W. J. Hallett and J. J. Morabito, "Components of Sodium Reactors," 31 October 1964. [Online]. Available: https://www.osti.gov/biblio/4035980. [Accessed 20 May 2020].

[63] R. E. Mueller and H. A. Wilbur, "Determination of Control Rod Float in the Enrico Fermi Reactor," Atomic Power Development Associates, Inc., Detroit, Mich., Detroit, 1964.

[64] M. Ragheb, "Fermi-I Fuel Meltdown Incident," 2014.

[65] H. W. Bertini, "Descriptions of Selected Accidents that Have Occurred at Nuclear Reactor Facilities," Oak Ridge Natoinal Laboratory, Oak Ridge, 1980.

[66] N. Tsoulfanidis, The Nuclear Fuel Cycle, La Grange Park: American Nuclear Society, 2012.

[67] International Atomic Energy Agency, "Decommissioning of Fast Reactors after Sodium Draining," International Atomic Energy Agency, Vienna, 2009.

[68] Department of Energy Hanford Site, 2013. [Online]. Available: https://pdw.hanford.gov/document/D197320118.

[69] P. L. O. S. E. Jensen, "Description of the Prototype Fast Reactor at Dounreay," Riso National Laboratory , Roskilde, Denmark, 1995.

[70] S. McKenzie, "Fire at Dounreay led to release of radioactivity," BBC, 21 November 2014. [Online]. Available: https://www.bbc.com/news/uk-scotland-highlands-islands-30143655. [Accessed 8 January 2021].

[71] "https://en.wikipedia.org," Wikipedia, 9 June 2009. [Online]. Available: https://en.wikipedia.org/wiki/File:CEA_Marcoule_Site.jpg. [Accessed 25 May 2020].

[72] R. Carle, "The Phenix Reactor, France," Commissariat a I'energie atomique.

[73] J. Guidez, "Gen IV International Forum," 12 2017. [Online]. Available: https://www.gen-4.org/gif/upload/docs/application/pdf/2017-12/gifiv_webinar_Phénix_superPhénix_final_guidez. [Accessed 25 May 2020].

[74] J. M. Chaumont, D. Goux and L. Martin, "Some Safety Related Characteristics of Phenix, a 250 MVVe Fast Reactor," Centrale Phénix, BAGNOLS SUR CEZE, 1990.

[75] J. Bouchard, "Phénix 30 years of history: the heart of a reactor," French Atomic Energy Commission, 1973.

[76] M. Schneider, "Fast Breeder Reactors in France," Taylor & Francis Group, LLC, 2009.

[77] International Atomic Energy Agency, "Operational and decommissioning experience with fast reactors," International Atomic Energy Agency, Cadarache, 2002.

[78] G. A. Vendryes, "Superphenix A Full-Scale Breeder reactor," Scientific American, 1977.

[79] "https://fr.wikipedia.org," Wikipedia, 31 July 2007. [Online]. Available: https://fr.wikipedia.org/wiki/Fichier:Superphénix_4.jpg. [Accessed 25 May 2020].

[80] C. Le Renard, "The Superphénix fast breeder nuclear reactor Cross-border cooperation and controversies," Journal for the History of Environment and Society, 2018.

[81] Jaoan Atomic Energy Agency , "Basic Specifications -Monju Plant -," [Online]. Available:

https://web.archive.org/web/20130123183123/http://www.jaea.go.jp/04/monju/EnglishSite/contents02-1.html.

[82] A. Mikami, "Sodium Leak at Monju (I)," Reactor and System Engineering Section,, Shiraki, Tsuruga-shi, Fukui-ken,, 1995.

[83] Nuclear Engineering International, " Global Trade Media," 2013. [Online]. Available: https://archive.vn/20130130012503/http://www.neimagazine.com/story.asp?storyCode=2059044.

[84] H. Tabuchi, "New York Times," 2011. [Online]. Available: https://www.nytimes.com/2011/06/18/world/asia/18japan.html?_r=1&pagewanted=all.

[85] Japan Atomic Energy Agency, "JOYO User Guide," [Online]. Available: https://www.jaea.go.jp/04/o-arai/joyo_users_guide/joyo/index.html.

[86] International atomic energy agency, "in-pile testing and instrumentation," IAEA-tecdoc-CD-1726, Halden, Norway, 21–24 August 2012.

[87] S. A. Rogozhkin, S. L. Osipov, S. F. Shepelev, A. A. Aksenov, M. L. Sazonova and V. V. Shmelev, "Verification calculations as per CFD FLOWVISION code for sodium cooled reactor plants".

[88] E. Mearns, "The BN-800 Fast Reactor – a Milestone on a Long Road," http://euanmearns.com, 4 November 2016. [Online]. Available: http://euanmearns.com/the-bn-800-fast-reactor-a-milestone-on-a-long-road/. [Accessed 28 May 2020].

[89] R. W. Schaefer, R. T. Klann, S. M. Koltyshev and S. Krechetov, "Criticality Safety Issues in the Disposition of BN-3S0 Spent Fuel," Argonne National Laboratory-West, San Diego, 2000.

[90] Nuclear Threat Initiative, "Kazakhstan," Nuclear Threat Initiative, April 2018. [Online]. Available: https://www.nti.org/learn/countries/kazakhstan/. [Accessed 28 May 2020].

[91] O. G. Romanenko, K. J. Allen, H. P. Planchon, P. B. Wells, J. A. Michelbacher, P. Nazarenko, I. Dumchev, V. Maev, B. Zemtzev, L. Tikhomirov, V. Yakovlev and A.

Synkov, "Cleaning Cesium Radionuclides from BN-350 Primary Sodium," Taylor & Francis Online, 2017.

[92] T. B. Cochran, H. A. Feiveson, W. Patterson, G. Pshakin, M. V. Ramana, M. Schneider, T. Suzuki and F. V. Hippel, "Fast Breeder Reactor Programs: History and Status," Creative Commons, 2010.

[93] O. M. Saraev, "Operating Experience with Beloyarsk Fast Reactor BN600 NPP," Beloyarsk Nuclear Power Plant, Sverdlovsk Region.

[94] POWER, "Russian Fast Reactor Connected to the Grid," POWER, 31 January 2016. [Online]. Available: https://www.powermag.com/russian-fast-reactor-connected-grid/. [Accessed 29 May 2020].

[95] Y. I. Kim, A. Stanculescu, P. Finck, R. N. Hill, K. N. Grimm, G. Rimpault, T. Newton, Z. H. Li, P. Mohanakrishnan, M. Ishikawa, H. Song, M. Farakshin and V. Stogov, "BN-600 Hybrid Core Benchmark Analyses," PHYSOR, Seoul, 2002.

[96] B. A. Vasiljev, A. I. Zinovjev, A. I. Staroverov, V. V. Maltsev and A. N. Ogorodov, "Status and Possibility of Fuel and Structrual Materials Experimental Irradiation in BN-600 Reactor. Stages of BN-600 Reactor Core Development," Experimental Machine Building Bureau, Nizhny Novgorod.

[97] Nuclear Enginering International, "Fast reactor progress at Beloyarsk," Nuclear Enginering International, 14 January 2016. [Online]. Available: https://www.neimagazine.com/features/featurefast-reactor-progress-at-beloyarsk-4784803/. [Accessed 28 May 2020].

[98] M. Kutt, F. Frieß and M. Englert, "Plutonium Disposition in the BN-800 Fast Reactor: An Assessment of Plutonium Isotopics and Breeding," Taylor & Francis, Darmstadt, 2014.

[99] I. Pakhomove, "BN-600 and BN-800 Operationg Experience," Gen IV International Forum, 2018.

[100] World Nuclear News, "Russia to build 11 new nuclear reactors by 2030," World Nuclear News, 10 August 2016. [Online]. Available: https://www.world-nuclear-news.org/NP-

Russia-to-build-11-new-nuclear-reactors-by-2030-10081602.html. [Accessed 28 May 2020].

[101] World Nuclear News, "Russia targets 2030 for BN-1200," World Nuclear News, 22 July 2014. [Online]. Available: https://www.world-nuclear-news.org/NP-Russia-targets-2030-for-BN-1200-22071401.html. [Accessed 28 May 2020].

[102] The Hindu, "FBTR Completes 20 Years," The Hindu, 5 10 2009. [Online]. Available: http://www.igcar.ernet.in/press_releases/press15.htm. [Accessed 5 June 2020].

[103] P. Pavlicek, Artist, *A Fast-Breeder Test Reactor at the Kalpakkam Nuclear Complex, India.*. [Art]. International Atomic Energy Agency, 2013.

[104] P. Chellapandi, "Overview of SFR Safety in India," Idira Gandhi Centre for Atomic Research, Kalpakkam, 2011.

[105] T. Camacho-Lopez, "Molten Salt Test Loop Commissioning," Sandia National Laboratory, 10th October 2012. [Online]. Available: https://energy.sandia.gov/molten-salt-test-loop-commissioning/. [Accessed 11 June 2020].

[106] D. Gill, W. Kolb and R. Briggs, "An Evaluation of Pressure Measurement Technology and Operating Performance Using Sandia's Molten Salt Test Loop," Sandia National Laboratories, Albuquerque, 2013.

[107] S. Kales, "Injuries Caused by Hazardous Materials Accidents," *Annals of Emergency Medicine,* vol. 30, no. 5, pp. 598-603, 1997.

[108] K. Andrews, "The treatment of alkaline burns of the skin by neutralization," PubMed, 2003.

[109] M. L. Siri Shastry, "Electronic Vapor Cigarette Battery Explosion Causing Shotgun-like Superficial Wounds and Contusion," The Western Journal of Emergency medicine, 2016.

[110] J. Domenic B. Sanginiti, "E-Cigarette Explosions Cause Devastating Injuries: Torn Flesh, Caustic Burns and Heat Burns," Stark & Stark Attorneys At Law, 2016.

[111] C. Kunz, May 13, 2021.

[112] E. Uva, "Why Scary Lab Accidents Happen," UVA, 2012.

[113] J. Reindl, "Did we really 'almost lose Detroit' in Fermi 1 mishap 50 years ago?," Detroit Free Press, Detroit, 2016.

[114] P. Radford, Interviewee, [Interview]. December 2020.

[115] *LIVE UPDATE: Industrial fire forces evacuations in Morris, Illinois.* [Film]. Chicago: FOX 32 Chicago, June 29, 2021.

[116] J. Garcia, "Morris battery fire: Evacuation order lifted; drone footage of blaze released," ABC 7 Chicago, 2021.

[117] nuclear-power.net, "Transport Mean Free Path," nuclear-power.net, . [Online]. Available: https://www.nuclear-power.net/nuclear-power/reactor-physics/nuclear-engineering-fundamentals/neutron-nuclear-reactions/mean-free-path/transport-mean-free-path/. [Accessed 16 June 2020].

[118] R. Adams, "Atomic Insights," 24 August 2015. [Online]. Available: https://atomicinsights.com/sad-ending-story-of-ebr-ii-told-by-three-of-its-pioneers/.

[119] LLC(TP), "TerraPower," 2020. [Online]. Available: https://www.terrapower.com/about/.

[120] Google images , [Online]. Available: https://www.google.com/search?q=dead+sea&tbm=isch&ved=2ahUKEwjKiqbTyO7pAhUOmJ4KHYUmA4cQ2-cCegQIABAA&oq=dead+sea&gs_lcp=CgNpbWcQAzIFCAAQsQMyBQgAELEDMgIIADICCAAyAggAMgIIADICCAAyAggAMgIIADICCAA6BAgjECc6BAgAEEM6BQgAEIMBUNmeFljNqhZgmK0WaABwAHgAgAFZiAHPBJIBATiY.

[121] Asit Roy, "KPL International," 18 July 2014. [Online]. Available: http://www.kplintl.com/blog/sodium-metal-facts-dangers-and-safety-precautions/#:~:text=So%20it%20is%20a%20combustible,corrosive%20and%20highly%20water%2Dreactive.. [Accessed 06 June 2020].

[122] D.Gerstner, "ANS Summary of Safety Design Strategy for the Versatile Test Reactor," Idaho National Laboratory , 2019.

9 Appendix A: Chemical and Physical Properties of Sodium

Table 11. Chemical Properties of Sodium [9]

Chemical Properties of Sodium	
Atomic number	11
Atomic mass	22.98977 $g.mol^{-1}$
Electronegativity according to Pauling	0.9
Density	0.97 g.cm -3 at 20 °C
Melting point	97.5 °C
Boiling point	883 °C
Vander Waals radius	0.196 nm
Ionic radius	0.095 (+1) nm
Isotopes	21
Electronic shell	[Ne] 3s1
Energy of first ionization	495.7 $kJ.mol^{-1}$
Standard potential	- 2.71 V

Table 12. Physical Properties of Sodium

Physical Properties of Sodium	
Atomic weight	22.9898 g/mol
Crystal form	BCC
Atomic radius	1.896 Å
Ionic radius	0.95 Å
Atomic volume	23.7 c.c./g-atom
Lattice constant	4.24 A-173°C
Ionization potential	5.12 V
Electron work function	2.28 eV
Electrode potential	2.714 V
Electron emission wavelength	0.6 m
Thermal conductivity (cal/sec °C cm.), m.p.	
200°C	0.193
400°C	0.17
Specific heat (cal/°C g), 0°C	
20-25°C	0.092
50~100°C	0.33

10 Appendix B: History of Different SFRs

10.1 US Sodium Cooled Reactors

10.1.1.1 *PRISM*

PRISM, Power Reactor Innovative Small Module, is a type of fast neutron reactor designed by General Electric and Hitachi. PRISM had its initial concept and design plans started in the early 1980s and has been an ongoing project. PRISM reactors are pool type, metal fueled, SFRs. It has a rated thermal power of 840 MW, with an electrical output of 311 MW. The unique features of PRISM are the metallic fuel that it uses and its liquid metal coolant. There is no set location for the PRISM reactor yet due to certain characteristics for its placement that were considered. For example, site boundaries of 0.8 km and 3.22 km are needed, as well as a low population zone. Dose calculations at these distances, performed by General Electric (GE), had a basis from source terms determined from their studies.

Figure 47 depicts the typical layout of what the PRISM reactor facility would look like.

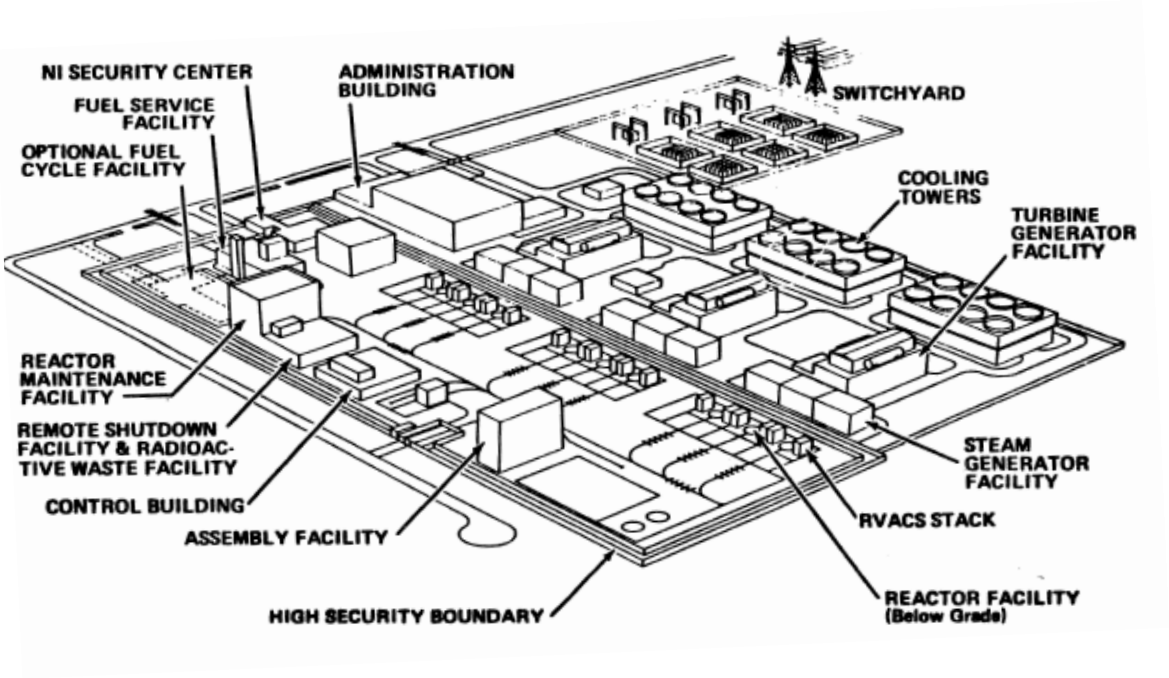

Figure 47. PRISM reactor facility overview

Table 13 highlights plant characteristics and design data for PRISM reactors. There are three categories pertaining to the plant characteristics mentioned: overall plant, reactor modules, and the reactor core. The PRISM reactor design proposed by GE is for a small, modular, pool-type,

liquid metal sodium cooled reactor producing 471 MWt power. Figure 48 is a cut-away view of the reactor module. The standard plant produces 465 MWe per block, for a total electrical rating of 1395 MWe.

Each power block depicted in Figure 49 comprises three reactor modules, each with an individual thermal rating of 471 MWt. Each module is in its own below-grade silo and is connected to its own intermediate heat transport system (IHTS) and steam generator system. The steam generator and secondary system hardware are located in separate buildings and are connected by a below-grade pipe way. All reactors on site share a common control center, reactor maintenance facility, remote shutdown, radwaste facility, and assembly facility. Each power block shares a sodium service vault containing sodium purification equipment.

Table 13. PRISM Plant Characteristics and Design Data

Overall Plant	
Number of reactors per power block	3
Number of power blocks	1/2 or 3
Net electrical output	465/930 or 1395 MWe
Net station efficiency	32.90%
Turbine throttle conditions	6653 kPa/555 K (965 psia/540 F)
Reactor Modules	
Thermal power	471 MWt
Primary sodium inlet/outlet temp	611 K/758 K (640 °F/905 °F)
Primary sodium flow rate	174,128 L/min (46,000 gpm)
Intermediate sodium inlet/outlet temperature	555 K/716 K (540 °F/830 °F)
Intermediate sodium flow rate	156,148 L/min, (41,250 gpm)
Reactor Core	
Fuel	Metallic
Refueling interval	18 months
Breeding ratio	1.05

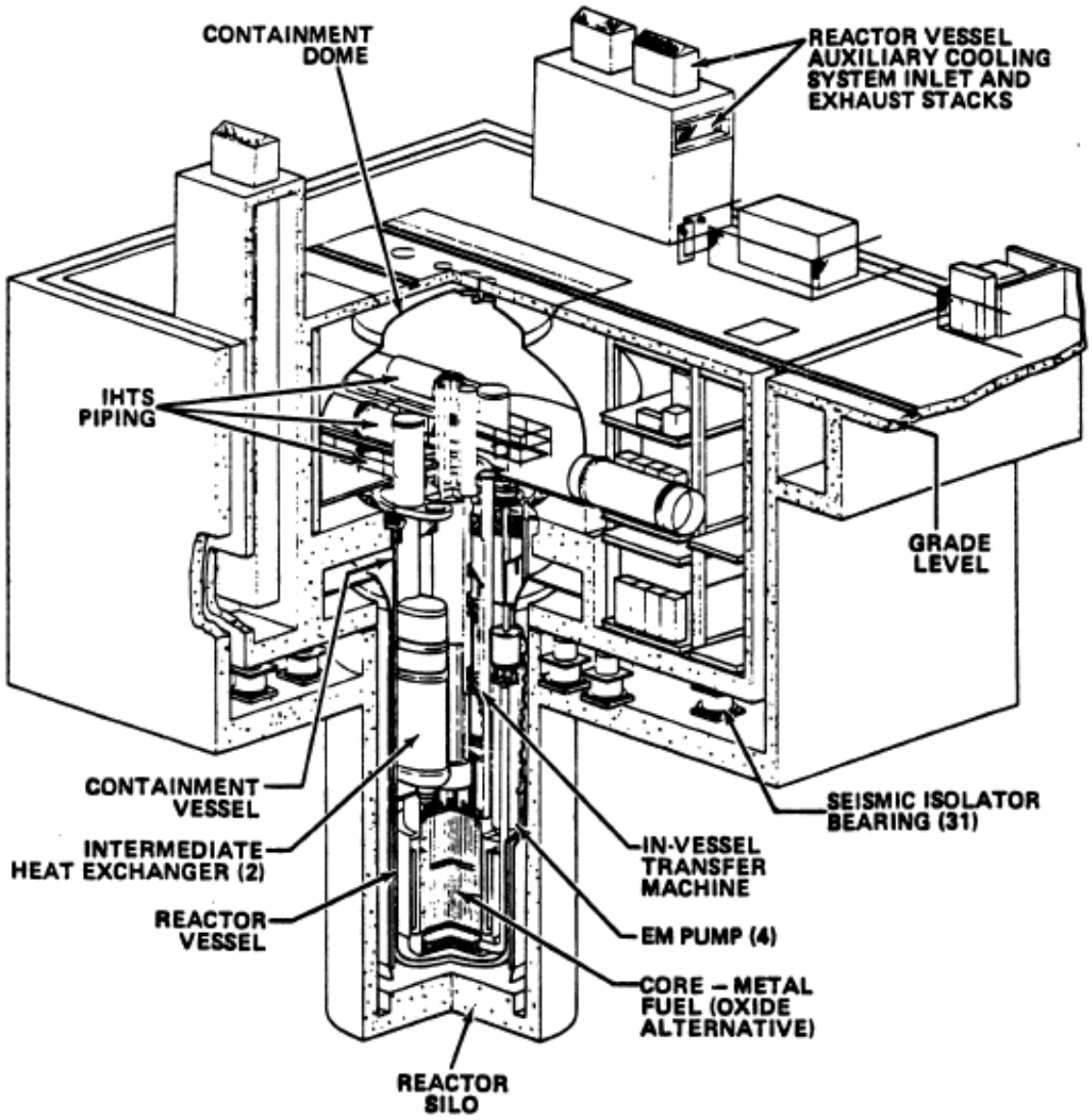

Figure 48. Isometric view of PRISM reactor.

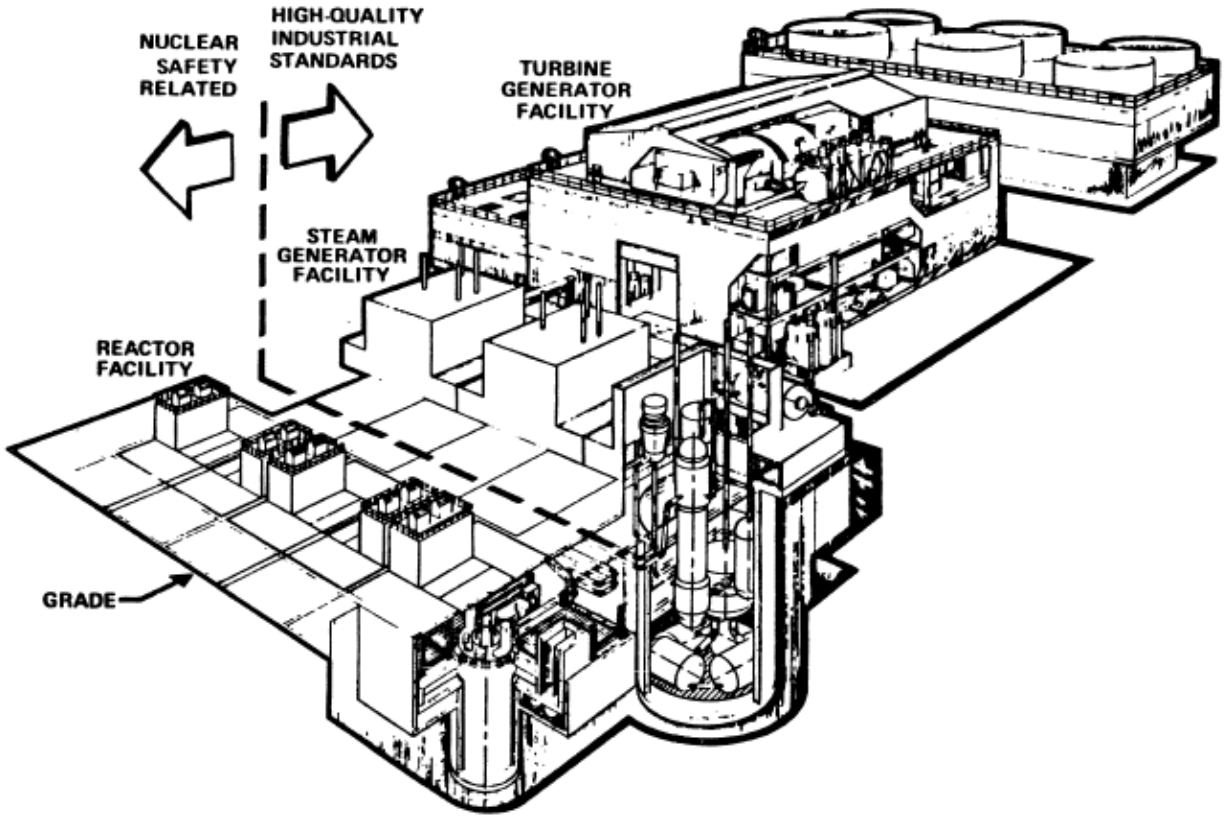

Figure 49. PRISM reactor power block.

The facility is designed to permit operation at 90 percent of existing continental United States sites. The designer has proposed a 60-year design life for the facility. Each power block contains a single turbine generator which is fed by three steam generators: one steam generator for each reactor module. The reactor module is 19 m (62 ft) high and about 6 m (20 ft) in diameter and is positioned in a silo below grade level. The reactor module and its associated components are seismically isolated to reduce horizontal oscillations.

The reactor module enclosure consists of the reactor vessel, the containment vessel, and the reactor closure head. The reactor vessel is a 5.08 cm (2 in.) thick stainless-steel vessel, 5.74 m (18.83 ft) in diameter and 16.9 m (55 ft 7 in.) high. The reactor containment vessel is a 2.5 cm (l in.) thick stainless-steel vessel and approximately 6.04 m (19.83 ft) in diameter as shown in Figure 51. The reactor closure head is common to both vessels. A 15.2 cm (6 in.) diametral gap filled with argon gas exists between the reactor vessel and the containment vessel. The vessels are

designed to allow in service visual inspection of the two vessels. The gap between the two vessels is also intended to contain a primary coolant leak without resulting in core uncover.

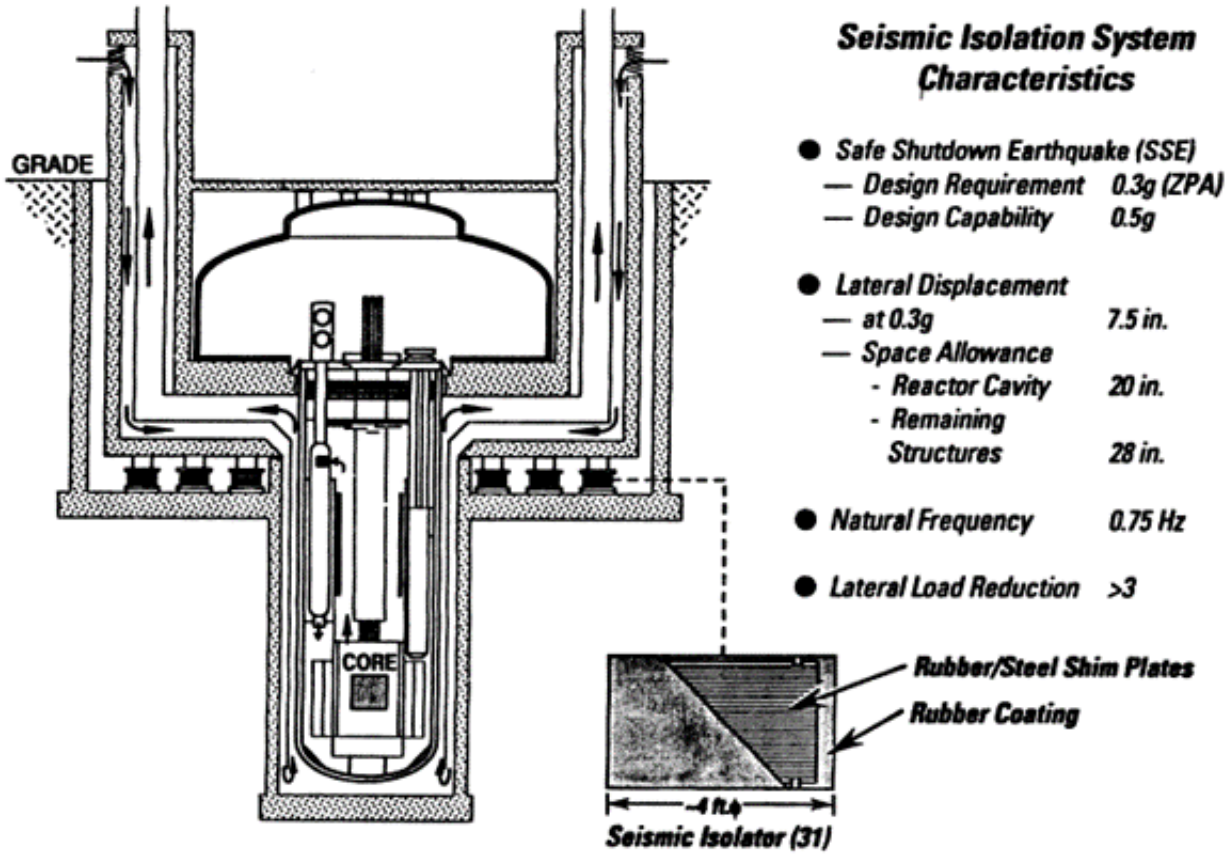

Figure 50. PRISM reactor seismic isolation system characteristics.

The closure head is a 0.3-m (1 ft) thick steel plate with a rotatable plug (Figure 52) for refueling, and contains penetrations for the primary coolant pumps, the intermediate heat exchanger system, and instrumentation and hardware. The system is designed so that all the reactor containment penetrations only penetrate through the closure head.

The PRISM core, shown in Figure 53, is designed to use metallic fuel rather than oxide fuel. The core is designed to have a 21¢ reactivity swing during the fuel cycle. Reactivity and power are controlled by six independently regulated absorber assemblies (control rods). Any one of the six absorber assemblies is capable of shutting down the reactor and maintaining the core in a hot-shutdown condition. In addition, the reactor core is designed to utilize passive reactivity

feedback mechanisms to give a negative reactivity coefficient for all design-basis transients. Three GEMs, on the core periphery, insert negative reactivity (approximately -69¢) following a loss-of-flow event [45].

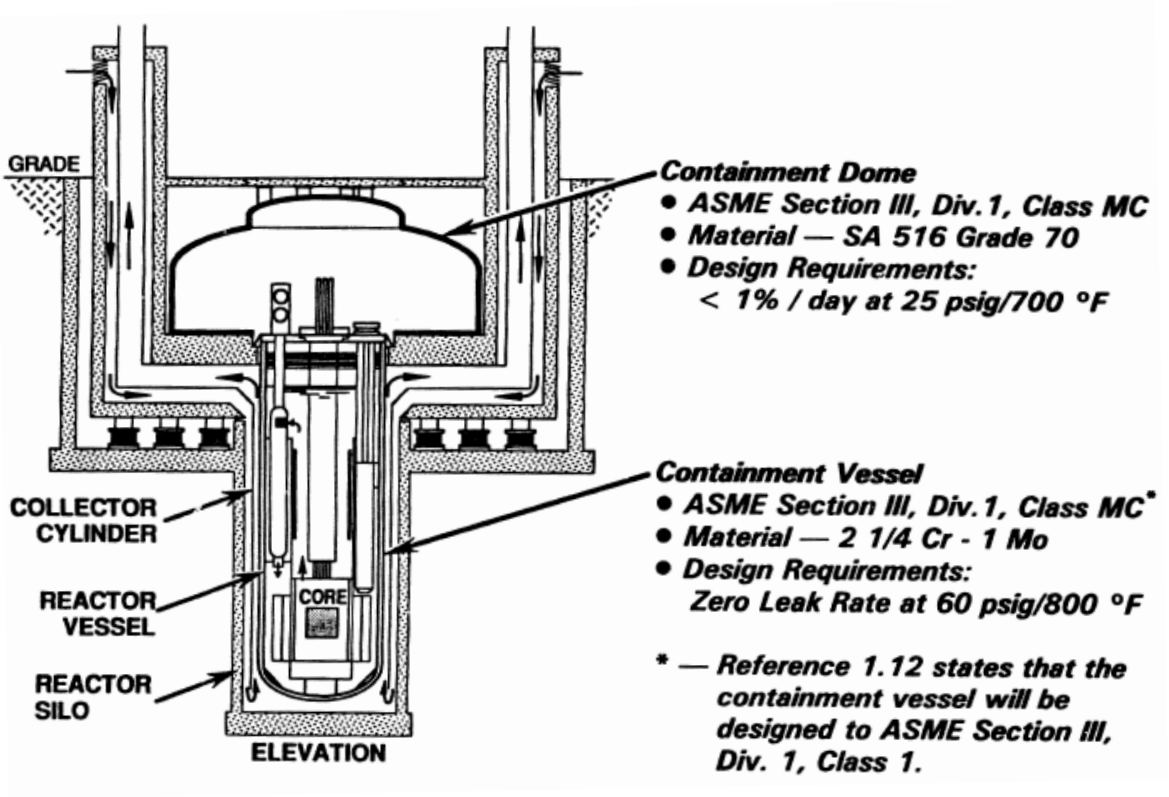

Figure 51. PRISM reactor containment dome and vessel information.

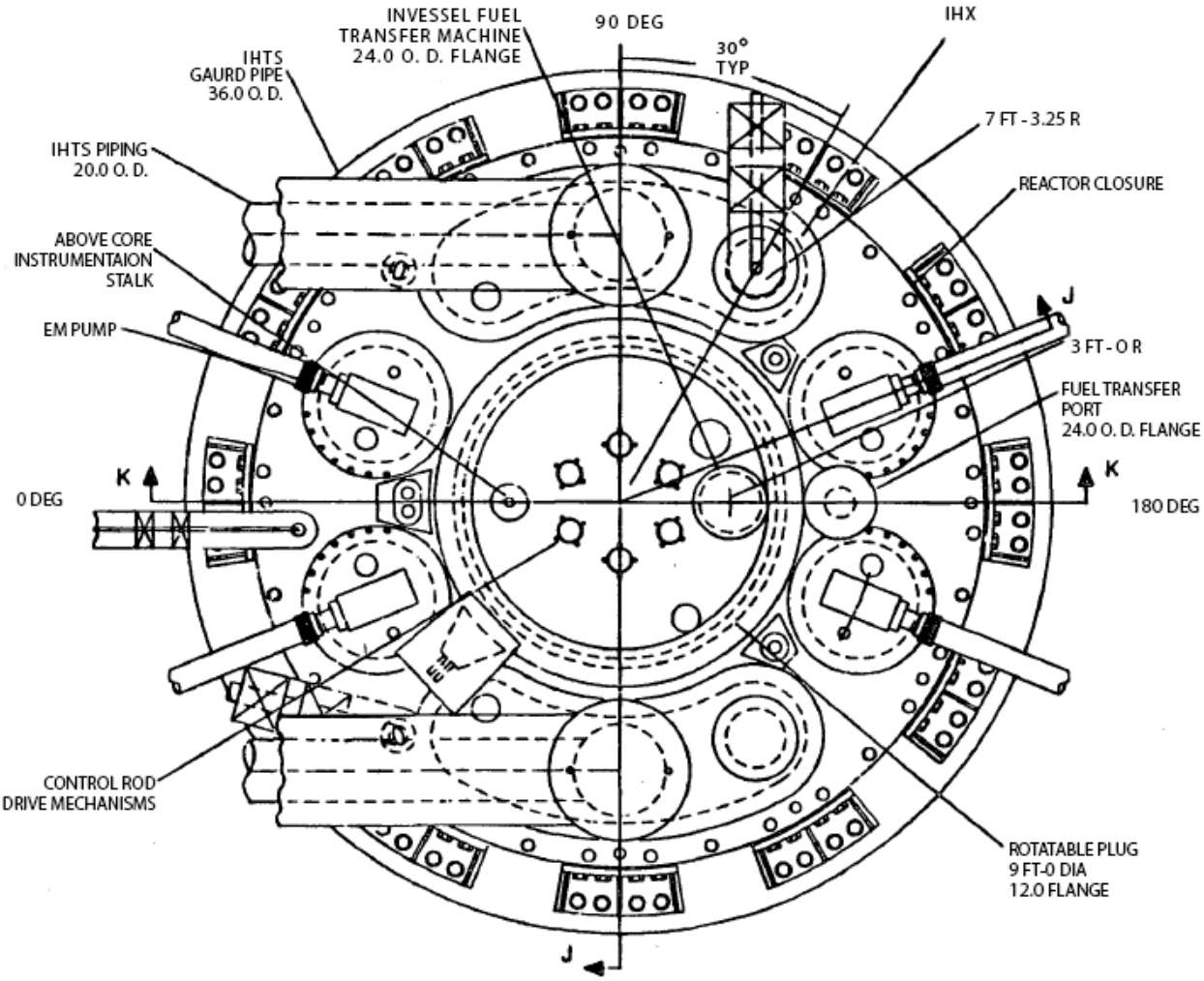

Figure 52. PRISM reactor closure head.

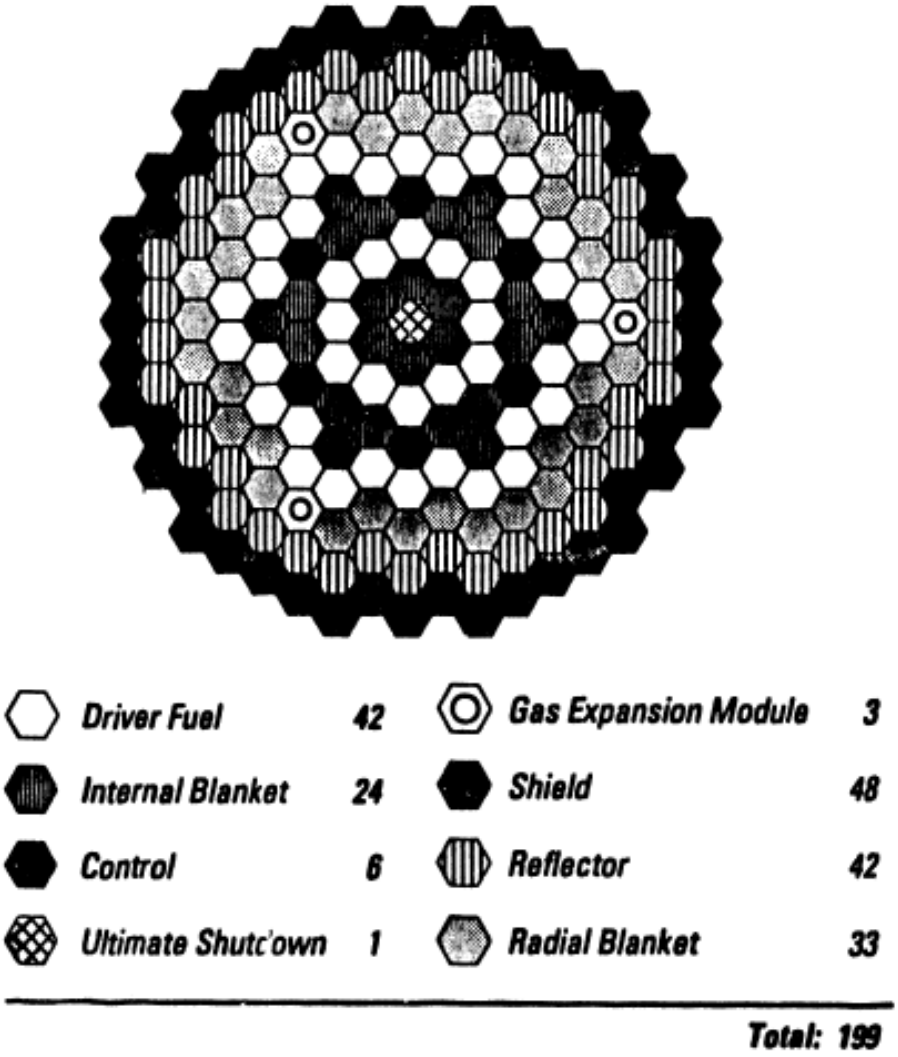

Figure 53. PRISM reactor fuel configuration.

10.1.2 Sodium Advanced Fast Reactor

The SAFR is an alternative design to the PRISM trying to meet similar needs. The SAFR plant aims to employ “multiple 330MWe, shop---fabricated, barge shippable power paks” [46]. The four goals of the SAFR design was to:

1. maximize the inherent safety characteristics
2. be scalable to the local economics

3. reduce investment risks
4. match the electrical capacity to the demand

An artist rendition of the SAFR plant is shown in Figure 54, and it highlights the four power paks the facility would contain.

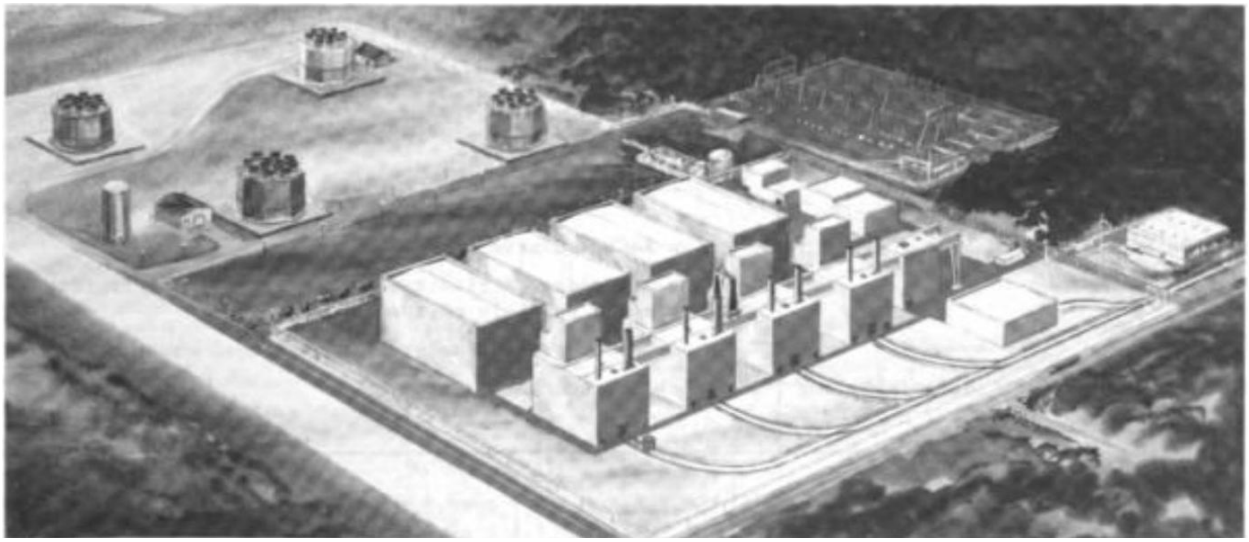

Figure 54. Artist rendition of the SAFR plant [46].

With the main goal being inherent safety designs, the SAFR design team created a list of goals for the plant shown in Table 14. The inherent safety features use a "self-actuated shutdown system (SASS)" where the poison control rods are held out of the core by an electromagnet; following an inadvertent SCRAM or the sodium temperature exceeds normal operating temperature, a curie point material is heated and "loses its magnetic flux permeability." The control rod then falls into the core through gravity and shuts down the reactor.

Designed as a collaboration of Rockwell International Corporation and Argonne National Laboratory, SAFR varied in design from most sodium cooled pool type reactors due to Rockwell's involvement. Although never built, the SAFR had an expected plant design lifetime of 60 years. Each of the power paks was predicted to produce 330 MWe and have a sodium exit temperature of 950 ˚F. Each power pak was planned to contain two pumps that could passively remove heat following a reactor shutdown. Inherent decay heat removal occurs through two natural circulation

systems known as the Direct Reactor Auxiliary Cooling System (DRACS) and the Reactor Air Cooling System (RACS).

Table 14. SAFR Top -Level Safety Goals [46]

Top Level Safety goals
Inherent safety responses to all credible events
Inherent reactor shutdown
Inherent decay heat removal
Inherent guillotine pipe protection
Inherent Vessel leak protection
Inherent spent fuel cooling
Passive sodium fire mitigation
Reactor deck and cavity natural circulation cooling
Minimize potential for sever accidents
Accommodate ATWS events (LOFTWS, TOPWS, and LOHSWS)
Long grace period for corrective action
Diversity in major safety functions:
Reactor shutdown
Decay heat removal
Minimize dependency on supporting safety equipment

The DRACS releases helium into the vessel heat exchanger to cool down the reactor. The RACS allows for air to travel through the vessel under natural circulation to remove around 1.5 MWt during a power operation and 5 MWt during the maximum decay heat removal load. As seen in Figure 55, the circulating air in the RACS is protected from the sodium by insulation, a finned shell, and a nitrogen layer. Table 15 shows a summary of the SAFR safety mechanisms.

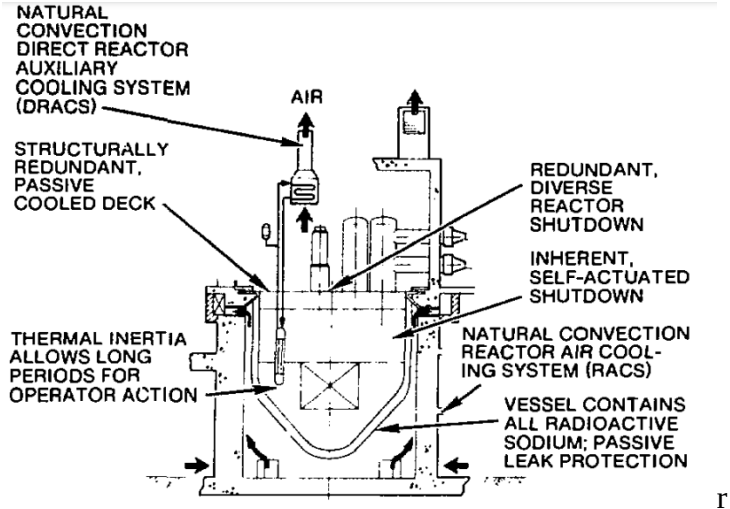

r

Figure 55. SAFR cooling systems.

Table 15. Examples of SAFR Safety [46]

Reactor Shutdown	Decay Heat Removal	Spent Fuel Cooling	Structural Cooling	Structural Integrity	General
Spring-assisted primary control rod system	Air natural convection cooling of vessel	Air natural convection, redundant DRACS	Air natural convection cooling of deck	Redundant box beam deck structure assures support of shutdown system	Heterogeneous core has inherent low energetics
Self-actuated inherent shutdown	Na-Na-air cooling natural convection DRACS	N/A	Air backup natural convection cooling of cavity	Redundant, monitorable core support system	no safety-related components / systems in IHTS or BOP
Inherent ability to shutdown after LOF without SCRAM	N/A	N/A	N/A	Simple vessel configurable / backup guard vessel assures safe sodium level	Long Grace Period for operator action.

Should a severe accident occur in the SAFR, the system's inherent ability to remove decay heat "provides long grace periods for corrective action." The designers estimate that the SAFR

design can withstand 30 hours of abnormal operation before the sodium starts to boil. The SAFR design was created prior to the study of metallic fuels in reactors, where the designers mentioned there is a “substantial margin for uncertainty in the metal fuel performance”. If an oxide fuel were chosen, the 30 hours of abnormal operation would instead become 25 minutes for the sodium to reach boiling, making the design less desirable.

The SAFR design approach for fire suppression was a modified form of the CRBR [30]. Figure 56 shows the design of the fire suppression system for the steam generator building. The image shows the drain line entering the header “where the sodium is conducted to the sodium water reaction protection system (SWRPS) vault” [30]. In the event of a leak within the SAFR plant, the leak collects in the leak collection header as shown on the left of Figure 56. The SAFR plant required the use of “sensitive, reliable leak detectors,” the implementation of said leak detection resulted in testing various methods [30]. Five different detection methods evaluations: “two conductivity-types and three aerosol-type,” but as SAFR is not a constructed reactor none of these have been implemented [30].

The overall fire protection system has two types of systems: a “non-sodium fire-protection system (NSFPS)” and a “sodium-fire-protection system (SFPS)” [30]. The non-sodium fire-protection system will be equipped with “300,000-gallon redundant storage tanks,” with a series of “sprinklers,” “pumps,” and a “water spray” [30]. For rooms with water sensitive equipment, such as computers and electronics, “pressurized storage cylinders located outside the rooms and cable ways” will be equipped with a “flooding system” filled with “Halon 1301” (Bromotrifluoromethane) [30]. The sodium-fire-protection system is equipped with “fire-detection and alarm instrumentation,” aerosol release-limiting instrumentation, a “leak-collection and catch-pan system,” and transportable fire extinguishers coupled with protective clothing to mitigate the risk of sodium leaks and fires. [30]. These components all work to prevent the “uncontrolled release of a moderate energy fluid system (MEFS)-size leak” by design. The philosophy behind the system “consists of three principal features: an insulation confinement and collection system, a system of piping to carry away sodium leakage, and catch-pans to safely collect accumulated leakage” [30].

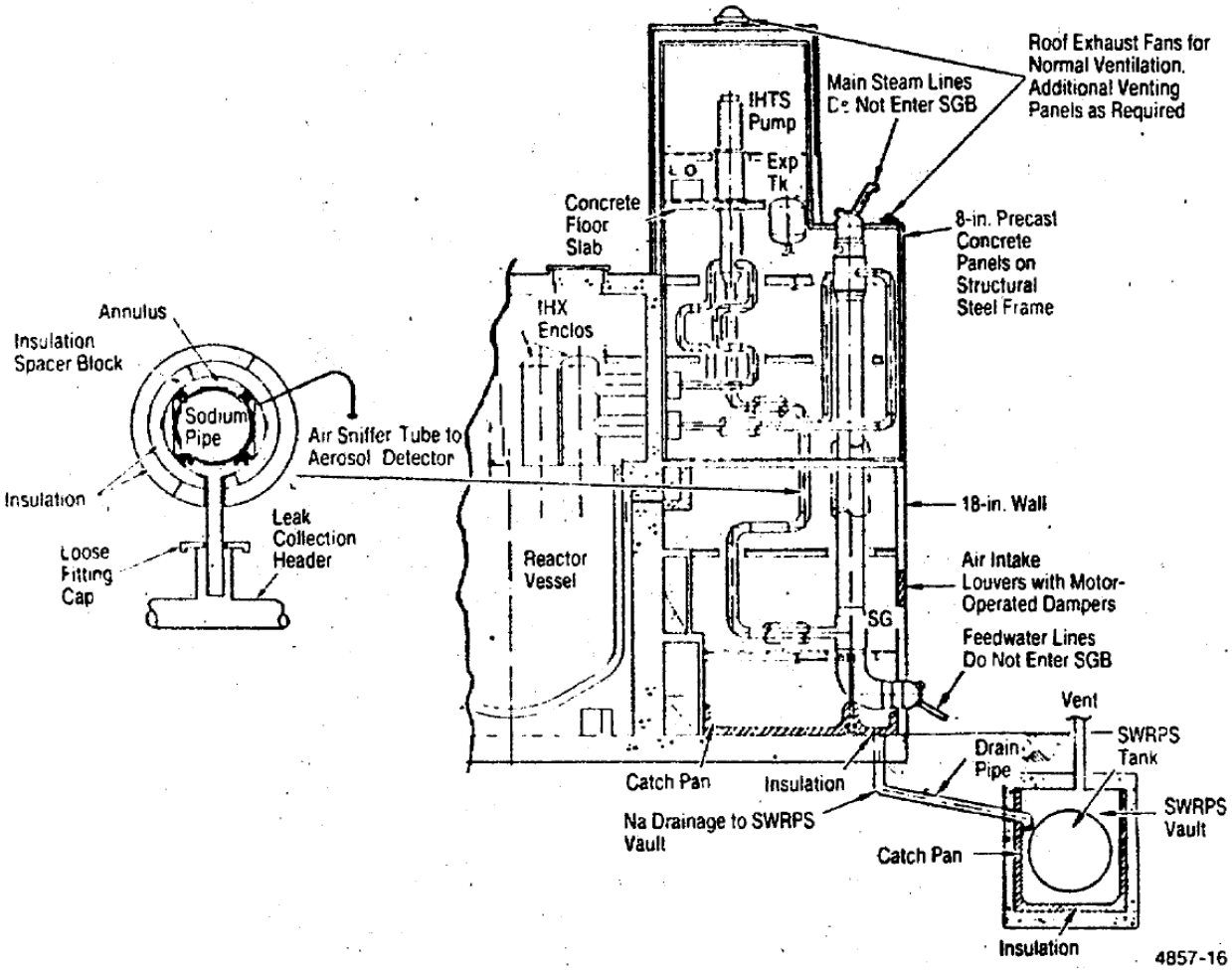

Figure 56. Passive sodium fire mitigation provided by SAFR steam generator building [30].

10.1.3 Advanced Burner Reactor

The Advanced Burner Reactor (ABR) was a reactor concept deigned by Argonne National Laboratory. ABR was projected to be steady state at 1,000 MWt and 380 MWe. The primary objective of the ABR project was to research and demonstrate the feasibility of separating transuranics from the used fuel of the current fleet of LWRs and burning it in a fast neutron spectrum. This concept will not only allow the transuranics to be transmuted to produce energy but also reduce the radiotoxicity and the decay heat load on the repository. This recycling of the spent nuclear fuel will help manage the growing system of nuclear waste.

The initiative to design and build ABR was started in the early 2000s. There were two phases in the initiative. The first phase was to build a prototype reactor, the Advanced Burner Test Reactor (ABTR), which was to be a fraction of the size of a normal nuclear reactor plant. The second phase was to build full scale ABR's once the fuel cycle was demonstrated as a success. The reactor was to be sodium cooled, which would allow the use of a fast neutron spectrum. Many design concepts were similar to that of the SAFR. ABTR had much of the design work done but was ultimately never built. An artist's rendition of the site can be seen in Figure 57 [47] and is noted that all nuclear components and systems are to be isolated on the nuclear island, separate from the energy island.

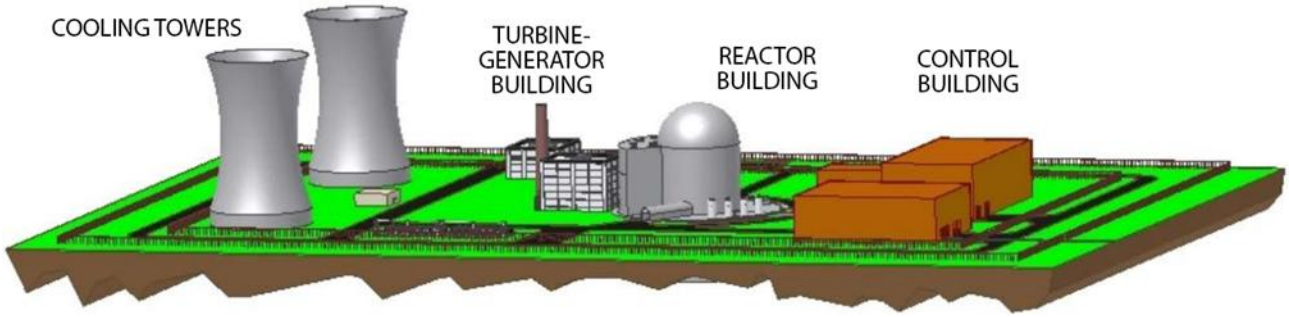

Figure 57. Artist's rendition of the ABR plant.

Key plant characteristics of the proposed ABR by ANL can be seen in Table 16 [47]. The plant was initially to be licensed for 30 years but was designed to last up to 60 years with an expected license renewal. The different materials used for the sodium systems, such as HT-9 and austenitic stainless steel were chosen for their corrosion resistance, high strength, and irradiation resistance.

The reactor core was designed to be a pool type reactor, with all primary sodium components being enclosed by the reactor vessel, thus ensuring a primary sodium containment in case of a leak. As an extra layer of protection, a guard vessel will surround the reactor vessel to ensure any leaks are contained. The core can be seen in Figure 58, where the hot and cold pool of primary sodium are separated by a conical structure called the redan. Cold pool sodium is heated as it is pumped through the core into the hot pool. Heat is then transferred between the primary and secondary sodium via four intermediate heat exchangers (IHX). It can be seen in the figure

that the hot pool sodium operates at a higher level than the cold pool sodium. The redan is designed to completely isolate the hot pool and cold pool sodium from each other, even during a seismic event, to prevent unwanted heat transients.

Table 16. Key Plant Characteristics of ABR.

Reactor Power	1,000 MWt, 380 MWe
Coolant	Sodium
Coolant Temperature, Inlet/Outlet	355°C/510°C
Driver Fuel	Both metal and oxide startup and recycle cores were evaluated
Cladding and Duct Material	HT-9
Cycle Length	12 months
Plant Life	30 years with the expectation of life extension to 60 years
Reactor Vessel Size	14.1 m diameter, 14.8 m height
Structural and Piping Material	Austenitic Stainless Steel
Primary Pump	Four (4) Mechanical (centrifugal) primary pumps
Power Conversion Cycle	Reference: Rankine Steam Cycle
Thermal Efficiency	38%

To ensure that the reactor vessel is not leaking or cracking, a series of measures will be taken which includes sensors, measurement techniques, and physical examinations inside the guard vessel. Sensors will monitor for sodium and gas leaks. Radiation sensors and gas pressure gauges will help detect cover gas leaks from inside the reactor. Physical examination of the reactor vessel will be accomplished through the use of a remotely operated vehicle (ROV) with a camera system. The ROV will be able to transverse the outside of the entire vessel through a series of winches and cables as seen in Figure 59.

The core is designed to hold a total of 180 fuel assemblies, with 78 of them comprising the inner enrichment zone and 102 of them comprising the outer zone. The fuel type proposed for ABR was ternary metal and mixed oxide. Two in-vessel storage rings will surround the core barrel in ABR. The rings will hold new subassemblies that will allow fresh fuel to be preloaded into the core. The rings will also contain spent fuel that will allow time for used fuel assemblies to decay before being removed to a long-term storage. These fuel storage rings can be seen in Figure 60.

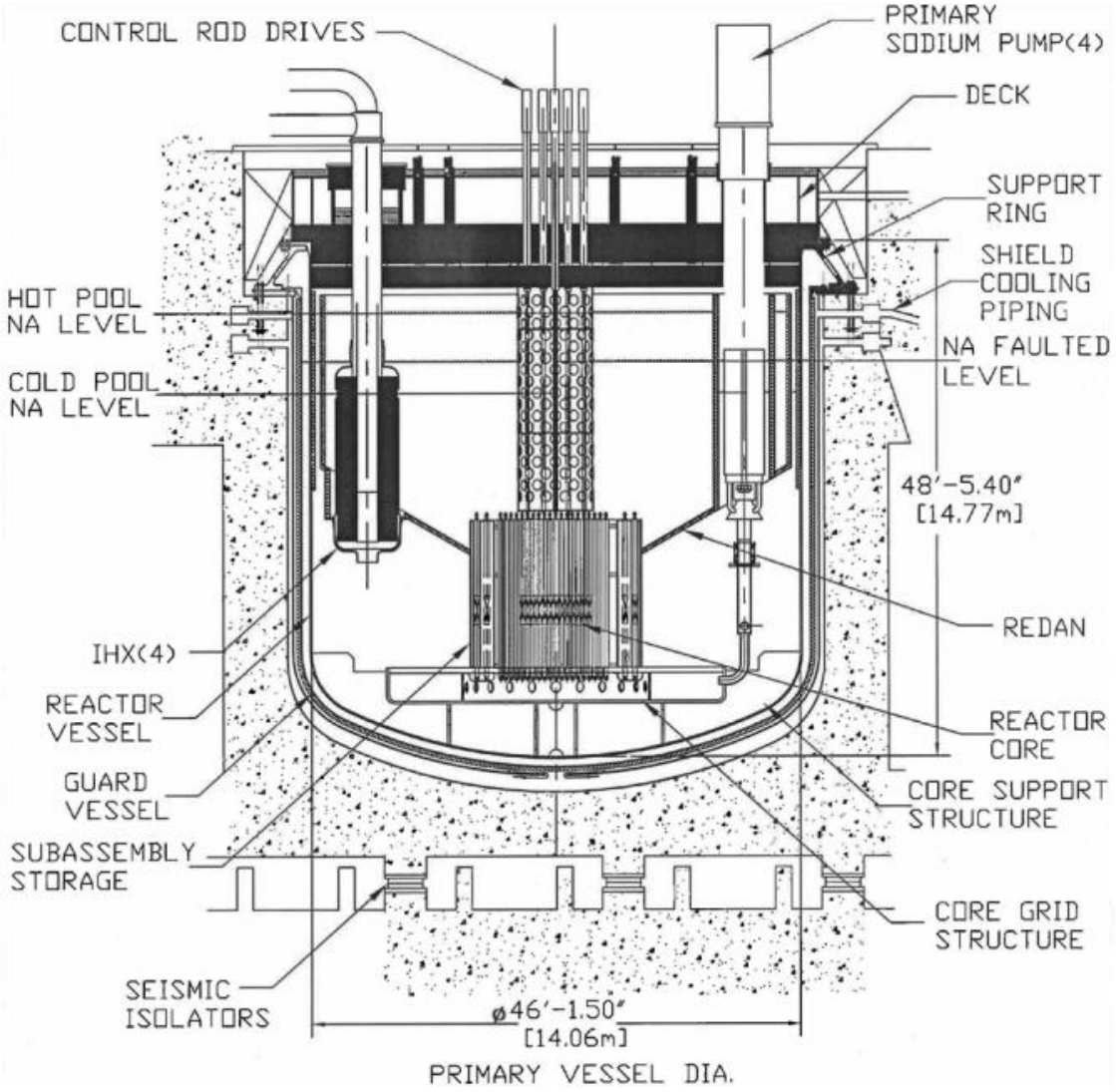

Figure 58. ABR core assembly.

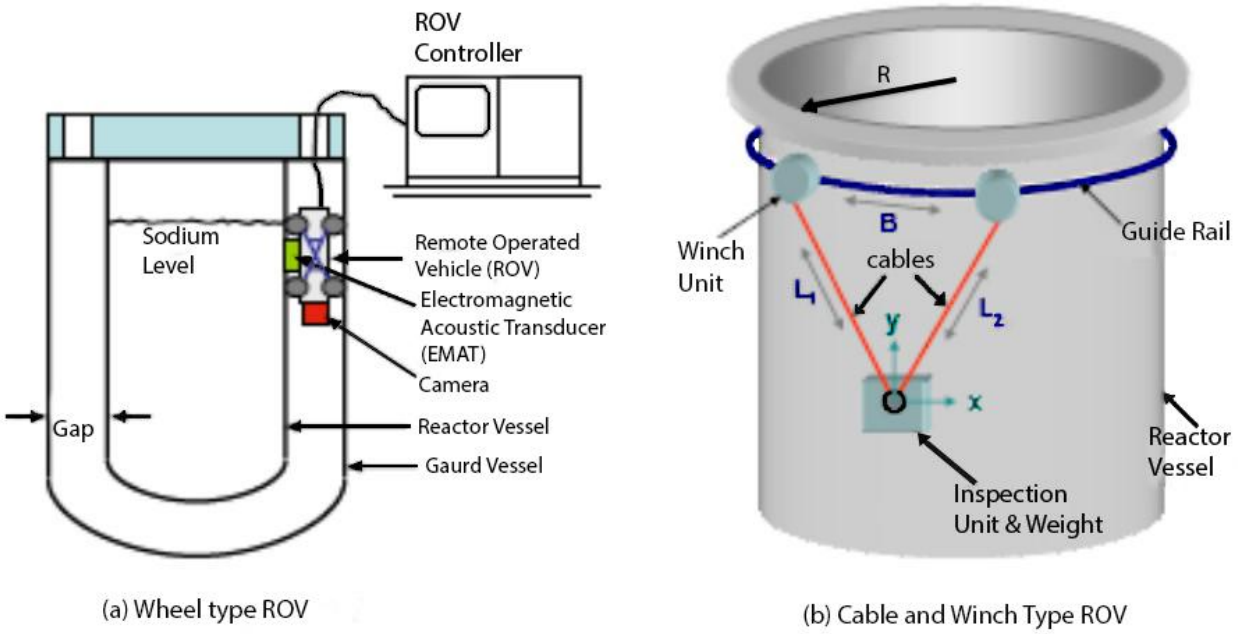

Figure 59. Physical inspection of the reactor vessel using an ROV.

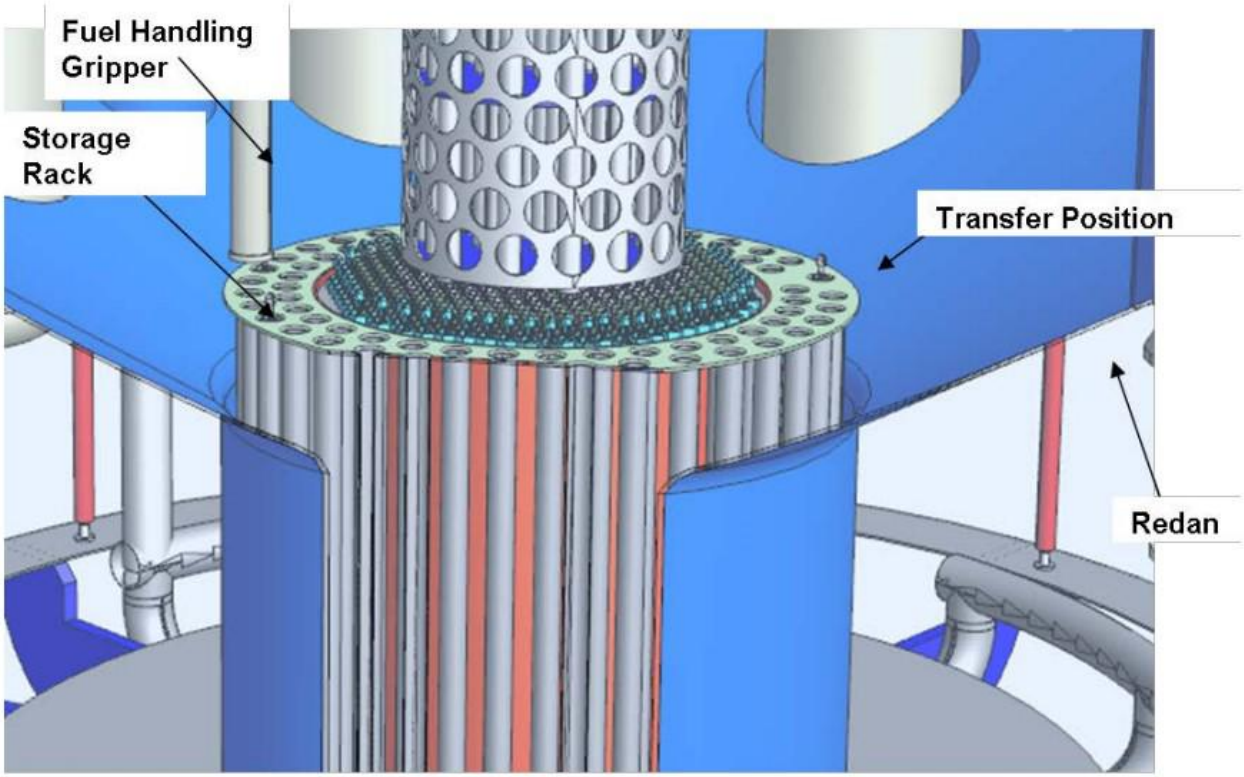

Figure 60. Fuel storage rings surrounding the core barrel.

10.1.3.1 Primary Purification System

A continuous purification system is needed to maintain purity in the primary sodium coolant supply in order to: lesson the corrosion rate of reactor vessel, piping, and materials since sodium impurities could cause metal surface removal (which could affect the load carrying capability of reactor materials), fouling of heat transfer surfaces through surface deposits, and reduced mechanical properties of materials caused by changes in base alloy composition [47]. Several components of the purification system include a surge tank, a nuclide trap, a cold trap, a NaK loop, and a silicon loop.

The purpose of the nuclide trap is to capture and retain radioactive Cs-137 and other fission products that might be contained in the primary sodium. The trap uses a porous, low density filter made from carbon that will be able to trap a significant amount of Cs-137. A final filter in the trap is made of stainless steel and ensures that no carbon escapes into the primary sodium.

The cold trap utilizes a crystallizer tank that traps sodium impurities like sodium hydride, sodium oxide, and sodium monoxide. A regenerative heat exchanger reduces the sodium down to an effective cold trapping temperature, and then reheats the purified sodium before re-entering the primary tank. The crystallizer precipitates the impurities out of the sodium using wire mesh cylinders and is cooled by the NaK loop [47].

Many systems and auxiliary units for the proposed ABR are fairly similar to SAFR, such as the DRACS, the redan assembly, seismic isolation, etc. For more information on these other systems, see the SAFR section of this handbook.

10.1.4 Clinch River Breeder Reactor

10.1.4.1 History

The CRBR was a Liquid-Metal-Cooled Fast Breeder Reactor (LMFBR). Figure 61 depicts an artist’s rendering of the CRBR facility. The CRBR was meant to be part of a proven technological and engineering base, with joint utility and industry participation in the commercial breeder reactor industry [31]. CRBR was located on the Clinch River site in Oak Ridge, Tennessee,

bordering DOE's Oak Ridge reservation. Within 30 miles of the site is metropolitan Knoxville (Figure 62) [48].

Figure 61. CRBR facility.

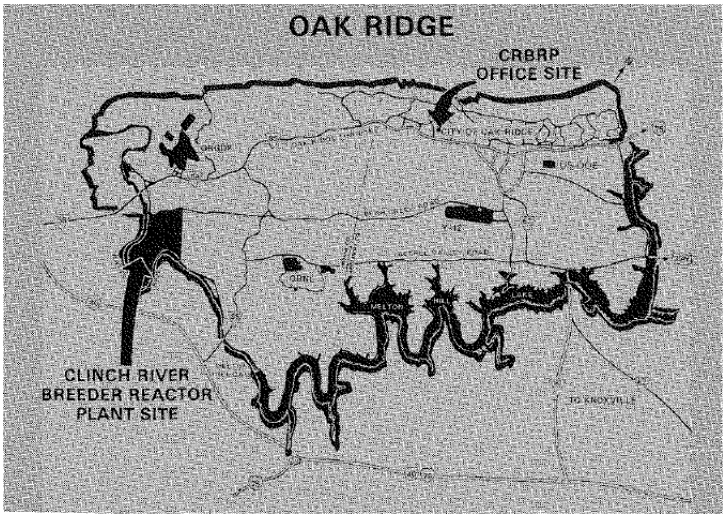

Figure 62. Map of Oak Ridge.

The Clinch River Breeder Reactor Plant Project (CRBRP) has its beginnings at the Atomic Energy Commission (AEC) Authorization Act for Fiscal Year 1970 (Pub. L. No. 91-44) which authorized AEC to conduct the "project definition phase" of a liquid metal fast breeder reactor demonstration program under cooperative arrangements with reactor manufacturers and others.

By 1970, the DOE announced funds would be used for construction of a new SMR–powered reactor plant at the former CRBR site in Oak Ridge, Tennessee [49]. The basic CRBRP authorization followed 1 year later in the AEC Authorization Act for Fiscal Year 1971 (Pub. L. No. 91-273) which authorized AEC to enter into cooperative arrangements for the design, construction, and operation of the plant in accordance with criteria submitted to the Joint Committee on Atomic Energy (JCAE). The AEC Authorization Act for Fiscal Year 1972, Pub. L. No. 92-84, increased the Government's participation in the project by increasing direct assistance funding and by increasing the assistance allowed from the base program to 50 percent of the estimated capital cost of the plant [50].

10.1.4.2 Design

As seen in Figure 63, the schematic elevation of the reactor is shown and identifies the reactor vessel, closure head, and inlet/outlet nozzles. The reactor internals are comprised of removable fuel, blanket and control assemblies, removable radial shielding, and the upper and lower internal structures' which provide support and positioning for the core and the core restraint system. The lower internals structure consists of the core support structure plate and cone, the core barrel, horizontal baffle, fixed radial shielding, and inlet/bypass modules.

Most of these components are shown in Figure 64. The core barrel provides support for the upper and lower core restraint former rings and the bypass modules provide support for the removable radial shielding. Together these comprise the core restraint system. The lower internals structure is welded into the reactor vessel. The core support structure includes features to prevent large debris from completely blocking flow to any of the inlet modules.

The upper internals structure consists primarily of the four lifting columns, two transverse interconnected plates, thirty-five outlet modules, and flow chimneys. The structure, shown in Figure 65, provides lateral stabilization for the control rod shrouds and outlet module flow tubes, supports the in-vessel instrumentation, and provides mechanical backup hold down for the core assemblies. The shroud and flow conduits are designed to mitigate transient' temperature effects on the structure from the reactor core effluent. The upper internals structure is supported from the

intermediate rotating plug of the vessel closure and is radially keyed to the upper core restraint former ring attached to the core barrel.

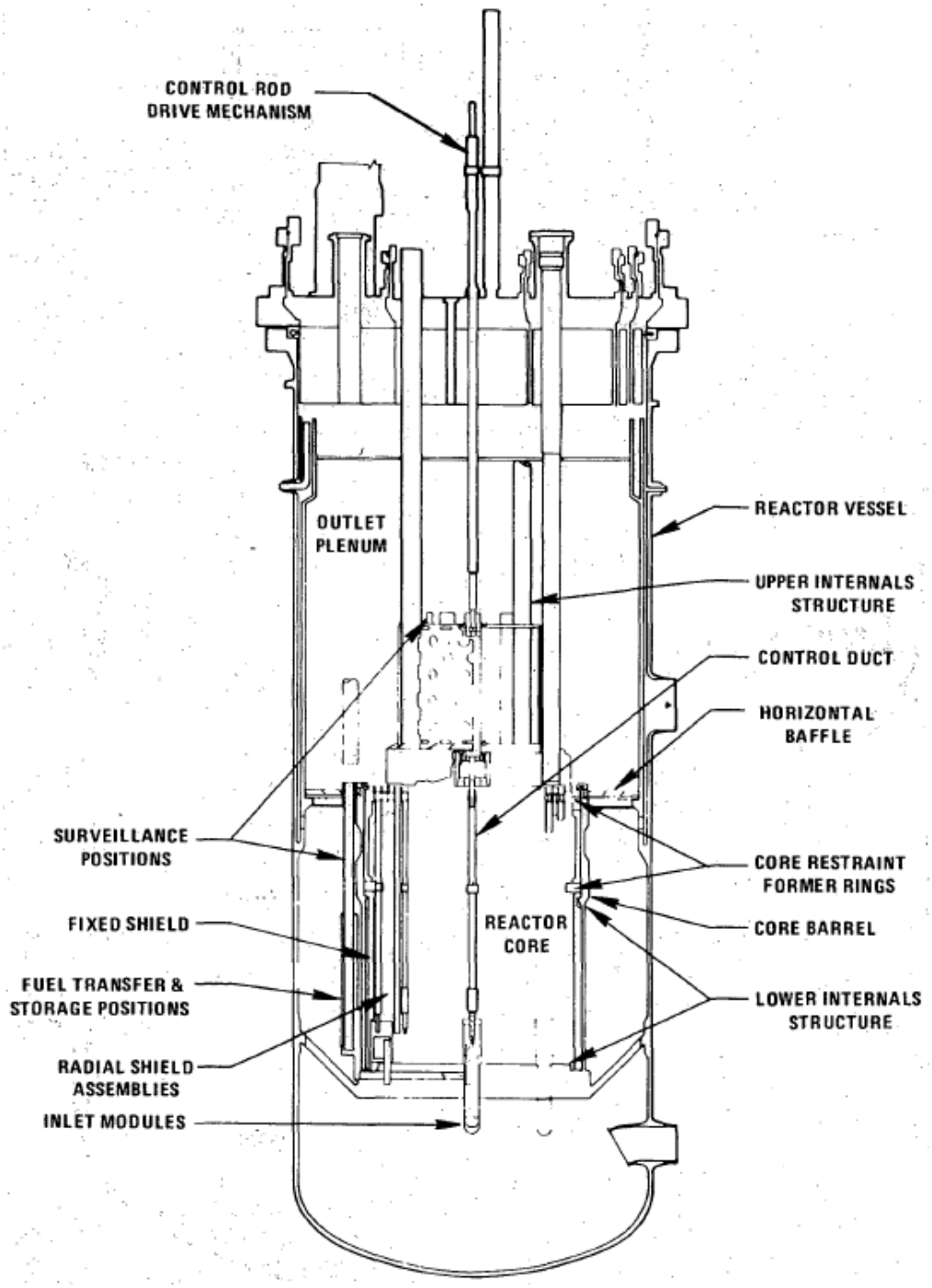

Figure 63. Reactor elevation.

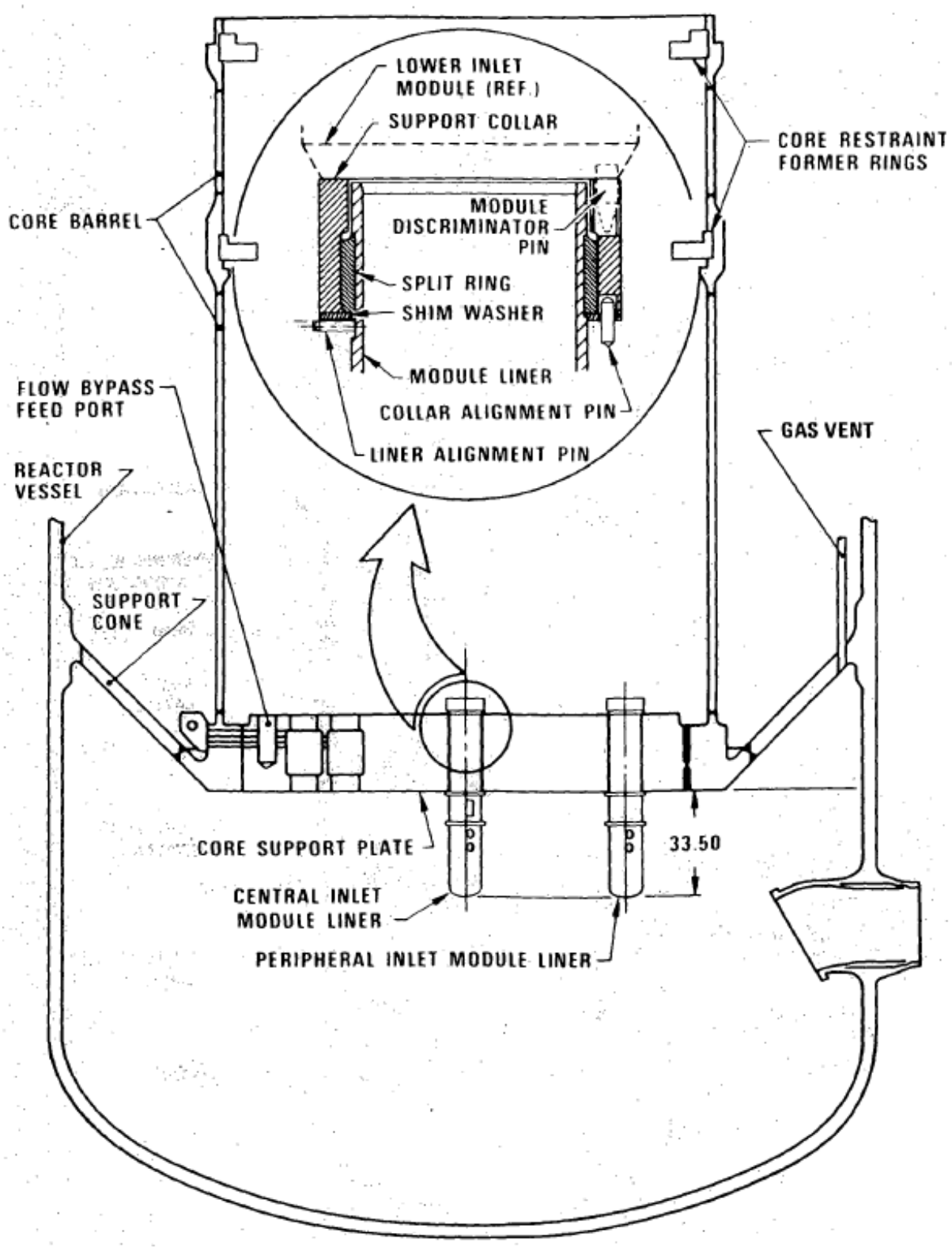

Figure 64. Lower internal structure.

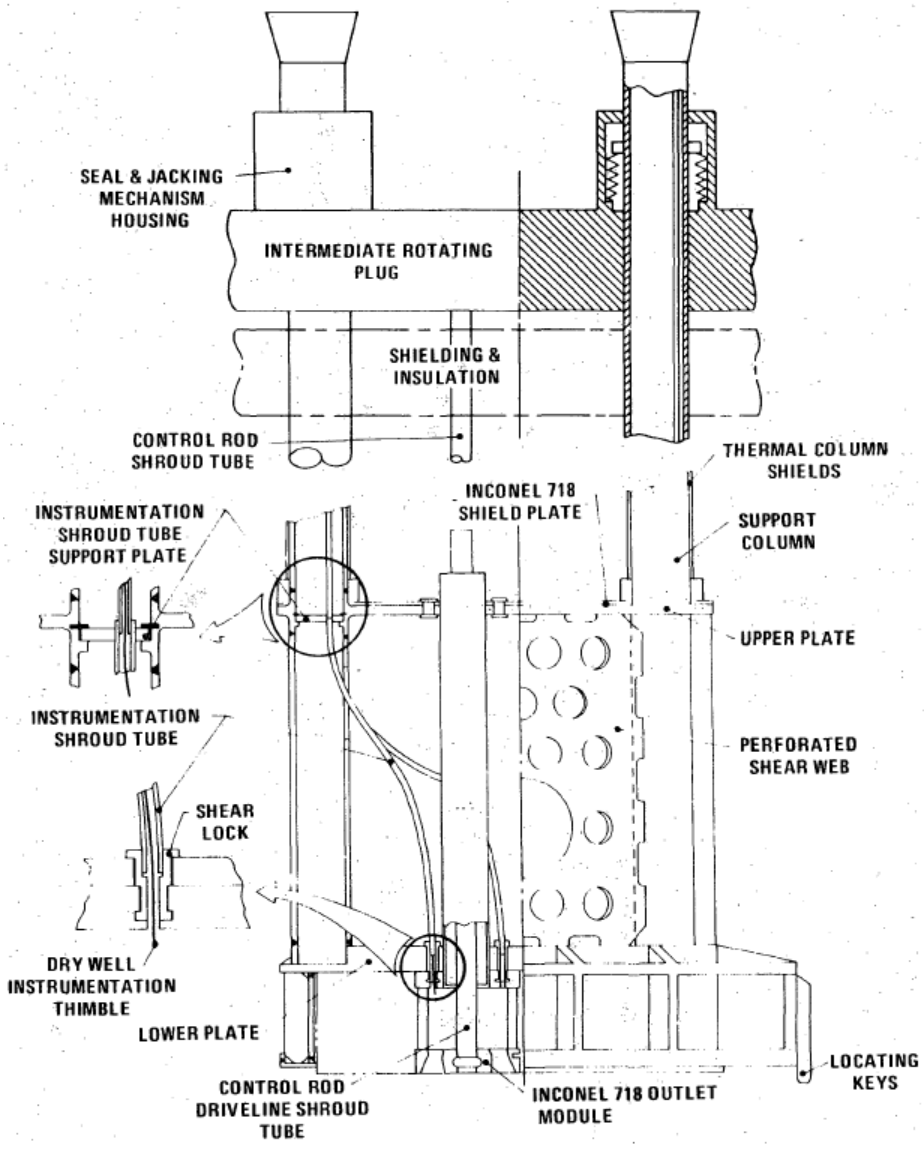

Figure 65. Upper internal structure.

The active fueled region is 36 inches long with a diameter equivalent of 73.6 inches. The fuel region consists of two radial enrichment zones with a total initial fissile plutonium loading of 1l,150 kg. The primary system has 15 mechanically scram assisted control rods while the secondary system has 4 hydraulically scram assisted control rods. Each system is independently capable of shutting down the reactor from full power to hot standby conditions. Each of the core assemblies and the removable radial shields have two load pad areas which match the elevation of the core restraint former rings to position the core and restrain core assembly motion during

operation. The fuel, blanket, and control assemblies each contain a tag gas to permit the detection and identification of failed elements. Fuel transfer and storage positions are provided in the annulus between the core barrel and the reactor vessel. A plan view of the reactor details is shown in Figure 66 [31].

The Clinch River Breeder Reactor possess three engineered safety features: the containment system, the containment isolation system, and the control room habitability system. The containment functional design is described, and the containment design basis accident is identified as a barrier against a failure of the primary sodium tank. A “negative pressure differential” will be maintained in the annulus, thus ensuring any leaks are directed into that location and can be monitored [31]. The accident condition in containment pressure and temperature transients are provided and the calculated radioactivity in the containment atmosphere are presented. Details of

calculated site boundary doses are provided and are shown well below the 10 CFR 100 guideline exposures as shown in Table 17.

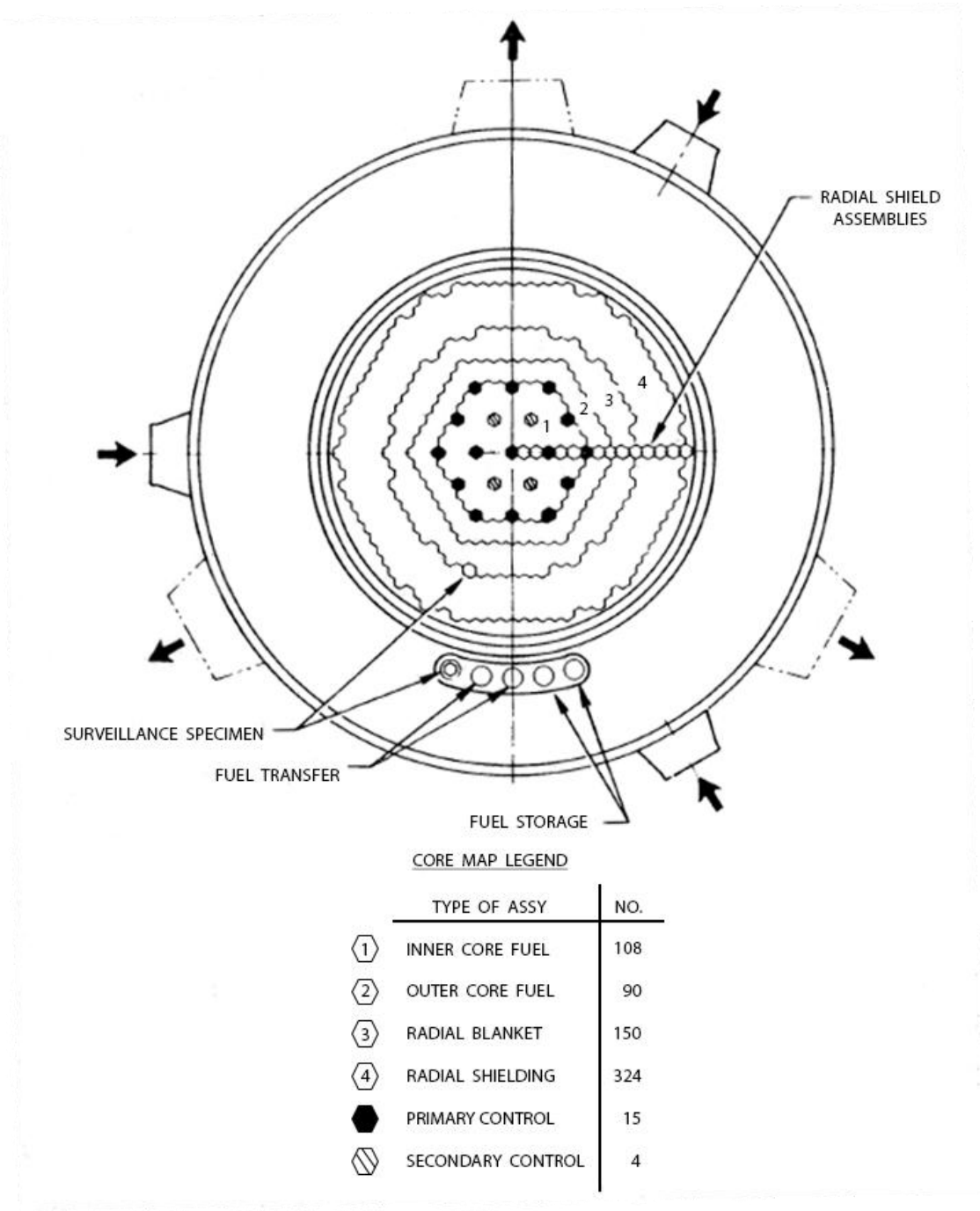

Figure 66. Plan view of the reactor.

Table 17. Dose calculation results

Organ	Dose (Rem)		
	Guidelines of 10CFR100	Site Boundary (0.41 mi) 2-Hour	Low Population Zone (5.0 mi) 30-Days
Beta Skin	none	1.18E-8*	5.66E-08
Whole Body**	25	4.55E-06	2.17E-05
Thyroid	300	2.61E-05	1.25E-04
Bone	150'	1.21E-04	5.76E-04
Lung	75+	2.83E-05	1.36E-04

*1.18E-8 =l1.18x10 8
**Includes both inhalation and external gamma exposure,
+Not covered in 10CFRO00; used as guideline values

10.1.4.3 CRBR Sodium to Atmosphere Leak Detection Systems

The sodium to atmosphere detection systems proposed for CRBR are as follows: sodium ionization detection, a hydro detector, surface ionization monitor for particulates, and liquid sodium detection. Sodium to atmosphere leaks occur due to a positive pressure differential between sodium and the surrounding gaseous environment. The escaping sodium can react producing numerous by-products such as aerosols or vapors. In some reactions, hydrogen gas can be released. In addition, sodium can react exothermically, possibly producing heat, smoke, or fire.

The SID monitors sodium aerosol /vapor leaks from the primary and intermediate heat transport systems to the surrounding atmosphere. The SID is activated by the passage of a gas sample through an ionization chamber operating via a hot filament technique. The hot filament ionizes sodium and sodium species, generating a recordable signal. When the sample gas contains no sodium vapor or aerosols, the ionization current is low, 0.01 to 0.2 nanoampere. However, as the sodium aerosol concentration increases, the SID ionization current increases. This increase is proportional to the concentration of sodium vapor/aerosol in the gas passing through the SID chamber at any given time; the increase is not a function of sodium aerosol collection over time. The SID schematic is shown in Figure 67.

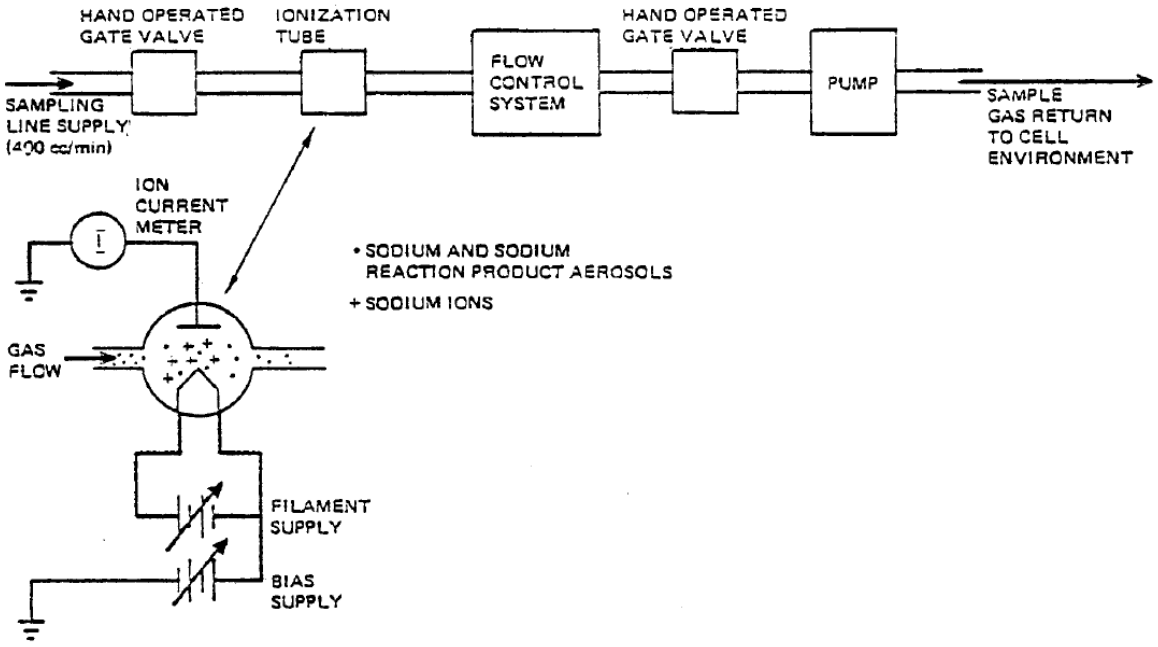

Figure 67. Sodium ionization detection schematic.

The smoke detector (Figure 68) proposed for CRBR is a commercially available unit and monitors the cell atmosphere for sodium aerosols. The smoke detector operates on an ionization principle; combustion products entering the detector's outer chamber disturb the balance between it and the inner reference chamber. This unbalance causes the gas discharge tube to ignite, generating a signal indicating the presence of combustion products.

The hydrogen detector (Figure 69) proposed for CRBR is a commercially available, laboratory-grade gas chromatograph. This device separates and analyzes sample gas' from the test cell environment. In the presence of moisture, a sodium leak will generate hydrogen gas that can be monitored by the detector and used as an indicator of a reaction.

A SIMP is proposed to monitor the cell environment for sodium and sodium reaction products in the form of aerosols. A schematic of this monitor can be found in Figure 70. The SIMP detector responds to sodium aerosol presence in two ways: to measure the average ion current and measure the "counts" of particulates. When particulate "counts" are measured, they

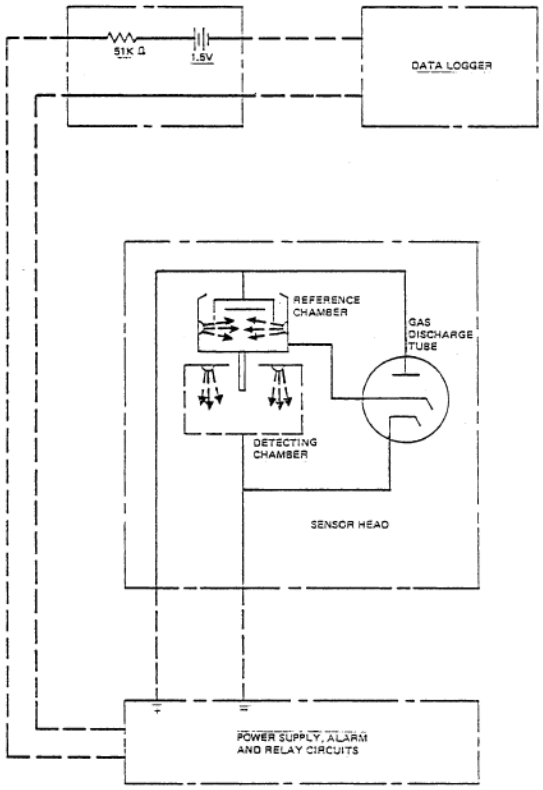

Figure 68. Sodium aerosol smoke detector.

can be displayed via a digital count meter through a signal processed within the SIMP, or a strip chart recorder signal, which is the integrated output of a sawtooth signal originating within a triggering unit synchronized to the detector's ionization current.

A liquid sodium leak can be detected through a cable detector or a contact detector. The cable detector consists of a thin, stainless steel-sheathed, mineral insulated (magnesium oxide) coaxia1 cable, with perforations in the outer (grounded) sheath. This detector can be seen in Figure 71. Liquid sodium penetrating the perforated sheath causes a low resistance path to ground, which then produces an increased voltage drop and activates an alarm. The response to liquid sodium is indicated on a strip recorder and data logger.

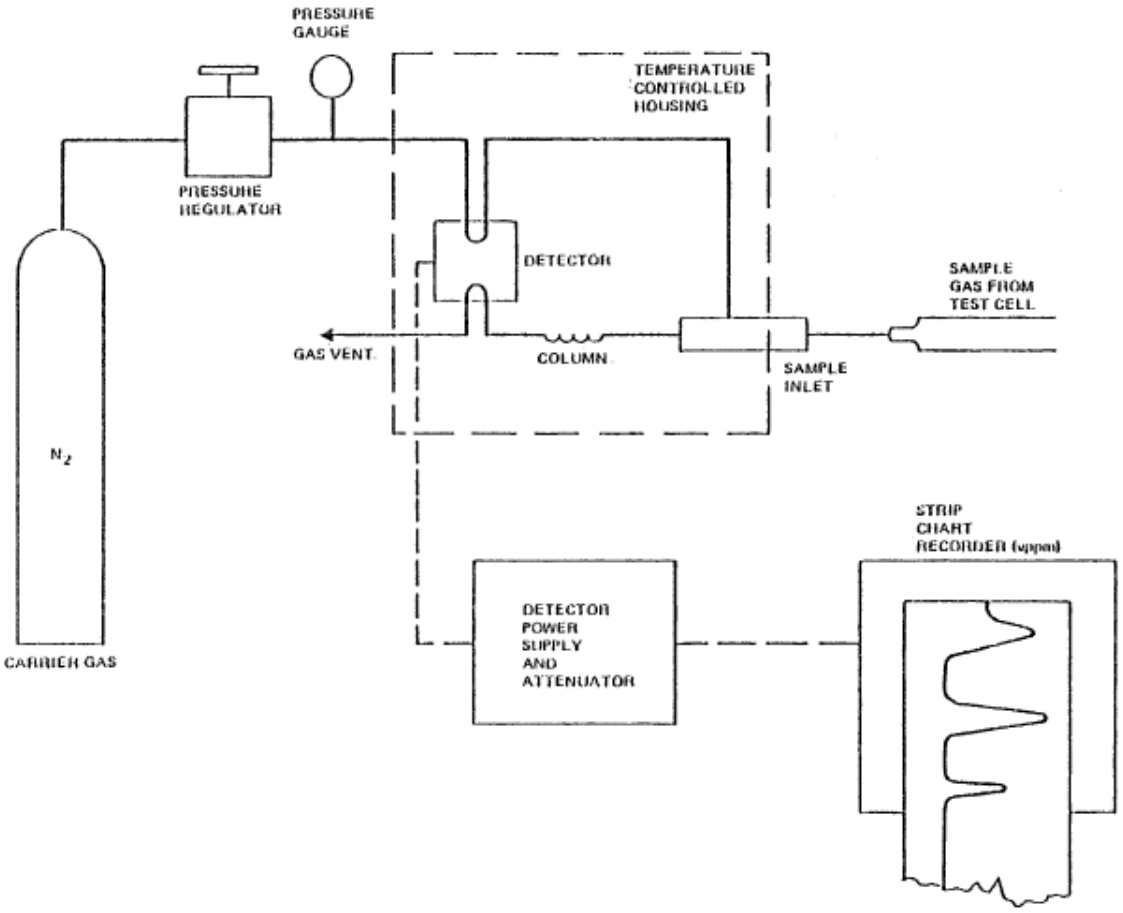

Figure 69. Hydrogen detection schematic.

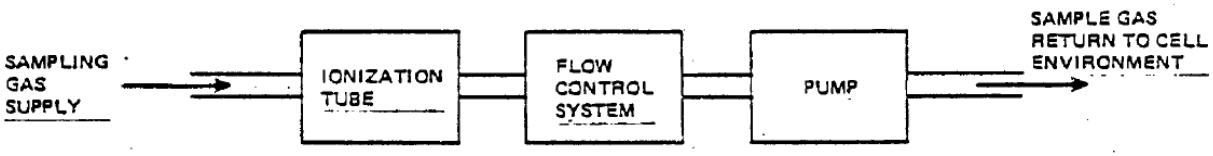

Figure 70. Surface ionization monitor for particulates.

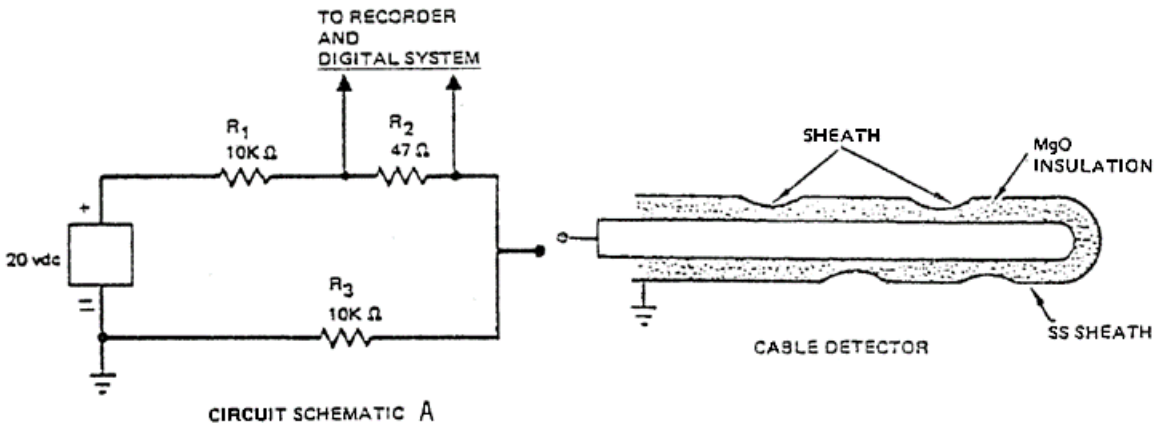

Figure 71. Cable detector.

The contact detector (spark plug) consists of a stainless steel-sheathed, mineral -insulated (MgO) coaxial cable, joined as an exposed junction within a bonnet at the end. Liquid sodium flowing into the gap between the electrodes provides an electrical short circuit between the exposed junction and the stainless-steel sheath [32]. The contact detector can be seen in Figure 72.

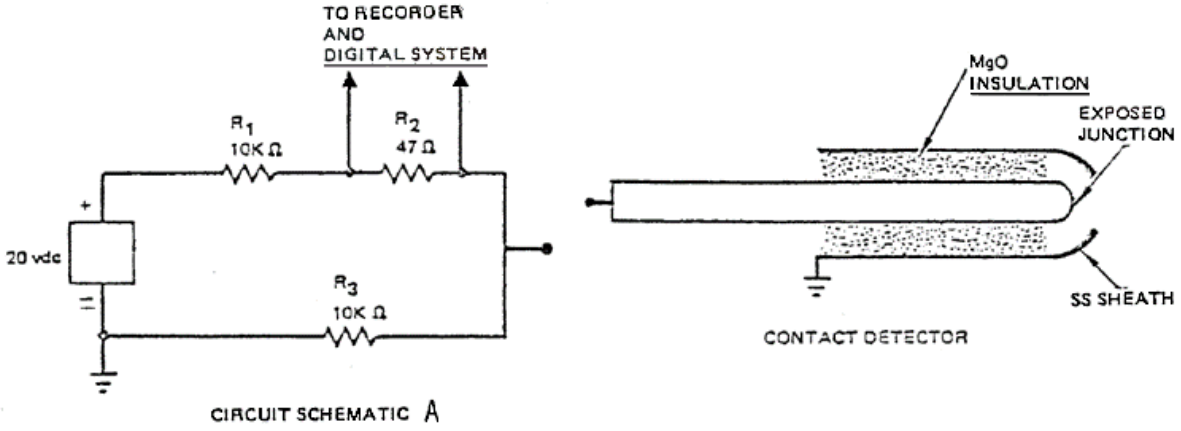

Figure 72. Sodium contact detector.

10.1.4.4 Sodium to Water Leak Detection

It is important to allocate where sodium to water interactions may occur. These locations are primarily at the steam generator, since the only localized place in the plant where sodium and water meet are in the process of transferring heat from the sodium to the water for the turbine.

The steam generator leak detection system is designed in such a way that it can detect the presence of hydrogen or oxygen gas. The leak detection is based on the measurement of the hydrogen concentration in both the sodium and in the cover gas spaces. Oxygen concentration measurements are found in the sodium only and are complementary to the hydrogen detectors, thus providing a diverse method to ensure early detection.

The measurement of hydrogen in the sodium is performed by allowing the hydrogen to diffuse through a thin-walled nickel membrane and then detecting the hydrogen with an ion gauge and an ion pump. The monitor may operate in a static mode using the ion gauge to monitor steady state hydrogen concentration, since hydrogen content is directly related to the pressure measured in the chamber. The monitor may also operate in a dynamic mode, using the ion pump to constantly pump the chamber since the hydrogen concentration is directly related to the ion-pump current.

The hydrogen detection in the expansion tank cover gas utilizes a gas chromatograph. A continuously monitoring hydrogen detector similar to the in-sodium detectors is also provided for the cover gas. The hydrogen detector proposed for CRBRP water to sodium leak detection is shown in Figure 73. The nickel membrane is inserted into the liquid sodium. On the other side of the nickel membrane is a vacuum created by an ion pumping system. Hydrogen resulting from a leak diffuses through the nickel membrane into the vacuum, where it can be detected through several means; measuring the pressure rise, employing a mass spectrometer, or monitoring the ion pump current [32].

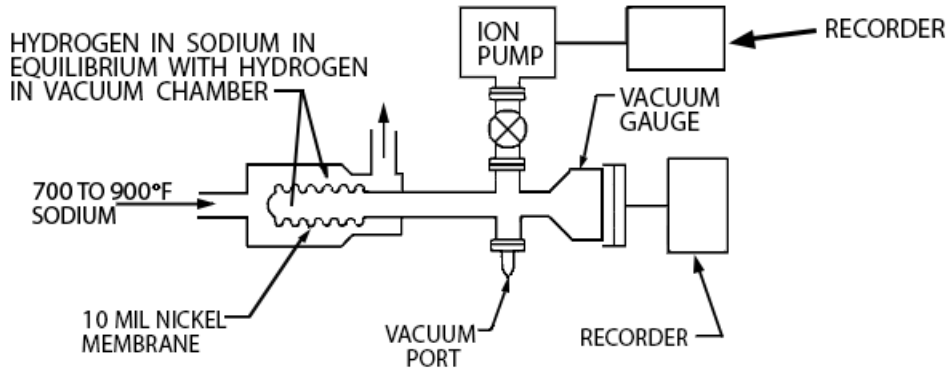

Figure 73. Hydrogen Detector Schematic.

Oxygen detectors are electrochemical cells immersed in sodium that continuously monitor in-sodium concentration and consist of a reference oxygen electrode separated from the sodium by a $ThO_2 - Y_2O_3$ solid electrolyte (see Figure 74).The electrical potential difference between the reference electrode and the sodium is a measure of the oxygen content in the sodium [32].

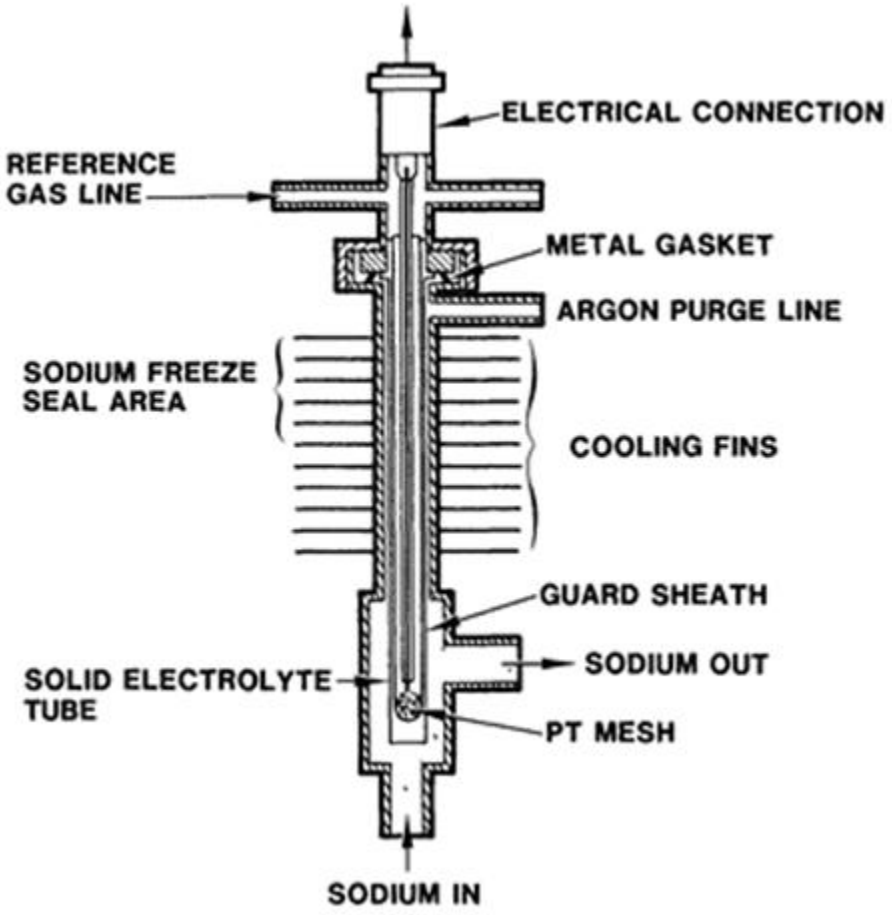

Figure 74. Oxygen detector schematic.

10.1.5 Experimental Breeder Reactor-I

EBR-I was the first liquid metal cooled fast reactor. EBR-I's design utilizes sodium-potassium (NaK) as the coolant. EBR-I utilized uranium fuel to then breed plutonium. An image of the facility is shown in Figure 75.

EBR-I was built on the National Reactor Testing Station in Idaho, 18 miles southeast of Arco, Idaho. EBR-I started power operation on August 24, 1951, and operated until 1963. Rated to produce 800 W [51], EBR-I's objective was to develop and test the concept of a nuclear breeder reactor, to breed plutonium from uranium. EBR-I contributed to the nuclear industry by demonstrating the possibility of breeding nuclear fuel, it proved that more atoms of fuel are created by the reactor than are used. This process makes it possible to utilize almost all of the

Figure 75. Image of the EBR-I facility.

uranium found in nature. Another accomplishment was to become the first reactor to produce electricity from a plutonium core [51]. Argone National Laboratory decided to build EBR-I near Arco, Idaho.

The earliest efforts associated with the design of EBR-I was considered by Dr. W. H. Zinn and Dr. Enrico Fermi when they considered the feasibility of a fast reactor consisting of a solid mass of fissionable material [52]. Construction at the INEL site began in October 1949. Criticality was reached in August 1951, and the system was brought to full operating power, 1.1 MWt, on

December 19, 1951. On the following day, December 20, 1951, steam was led to a turbine-generator and for the first-time nuclear heat was transformed into electrical energy [35].

The reactor consisted of three principal regions: a core, a light inner blanket that surrounded the core axially and radially, and a dense outer blanket in the form of a cup which could be moved vertically with respect to the core. The core consisted of a hexagonal assembly of 217 fuel elements which, in turn, were stainless steel tubes filled with fully enriched metallic uranium slugs. A 0.010-in. annulus between the tubes and the slugs was filled with NaK, which served as a heat-transfer bond. Upper and lower axial blankets were formed by the inclusion of natural metallic uranium slugs above and below the fuel. Inner radial blanket rods consisted of larger stainless-steel tubes filled with natural metallic uranium slugs. All core and inner radial blanket components were contained within a double walled stainless-steel tank. The outer blanket or cup consisted of an assembly of stainless-steel clad keystone-shaped bricks of natural uranium metal.

The entire assembly was mounted on a pedestal which could be raised or lowered relative to the core. Twelve stainless-steel-clad uranium rods which penetrated holes in the vertical columns of brick, served as control and safety rods. Controlled movement of the cup served as a coarse variation of reactivity and upon the receipt of a scram signal the cup dropped away from the core to reduce reactivity by approximately 6% $\Delta k/k$ [35]. A schematic layout of the plant is given in Figure 76. After leaving the outlet plenum, the coolant flowed via gravity to a primary-secondary (NaK to NaK) heat exchanger, then into a receiving tank in the basement. A pump, operated at a capacity slightly higher than the main coolant flow, returned the coolant to the gravity supply tank. An overflow system connecting the supply tank to the receiving tank guaranteed a constant delivery rate of coolant to the core and blanket. Heat from the secondary NaK was removed in a steam generator which consisted of a water heater, boiler, and superheater. Water, in the form of a film, traveled downward through the heat exchanger tubes. Heat transferred from the counter-flowing secondary NaK and in turn generated steam which, after superheating, was used to drive a conventional turbine-generator. Approximately 200 kilowatts of electricity were generated -- enough to satisfy the needs of the EBR-I facilities. In the course of its useful life (1951-1964), EBR-I operated with four different fuel loadings, each designed to establish specific benchmarks of Fast Breeder Reactor (FBR) technology [52].

EBR-I successfully tested the ability to breed fuel, to gain experimental data in handling radioactive liquid metals at high temperatures, and to obtain data on the operation of high energy neutron range. It also brought about proof that the operating characteristics of fast reactors are similar to those of thermal systems, as well as proof that a breeder reactor can produce more fuel than it consumes (A conversion ratio of 1.01 ± 0.05 was established for the first uranium-fueled loading.) It accomplished the first production of "super-pure" plutonium and gave data for the measurement of nuclear parameters needed for the design of more advanced LMFBR systems. Other accomplishments were; a demonstration of the simplicity of working with liquid metal coolants, an evaluation of the effects of alloying materials on the behavior of metallic fuels, an evaluation of the effects of structural features on operational stability, and the first plutonium-fueled reactor loading which proved that a breeder reactor fueled with plutonium enjoys a higher breeding ratio than one fueled with uranium. (A breeding ratio of 1.27 ± 0.08 was established for the plutonium loading) [52].

In 1955 EBR-I's core melted down (Figure 77) during an experiment. Scientists were testing the capabilities of EBR-I and decided to turn the coolant off while increasing the criticality [53], which led to the meltdown.

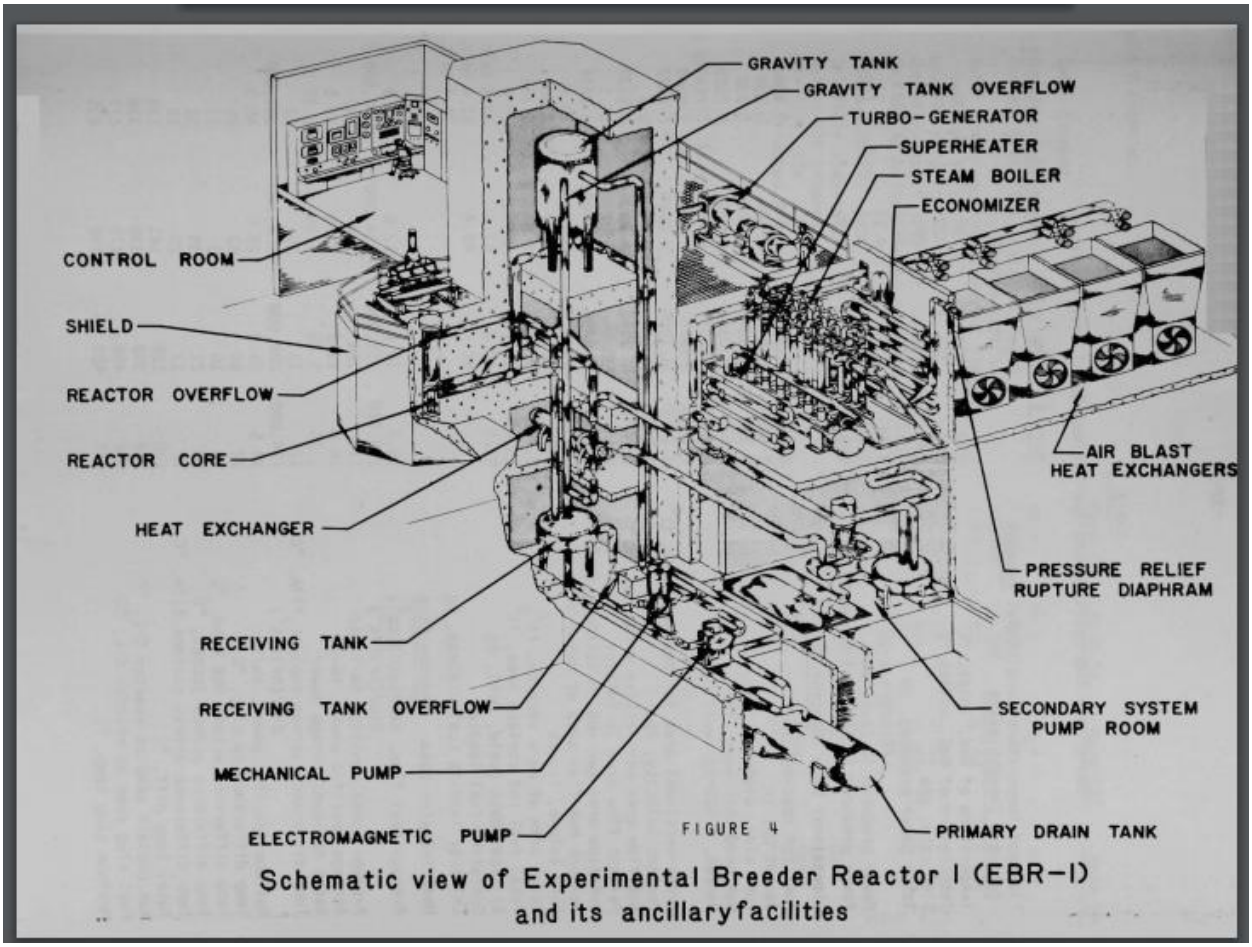

Figure 76. EBR-I schematic.

Following the completion of tests with the plutonium loading in 1964, EBR-I was shut down, placed in standby status, and in 1966 declared a National Historic Landmark under the stewardship of the United States Department of the Interior. The facility was opened to the public in June 1975. Visitors may tour the facilities, located on U.S. Route 20 between Blackfoot and Arco, during the period from June 15 to September 15 [35].

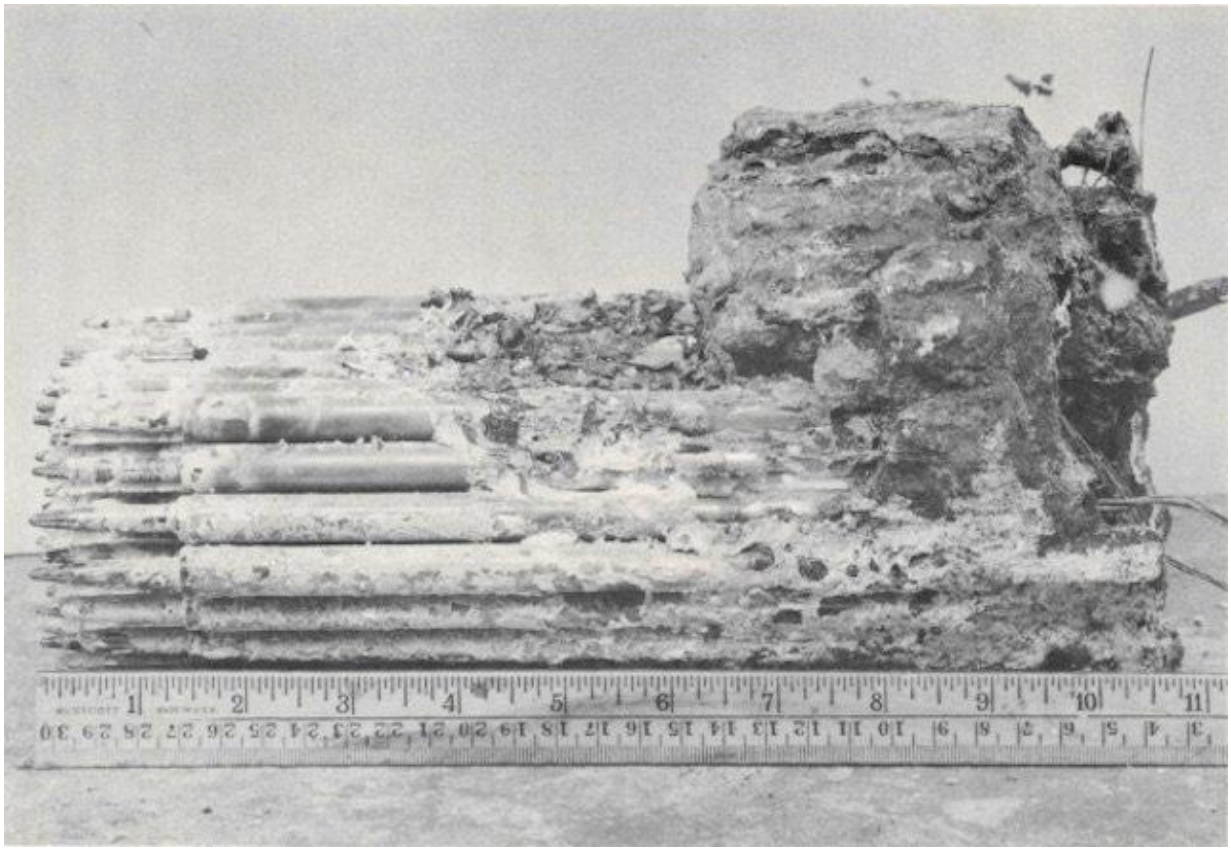

Figure 77. EBR-I melted core.

10.1.6 Experimental Breeder Reactor II

EBR-II was an LMFBR using molten sodium metal for the coolant. EBR-II's fission chain reactor occurred in the fast spectrum hence "Fast" and "Breeder" because it had the potential for breeding more fuel than it consumed. This LMFBR reactor was built in Idaho Falls, Idaho in 1961 by Argonne National Laboratory West, now known as Idaho National Laboratory, and is found in Figure 78.

EBR-II's purpose was simple: create a civilian power reactor producing fissile material--in the form of plutonium-239--meant for use later in fuel. EBR-II was in operation from 1964 until 1994 and was power rated at 62.5 MW.

Figure 78. Image of EBR-II facility design [35].

EBR-II provided insightful data about how fast reactors are possible on a large scale and with passive safety measures over its lifetime. The negative temperature reactivity coefficient showed the potential to drive the reactor power down without a SCRAM and a loss of coolant and heat sink. The tests showed the inherent safety of designs like EBR-II and other similar projects within the Integral Fast Reactor program [35].

EBR-II was located in the southeastern corner of INL as shown in Figure 79. The EBR-II complex was built in this location because in 1949 it was selected to be a national site for centralizing the construction, operation, and testing of reactor concepts. It is important to mention that EBR-II was not only a reactor, but a series of complexes dedicated to the research of breeding technology, like the reprocessing of EBR-II's spent fuel.

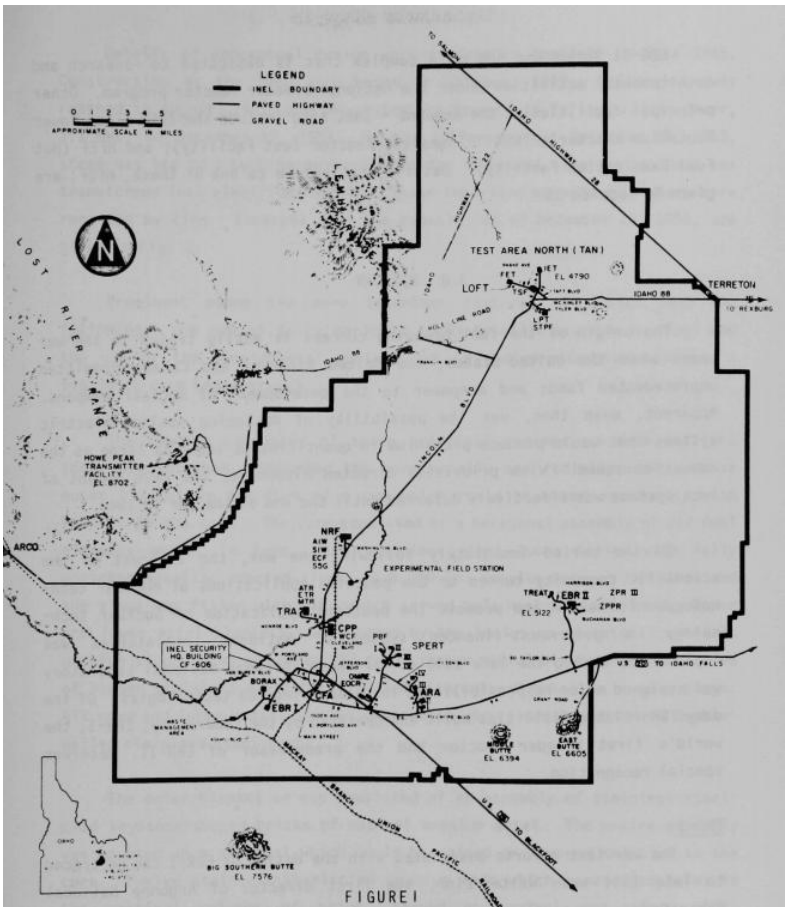

Figure 79. EBR-II location [35].

EBR-II's conception came as an outcome of the national breeder reactor program amongst EBR-I; ZPPR (Zero Power Physics Reactor); TREAT (Transient Reactor Test Facility); and HFEF (Hot Fuel Examination Facility).

After the success of EBR-I the "Atoms For Peace" program in the early 1950s prompted studies of a larger metallic-fueled, sodium-cooled system which eventually became known as EBR-II. The early intention or EBR-II was to show the feasibility of a metallic sodium cooled reactor to produce electricity and demonstrate the potential of reprocessing spent fuel [35]. Important dates in the design of EBR-II can be found in Table 18.

Table 18. EBR-II Important Dates [35]

Action	Date
Primary design features proposed to US Army Environmental Command	December 1953
Federal funds were authorized	July 1955.
Site preparation began	October 1957
Formal construction of the power plant, reactor plant, and cooling tower	June 58
Fabrication of the reactor vessel started	October 1958
The containment building was completed	December 1958
A rotary bridge crane was erected in the containment building	November 1959,
Plans for the FCF (Fuel Cycle Facility) and Sodium Boiler Plant were finalized	March 1959
Construction of these facilities began	July 1959.
Construction and installation work in the primary tank was essentially completed.	May 1961
All systems were ready for operation	June 1964

The EBR-II complex had three main facilities: the reactor housing, steam generation system, and power plant. From left to right in Figure 80 are depicted the sodium boiler building, the reactor and its containment building, and the power plant building.

EBR-II works by generating heat in the core, and then transferring that heat into the primary sodium coolant that is pumped through the core. The grid plenum assembly, as depicted in Figure 81, is responsible for directing sodium flow through the core and consists of upper and lower grid plates that are interconnected through a system of stainless-steel tubes. The plates are then surrounded by a cylindrical stainless-steel structure that also seal the pumped sodium flow. After the primary sodium leaves the core, a primary-to secondary heat exchanger is used, which is then discharged directly to the sodium-filled primary tank. The heated secondary coolant is then pumped from the heat exchanger to the sodium-boiler building where steam is produced and superheated. From this point the steam rotates a turbine which converts the kinetic energy of the rotation into electricity. With this design the EBR-II was capable of 62.5 MWt.

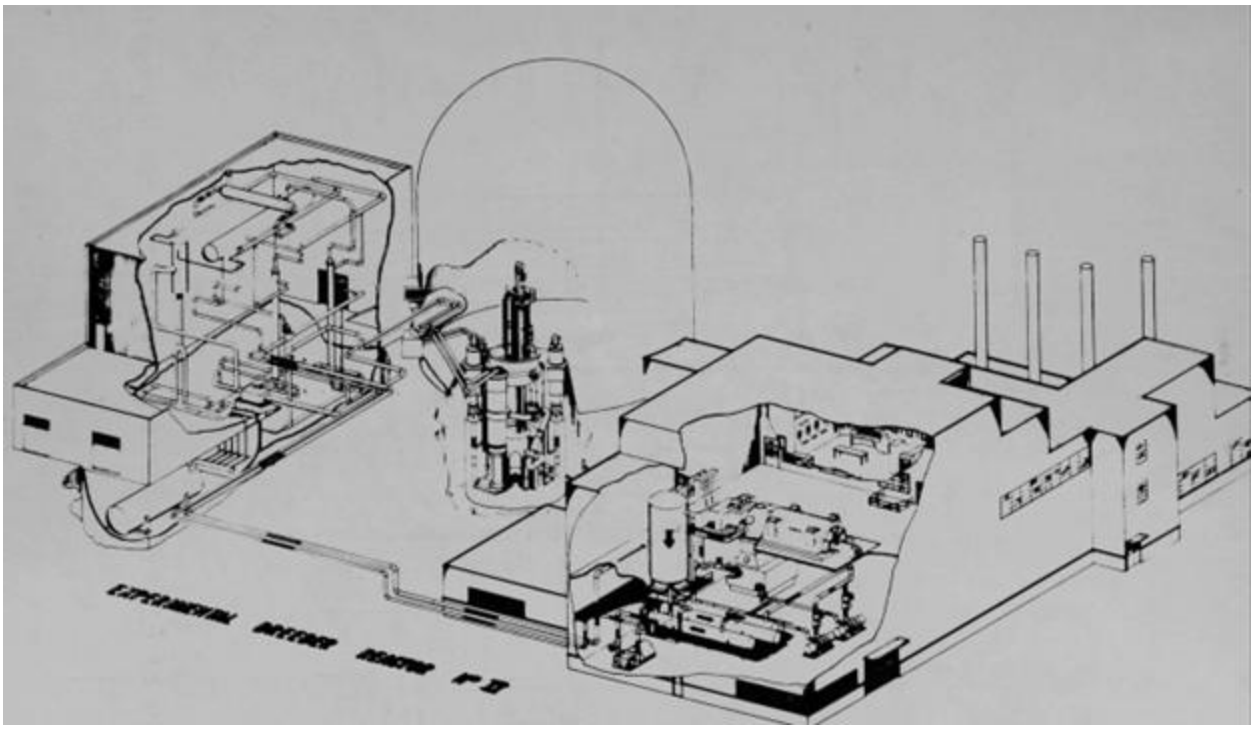

Figure 80. EBR-II complex [35].

Additional facilities related to the main complex are the HFEF/S and HFEF/N where discharged fuel and irradiation experiments are processed for ultimate disposition.

The reactor vessel consists of two concentric shells which form a cylindrical annulus filled with stainless-steel-clad graphite bricks. This can be seen in more detail in Figure 82.

EBR-II had many successes within its lifetime. The reactor core had a hexagonal assembly allowing placement of either the fuel or the material that needed to be tested [35]. Fifteen years of successful experience with the sodium-to-water steam generator (evaporators and superheaters) with no leakage of water into sodium. It was capable of loss of flow without scram and a loss of heat sink without scram, both from 100% initial power. Fifteen years of experience with under-sodium components such as pumps, flowmeters, intermediate heat exchanger, fuel handling equipment, etc., with only minor and repairable problems. Use of EBR-II plant steam for domestic heating at the ANL-W site since September 1974. Extensive experience in maintenance of sodium components; practical demonstration that maintenance and

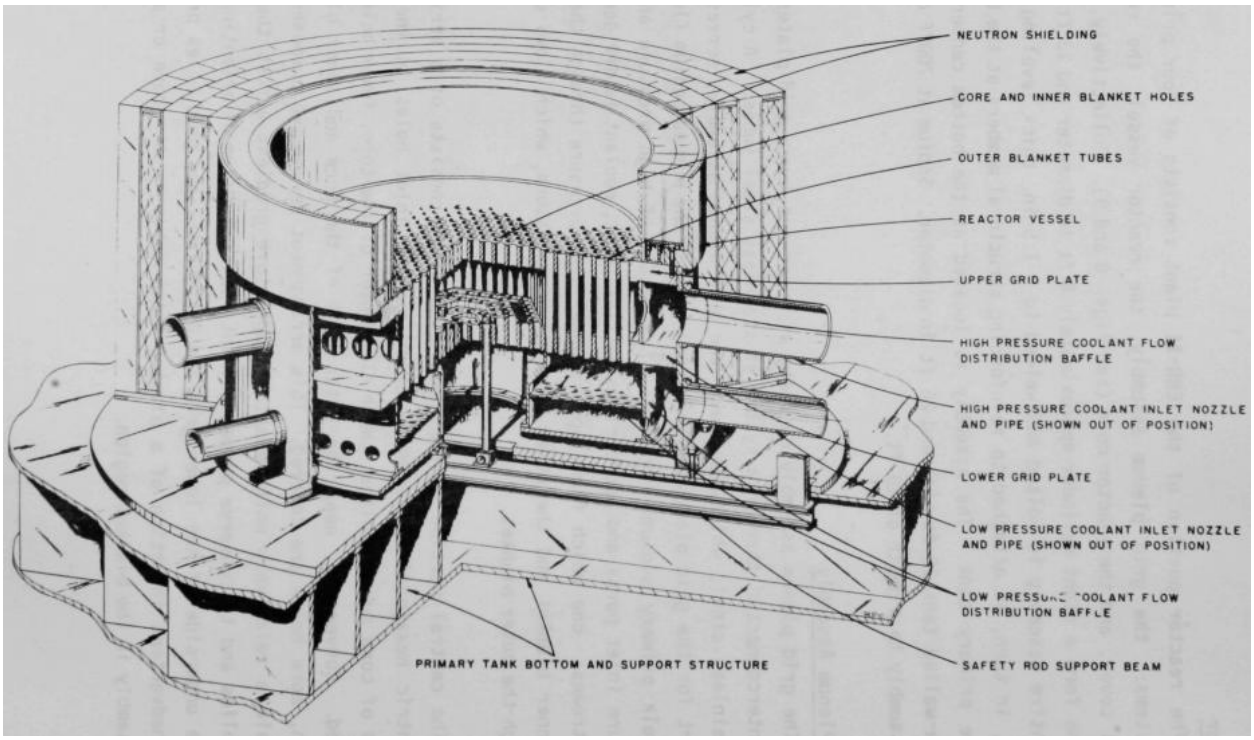

Figure 81. EBR-II grid plenum assembly [35]

repair of such components can be accomplished by straightforward techniques, with relatively simple equipment, and without undue hazard to personnel. Operation of the plant with minimal release of radioactivity to the environment [35].

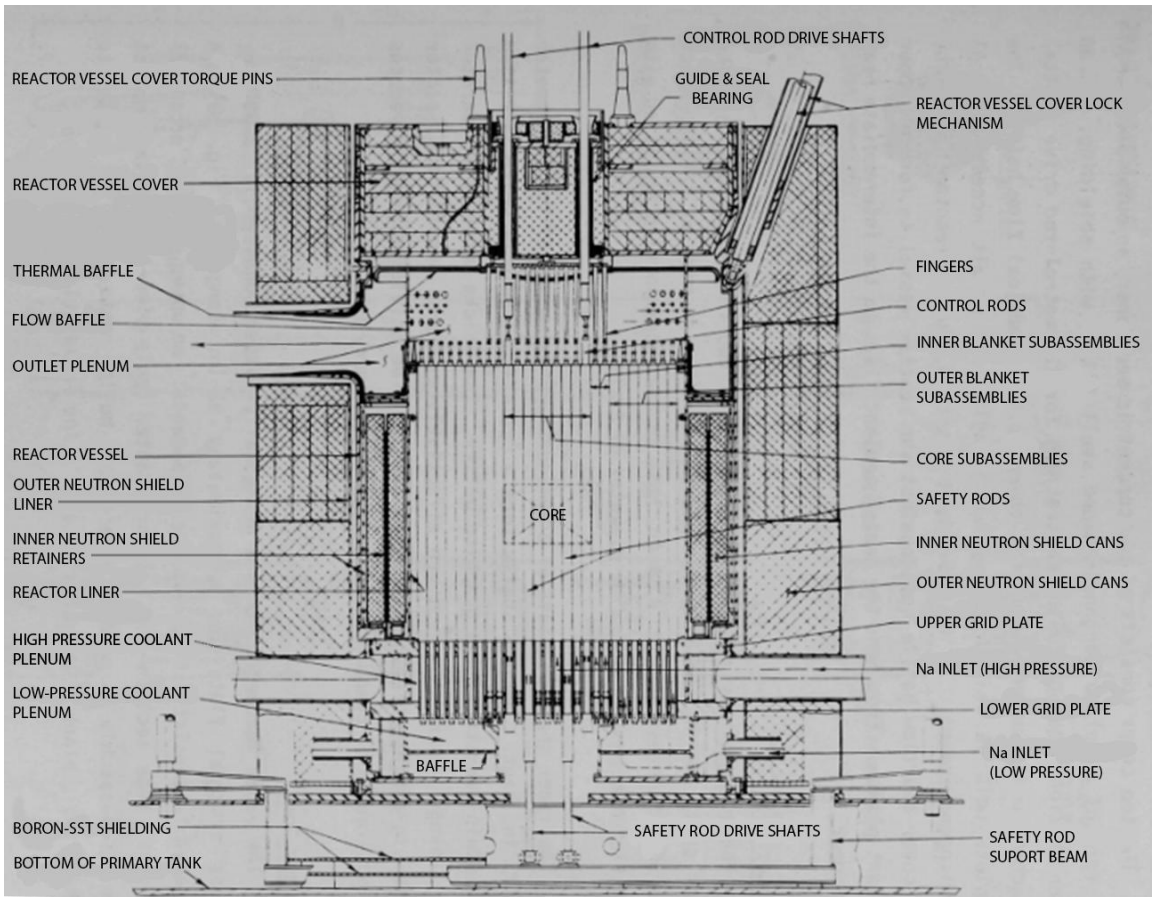

Figure 82. Reactor vessel assembly [35]

In 1968, a sodium leak took place in the secondary sodium system. Melted sodium (approximately 100 gallons) was spilled onto the floor of the secondary sodium control system. Prior to the accident "repairs were taking place on a bellows-seal isolation valve in the secondary-sodium plugging loop, freezing the sodium in the line, cutting out a section and then re-welding the section into the original line" [54]. Unfortunately, the frozen sodium plug did not extend as expected beyond the removed section and when it was welded into the pipe, the sodium melted and spilled to the floor. A major fire erupted but was contained and extinguished by application of Metalex (a mixture of salts which cover the burning sodium and starve the fire of oxygen). Cleanup was accomplished in 13 days and there were no injuries [54]. The incident can be seen in Figure 83.

In 1981, the super heater was separated from EBR-II's assembly for destructive examination. During the operation it was found that the SG tube-to-tube sheet had welding

discontinuities. These inadequate welds default in the baffle nest falling 22 inches away from its original location to the sodium flow stream. It is important to notice that during the 16 years of operation of EBR-II this accident did not produce catastrophic failure to its performance. Also note that this incident was not found or known about prior to the EBR-II disassembly of the steam generator in 1981 [55].

In 1994, funds for operations and research associated with the Integral Fast Reactor (IFR) project, including EBR-II, was terminated.

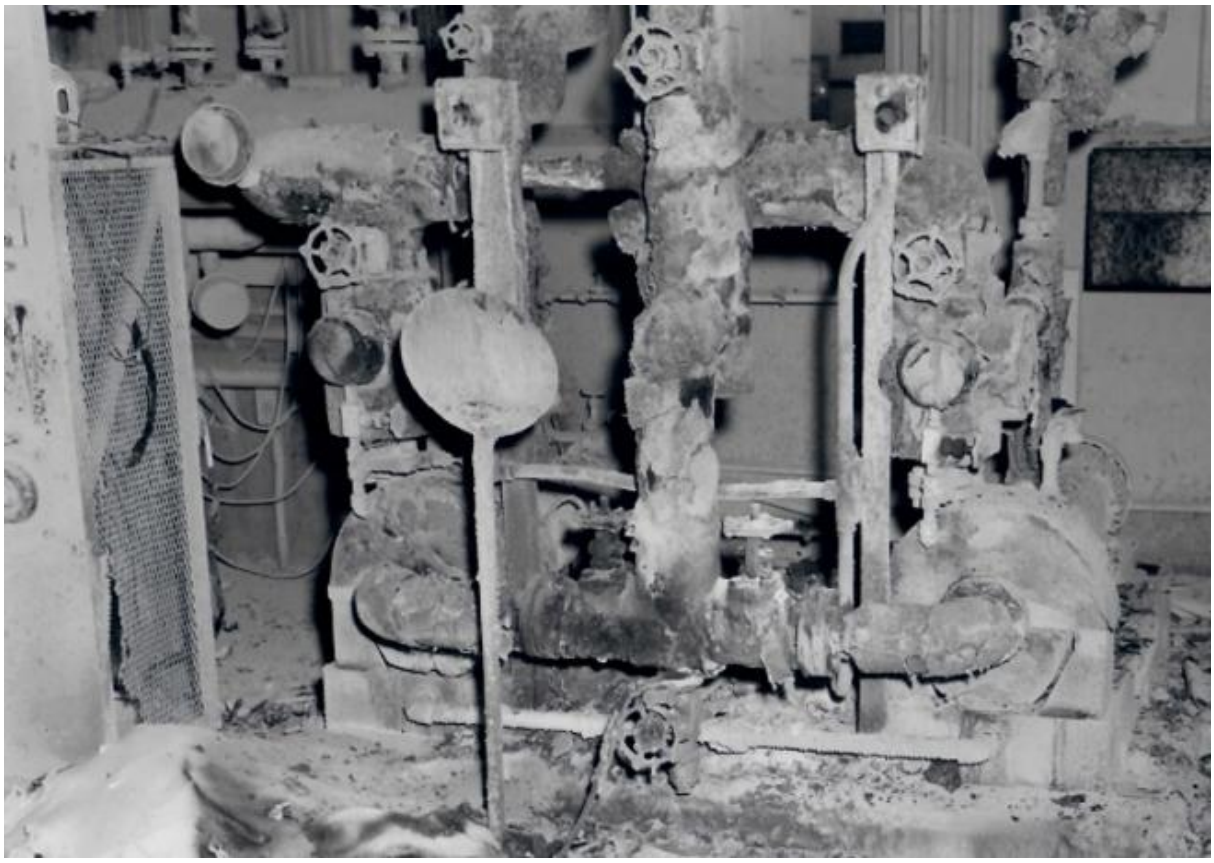

Figure 83. EBR-II sodium incident.

10.1.7 Sodium Reactor Experiment

The Sodium Reactor Experiment (SRE) was a graphite moderated, sodium cooled thermal reactor. The SRE was primarily used for experimenting, and secondarily used for generating electricity. The SRE was located 30 miles from the center of Los Angeles in the Semi Hills [56].

Design Concept

The SRE utilizes graphite as a moderator and reflector. Graphite is sufficient at slowing down neutrons to a thermal level and thus allowing the blend of uraniun-235 and thorium-232 fuel to be used. The reactor used liquid sodium as a coolant coupled with an inert gas cover comprised of helium. The basic layout of the heat exchange system is similar to other sodium cooled reactors. A radioactive primary sodium loop travels through the core and removes heat. This heat is then transferred to the nonradioactive secondary sodium loop through a heat exchanger, and then finally to steam generators for generating electricity. If generating electricity is not desired, the secondary sodium loop can instead be cooled through large cross flow air fans. The sodium loops operate near atmospheric pressure. The reactor core was situated below ground level, with a concrete foundation and the earth acting as shields [56].

The sodium coolant system played a critical role in reactor startup and shutdown. Before startup, the sodium is heated to 350°F using electric heaters and then pumped through the reactor. The reactor was brought up to critical, and then moderated to the desired level by reducing or increasing coolant flow. Care must be taken during startup to ensure temperature gradients are controlled and not allowed to cause damage to components and vessels.

Shutdown of the reactor utilizes four safety rods and four control rods. Each rod is about $2.5 of reactivity. The safety rods can be completely dropped into the core in about 0.5 seconds, while the control rods are actuated at about 0.3ft/min. Reactor scram is accomplished and monitored through several safety circuits, including: “a high flux level; a short period of neutron flux; loss of flow in the main sodium loops; a high temperature at the fuel element outlets; failure of electrical power; earthquake; loss of feedwater when operating steam plant; loss of air-blast fans when operating with air-blast heat exchangers.” Sodium flow during shutdown should be carefully monitored to negate any severe temperature transients [56].

The safety features incorporated into the reactor and its facility were well thought out. No reactions are plausible between many of the reactor components, such as sodium, uranium, steel, graphite, zirconium, cover gases, and NaK. Because of this lack of reaction, it can actually be difficult to detect when components fail, such as a cladding rupture [56]. Graphite has a large heat

capacity and operates between a temperature of 600-1,000°F, thus ensuring a minimum temperature transient and provides “relatively long time responses for control” [56].

The primary sodium loop is enclosed by a stainless-steel envelope which provides a gas-tight barrier which prevents air from mixing with the sodium and causing any reactions. Gaskets and O-ring seals at access plugs prevent sodium leaks at pump, pipe, and heat exchange locations. This gas tight barrier also provides an inert atmosphere of a helium cover gas to moderate the sodium in case of any leaks. These features a part of the primary loop can be seen in Figure 84.

The secondary sodium loop has potential of mixing with water as it enters the heat exchanger to generate steam. SRE incorporated double tube steam generators with a monitoring system that indicates fluid mixture to deal with this issue. A proper pressure relief system was put in place to handle any reactions that might occur.

The sodium pumps used in SRE are modified hot oil pumps of the impeller type. The pumps have two separate seals made from frozen sodium that prevent any leaks. The first seal is surrounding the impeller, with the second seal being between the impeller and pump housing. The sodium is kept frozen through an organic shield cooling system that uses Tetralin. A helium cover gas is maintained inside the pumps above both seals to mitigate any effects of frozen sodium failure. The sodium pump can be seen in Figure 85.

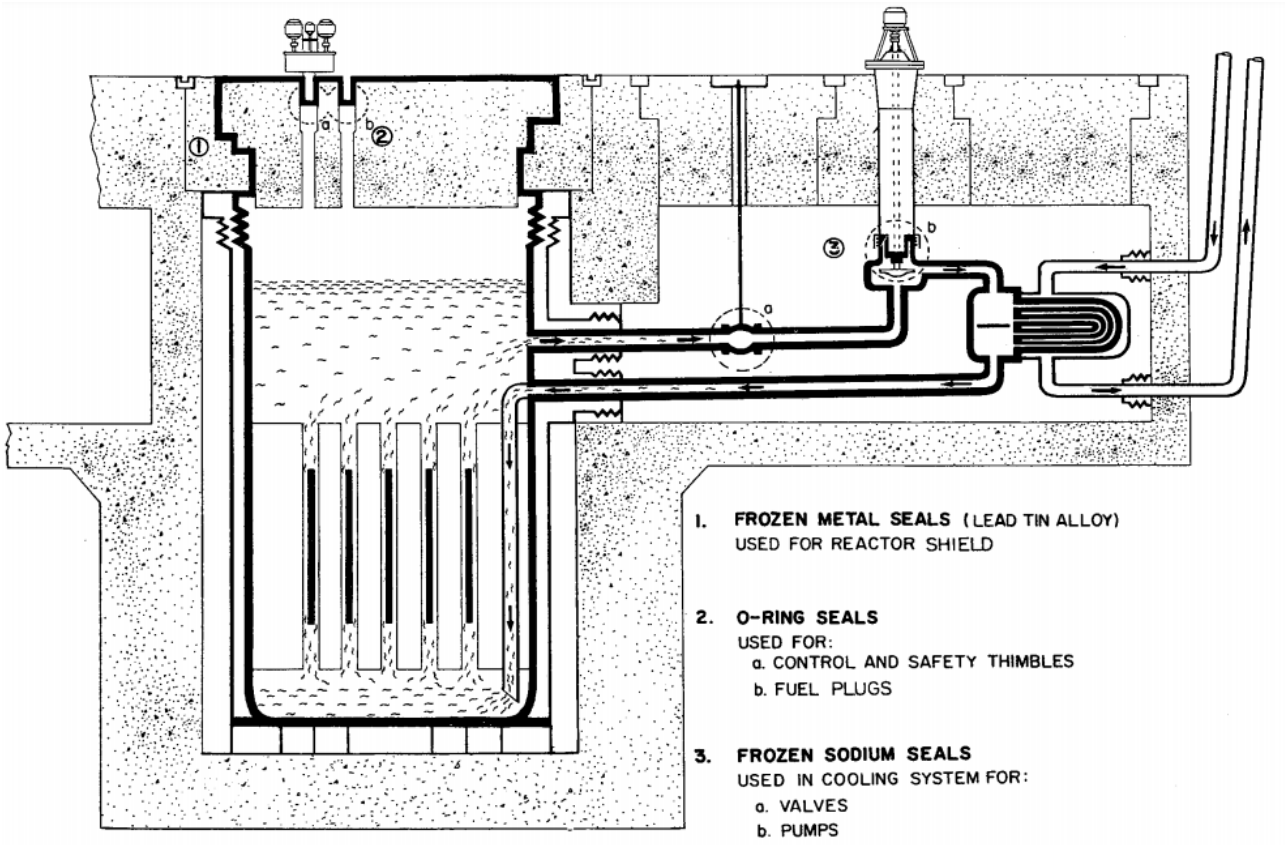

Figure 84. Reactor core and primary sodium loop. Heavy line indicates gas tight barrier [56].

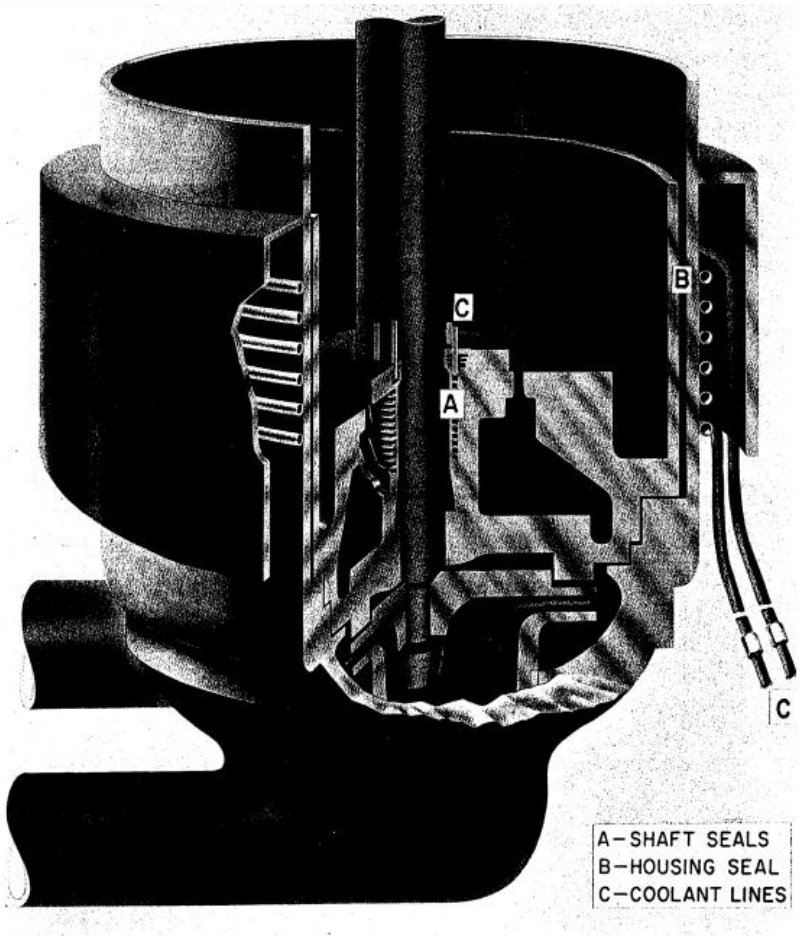

Figure 85. Sodium pump utilizing frozen sodium seals.

Accidents

During a test run between July 14-26, 1959, operators noticed signs that the reactors temperature was fluctuating and overheating. When the reactor was shut down and examined, it was seen that 13 out of its 43 fuel elements were partially melted or ruptured. A partially melted fuel element can be seen in Figure 86. After investigation, it was found that tetralin from the sodium pumps had been leaking into the sodium over a period of two weeks and was the ultimate cause of the fuel damage. The Ad Hoc committee that was assigned to investigate the incident listed the sequence of events as follows:

a) "Tetralin slowly leaked into the primary sodium vis a freeze seal on the main primary pump. The tetralin leaked into 1,000°F sodium for a period of about five days. The reactor was shut down to repair the pump, the tetralin continuing to leak into 350°F sodium for an additional 9 days.
b) Nitrogen was admitted to the system to purge the sodium of tetralin and some of its decomposition products. Seventeen fuel elements were removed from the core for the operation. These were viewed in the handling machine and appeared to be in good condition.
c) The pump and fuel elements were reinstalled and run 14 started at low power. Carbon and other tetralin decomposition products, as well as quantities of oxide, were still present in the core, though undetected. Partial plugging of several fuel channels is evident from the spread in fuel channel outlet temperatures.
d) The partial plugs in the channels were located randomly in the core and in the channels. It is possible that some of the elements were plugged before the run started. A few of those which had been removed and re-inserted between runs 13 and 14 plugged shortly after re-insertion.
e) In addition to excluding coolant locally, the plugs resulted in fluctuations in coolant flow. The fluctuation in flow produced severe thermal cycling of the fuel. The thermal cycling caused the fuel slugs to expend to such an extent that the cladding tubes were ruptured. The severity of the fuel distortion forces the conclusion that the fuel was cycled through the uranium α-β phase transformation temperature (1,220°F). In at least one area (the

"burst" area of the element from R-24) the temperatures were not sufficiently high to promote accelerated Fe-U diffusion.

f) The plugging interfered locally with heat transfer to such an extent that very high (above 1,400°F) temperatures were reached in several places even at low power, and Fe-U alloys were formed and melted."

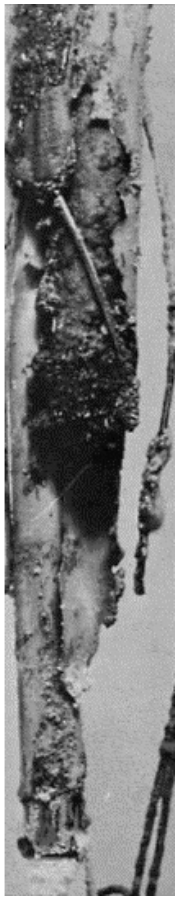

Figure 86. Partially melted fuel elements. [57]

The effected fuel slugs can be seen in Figure 87. The thermal cycling that occurred presented stresses that caused several fuel rods to eventually break. After this incident, the tetralin coolant was no longer used in the sodium pumps.

The problems that arose from the coolant leak took over a year to address, and the reactor was restarted on September 7, 1960. During the recovery process, radiological activity and airborne contamination was constantly monitored not only inside the facility to keep personnel

safe, but also in the stack to limit release into the atmosphere. Some individuals were exposed up to 600 mrem during a week's time to complete certain tasks of recovery. These individuals were then secluded from radiation for at least a week after such exposure was necessary. Overall, the average exposure for the 150 personnel directly involved in the recovery process was 2 rem/year [58].

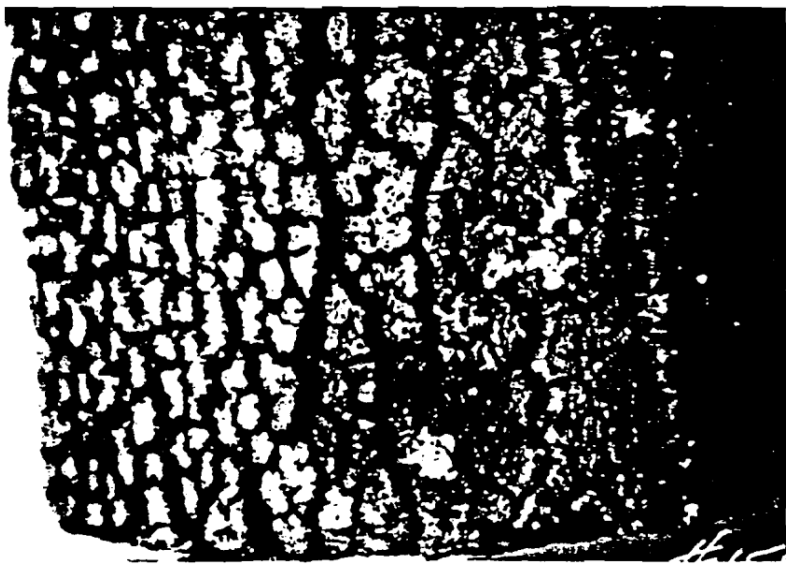

Figure 87. A fuel slug showing effects from thermal cycling.

10.1.8 Fermi 1

The Enrico Fermi Atomic Power Plant Unit 1 (Fermi 1) was a fast breeder reactor located in Monroe County, Michigan [59]. The coolant utilized in Fermi 1 was molten sodium near "atmospheric pressure" [59]. Fermi 1's design allowed for operations at 430 MWt; the maximum power achieved was 200 MWt [59]. Fermi 1's first commercial startup was on August 7, 1966 [60].

The design of the reactor's vessel is shown in Figure 88. The reactor is made of stainless steel "sealed at the top by a rotating shield plug which supports the control mechanisms, the hold down mechanisms, and the fuel handling mechanism" [61]. Over the years, the reactor vessel of

Fermi 1 had “only encountered insignificant operational problems” [62], where the design of the vessel was nearly identical to that of EBR-II, known as the Hallam vessel [62].

The core and blanket consisted of square subassemblies which held cylindrical “fuel pins and blanket rods” with a diameter of 80 inches and 70 inches in height, as shown in Figure 88 and Figure 89. The fuel pins were zirconium-clad pins with molybdenum alloyed to 25.6% enriched uranium. The fuel subassemblies consisted of 140 pins “for a total mass of 4.75 kilograms” [61].

The reactor was controlled by two control rods and eight poison safety rods, as seen in Figure 90. One of the control rods was for “regulating purposes and the other for shimming”, resulting in the average reactivity rate for the control rods to be $0.01 per second and $1 per minute, respectively [61]. The safety rods were composed of boron carbide, where the boron was enriched with boron-10. The eight safety rods were uniformly spaced around the center of the core to provide a total negative reactivity of $9 [63]. While in operation, the safety rods were “held just above the axial blanket section of the core so that they can be rapidly inserted into the core if a scram becomes necessary” [61].

Fermi 1 serves as an example as one of the first commercial power plants to experience a nuclear accident and the second sodium cooled fast reactor in the United States to melt fuel. The event that occurred yielded a partial meltdown of two fuel assemblies out of the original 93 [64]. The cause of the meltdown was from an experiment performed to investigate abnormal temperatures in two fuel assemblies in a location within the reactor core [65].

Fermi 1’s melt down occurred on October 5, 1966 during power ascension [64]. The occurrence was originally believed to be a thermocouple fault. The method employed to investigate the fault was to move the two affected fuel assemblies and using different thermocouples at a lower power of 67 MWt [64]. During the approach to 67 MWt, the reactor operator received “erratic neutron population” at a power of 20 MWt, this was corrected by placing the reactor into a manual control mode and waiting for the behavior to cease before returning to automatic control; the fluctuations reoccurred at 27 MWt [64].

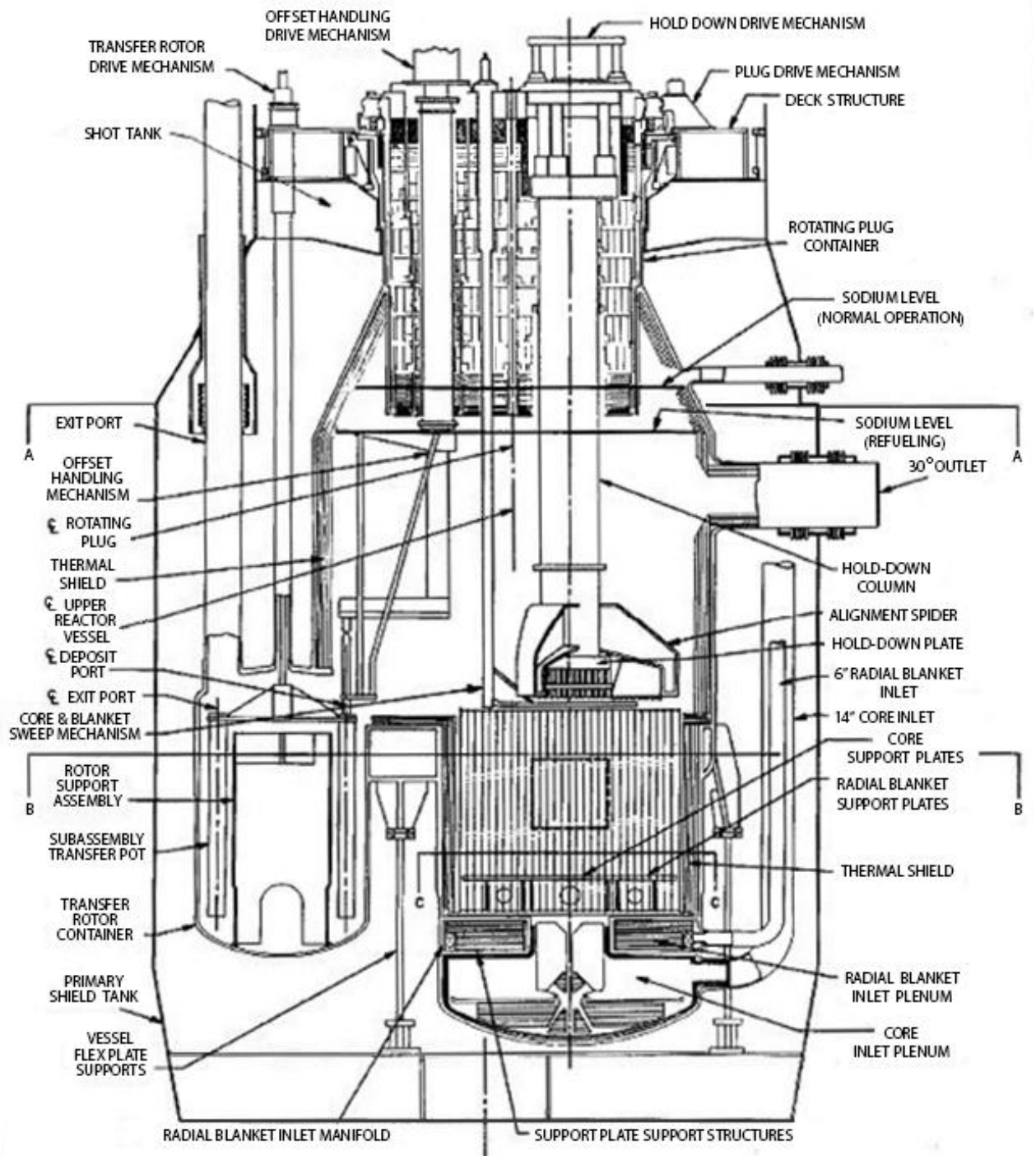

Figure 88. Elevation view of the Fermi 1 reactor vessel [64].

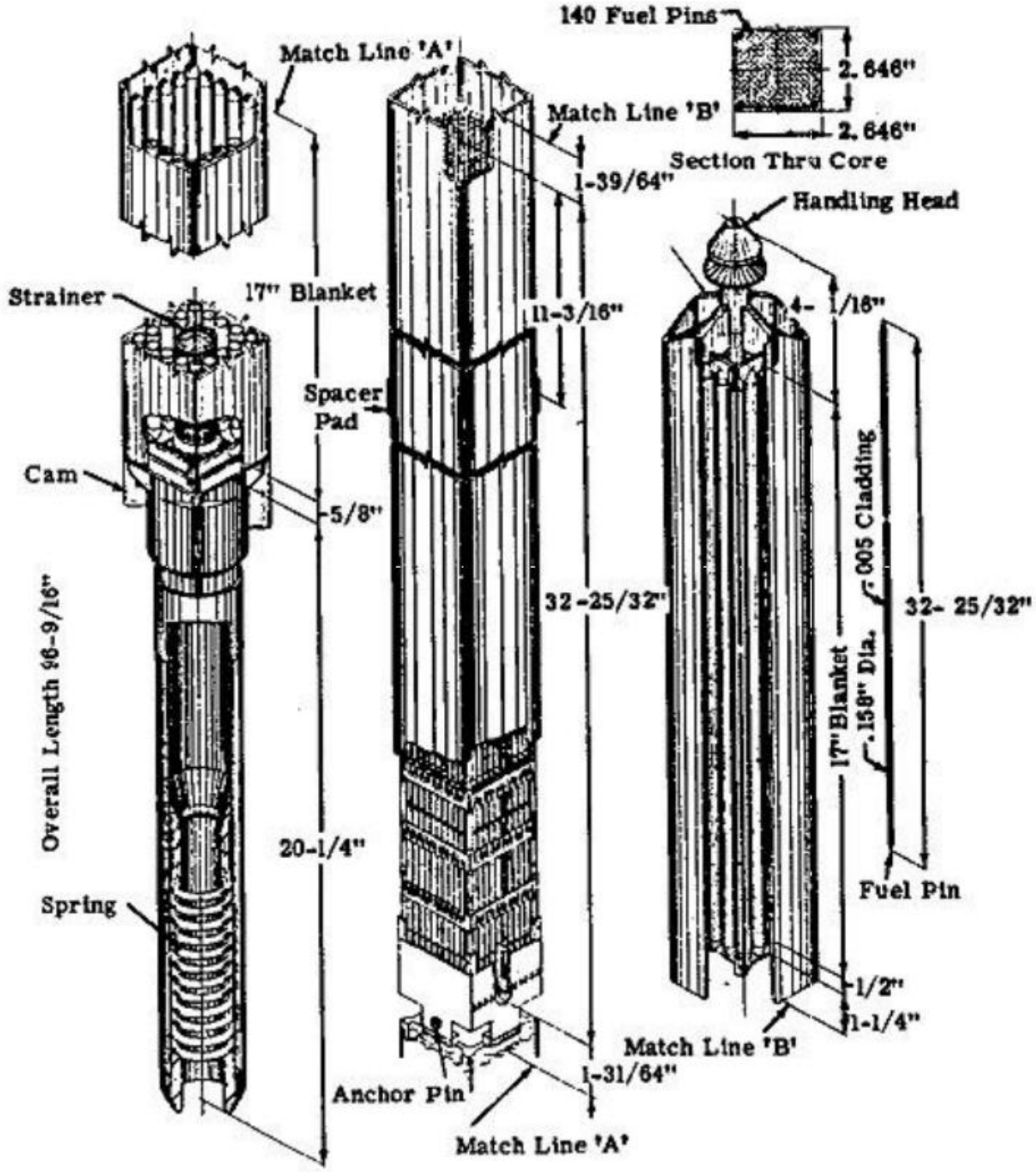

Figure 89. Isometric view of Fermi 1 fuel assembly [64].

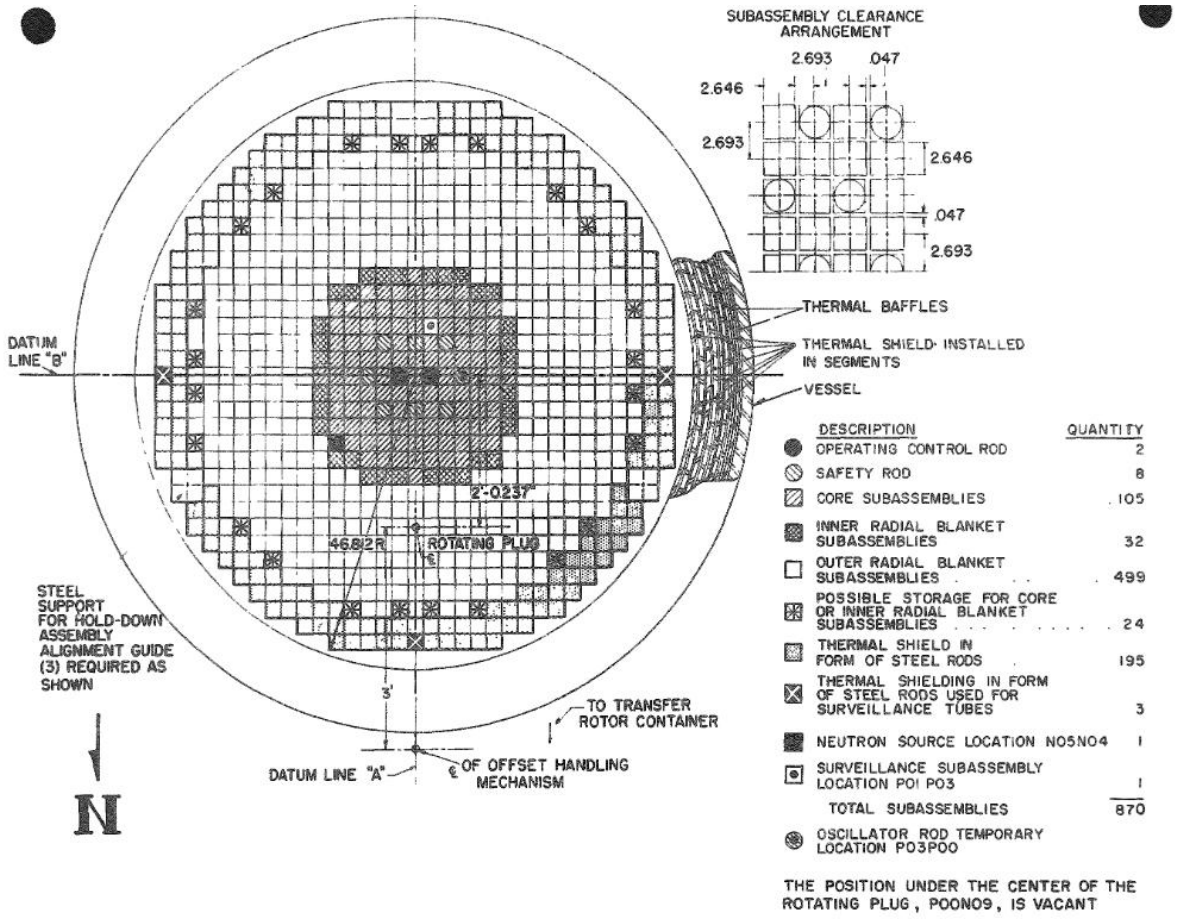

Figure 90. Cross section of Fermi 1 reactor core [61].

The operators also noted that the reactor control rods were withdrawn farther than normal for usual operations. Figure 91 shows the area where the accident occurred in the reactor and shows the various components in the vicinity of the reactor. The debris within the reactor that caused blockage was the deflector plate. The deflector plate, while small, was sufficient enough to increase the temperature of the two fuel assemblies and cause a meltdown of the metallic uranium fuel.

Fermi 1's decommission was due to the fuel within the core "approaching the burnup limit," in 1972 [59]. The reactor was decommissioned via a safe storage method [59]. The Safe Storage Method of Decommissioning is a decommissioning method involving the removal of "all liquid radioactive material" and the removal of "all portable solid radioactive materials" [66].

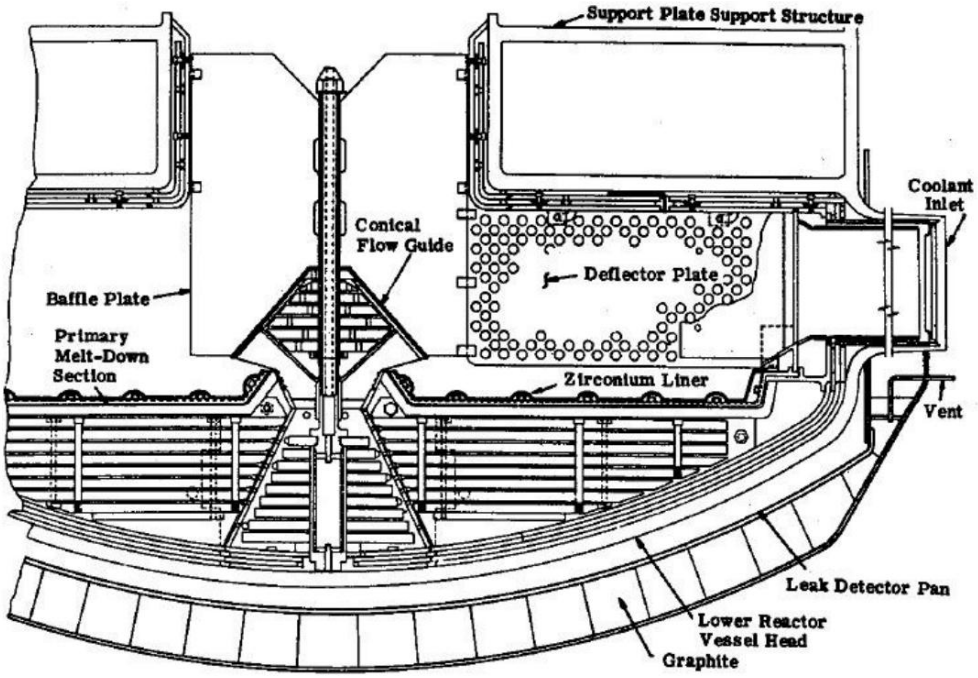

Figure 91. Elevation view of the accident segment [64].

However, the structures and equipment that remain are secured and kept under surveillance, ensuring the "protection of the public" [66].

The "primary and secondary coolant loop were drained" and the primary loop was subjected to carbon dioxide to form sodium carbonate, a substantially less reactive substance, from the residual sodium left in the loop. The secondary sodium loop was "cut and sealed" [67].

In 1997, a study conducted by the Detroit Edison company exhibited excess buildup of liquid sodium potassium and sodium carbonate in areas where the secondary loop was "cut and sealed", resulting in a sodium hazard where exothermic reactions from both the unused sodium potassium and sodium carbonate could occur if oxygen or propane are present, respectively [67]. There have been significant efforts to fully finish the decommissioning following the discovery in 1997, however due to the exothermic reaction resulting from processing the primary coolant loop in a scrubber, the process vessel cracked and the need for more effective processing has postponed the project as of 2009 [67].

The Fermi-1 accident showed the importance of educated operators on heat transfer and the implications of heat within a reactor vessel. The thermocouple should have been checked prior to operation and the fluctuations in power should have been an indicator of the necessity to SCRAM.

Following the accident, the decommissioning process exhibited the need for more controlled and consistent decommissioning of sodium cooled fast reactors, as the scrubber used to process the primary coolant loop exhibited faulty engineering which resulted in a cracked process vessel, costing the decommissioning company and Detroit Edison a lot of money and years spent repairing the vessel, ultimately lengthening the decommissioning process. The secondary coolant loop's decommissioning was faulty as the loop should have been processed instead of sealed up, as ultimately the resultant residue and liquid found in 1997 posed a threat to the wellbeing of people and the environment.

10.1.9 Fast Flux Test Facility

FFTF is a 400-MW, liquid sodium-cooled reactor located at the Hanford Site in Richland, WA. FFTF was built as part of the U.S. liquid metal reactor program in the 1970s. The Facility operated successfully from 1982-1992 performing tests of reactor fuel assemblies and materials, studies on operational safety and reliability of liquid metal reactors, and tests of the ability of FFTF to produce a wide variety of radioisotopes for applications in medicine, industry and research [68]. An aerial view of the facility can be seen in Figure 92.

Figure 92. Aerial view of FFTF.

Figure 93 depicts the Hanford Site and the surrounding area. FFTF is situated in area 400 of the site, with laboratory facilities at the 325 building that provided 22 different isotope processing lines.

The FFTF began its 400 MWT power operation in April 1982. The plant was designed and analyzed for a 20-year lifetime (at 400 MWT and 75% capacity factor). Several replaceable components in the reactor vessel (in the high neutron flux) were analyzed for 10 years of operation with the intent that they either be replaced or re-analyzed if operation after 10 years was desired. In 1985, as the 10-year limit was approaching, the project 1) began analysis to extend the life of the 10-year components, based on actual core structural specimen radiation damage data, and 2) revised (updated) flux profiles using more recent in-core dosimetry measurements [34].

In 1986, a significant study was undertaken to consider using FFTF for electrical power generation and/or liquid metal reactor (LMR) steam generator testing. Thus, an additional 20 years of operation beyond the 10 years at projected restart for the new mission was desirable.

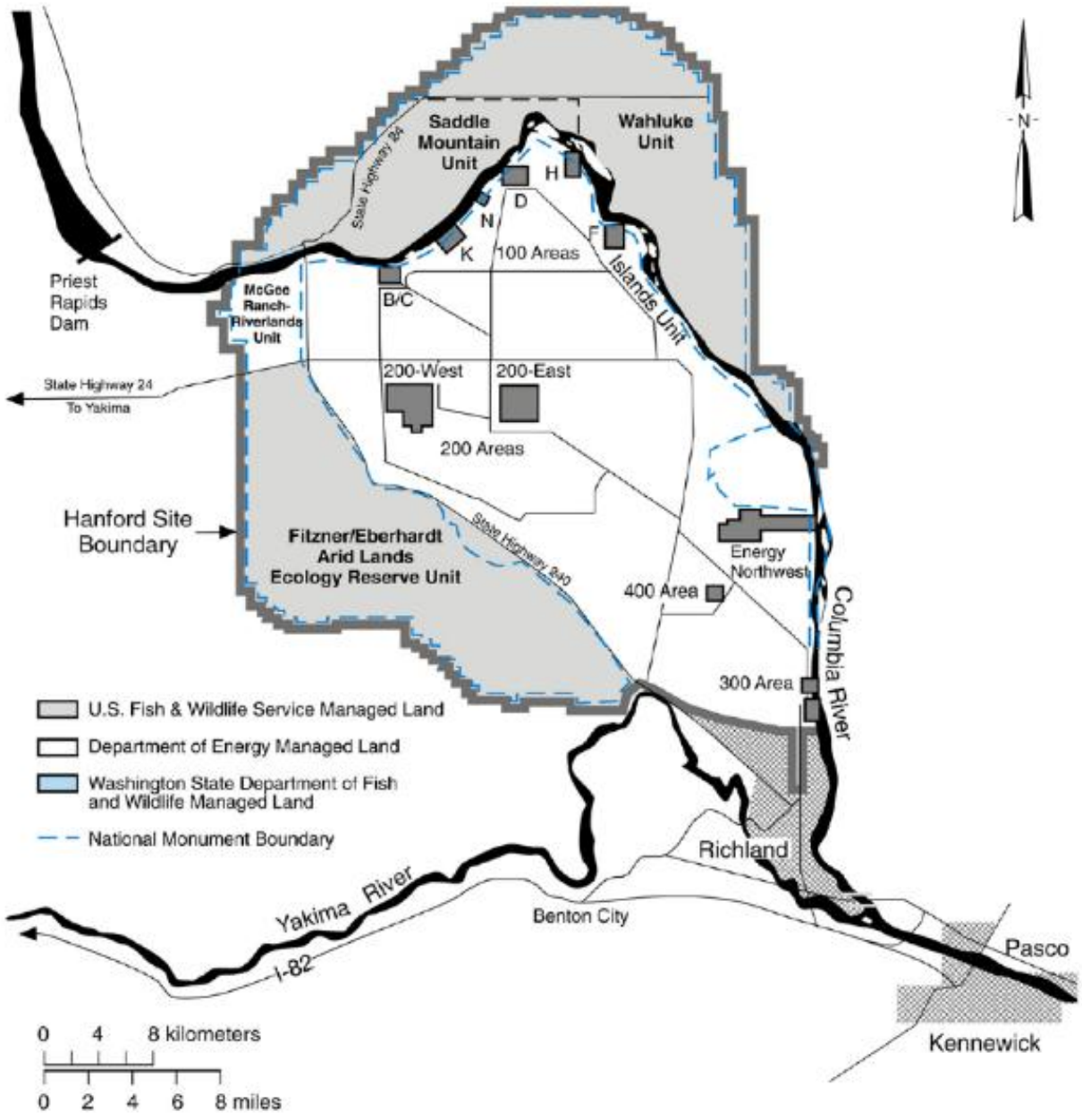

Figure 93. FFTF location.

In April 1990, the analysis of the 10-year components for 30-year life was completed and transmitted to the DOE-Richland Operations (DOE-RL) for their review and approval. All analysis was based on the latest LMR design/analysis criteria and all reports were peer-reviewed by Stone and Webster. DOE-RL approved the 10-year component life extension documentation in January

1991. The 20-year reactor component extension to 30 years was completed in December 1992, using the same analytical methods followed for the 10-year components [34].

The FFTF reactor is positioned in a heavily shielded cell at the center of a domed containment building. Heat is removed from the reactor by liquid sodium circulating under low pressure through three primary cooling loops. Intermediate heat exchangers separate the radioactive sodium in these primary loops from the nonradioactive sodium in the secondary system. Three secondary sodium loops transport the heat from the intermediate heat exchangers to twelve dump heat exchangers, which are cooled by air. Figure 94 depicts the main heat transport system utilized by FFTF [34].

The ability to perform the above tasks proves the flexibility, reliability, and safety of the FFTF and the capabilities of the Physics and Engineering staff

Examples of some of the FFTF's various missions include: Fusion Program material testing; Space Isotope Program testing (Pu-238); Space Reactor Program materials testing; International Testing Program, specifically for Japan and the European Fast Reactor Programs; Liquid Metal Reactor (LMR) fuel testing; LMR passive safety testing; and medical/industrial radioisotope production [34].

Although FFTF achieved an outstanding record of performance and operational safety during its decade of operation, the lack of a long-term mission forced DOE in 1993 to place the reactor in a standby condition during preparation for a phased shutdown [34].

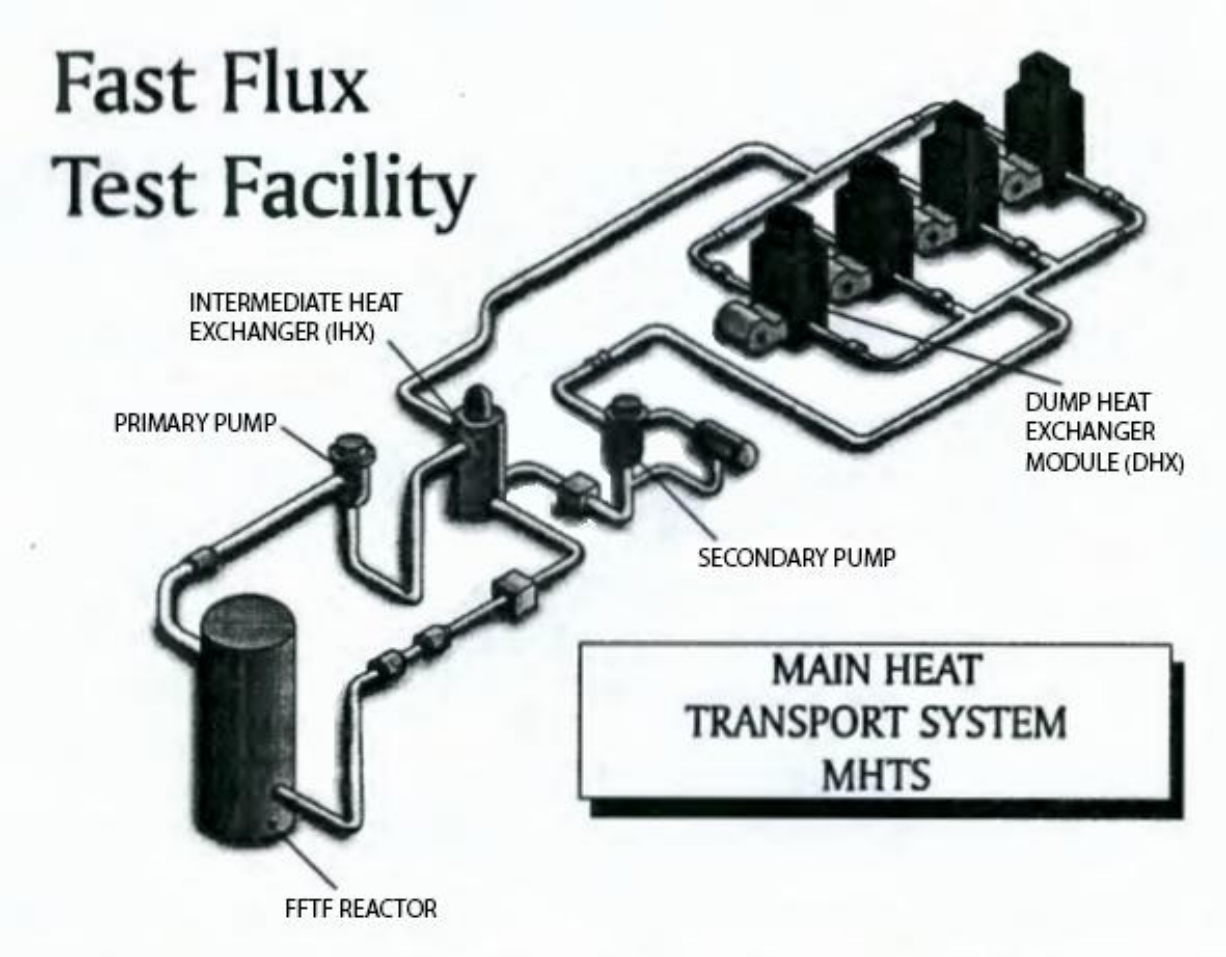

Figure 94. Main heat transport system.

10.2 United Kingdom Fast Reactors

10.2.1 Prototype Fast Reactor

The Prototype Fast Reactor (PFR) was the second reactor to be constructed in Dounreay, Scotland as part of a British nuclear research initiative. PFR was first connected to the grid in 1975 and operated until 1994. Key characteristics associated with the PFR reactor can be found in Table 19 [1]. PFR was primarily built as a research reactor for testing different types of fuel assemblies and secondarily for electricity generation. The site layout for PFR can be seen in Figure 95.

The core of PFR contains 78 fuel assemblies with an inner and outer zone. The inner zone is comprised of 28 assemblies that have a plutonium/uranium content of 22%/78%. The outer zone is comprised of 44 assemblies with a plutonium/uranium content of 28.5%/71.5%. A more uniform power density is resulted from the outer core containing a higher plutonium density. The core layout of PFR can be seen in Figure 96. The core has six different locations available within the inner zone that can hold experimental assemblies. Depending on what needed to be tested, it could be used for fuels, materials, or anything else that was desired.

Table 19. Key Characteristics of PFR.

Thermal Power	630 MWt
Electric Power	250 MWe
Efficiency	39.7%
Coolant	Na
Number of Primary Cooling Loops	3
Core Inlet/Outlet Temperature	562°C/700°C
Mass of Na in Reactor Tank	919 t
Fuel Material	$PuO_2 + UO_2$
Number of Turbo Generators	1
Turbine Inlet Temperature	538°C
Turbine Inlet Pressure	161.7 kg/cm^2
Steam mass flow rate	854 t/hr

A rotating shield plug is placed above the core and holds the refueling machine. Rotation of the plug gives the machine access to every reactor assembly. Spent fuel that has a heavy nuclide burnup of about 10% is taken and stored in a transfer rotor for a month until decay heat reduces to 15 kW. The spent assemblies are continuously cooled by liquid sodium. After the assemblies have had enough time to decay, they are transferred to an irradiated fuel cave where they are examined and then sent to a reprocessing plant via sodium tanks. The assembly transfer system can be seen in Figure 97.

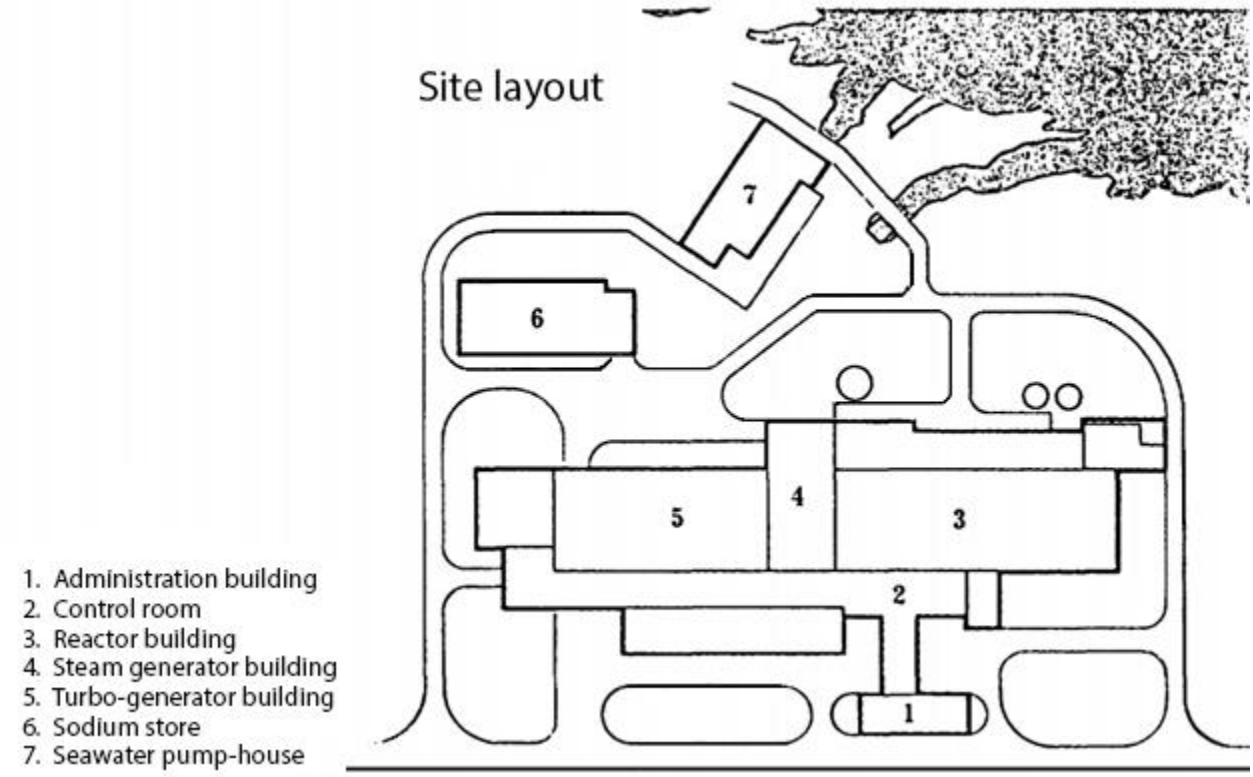

Figure 95. Site layout for PFR in Dounreay, Scotland.

All equipment used for processing and handling assemblies are done below sodium level. A viewer utilizing 1 MHz ultrasonic signals was successfully used to scan and examine equipment. These viewers provided high quality pictures.

The fuel type used was a mixed oxide made from $(Pu+U)O_2$. The fuel rods were arranged into a triangle lattice structure and had a standard length of 2.25 m and an OD of 5.84 mm, with a cladding thickness of 0.381 mm. The fuel element was comprised of a 0.915 m region of active plutonium that was bound above and beneath by a blanket of depleted UO_2 pellets, along with a 1.19 m long plenum to catch fission gas and prevent it from releasing into the primary sodium coolant.

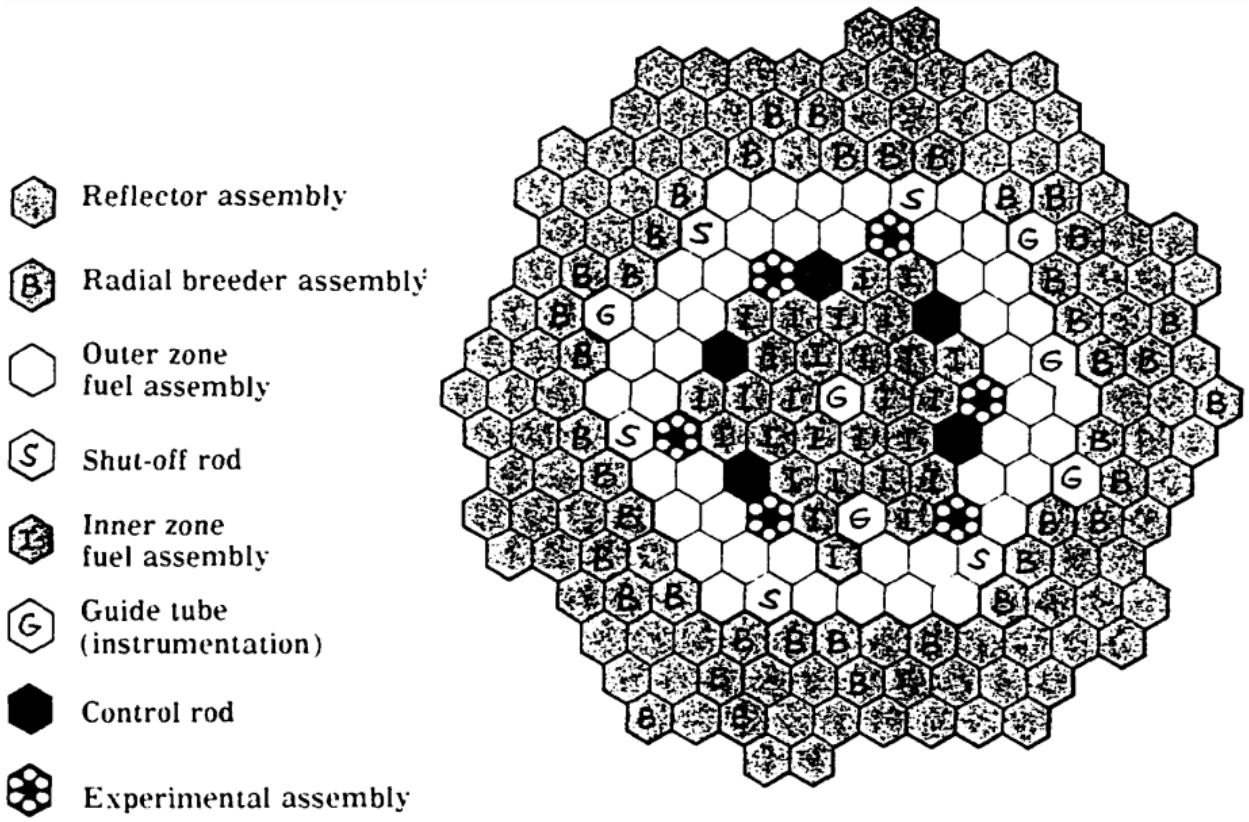

Figure 96. PFR core layout.

In case a fuel pin does fail, a detection system is put in place to monitor the presence of fission gases. Within the blanket region, the fuel rods have heavy fins attached on the outside region to promote uniform mixing of the passing sodium before a sample is taken. The sample is measured for delayed neutrons in the coolant and will shut down the reactor if a failure is detected. Only a few fuel pins have failed out of the 93,000 that were used throughout PFR's lifetime.

Control rods were first made of tantalum but later changed to boron carbide. A complete withdrawal of all control rods would lead to an increase in reactivity of 2.64 cents/s in the core. If an uncontrolled power increase does occur, it will be stopped by either a power deviation trip or by the core outlet temperature trip. Each of these trips will prevent the cladding temperature from exceeding 740°C and prevent sodium boiling. These trip systems were very important because sodium boiling introduces gas bubbles into the core and can lead to unpredictable reactivity.

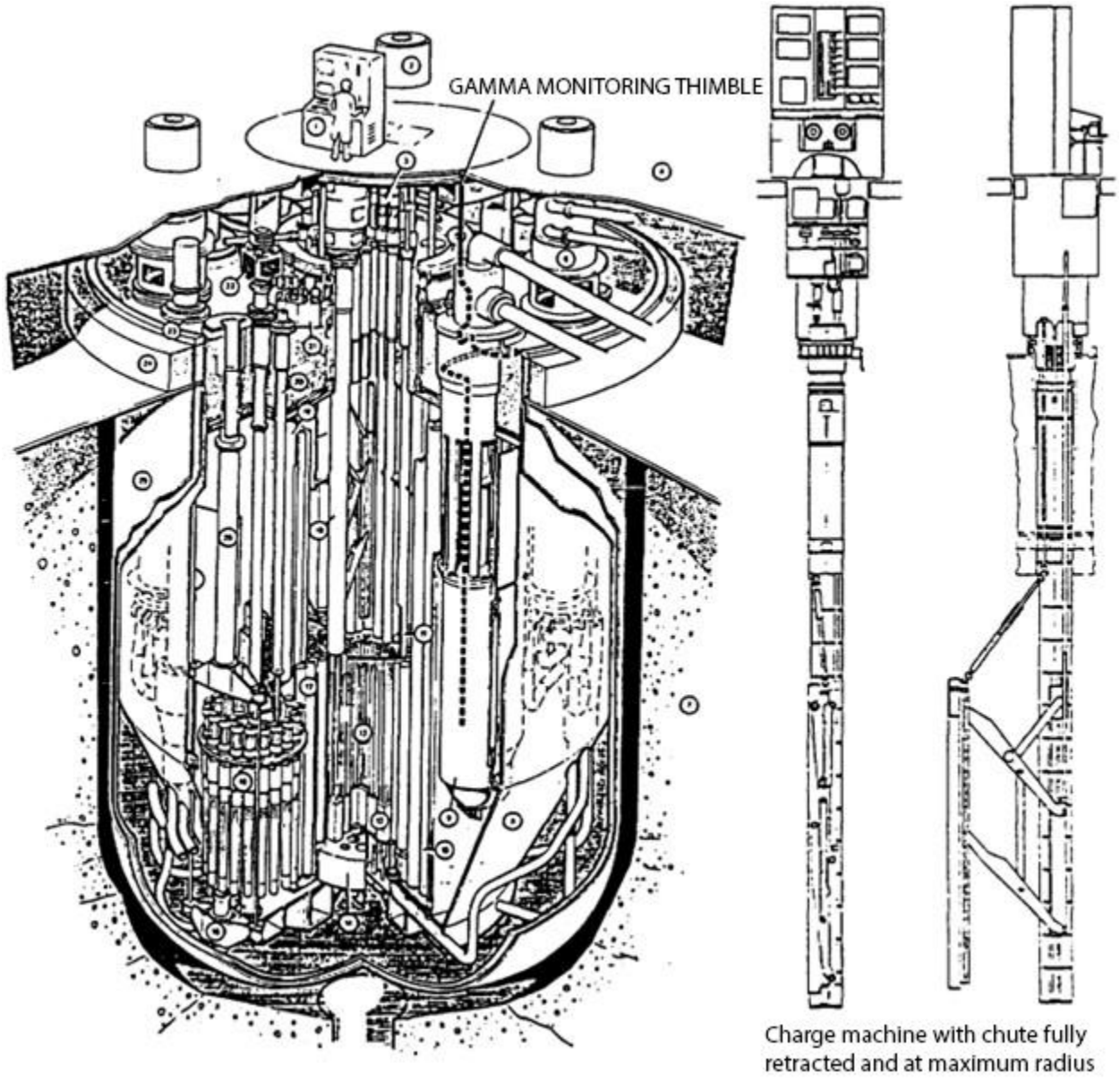

Figure 97. Assembly transfer system utilized inside reactor vessel.

PFR tested many different types of cladding material for their properties at high temperatures and under different neutron radiation loads. Among the materials tested were advanced optimized austenitic steels, ferritic steels, and Nimonic alloys. The Nimonic PE16 alloy proved to be the cladding of choice.

The PFR is a pool type reactor consisting of a primary and secondary sodium circuit. A few advantages to the pool type reactor are;

1) “The whole primary cooling system is submerged in the pool tank. Any leak in the primary system is unable to lower the sodium level in the pool

2) The main pool tank is surrounded by a safety tank, which should guarantee that a ‘Loss of Coolant Accident’ which leads to the uncovering of the core is almost impossible.

3) The sodium circuits are not pressurized, and a temperature increase of almost 400°C is possible before boiling takes place.” [69]

The primary circuit is completely enclosed inside the reactor vessel to prevent radioactive sodium from escaping and possibly releasing into the atmosphere. The reactor pool tank, the reactor core, and all the core components are suspended from a fixed roof structure to reduce stresses on the reactor vessel. The vessel has a secondary leak jacket surrounding it to catch any sodium leakage, and is also suspended from the fixed roof structure. The vessel has a graduated thickness which permits an acceptable axial temperature from a material safety standpoint [69].

Heat is transferred between the primary and secondary sodium through six IHXs using three primary mechanical pumps and three secondary mechanical pumps. The heat exchangers utilize counterflow shells with 1,540 tubes of an outside diameter of 19 mm and a length of 4.57 m. The number of tubes increases the surface area and the effectiveness of the heat transfer system. The heat exchangers are also suspended from fixed roof structure. The secondary circuit has three independent loops with 200 MW steam generators each. The secondary loop is comprised of an evaporator, reheater, and superheater. This allows for the sodium to be heated and reheated to increase the plant efficiency. A schematic of the steam generating process can be seen in Figure 100.

PFR experienced early on many problems with the leaking in the steam generators. The welds for the tube and tubeplate for the evaporators could not be stress relieved after fabrication. Cracking was caused by delayed reheat that led to stress corrosion. The problem was solved by implementing a sleeve technique that was applied to 1,000 welds in the steam generation system. In the case of the reheater, cracking was so bad the system had to be redesigned. A later technique

was developed for addressing cracks in the steam generator that involved finding, removing, and fixing defects.

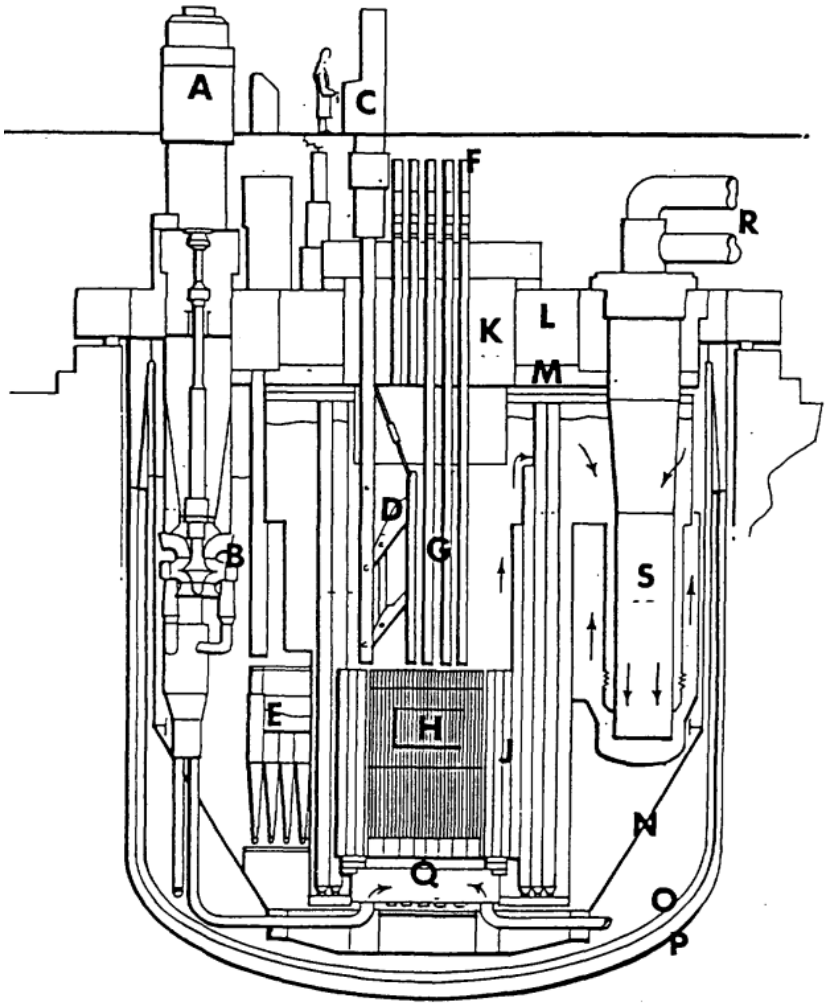

A.	Sodium pump motor (3)	K.	Rotating shield
B.	Primary sodium pump (3)	L.	Biological shield
C.	Charge machine console	M.	Stainless steel insulation
D.	Charge machine	N.	Diagrid support structure
E.	Rotor	O.	Primary vessel
F.	Control rod drives	P.	Leak jacket and insulation
G.	Control rods	Q.	Diagrid
H.	Core	R.	Secondary sodium pipes
J.	Neutron shield	S.	Intermediate heat exchanger

Figure 98. Reactor vessel of PFR.

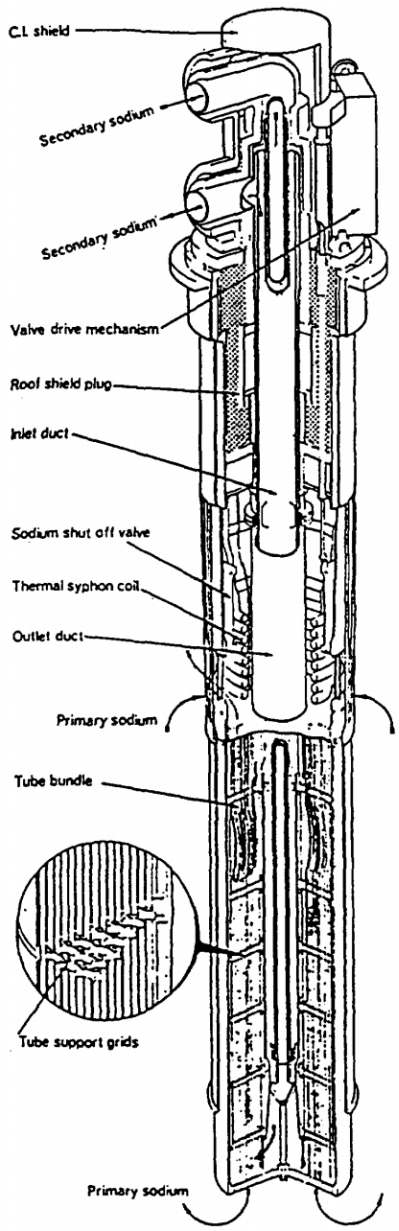

Figure 99. Intermediate Heat Exchanger for PFR.

The mechanical pumps were specially designed to spin on roller bearings and provide leak tight seals between the cover gas and lubricating oil. The pump impellers were specially designed to reduce high frequency noise in the sodium. Noises and vibrations produced from pumps can disrupt sensitive instruments that monitor for sodium boiling. At one point, 200 L of oil from a mechanical pump leaked into the primary sodium and required an entire primary circuit cleanup.

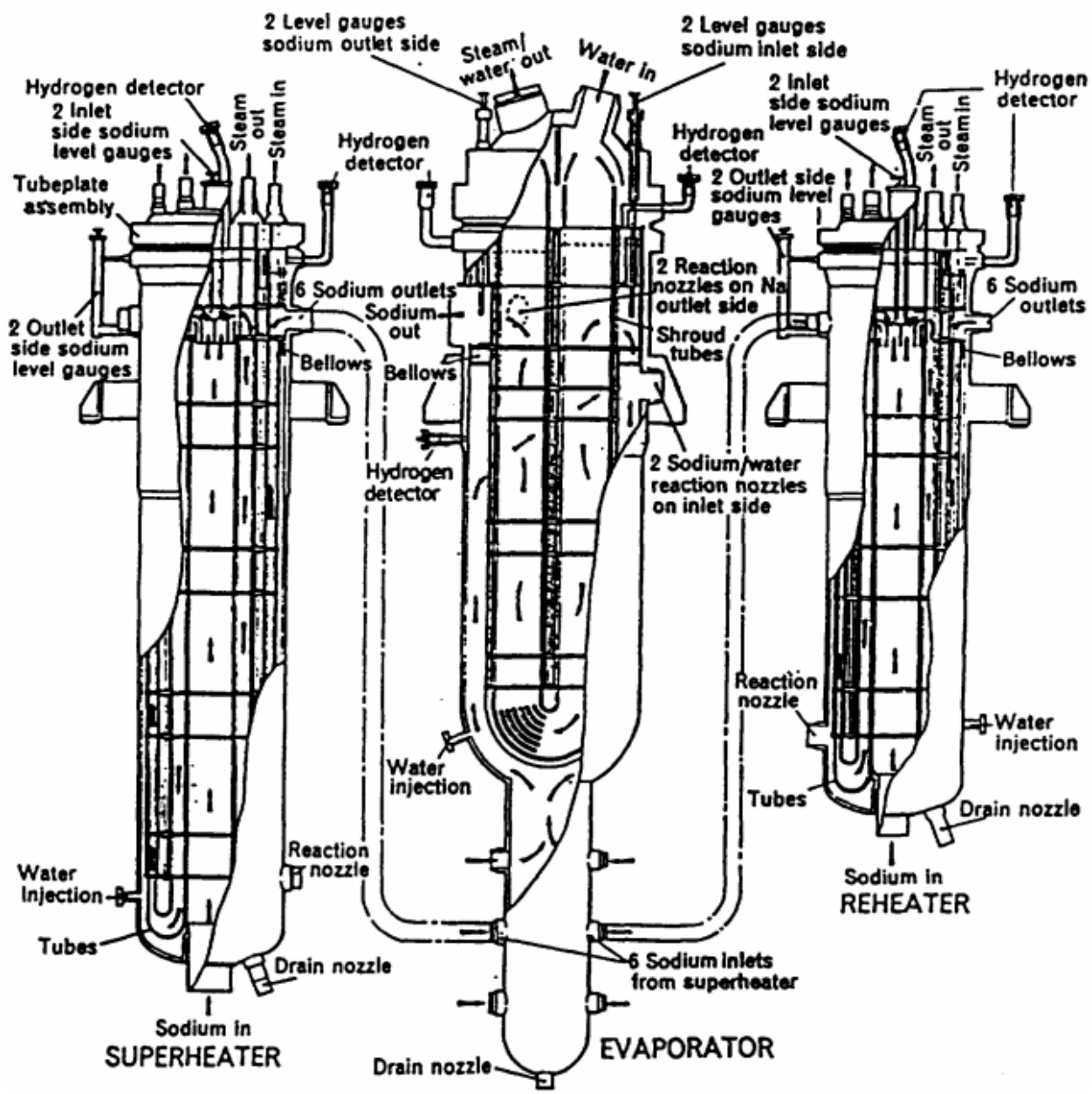

Figure 100. Steam generation process in PFR.

Sodium purification is required in all sodium systems as sodium impurities dissolve structural materials inside the core and reactor vessel. Cold traps are placed in bypass lines that are connected to the primary sodium loops [69]. These cold traps cool the sodium to a temperature of 110°C at which point the impurities (oxides and hydrides) can be crystalized out of the sodium

in the cold trap packing material made of a stainless steel wire mesh. The cold trap is designed to get the sodium impurity level between 5 – 10 ppm. A typical cold trap can crystallize around 100 kg of impurities before replacing the packing material, which happens around every 20 months of service.

The cold trap is placed inside of a regenerative heat exchanger and is supplied sodium through a 7 kg/sec pump. The cold trap is double walled, with the inner vessel being made of 18.8.1 stainless steel and the outer vessel being 2.25 Cr-1 Mo steel. 300 cooling fins are attached to the outer vessel and cooled by air, effectively reducing the sodium from 140°C to 110°C. The sodium is first pumped between the inner and outer vessel walls to cool the sodium and is then directed through the central cavity of the cold trap which contains the wire mesh for crystallization.

After shutting down in 1994, the decommissioning process began to safely dispose of the thousands of tons of sodium along with the thousands of fuel elements. On October 7, 2014, a fire broke out in a sodium holding tank on the PFR site. The Dounreay fire brigade safely put the fire out within 30 minutes and no one was hurt. After investigation, it was found that radioactive tritium was released into the atmosphere but posed no threat to the environment or the local population. The investigation found that unacceptable practices and diverging from procedures caused the fire to occur [70].

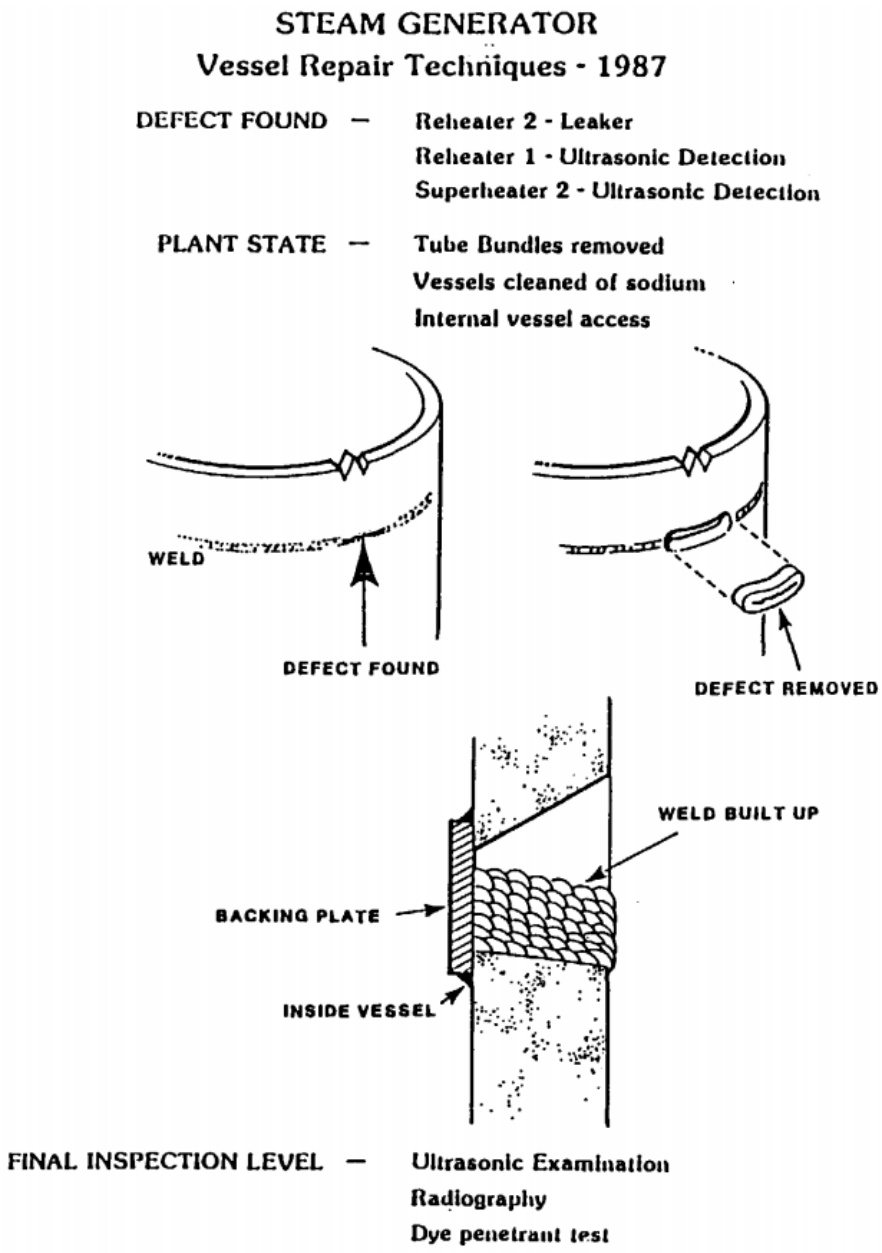

Figure 101. Vessel repair procedure.

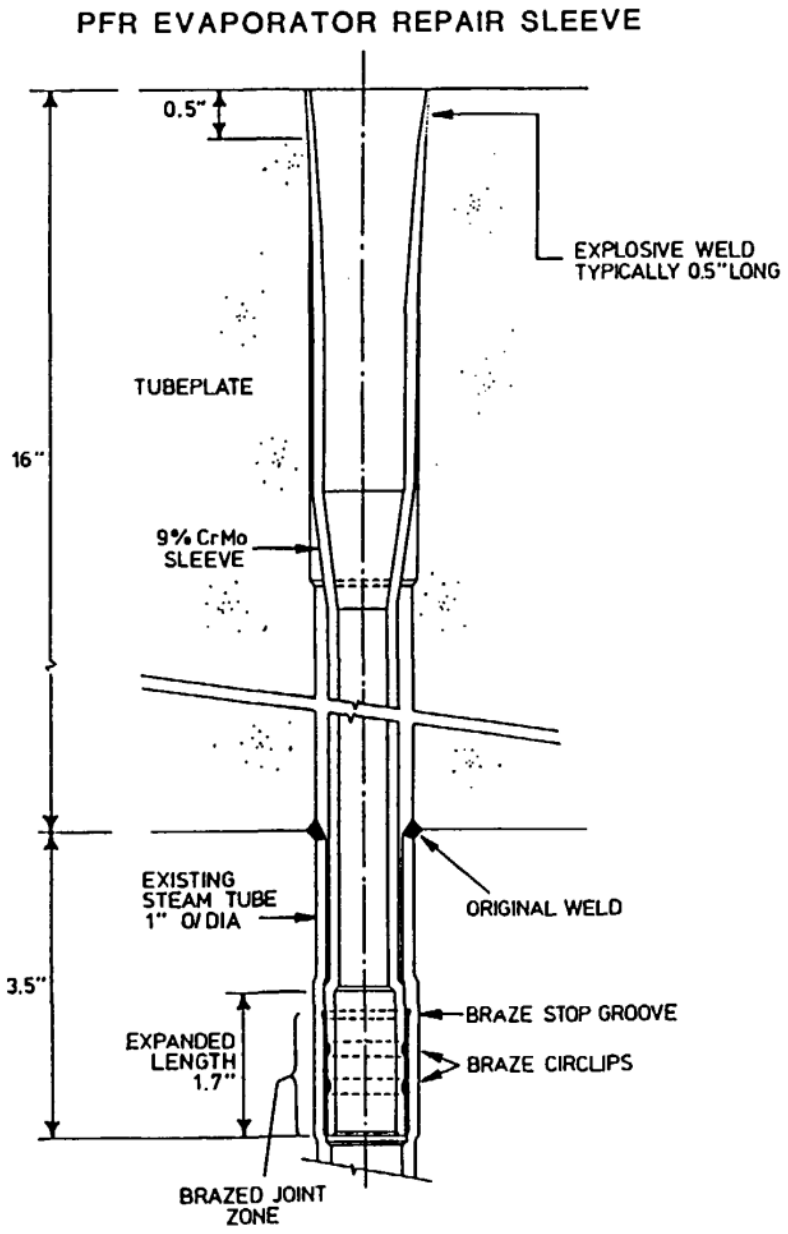

Figure 102. Repair sleeve for evaporator.

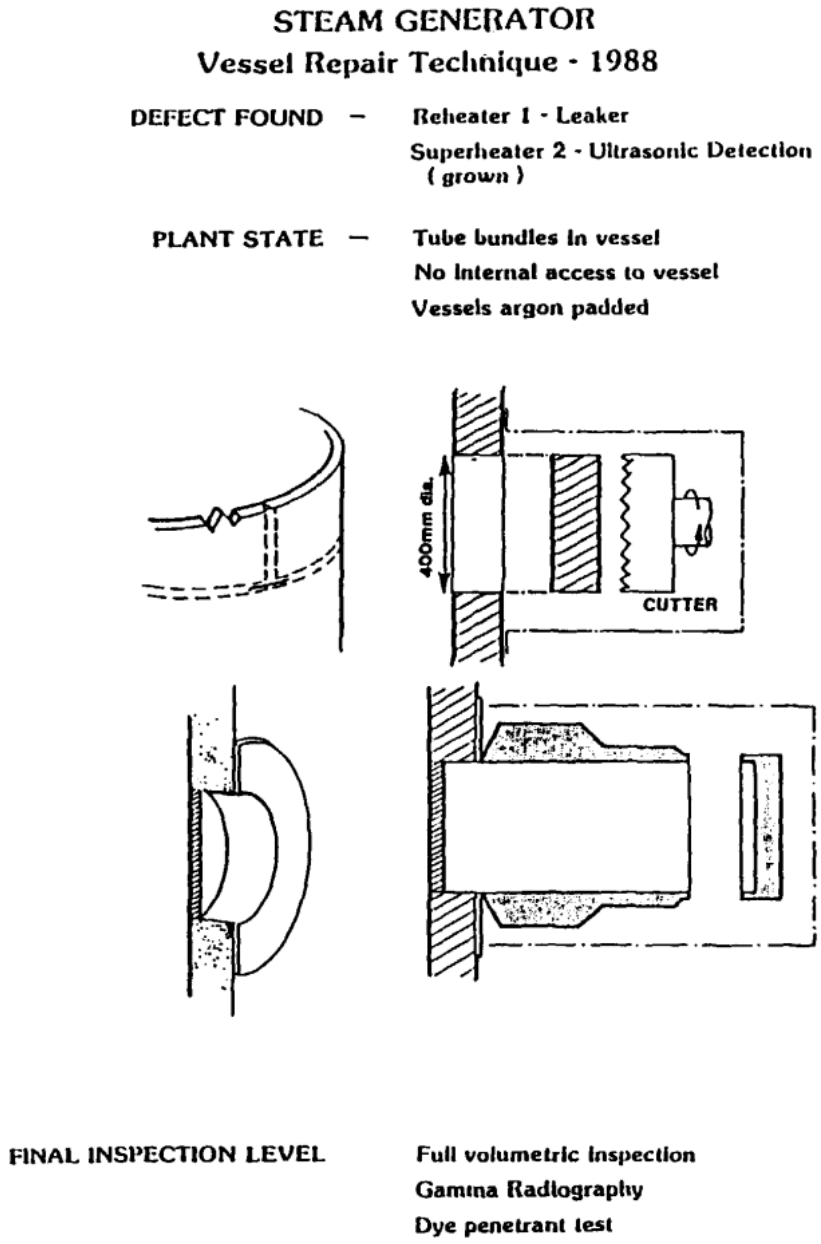

Figure 103. Steam generator vessel repairs.

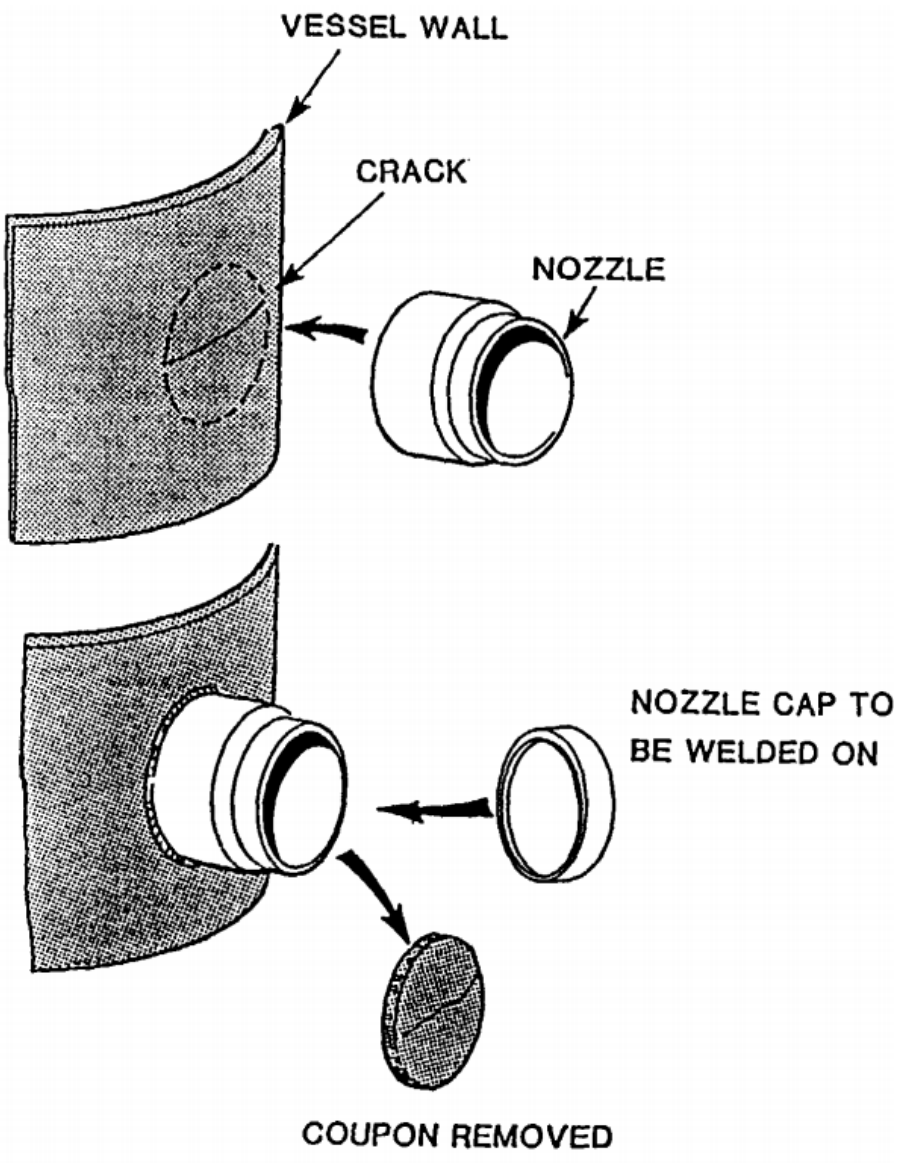

Figure 104. Method to repair defects.

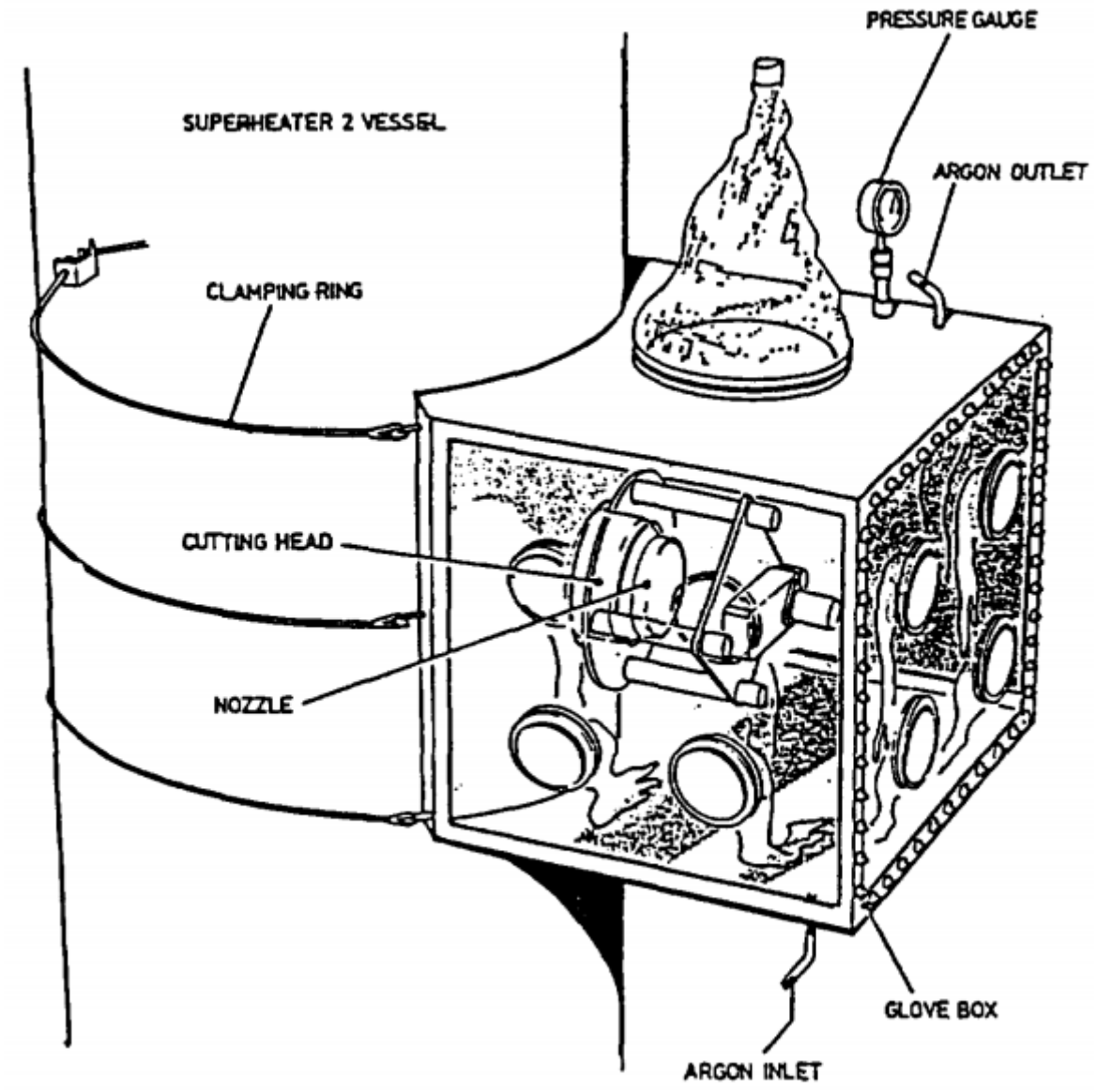

Figure 105. Method to removing coupon from vessel wall.

10.3 French Fast Reactors

Of the five SFRs studied, developed, and operated in France, the Phénix and Superphénix are two reactors of note and will be discussed in depth. Both reactors utilized molten sodium as a coolant and operated on a fast neutron population. France used both Phénix and Superphénix for commercial power generation, but both were also used for fuel breeding. Figure 106 shows the timeline for all five French SFRs depicting the study and design, construction, operation, and decommissioning of all five reactors. Phénix, as shown, was the longest running SFR France produced and Superphénix is the most powerful SFR produced by France.

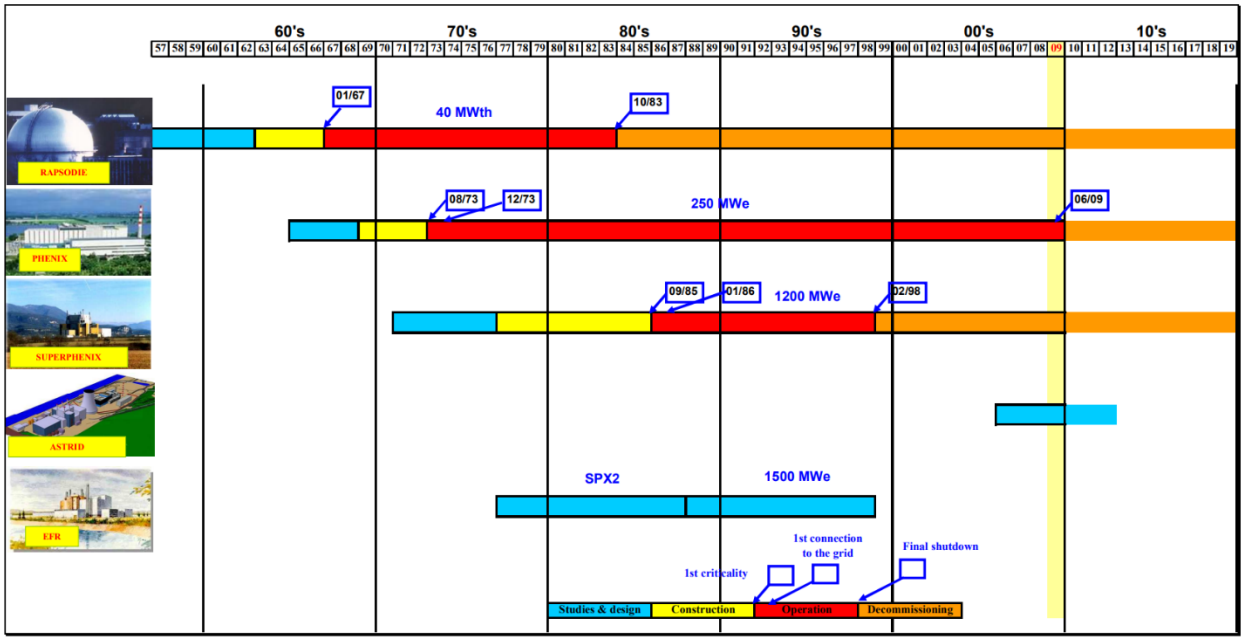

Figure 106. French SFR's timeline [77]

10.3.1 Phénix

The Phénix was built in the Orange, France region at the Marcoule Nuclear Site and can be seen in Figure 107. The Orange, France is located in Southern France.

Figure 107. Regional view of Marcoule nuclear site [71].

The Phénix reactor achieved criticality on August 31, 1973, with a capacity of 250 MWe which was “large enough to permit study of all the industrial problems associated with fast breeder power generation without excessively high investment” [72]. For 35 years, the Phénix generated electricity and functioned as a research reactor, showing the “design and operation, breeding potential, and transmutation possibilities” of fast breeder reactors [73]. Figure 108 shows an aerial view of the building housing the Phénix reactor.

The Phénix utilized a “sodium coolant and mixed plutonium oxide -uranium oxide fuel with stainless steel cladding” [72]. There were six control rods equidistantly spaced from the core where each control rod was worth $2-$3.5 each [74].

Figure 108. Aerial view of Phénix site building [75].

Over the course of Phénix's lifetime, 520 fuel assemblies were reprocessed and produced 3.3 tons of plutonium and 26 tons of uranium which was used to fuel around 40% of Phénix's core, yielding an overall breeding rate of 1.16 and exhibited the feasibility of closing the fuel cycle [73]. The "mean length of reactor runs was 90 days and the fuel reached burn-ups of up to 150,000 MWd/t" [76]. Within the first few years of operation, Phénix experienced multiple sodium leaks between 1974 and 1983 [76]. Notably, on July 11, 1976, the intermediate heat exchanger experienced a sodium leak which resulted in what is labeled as the "first real sodium fire in the Phénix plant," which occurred again the following October [76]. Between 1982 and 1983, at least four incidents involving "sodium-water reactions in the reheater stages effected all three steam generators" of the Phénix plant, resulting in around 30 L of water leaking into the sodium and

creating a combustion that burned holes in the reheater [76]. The incidents resulted “in six months of outage and nine months of operation limited to two-thirds capacity” [76].

Beyond sodium leaks, Phénix experienced issues with steam generator failures, cladding failures, and reactivity transients. Three reactivity transients between 1989 and 1990 cost the Phénix plant “hundreds of millions of francs and 200 person-years of work.” It also caused reactivity and power drops of 28% to 45% within 50 milliseconds [76]. The cause of the transients was never determined.

10.3.2 Superphénix

The Superphénix reactor was another reactor built by France during the Phénix’s operating time. Beginning construction in 1976, the Superphénix operated until it was decommissioned in 1997 [76]. The facility site was in the Creys-Malville area of France. Figure 109 shows the plant and the surrounding area. Superphénix’s original core was designed to hold 5,500 kg of plutonium and be able to breed around 200 kg of plutonium per year at its full capacity of 1,240 MWe [77]. The initial core had 2 concentric rings of control rods consisting of 6 inner control rods and 15 outer control rods [77]. In total, Superphénix had a burnup of 70,000 MWd/t from its 271 fuel pins, producing a flux of 6.2×10^{15} n/cm^{2}s and a breeding ratio of 1.24 [78]. Figure 110 shows the core layout of Superphénix, as well as the reactor’s breeding blankets above and below the core.

The figure also shows the layout of the active region of the core and depicts the layers of sodium between the breeding blankets and the core. It is also seen that there is a density difference between the fertile fuel pins and the fissile fuel pins.

Superphénix faced significant opposition in its beginnings. One such example included a protest during the summer of 1976 where 20,000 people occupied the construction site of the reactor [76]. The prominent anti-nuclear demonstrators believed Superphénix to be “the central and most repugnant element of the entire system of nuclear power, an especially expensive, high-risk, and unproven technology that produced ‘the most toxic substance the world has ever

Figure 109. Regional view of the Superphénix site [79].

known'" [80]. The riot soon escalated to rioters throwing Molotov cocktails and police dispensing tear gas, ultimately killing one and injuring three people in the process [80].

Protests escalated to the point where on January 18, 1982, five missiles fired from an RPG-7 (Rocket Propelled Grenade launcher) at the Superphénix construction sight caught the attention of international media, even though there was little material damage done on the site [76].

Superphénix also experienced some sodium leaks, most notably on April 3, 1987, where 5,000 tons of sodium leaked and combined with plutonium, resulting in more advanced safety analysis following the incident [76]. The leak was from the main fuel storage tank and led to a 10-month shutdown. The cause was determined to "be the result of a design error" and a new fuel loading scheme was developed to compensate for the fact that the tank was irreparable [76]. Figure 111 shows the reactor with all sodium circuits and the sodium-to-water heat exchanger. The

figure shows that the reactor had 4 primary sodium loops leading to the four respective heat exchangers.

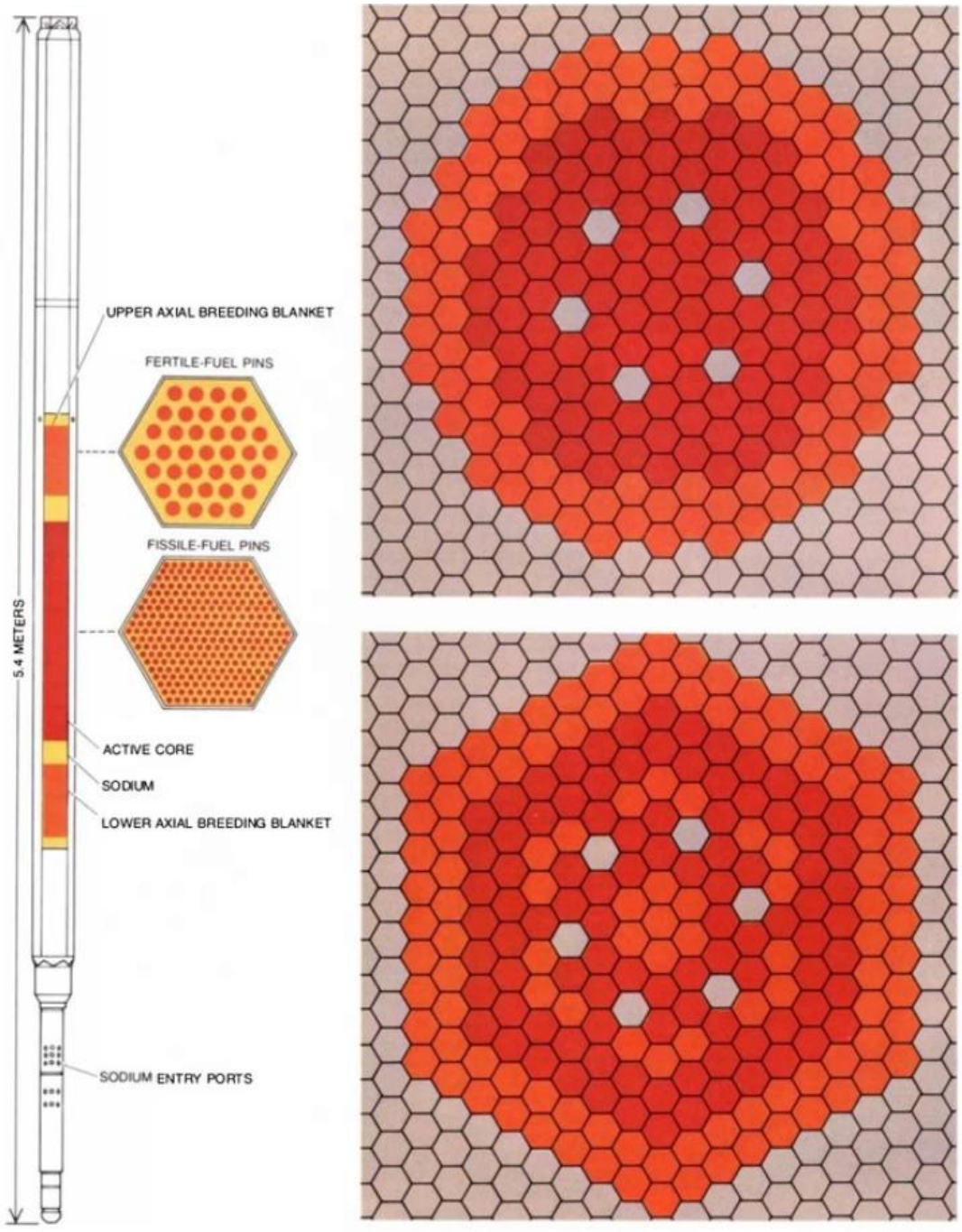

Figure 110. Superphénix core layout [78].

Superphénix was idealized as the future of the nuclear power industry for fast reactors; in 1976 the American Nuclear Society forecasted that by 2025 there would be 2,766 Superphénix sized Reactors in the world [76]. Superphénix's shut down was due to the excessive protests and terror attacks on the facility which lasted throughout its lifetime, which contrasts any other reactor's shut down.

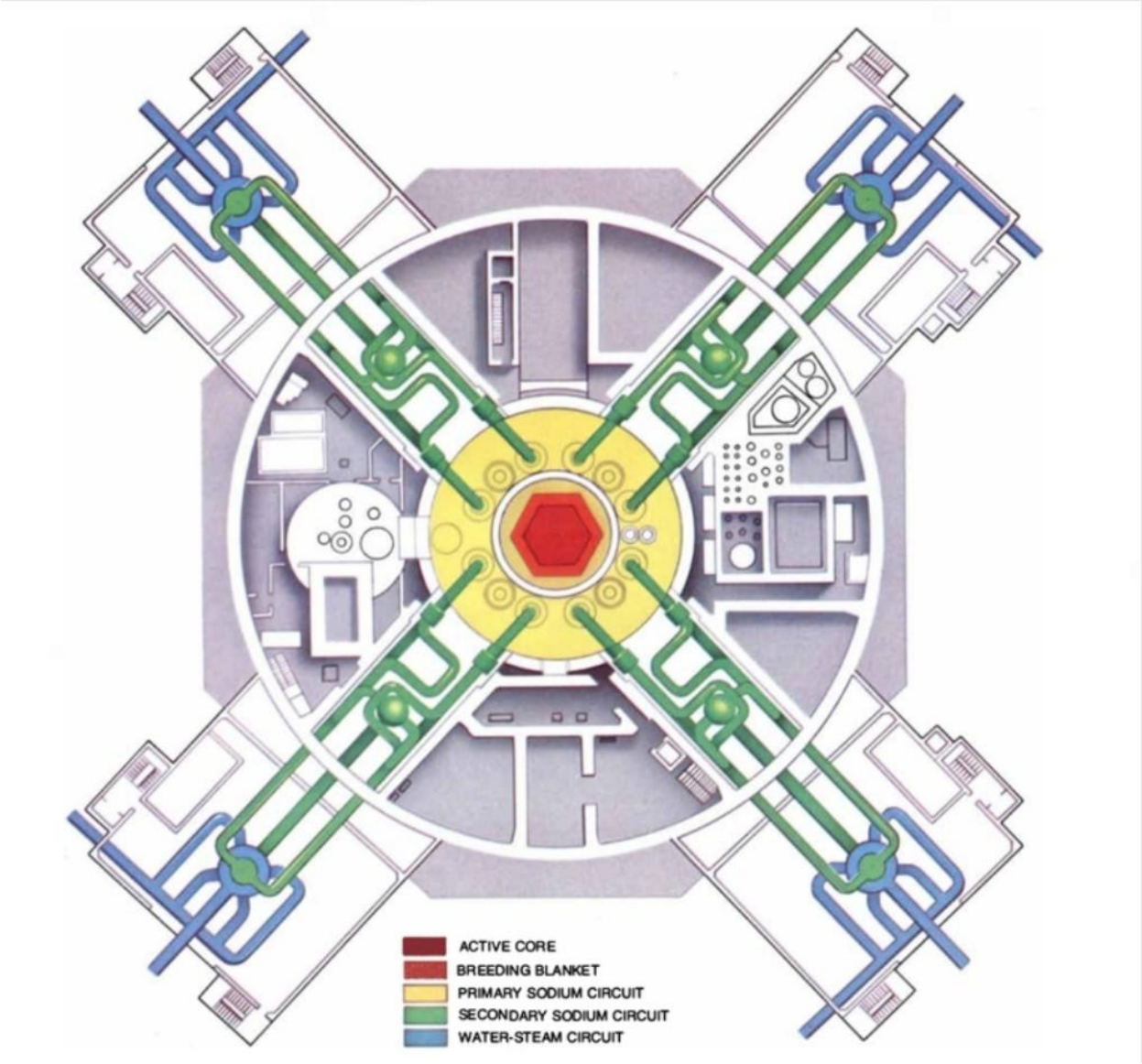

Figure 111. Aerial view of the Superphénix reactor vessel and heat transfer circuits [78].

10.4 Japanese Reactors

10.4.1 Monju Reactor

The Monju reactor was sodium cooled and fueled by Mixed Oxide Fuel (MOX), and can be seen in Figure 112. In this specific loop-type reactor there were three primary coolant loops with a breeding ratio of approximately 1.2. Monju was built on May 10, 1986, and decommission started on December 8, 1995. Monju went critical for the first time in April 1994 and was power rated at 280 MWe [81]. Monju was located in the Tsuruga, Fukui Prefecture (Figure 113).

A little over a year after Monju went critical for its first time, an accident occurred on December 8, 1995. A sodium leak from the Secondary Heat Transport System (SHTS) occurred in a piping room of the reactor auxiliary building. The sodium leaked through a thermocouple temperature sensor due to the breakage of the well tube of the sensor installed near the outlet of the IHX in the SHTS Loop C. There were no adverse effects for operating personnel or the surrounding environment. The reactor core remained cooled and thus, from the viewpoint of radiological hazards, the safety of the reactor was secured. On the basis of the investigations, it was concluded that the breakage of the thermocouple well was caused by high cycle fatigue due to flow induced vibration in the direction of sodium flow [82].

A subsequent scandal involving a cover-up of the scope of the accident delayed its restart until May 6, 2010, with renewed criticality reached on May 8, 2010 [83]. In August 2010, another accident, involving dropped machinery, shut down the reactor again. After the accident occurred, the Japanese government decided to decommission Monju. As of June 2011, the reactor has only generated electricity for one hour since its first testing two decades prior [84].

Monju was designed to use mixed fuel rods of uranium and plutonium to produce more fuel than it consumes and was seen as the key facility supporting the government’s policy for nuclear fuel recycling. A schematic of the plant can be seen in Figure 114.

Figure 112. Monju power plant.

Figure 113. Monju location.

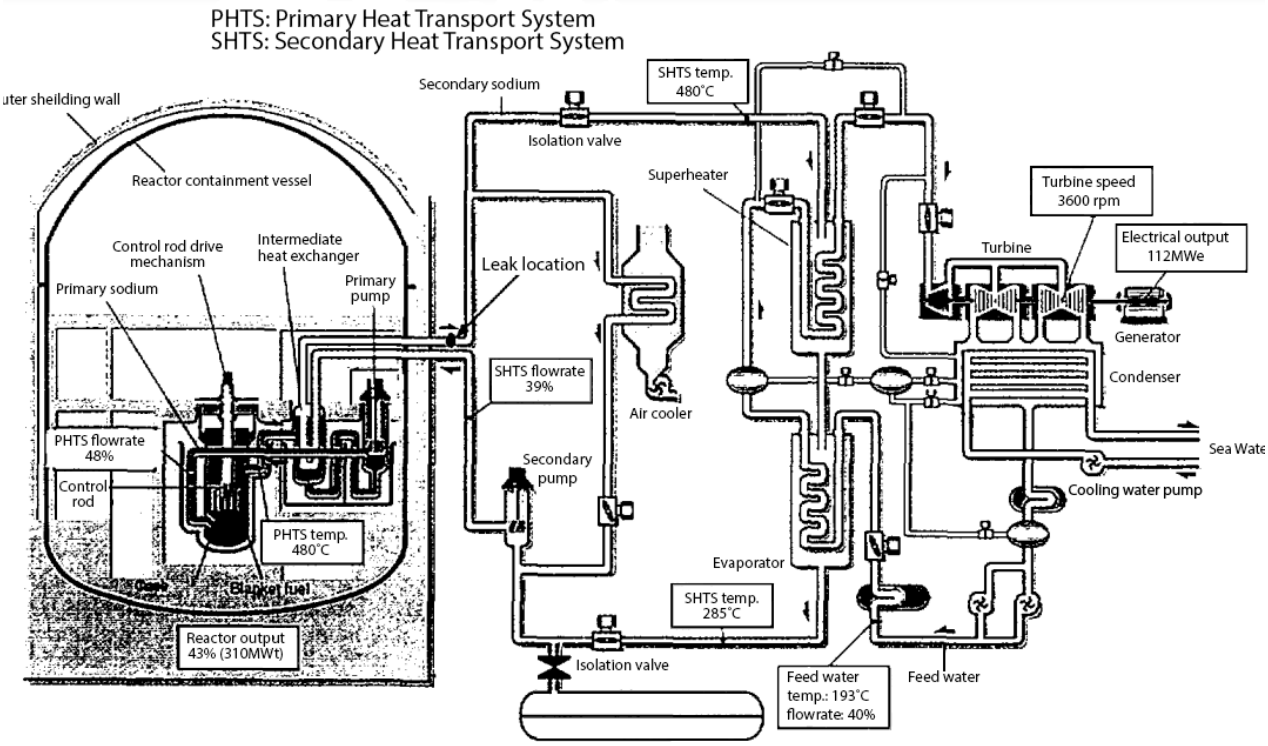

Figure 114. Monju power plant schematic [82].

10.4.2 Joyo Reactor

Joyo is located in Orai, Ibaraki, Japan (Figure 115). The Joyo reactor is a sodium cooled fast reactor fueled by uranium-plutonium MOX. In this specific design the breeding core is an MK-1 core. Joyo was built in 1977 and went critical for the first time on April 24, 1977 [85]. The facility itself can be seen in Figure 116.

The Joyo reactor, operated by Japan Atomic, was initially built with the intention of doing tests on and advancing the development of materials and activation experiments. Joyo, so far, has gone through 3 different core changes: MK-I April 24, 1977 - January 1, 1982, with a power output of 50-75 MWt, MK-II November 22, 1982 - September 12, 1997. This core surpassed 50,000 hours of operating time with 100 MWt. The third core was MK-III July 2, 2003–2007 (140-150 MWt). The Joyo complex consists of the reactor containment vessel and reactor auxiliary buildings and can be seen in Figure 117. The 54.3-m tall reactor containment vessel is carbon steel

with a 28-m inner diameter and a 12～27mm wall thickness. It is a closed system, containing the reactor vessel and major components of the primary cooling system [86].

Figure 115. Joyo location.

Figure 116. Joyo reactor.

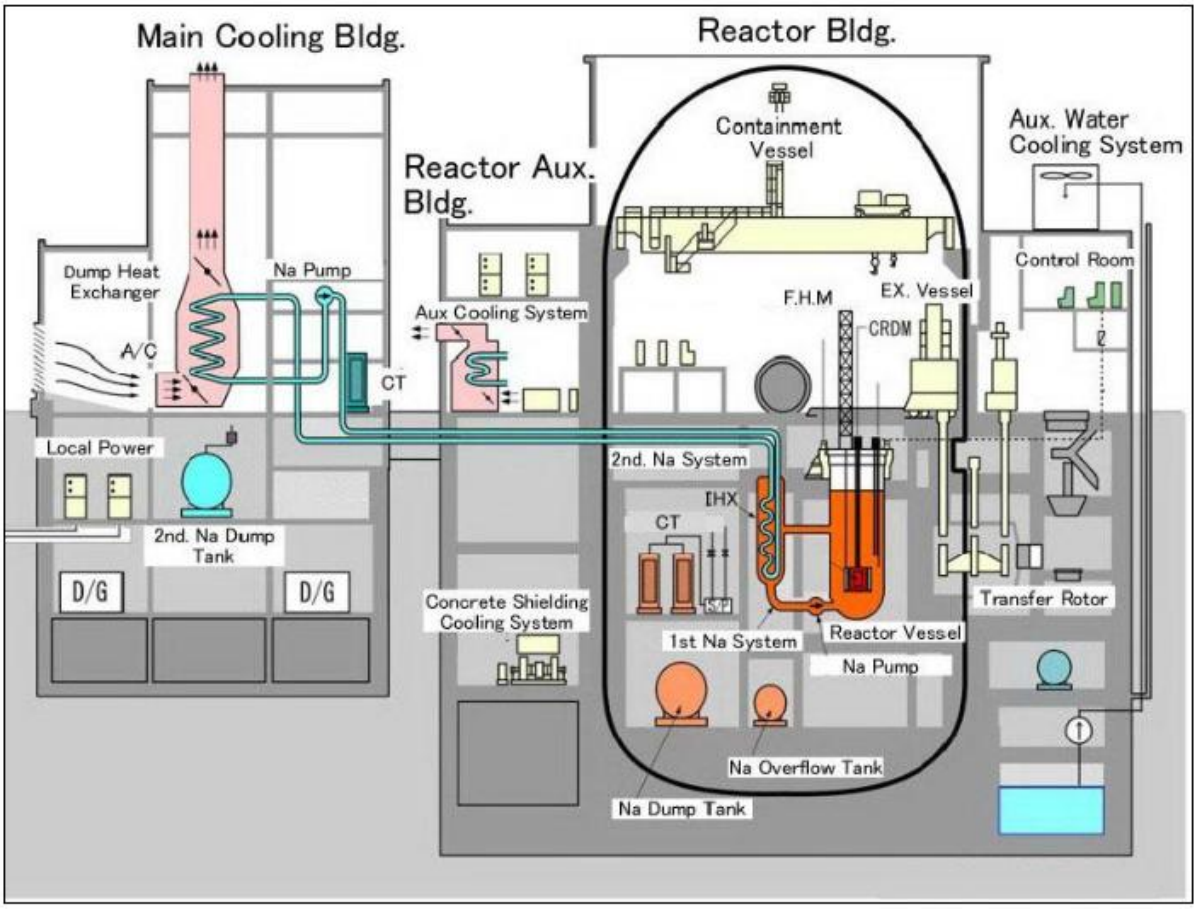

Figure 117. Joyo complex schematic.

10.5 Russian Reactors

Russian sodium fast reactor history is extensive, beginning in the 1960s with construction starting on BN-350, and extends to the present with the planning of BN-1200 (& BN-1600). A timeline of this development is shown in Figure 118. The reactors shown in the figure are very similar as they are of the same style BN-reactors, all built by OKBM Afrikantov, a Russian Nuclear Engineering Company [87].

Figure 118. Timeline of Russian reactors [88].

10.5.1 BN-350

The BN-350 was a liquid-metal-cooled, fast breeder reactor rated for 900 MWt within the city of Aktau, Republic of Kazakhstan [89]. Initial criticality was achieved in 1972 and provided heat and electricity to the local population. The reactor was shut down in 1999 as part of the Strategic Arms Reduction Treaty (START-I) and the Treaty on the Non-Proliferation of Nuclear Weapons (NPT) [90].

The core of the reactor contained over 600 fuel assemblies, 200 driver assemblies, and a dozen control rod assemblies. The assemblies had three different radial enrichment zones of 17%, 21%, and 26%. The zone with 26% enriched fuel was covered in a depleted uranium oxide radial blanket to breed new fuel [89]. Primary sodium coolant flowed upward through the core which then exchanged heat to the second sodium coolant loop and then finally to a third steam loop [91].

The BN-350 contained three heat transfer circuits in which the primary and secondary loops contained sodium and the third contained water and steam [91]. The primary loop contained six independent loops to remove impurities from the sodium and a system for storing the sodium after it was drained from a loop. Each of the three loops contained a heat exchanger and main pump that was outside of the reactor vessel. Any of the six independent loops could be isolated via

two gate valves in the case of a leak or other sodium related issue [91]. The primary loop system can be seen in Figure 119.

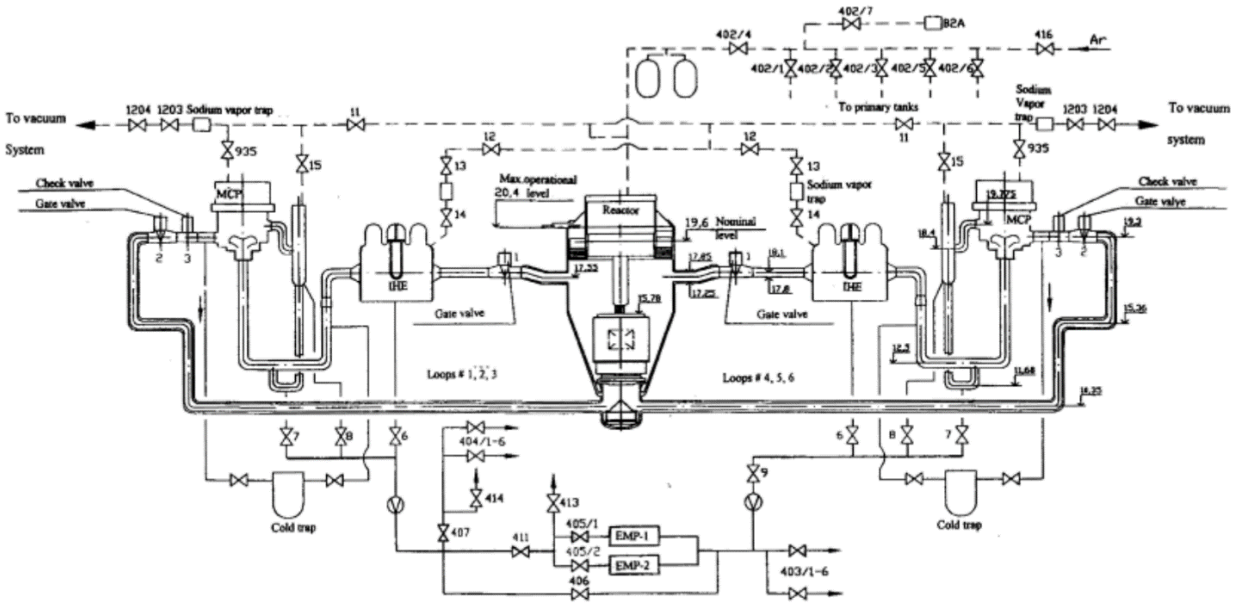

Figure 119. Primary loop system [91].

In 1973, the BN-350 "experienced a major sodium fire as a result of the failure of one of the steam generators" [92]. Defects in the fuel cladding first started to appear in 1975, where excessive amounts of Cs-137 in the primary sodium coolant was measured to be 2,200 MBq/kg [91]. To control the amount of cesium-137 within the primary loop, regular primary loop cleanings were conducted using reactor-grade graphite as an absorbent material known as "filters" [91]. In 1992 a "mass depressurization of fuel pins took place in the reactor core that resulted in an increase of the primary sodium cesium-137 specific radioactivity up to 300 MBq/kg" [91]. During decommissioning in 2001, the primary loop contained ~259,000 GBq of cesium-137, [91].

10.5.2 BN-600

The BN-600 was connected to the grid on April 8, 1980, and is rated to 600 MWe. It is touted as "reliable in control, safe and highly valuable for further commercial deployment of large fast reactor power plants" and can be seen in Figure 120 [93]. The BN-600 operates in Zarechny, Russia and has been licensed until 2025 [94].

The BN-600 has been used as an international benchmark for MOX fuel cores as a part of a three-year, eight country benchmark analysis [95]. The BN-600 contained 369 fuel assemblies, with 217 low to intermediate enriched fuel assemblies, 139-144 highly enriched fuel assemblies and 8 depleted uranium dioxide control rods [93]. The assemblies were enriched to 17%, 21%, and 26%-33% depending on the radial distance from the core [93].

Figure 120. BN-600 location [94].

A total of 104 failures have occurred over the life of the plant, 28 resulting in plant shutdowns and 18 shutdowns involving reactor scrams. 27 sodium leaks occurred in which five events involved sodium leakage from the primary loop. 14 sodium leak events resulted in fires, and five sodium leaks were the result of "personnel errors" [93]. The main causes of sodium leaks have been due to three main causes: material faults in the pipelines, "imperfect valve designs," and the degradation of rubber surrounding flange joints in sodium loops [93]. The most serious sodium leak occurred on October 7, 1993, where around 100 L of sodium spilled from the primary loop, resulting in only a 10 Ci release [93]. Figure 121 depicts the BN-600 reactor containment vessel.

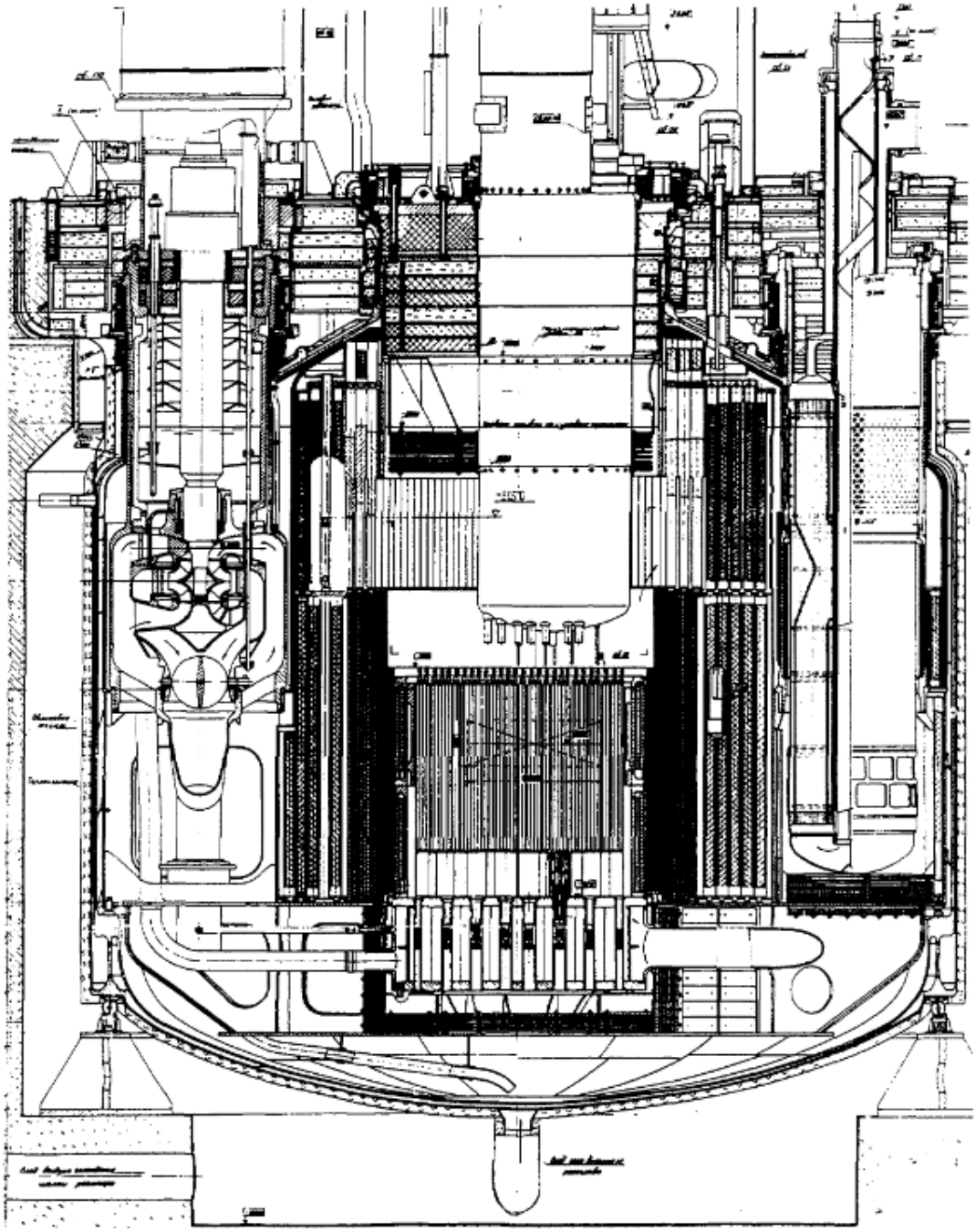

Figure 121. BN-600 reactor containment vessel [96].

10.5.3 BN-800

BN-800 is third in the line of BN-reactor designs constructed by Russia. The power rating of BN-800 was 780 MWe [97]. The BN-800 construction was to further the BN-600's initial purpose of establishing a closed nuclear fuel cycle [98]. Construction of the BN-800 started in 1984, and the subsequent start-up intended for 1992 [97]. Due to the Chernobyl accident, production of all nuclear plants temporarily ceased [97]. The physical construction of BN-800 occurred in Beloyarsk 4; an image of the surrounding area is shown in Figure 122.

Figure 122. Location of BN-800 [88].

BN-800 began operation in 2014, about 22 years later than initially intended [97]. Initial criticality occurred in June 2014 which means the reactor is still new in sodium history as a whole; however, the design being based on the well vetted BN-600 supports the improvement (Figure 123) [99]. There are no known leaks to date from the BN-800, as it has been improved on since BN-350 and other sodium fast reactor designs, making it one of the most reliable and scientifically interesting reactors to date. The BN-800 has exceptional potential to exhibit the reliability and design of generation IV reactors and their implementation [99]. Currently, the BN-800 is working with MOX fuel and the core layout can be seen in Figure 124 [99].

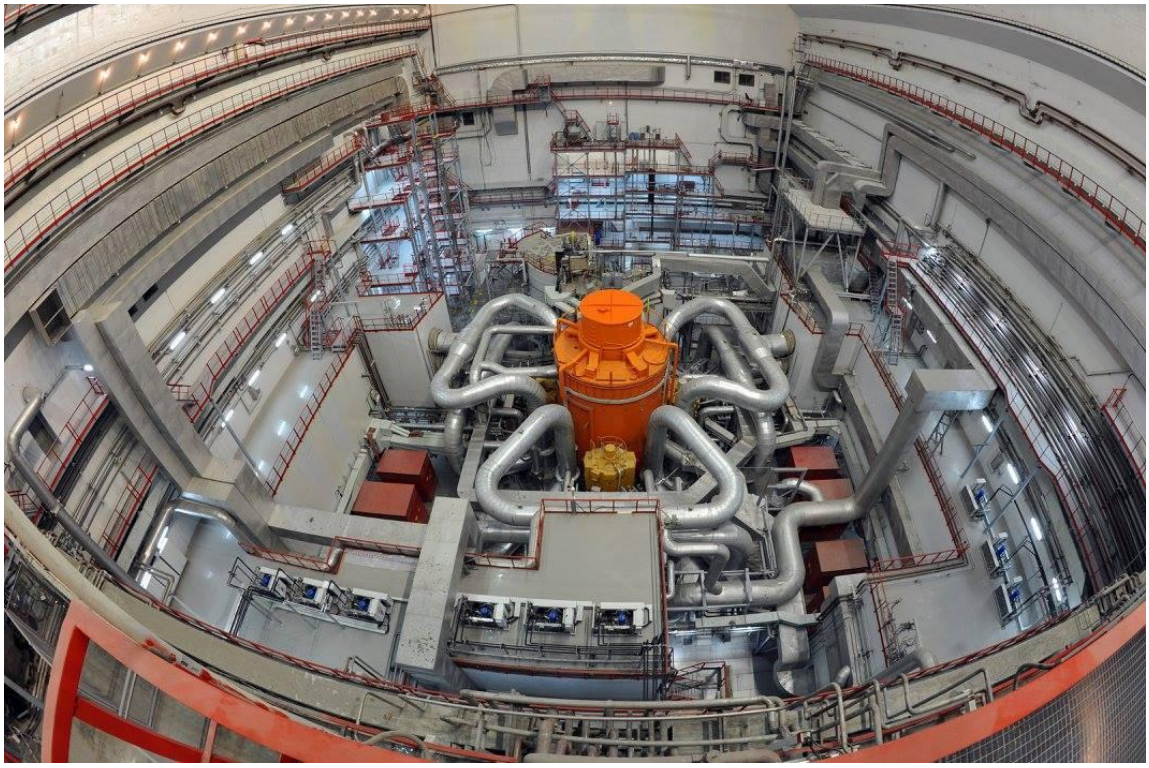

Figure 123. Visual of inside the BN-800 facility [88].

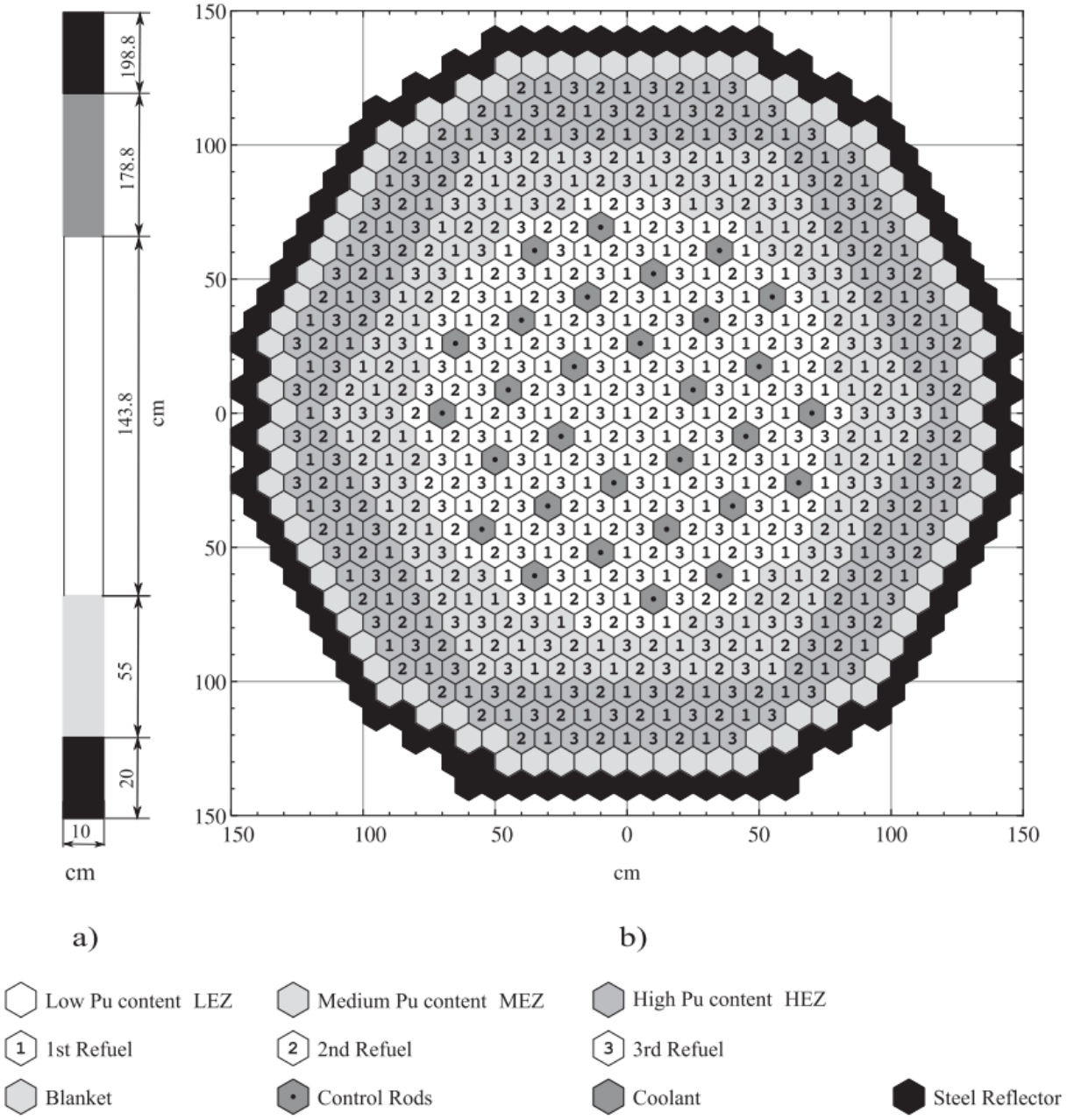

Figure 124. Core layout of BN-800 [98].

10.5.4 BN-1200

The BN-1200 is a nuclear reactor design currently being planned for with the construction to be completed in “Beloyarsk and South Urals” by 2030 [100]. The design is intended to meet the criteria for Generation IV reactor designs and be an improvement upon the BN-800’s design [101].

The design of the BN-1200 reactor’s intention is to further emphasize passive safety [100]. One such allowance from passive safety is a “72-hour grace period” post shutdown “requiring no operator intervention” [100]. BN-1200’s power rating is “1220 MWe” with a “60-year life”, making the design capable of producing the most power compared to any other SFR constructed by Russia [101].

10.6 Indian Reactors

India is another country that has sodium cooled fast reactors either in operation or planned in the future. The two reactors are the Fast Breeder Test Reactor and the Prototype Fast Breeder Reactor, both of which are in Kalpakkam, India [102]. Figure 125 shows the interior of the Madras Atomic Power Station which houses both the Fast Breeder Test Reactor and the construction site of the Prototype Fast Breeder Reactor.

Figure 125. Image of the Madras Atomic Power Station in Kalpakkam, India [103].

10.6.1 Fast Breeder Test Reactor

The Fast Breeder Test Reactor (FBTR) was a miniaturization design of the French Rapsodie Reactor [102]. FBTR achieved criticality first on October 18th,1985 [102]. The reactor operated at 13 MWe utilizing "plutonium-uranium carbide as a fuel" [102]. The reactor experienced three issues during the first 20 years of operating including one sodium leak and a manufacturing defect issue. Figure 126 depicts a diagram of FBTR, specifying the location of different components of the reactor as well as discretizing the separate loops within the reactor. The figure also shows the temperature of key sections in each loop and the direction of each loop.

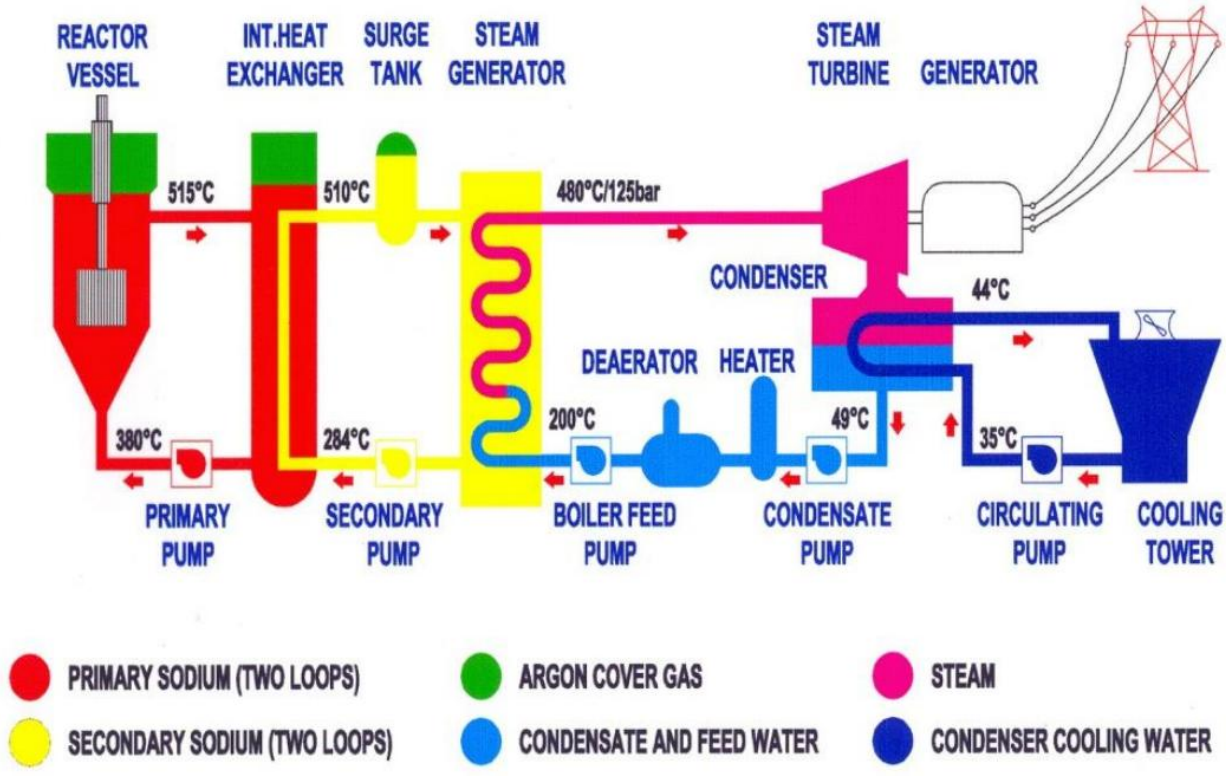

Figure 126. Flow sheet of FBTR [104].

The first issue occurred in May 1987 and involved a guide tube bending during loading [102]. The subassembly bent during the transfer from the 3rd ring to the storage [104]. In turn, this led to the gripper tube bending as it "jammed the fuel subassembly" due to the curtailed movement

[104]. FBTR rectified this with the use of remote machines to unjam the guide tube [102]. This issue caused the reactor to cease operating for two years, finally restarting in 1989 [102]. Figure 127 shows a diagram of the sodium assembly and depicts the pattern of the bent subassemblies with the trendline and the location of the control rods within the reactor. The diagram also labels the material at various distances from the fuel.

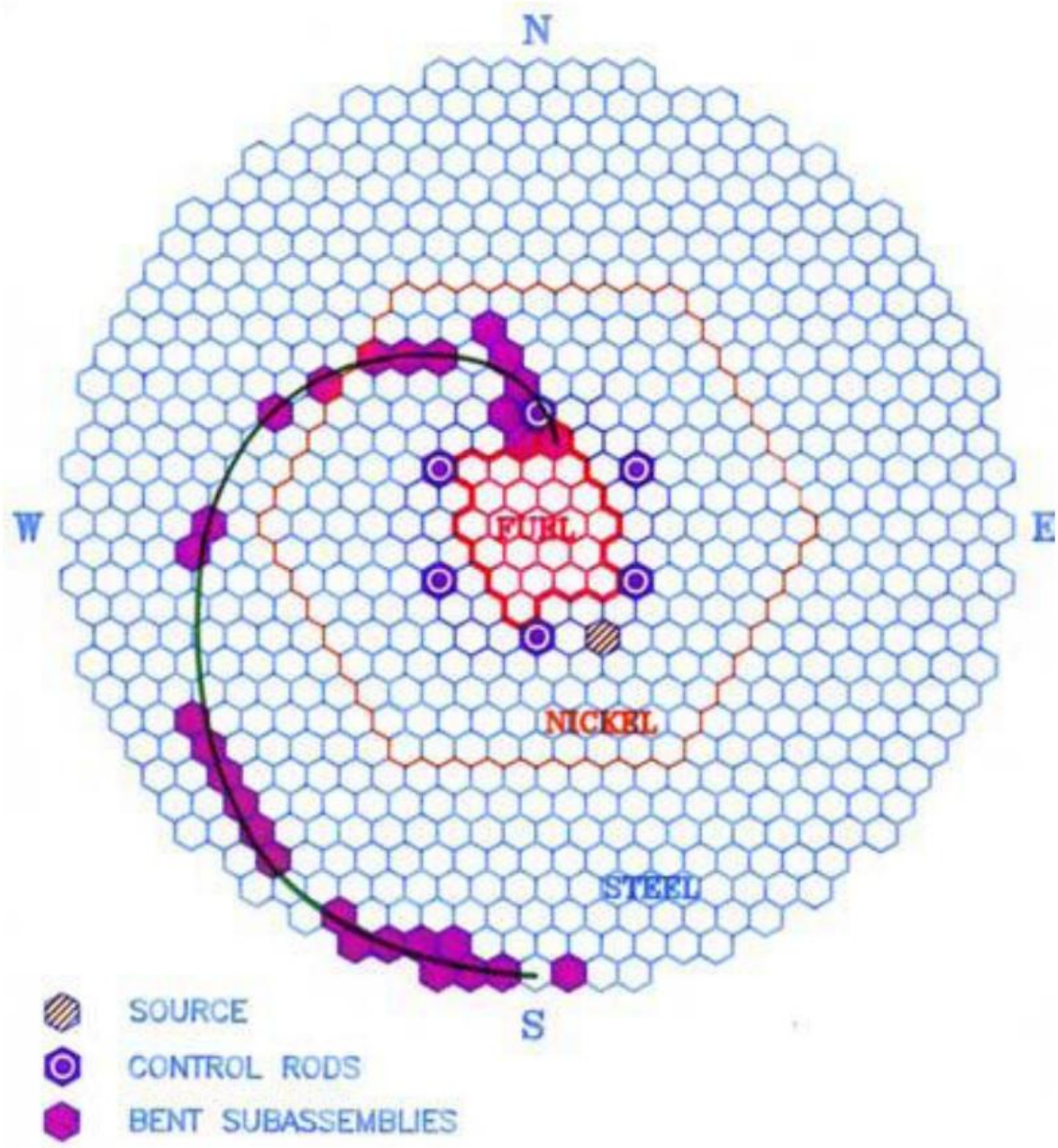

Figure 127. Guide tube bending aftermath [104].

The second issue occurred in 2002 when a sodium leak occurred [102]. The leak released 75 kg of irradiated sodium into the purification cabin. The cause of the leak was due to a "[m]anufacturing defect in an imported sodium valve" [102]. No radioactive material release occurred [102]. Figure 128 shows the generalized location of the sodium leak that occurred in FBTR. The image is from the exterior of the purification cabin of the reactor.

Figure 128. Sodiumn leak location on FBTR [104].

The third event occurred in 2011 when a fuel pin ruptured [104]. This occurred while operating at 18 MWt at a burnup on the order of "148 GWd/t," which is significantly larger than the normal burnup for the remaining fuel pins [104]. Reactor SCRAM took place successfully preventing this issue from becoming worse [104].

Overall, FBTR's reactor design has proven to be a successful miniaturization of the French reactor Rapsodie. FBTR has a successful use of the original "four sodium pumps" of "125,000 hours" with no reported issues [102]. FBTR was also able to operate the steam generators

without leaking for “20,000 hours” [102]. FBTR operated for “36,000 hours” without “fuel pin” failure [102]. FBTR is evidence that sodium reactors on a miniature scale are possible and can be used to produce plutonium and electricity. There were only two reported issues with the reactor showing that there is safe operation pertaining to the use and implementation of sodium.

10.6.2 Prototype Fast Breeder Reactor

The Prototype Fast Breeder Reactor (PFBR) is a reactor currently under construction in Kalpakkam, India and is designed to produce 500 MWe and 1250 MWt [104]. The construction plan expects the reactor to achieve criticality in 2020 [104].

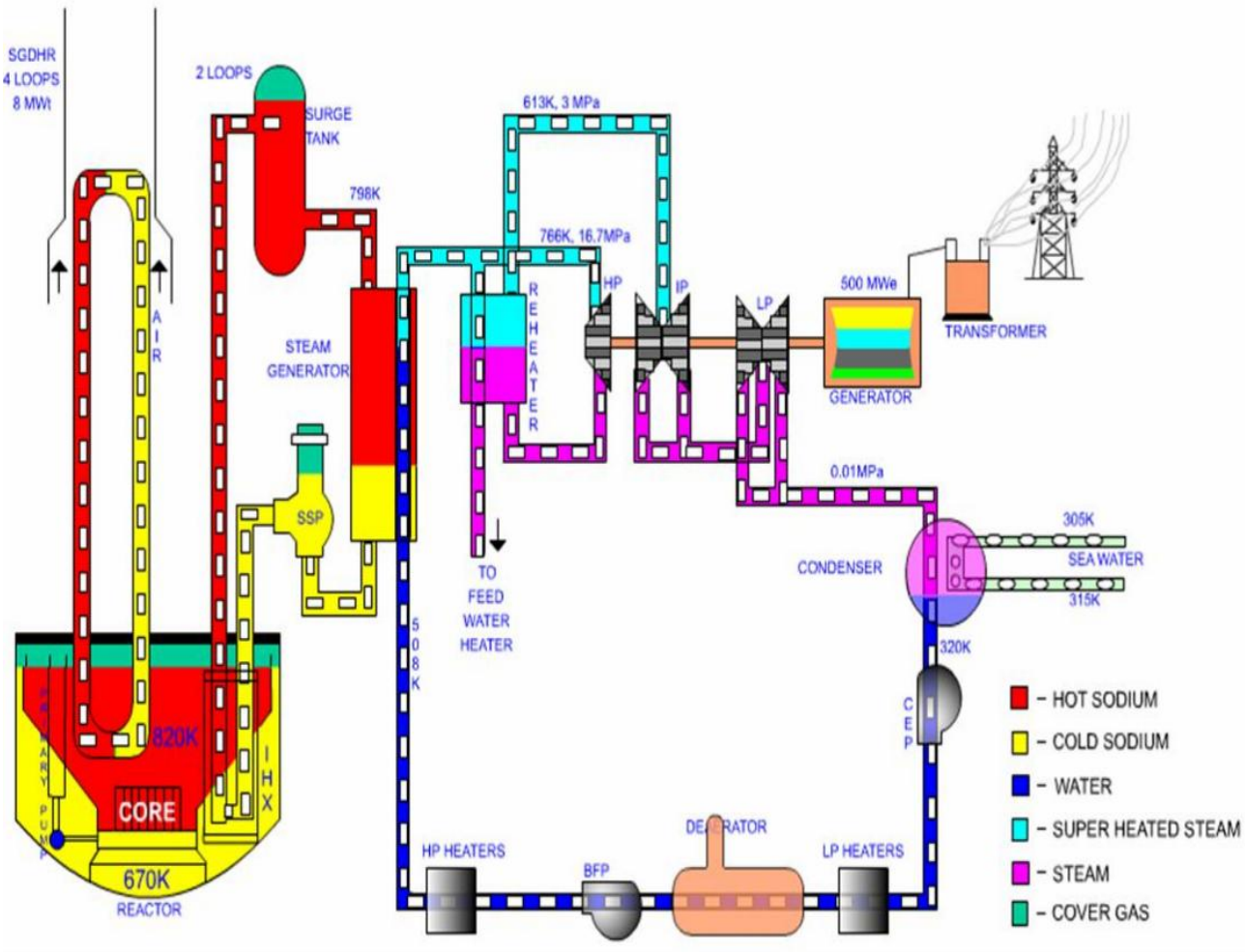

Figure 129. Reactor diagram of PFBR [104].

The Reactor will be loaded with MOX fuel [104]. PFBR expects to operate for 40 years with a plausible extension to 60 years and features an “efficient sodium fire handling” resulting from the extensive “leak detection system” [104]. Figure 129 shows the theorized design of the PFBR specifying the materials at each part of the loop. The figure also shows the relative temperature within the main loop of sodium as well as describes the temperature of the sodium, water, and steam at key points of the reactor’s loops.

10.7 Sandia Sodium Loops

SNL is a United States research facility located in Albuquerque, New Mexico. SNL performed several sodium experiments with the development of the “Sandia Sodium Purification Loop (SNAPL)” [28]. The sodium loop construction occurred to allow SNL to perform research into the safety of “liquid metal fast breeder reactors” furthering development of sodium safety and to investigate the “coolability of urania fuel debris beds within sodium” [28]. The Annular Core Research Reactor (ACRR), along with SNAPL, allowed for the experimentation with activated sodium as well [28].

Sodium purity from suppliers have no guarantee due to a lack of a standard for sodium [28]. These impurities are due to two things: “1) those impurities that are contaminants from the manufacturing process or source materials and, 2) those impurities that result from contact with other materials during the transport, storage and use of the sodium,” meaning that to successfully simulate a reactor loop the sodium must be purified [28] Another sodium loop produced by SNL is the “molten salt test loop” commissioned in 2012 at SNL’s National Solar Thermal Test Facility [105]. The loop contains three parallel test loops providing capabilities of operating three individual experiments at once [105]. The loop operates at up to 625 psi between 300-585°C [105]. The loop uses 60% molten sodium nitrate and 40% potassium nitrate [106]. The molten salt test loop is primarily used for experimentation with “concentrating solar collectors or individual components” under “plant-like conditions” [105]. Figure 130 shows the testing section of one of the three parallel testing locations.

Figure 130. Test loop experiment section for the molten salt test loop [105].

10.7.1 Description of Sandia Sodium Purification Loop

The sodium loop consists of machinery maintaining the sodium, the instruments used to monitor the sodium, and the power and controls involved in operating the sodium loop. Figure 131

depicts a box diagram of the sodium loop. The box diagram contains the various components and where control and information are spread between the various different components.

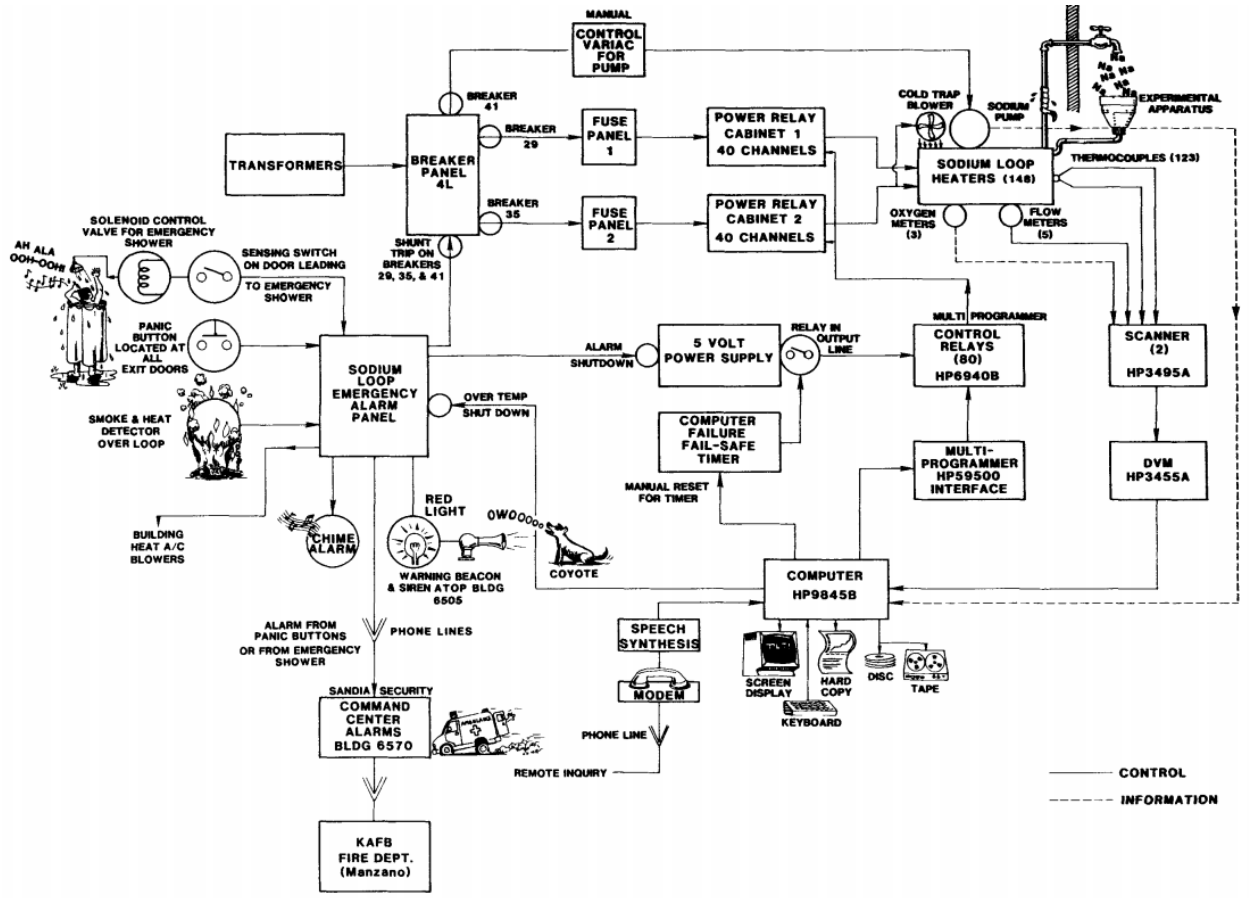

Figure 131. Sodium loop instrumentation, alarms and control schematic [28].

10.7.1.1 Mechanical Components

One mechanical component in SNAPL was the implementation of an electronic pump. The pump operates to circulate “sodium through both the loop but also through the Experimental Apparatus” when a specific voltage input is supplied [28]. The pump used is shown in Figure 132, which shows the direction of the current and flux of the magnetic field that moves the sodium through the pump.

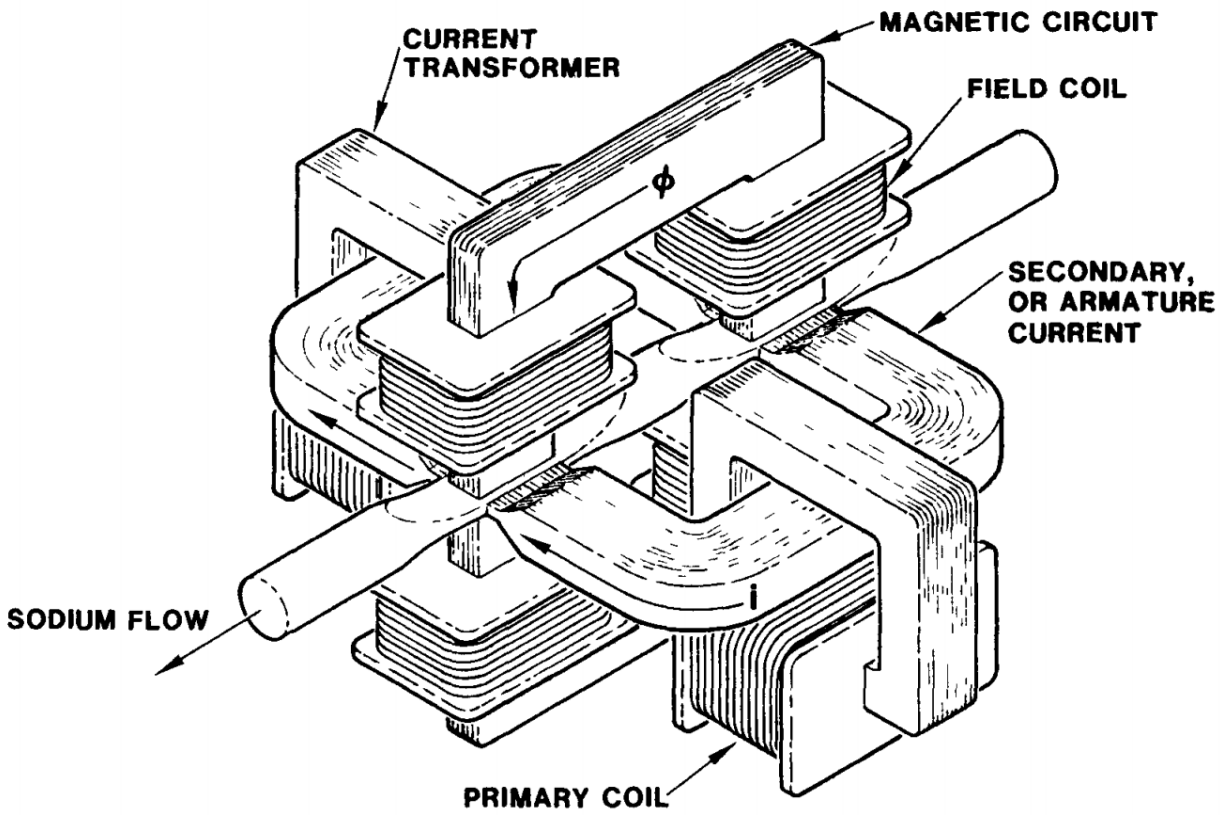

Figure 132. Two-stage electromagnetic pump [28].

The cover gas system acts to separate sodium from undesired interactions with “air and moisture” [28]. The cover gas used for the loop was argon, as argon prohibits air from reentering the system [28]. Figure 133 depicts the schematic of the cover gas system. The schematic shows some of the volume tanks used by the system as well as many of the valves in use by the sodium loop [28].

All piping used for the loop is stainless steel 304L for its “corrosion resistance” and “welding characteristics” [28]. Table 25 in Appendix D: Sandia National Laboratory Information goes through the procedure used for SNAPL valves and pipes intending use within the sodium loop. A sample valve shown in Figure 134 could expect use within the sodium loop. This valve type is a “bellows valve” because the valves’ stems “do not rotate” and provides a “positive barrier against leakage” [28]. One possible drawback from bellows valves would be misuse can lead to breakage. The bellows valves will likely rupture if an individual attempts operating the valves “when the sodium is still frozen” [28].

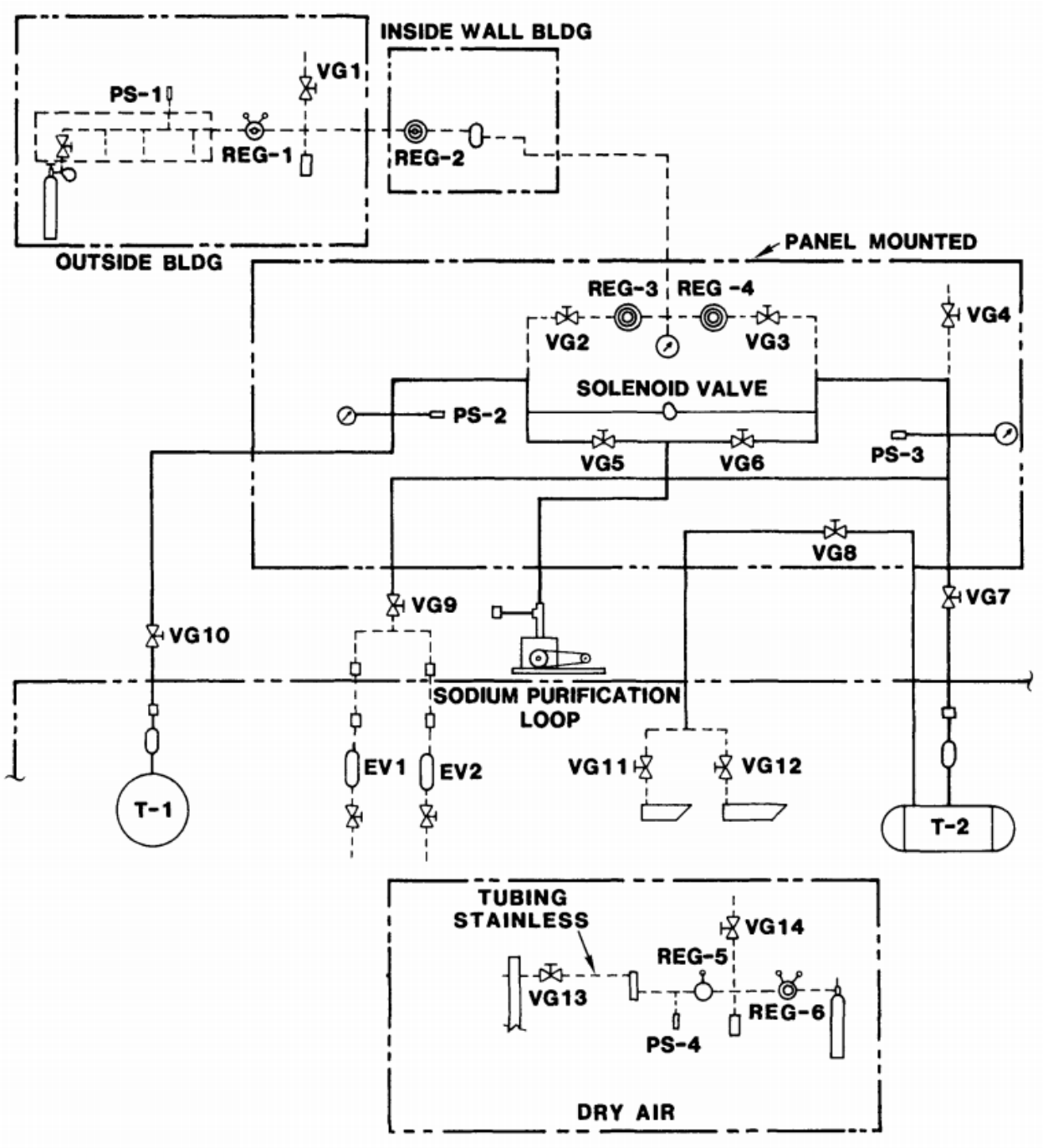

Figure 133. Cover gas system schematic [28].

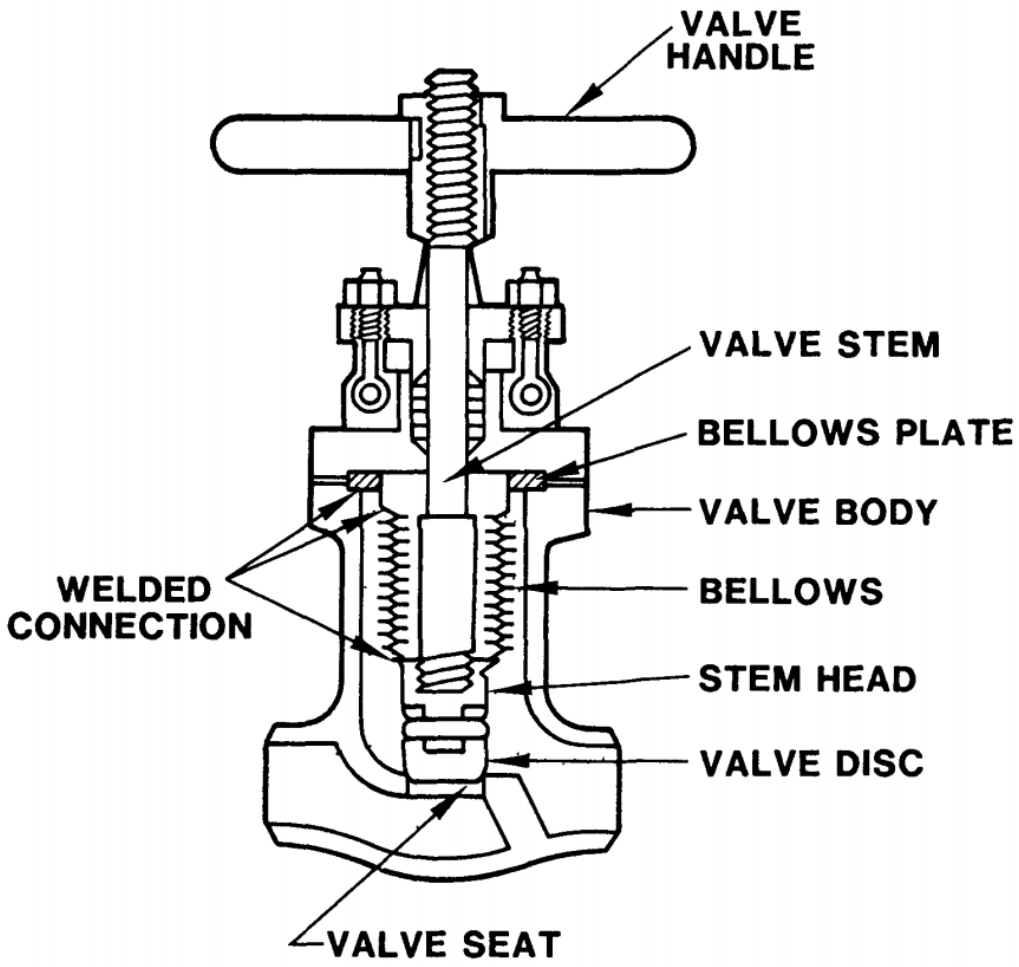

Figure 134. Bellows valve [28].

10.7.1.2 Instrumentation

Magnetic flowmeters measure the flow of the sodium as it moves through a section of pipe in the loop [28]. Effectively these flowmeters operate in the opposite of the electromagnetic pump by generating an output voltage as the sodium moves through the device. A schematic of an electromagnetic flowmeter is shown in Figure 135.

For the devices utilized by SNAPL, the electromagnetic field (emf) generated comes from Eq. (21). In the equation, Q is the sodium flow rate in gpm, d is the inside pipe diameter in inches, B is the flux density in gauss, $K1$ is the pipe wall shunting factor, $K2$ is the end effect factor, $K3$ is the magnet temperature factor, and $K4$ is the pipe expansion factor.

$$emf(mv) = \frac{QB(K1)(K2)(K3)}{3162d(K4)} \tag{21}$$

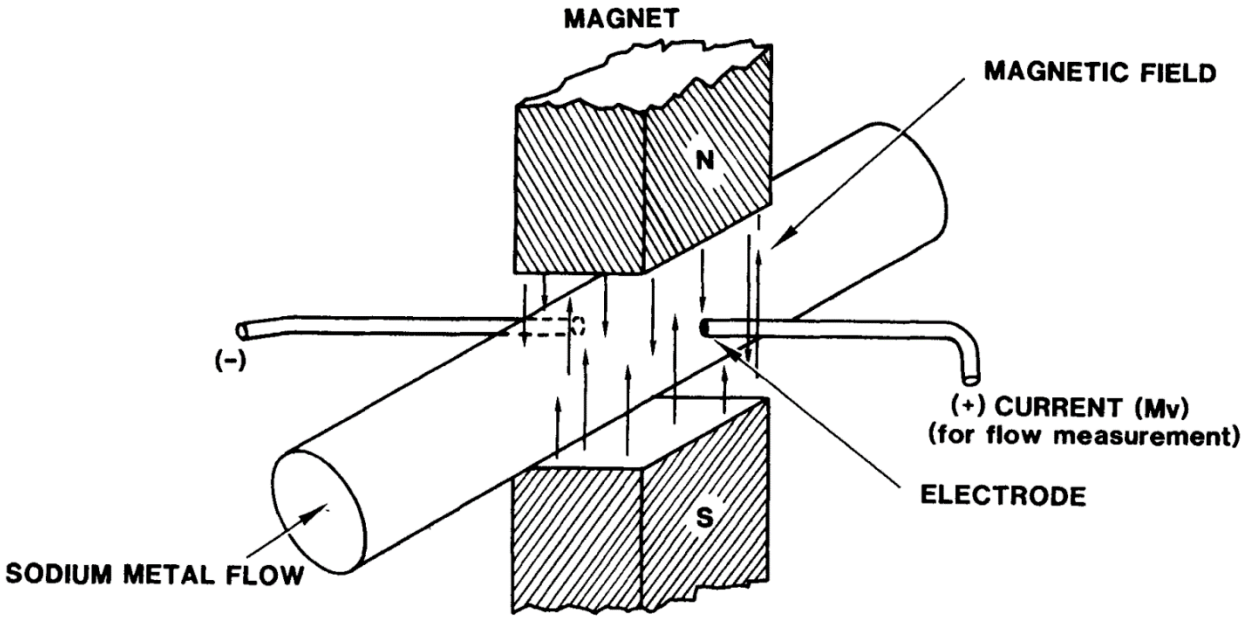

Figure 135. Schematic of electromagnetic flowmeter [28].

The pipe wall shunting factor, *K*1, is a derived value, and is presented in Eq. (22). The shunting factor represents the movement of an electric current from the movement of the sodium between two magnets of the flowmeter device. In Eq. (22), *D* represents the "pipe outside diameter" in inches, *p*1/*p*2 is the "ratio of electrical resistivities," and *d* is the "pipe inner diameter" [28].

$$K1 = \frac{2dD}{D^2 + d^2 + \left(\left(\frac{p1}{p2}\right)(D^2 - d^2)\right)} \tag{22}$$

The pipe expansion factor, *K*4, is another value that is derived and can be found from Eq. (23). The *K*4 value represents the expansion of the pipe, and resultantly, the increase in the sodium's flow rate due to temperature fluctuations. *K*4 is determined by the use of the pipe's "coefficient of thermal expansion," *a*, and the temperature of the pipe in °F [28]. The remaining factors are found using Figure 140 and Figure 141 in Appendix B.

$$K4 = 1 + a(T - T_0) \tag{23}$$

The thermocouples used within the sodium loop were specially designed to negate the requirement of welding it to the piping directly. The schematics of the thermocouple design is provided in Figure 136. The loop used 123 type J (iron-constantan) thermocouples to monitor the temperature of the loops. 58 of them were connected “to the computer,” 42 connected “to the manual control system” and 23 acted as backups [28]. The loop also had 14 thermocouples “available on the exit legs of the loop” [28].

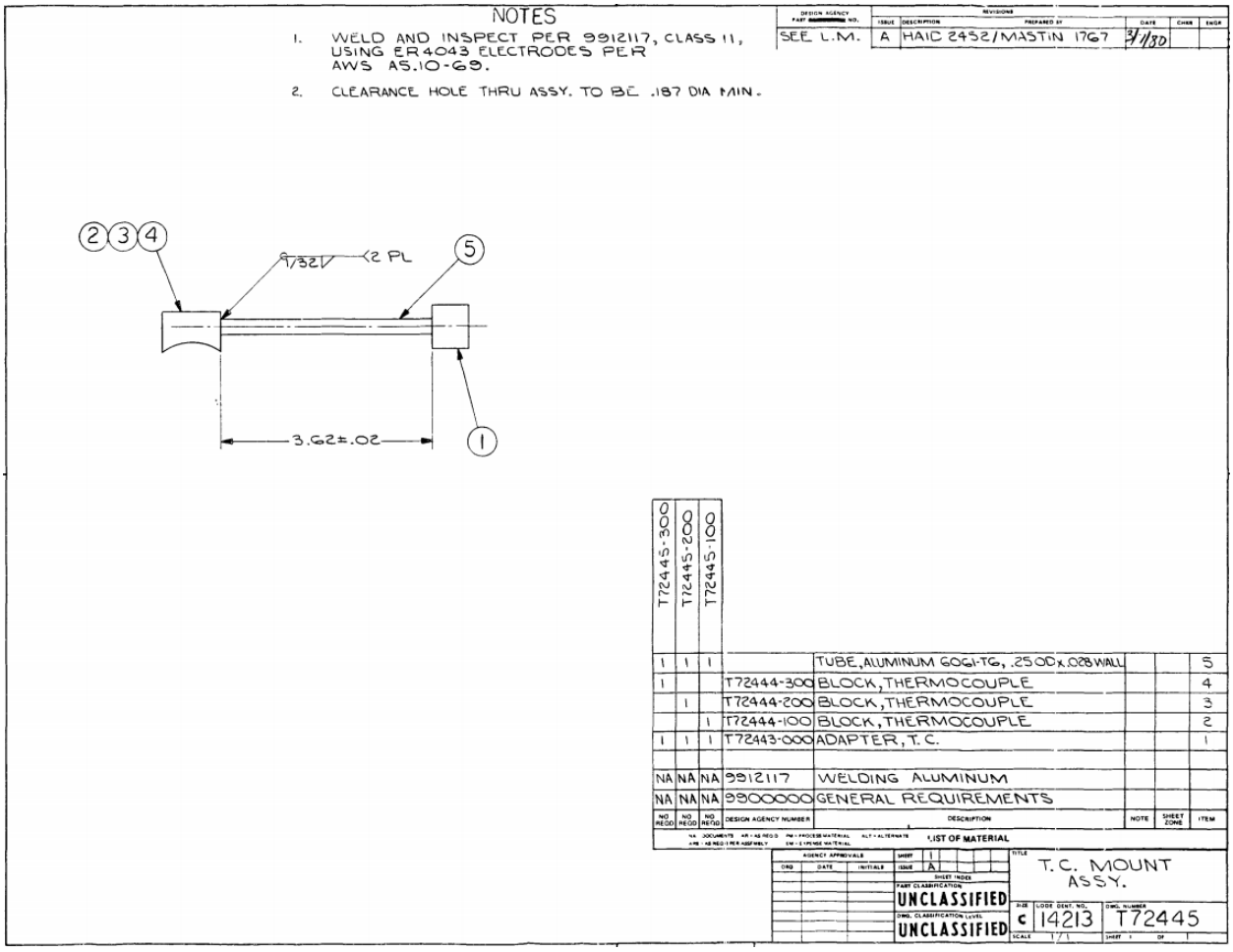

Figure 136. Thermocouple design.

The sodium loop had three oxygen meters installed, and all meters were built by either “General Electric Co. or by Westinghouse” [28]. Both meters have similar designs with “a solid electrolyte material” made of yttria doped thoria separating two electrodes [28]. The oxygen

meters ensure that the oxygen concentration does not cause undesired reactions with sodium. The voltage of the meter corresponds to a particular concentration of oxygen. Below are the equations for each oxygen meter.

For the General Electric Co. meter, the output voltage is found in Eq. (24), where *T* is the temperature in K. The meters temperature coefficient is given as 0.51 mv/K [28].

$$emf = 0.269 + \frac{160}{T}\ Volts\ (sensor\ at\ 773K) \tag{24}$$

The Westinghouse meter output voltage was found using Eq. (25), where *C* is the "oxygen concentration in ppm." Figure 137 shows a schematic of the oxygen meter used by Westinghouse [28]. The image highlights the flow of the sodium through the meter.

$$emf = 1.843 - 0.064Log(C)Volts(744K) \tag{25}$$

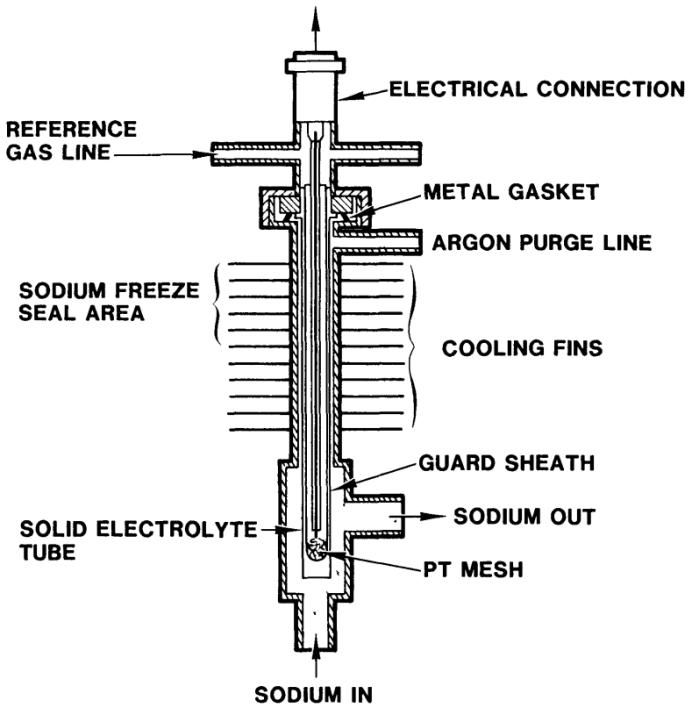

Figure 137. Schematic of Westinghouse oxygen meter [28].

The sodium loop uses two separate tanks to detect the level of the sodium and thus the volume of sodium within the loop. Figure 138 shows the schematic of tank T2 and depicts that

rods are used to determine the level within the tank. Different LED lights will turn on depending on which probes are in contact with the sodium.

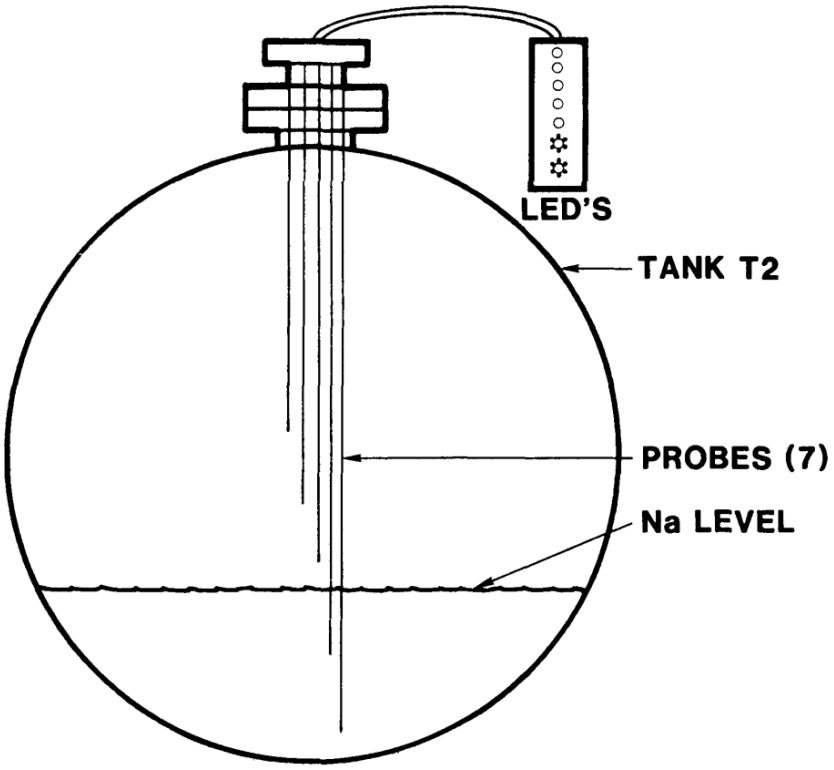

Figure 138. Probe level detector schematic [28].

10.7.1.3 Power and Control

The sodium loop control uses a "dedicated computer system" [28]. The computer system issues commands or alarms after reading the various instruments. The computer system is comprised of divisions, and each division operates independently. The system operates faster the larger the actual value is from the control value set in the computer [28]. Figure 139 shows a typical control circuit used by the computer system. The computer has five control functions: "heater on-off," "cold trap fan on-off," "E. M. pump on-off," "drain valve open-close," and "entire system on-off" [28].

The loop can also be manually controlled using a "very simple control system" [28]. The manual control's function is to ensure the "computer control program" is operating and ensuring

the loop is operating properly [28]. The manual system can also isolate operational problems that may arise, such as “illogical temperature readings.” [28].

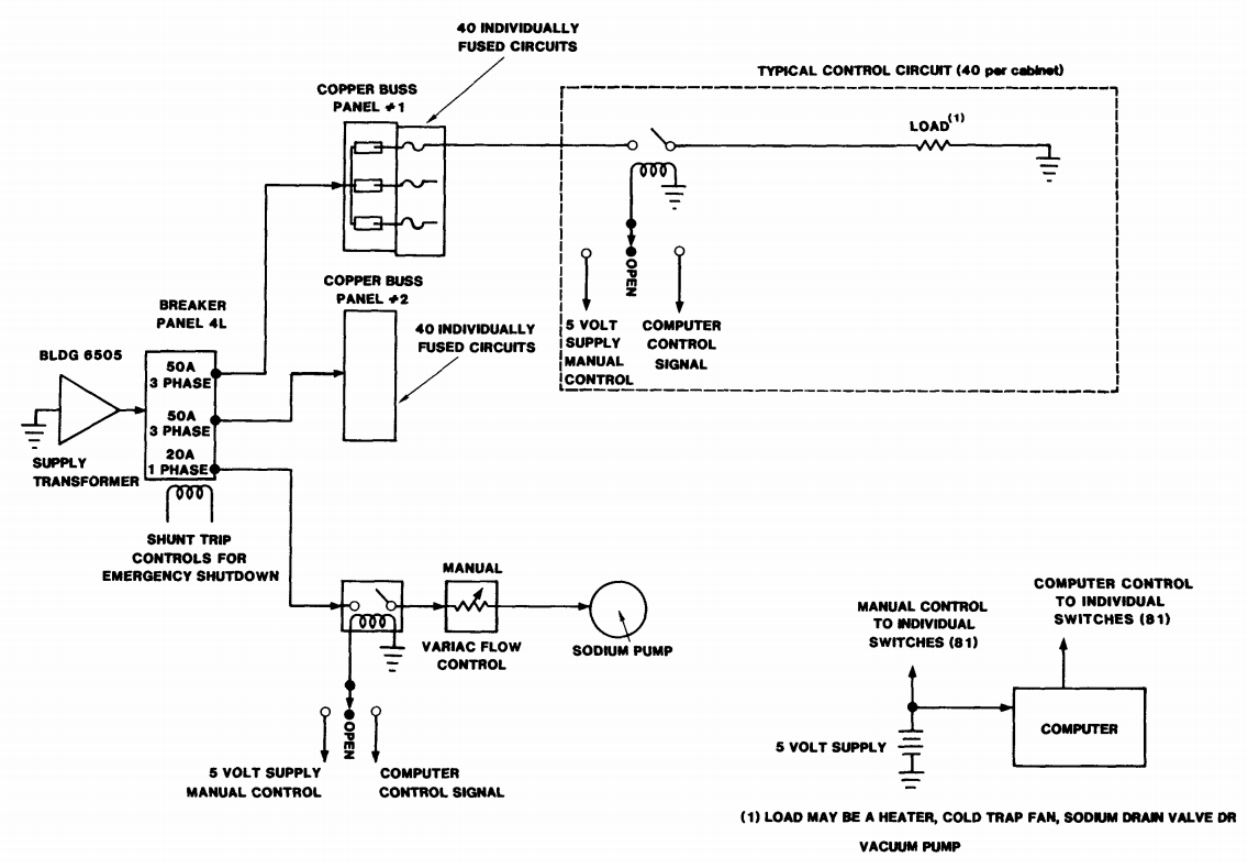

Figure 139. Typical control circuit [28].

11 Appendix C: Specifications of Various Components of Fermi 1

Table 20. Sodium-to-Water Steam Generator Characteristics [62]

Specifications	Value
Steam Generator Type	Once Through
Full Load Heat Transfer Per Unit [MW]	143
Number of Units	3
Steam Pressure [psig]	900
Shel1 Side Fluid	Sodium
Flow Rate, [lb/hr]	5.30×10^6
Temp "In" [°F]	820
Temp "Out" [°F]	520
Tube Side Fluid	Water & Steam
Flow Rate, [lb/hr]	4.76×10^5
Temp "In", [°F]	380
Temp "Out", [°F]	780
Heat Transfer Area [Ft2]	10,800
Number of Tubes	1,200
Outer Tube Size, in.	0.625 0.042
Inner Tube Size, in.	Single Tube
Water Side Materials	2 ¼ Cr- 1 Mo
Na Side	2 ¼ Cr- 1 Mo
Core Tube	---
Manufacturer	Griscom-Russel

Table 21. Fermi 1 Sodium to Sodium Heat Exchanger Characteristics [62]

Specification	Value
Full Load Heat Transfer Per Unit, [MW]	143
Number of Units	3
Shell Side Fluid (SSF)	Primary Na
SSF Flow Rate, [lb/hr]	5.30×10^6
SSF Temp "In" [°F]	900
SSF Temp "out" [°F]	600
Tube Side Fluid (TSF)	Secondary Na
TSF Flow Rate, [lb/hr]	5.3×10^6
TSF Temp "In" [°F]	520
TSF Temp "out" [°F]	820
Heat Transfer Area [Ft^2]	5,840
Number of tubes	1860
Tube size	0.875 OD 0.049 WT
Tube and Shell material	304 SS
Manufacturer	Alco

Table 22. Sodium Reactor Vessel Characteristics [62]

Specification	Value
Reactor Type	Fast
Reactor Power [MW]	430
Coolant Temperature “In” [°F]	600
Coolant Temperature “Out” [°F]	900
Coolant Pressure “In” [psig]	100
Coolant Pressure “Out” [psig]	Negligible
Vessel Height [Ft]	36
Vessel Diameter [Ft]	14
Material	304 SS
Fabricator	Combustion Engineering

Table 23. Primary Sodium Pump (Design) Characteristics [62]

Specification	Value
System Pump Type	Mechanical Free Surface
Number of Units	3
Capacity [gpm]	11800
Dynamic Head [Ft]	310
Design Temperature [°F]	1000
Motor Speed [rpm]	900
Motor Power [hp]	1060
Sealing Arrangement	Mechanical Shaft Seal
Material	304 SS
Type of Speed control	Wound Rotor Motor with Liquid Rheostat
Manufacturer	Byron-Jackson

Table 24. Secondary Sodium Pump (Design)

Characteristics [62]

Specification	Value
System Pump Type	Mechanical Free Surface
Number of Units	3
Capacity [gpm]	13000
Dynamic Head [Ft]	100
Design Temperature [°F]	1000
Motor Speed [rpm]	900
Motor Power [hp]	350
Sealing Arrangement	Mechanical Shaft Seal
Material	2 ¼ Cr- 1 Mo
Type of Speed control	Eddy Current Coupling
Manufacturer	Byron-Jackson

12 Appendix D: Sandia National Laboratory Information

Table 25. Cleaning procedure for piping system and correlated sodium parts [43]

1.	Vapors degrease with Trichloroethylene
2.	Caustic electro cleaner (sodium hydroxide)
3.	Tap water rinse
4.	Rinse in 50% by volume hydrochloric acid (to remove heavy oxides)
5.	Tap water rinse, DI (Deionized water) rinse followed by tap water rinse
6.	Rinse in 15% hydrogen peroxide at 125-130"?
7.	Tap water rinse
8.	DI water rinse (2 stages)
9.	Dry with isopropyl alcohol

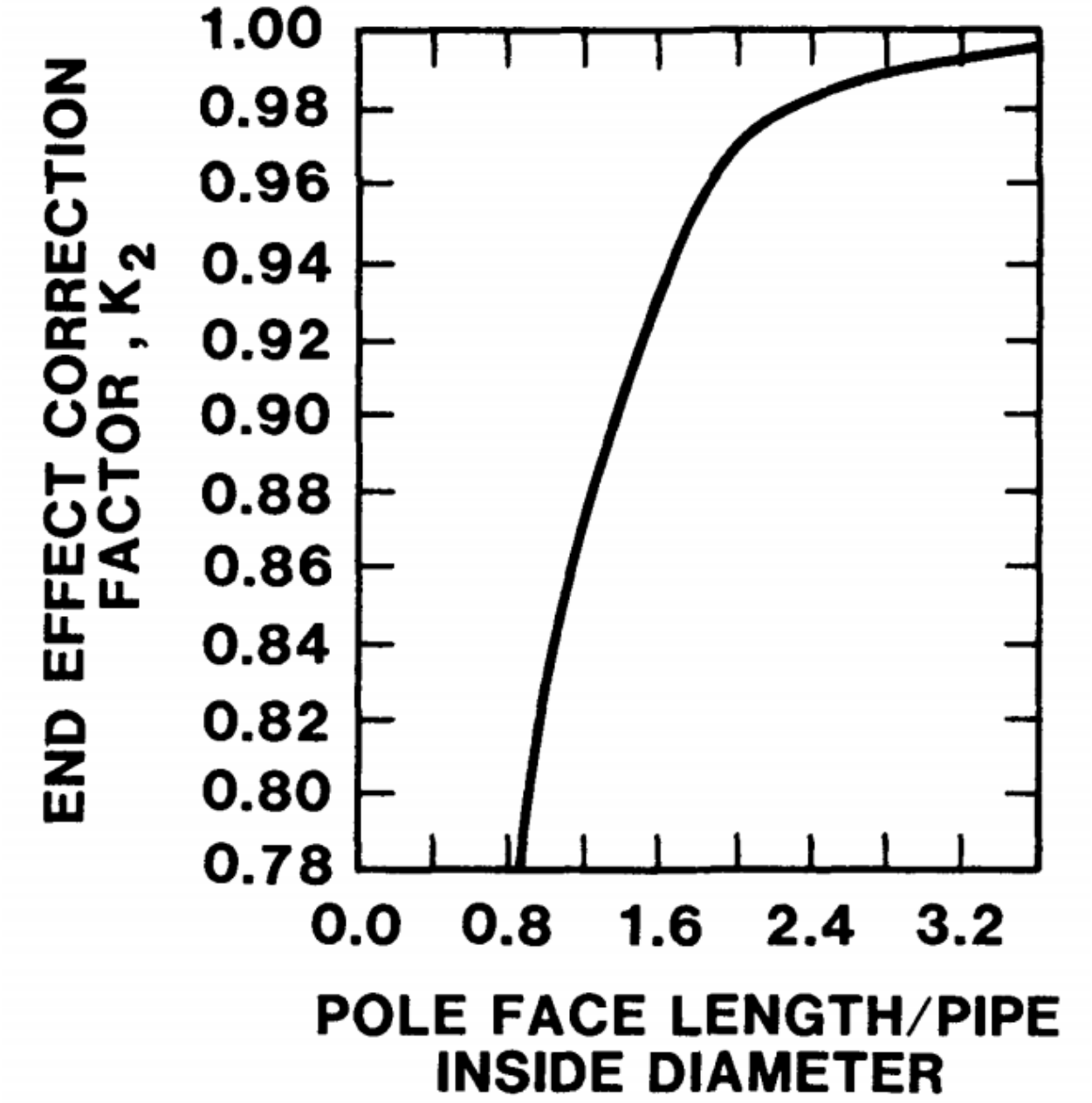

Figure 140. Flow meter end effect correction factor graph.

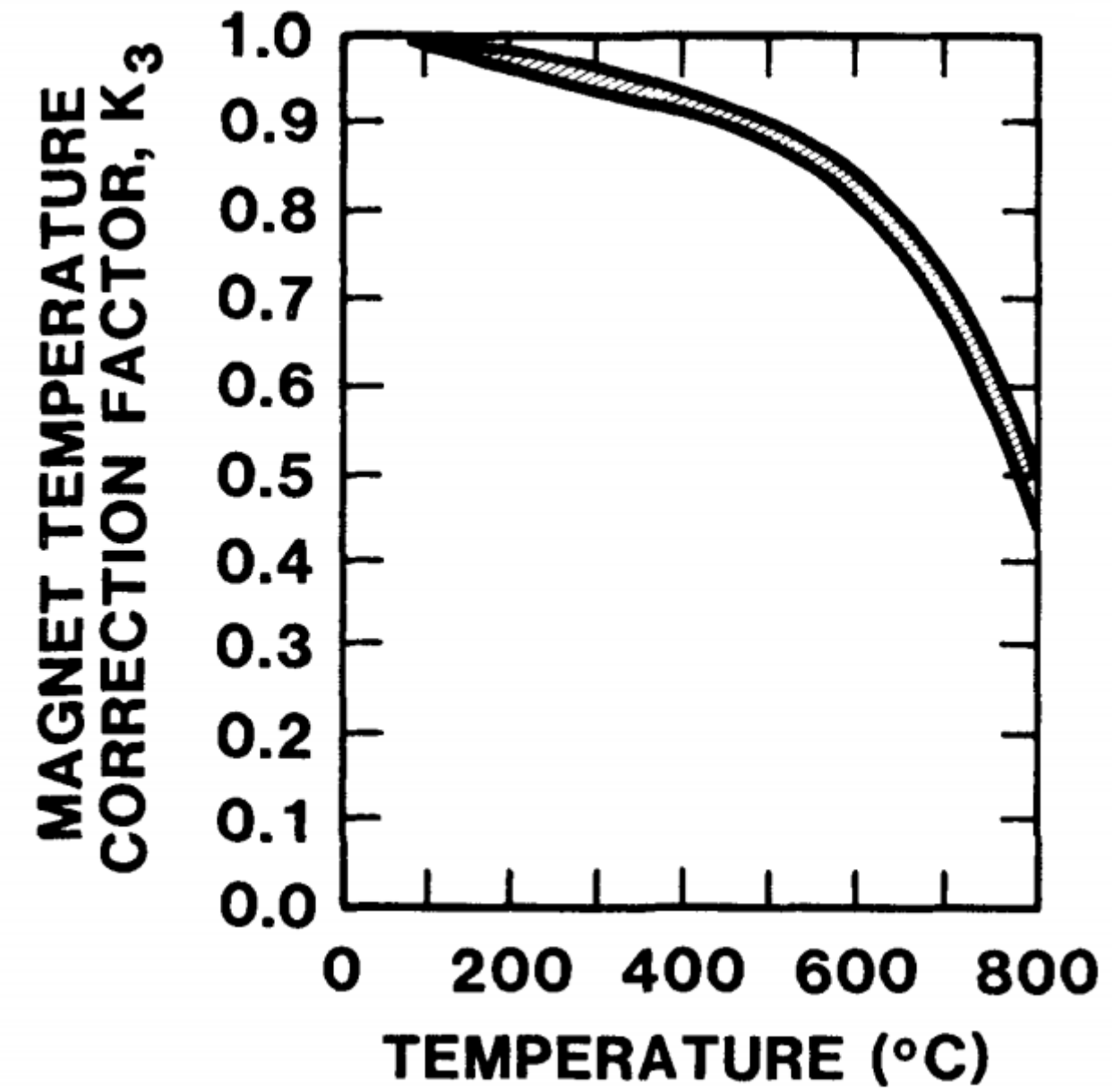

Figure 141. Flow meter temperature correction factor.

Table 26. Solubility of Oxygen in Sodium [43]

Temperature (°C)	Oxygen (ppmw)
120	1.2
125	1.5
130	1.7
135	2.1
140	2.4
145	2.8
150	3.3
155	3.9
160	4.5
165	5.2
170	6.0
175	6.9
180	7.8
185	9.0
190	10.2
195	11.6
200	13.1
205	14.8
210	16.7
215	18.7
220	21.0
225	23.5
230	25.2
235	29.1
240	32.4
245	35.9
250	39.7
255	43.9
260	48.4
265	53.2
270	58.5
275	64.1
280	70.2
285	76.8
290	83.8
295	91.3

Temperature (°C)	Oxygen (ppmw)
300	99.3
305	107.9
310	117.0
315	126.8
320	137.2
325	148.2
330	160.0
335	172.3
340	185.6
345	199.5
350	214.3
355	229.8
360	246.3
365	263.6
370	281.8
375	301.0
380	321.2
385	342.4
390	364.6
395	387.9
400	412.3

Table 27. Solubility of Hydrogen in Sodium

Temperature (°C)	Hydrogen (ppmw)
120	0.06
130	0.09
140	0.14
150	0.21
160	0.31
170	0.44
180	0.62
190	0.87
200	1.19
250	4.86
300	15.53
350	41.18
400	94.44

Table 28. Tank T1 Volume [43]

h1 (in)	V_Total (Gal)
0.250	0.357
0.500	0.828
0.750	0.370
1.000	0.968
1.250	0.613
1.500	0.299
1.750	0.020
2.000	0.774
2.250	0.556
2.500	0.364
2.750	0.196
3.000	8.048
3.250	8.920
3.500	9.810
3.750	10.714
4.000	11.634
4.250	12.565
4.500	13.508
4.750	14.461
5.000	15.422
5.250	16.391
5.500	17.366
5.750	18.347
6.000	19.331
6.250	20.318
6.500	21.307
6.750	22.297
7.000	23.287
7.250	24.275
7.500	25.262
7.750	26.245
8.000	27.225
8.250	28.199
8.500	29.168
8.750	30.130
9.000	31.084

h1 (in)	V_Total (Gal)
9.250	32.030
9.500	32.966
9.750	33.892
10.000	34.818
10.250	35.755
10.500	36.701
10.750	37.655
11.000	38.617
11.250	39.586
11.500	40.560
11.750	41.540
12.000	42.523
12.250	43.510
12.500	44.498
12.750	45.488
13.000	46.478
13.250	47.467
13.500	48.454
13.750	49.438
14.000	50.418
14.250	51.394
14.500	52.362
14.750	53.324
15.000	54.277
15.250	55.220
15.500	56.151
15.750	57.070
16.000	57.975
16.250	58.865
16.500	59.737
16.750	60.589
17.000	61.421
17.250	62.229
17.500	63.011
17.750	63.765
18.000	64.486
18.250	65.172

h1 (in)	V_Total (Gal)
18.500	65.817
18.750	66.415
19.000	66.957
19.250	67.428
19.500	67.785

Table 29. Tank T2 Volume [43]

h2 (in)	V_Total (Gal)
0.105	0.061
0.210	0.142
0.315	0.236
0.420	0.341
0.525	0.453
0.630	0.573
0.735	0.699
0.840	0.831
0.945	0.968
1.050	1.110
1.155	1.256
1.260	1.406
1.365	1.560
1.470	1.716
1.575	1.876
1.680	2.038
1.785	2.202
1.890	2.368
1.995	2.536
2.099	2.706
2.204	2.877
2.309	3.050
2.414	3.223
2.519	3.397
2.624	3.572
2.729	3.748

h2 (in)	V_Total (Gal)
2.834	3.923
2.939	4.099
2.939	4.274
3.044	4.449
3.149	4.624
3.254	4.798
3.359	4.972
3.464	5.144
3.569	5.316
3.674	5.486
3.779	5.655
3.884	5.822
3.989	5.988
4.094	6.153
4.199	6.320
4.304	6.489
4.409	6.659
4.514	6.831
4.619	7.003
4.724	7.177
4.829	7.351
4.934	7.876
5.249	8.052
5.354	8.228
5.564	8.403
5.669	8.578
5.774	8.752
5.879	8.925
5.984	9.098
6.089	9.269
6.193	9.439
6.298	9.607
6.403	9.773
6.508	9.938
6.613	10.100
6.718	10.259
6.823	10.415

h2 (in)	V_Total (Gal)
6.928	10.569
7.033	10.719
7.138	10.865
7.243	11.007
7.348	11.144
7.453	11.276
7.558	11.402
7.663	11.522
7.768	11.635
7.873	11.739
7.978	11.833
8.033	11.914
8.188	11.975

13 Appendix E: Atmospheric Dispersion Sample Calculation

Sample Calculations

$$C = \frac{\frac{m}{t}}{2\pi\sigma_y\sigma_z u} e^{-\frac{y^2}{2\sigma_y^2}} \left(e^{-\frac{(z-h)^2}{2\sigma_z^2}} + e^{-\frac{(z+h)^2}{2\sigma_z^2}} \right)$$

$$\sigma_y = 0.04x(1 + 0.0001x)^{-\frac{1}{2}} \left(\frac{60}{10}\right)^{0.2}$$

$$\sigma_z = 0.016x(1 + 0.0003x)^{-1}$$

$$u_{adj} = u_{10} \left(\frac{z}{10}\right)^p$$

Known or Assumed Quantities:

$$m = 100\ g\ ;\ t = 3600\ s\ ;\ x = 100\ m\ ;\ u_{10} = 1\frac{m}{s};\ z = 2\ m\ ;\ p = 0.55\ ;\ h = 0m\ ;\ y = 0m$$

After applying assumptions, we end with the following equation

$$C = \frac{m}{2t\pi\sigma_y\sigma_z u} \left(2e^{-\frac{(z)^2}{2\sigma_z^2}} \right)$$

Calculations:

$$u_{adj} = 1\left(\frac{2}{10}\right)^{0.55} = 0.4126\frac{m}{s}$$

Once $u < 0.5\frac{m}{s}$ it is negligibly different than $0.5\frac{m}{s}$ meaning: $u_{adj} \cong 0.5\frac{m}{s}$

$$\sigma_z = 0.016 * 100(1 + 0.0003 * 100)^{-1} = 1.6\ m$$

$$\sigma_y = 0.04 * 100(1 + 0.0001 * 100)^{-\frac{1}{2}} \left(\frac{60}{10}\right)^{0.2} = 5.7\ m$$

$$C(100\ g, 100\ m, 60\ min) = \frac{1000 * 100}{2 * 3600 * \pi * 5.7 * 1.6 * 0.5} \left(2e^{-\frac{(2)^2}{2(1.6^2)}} \right) = 0.92\frac{mg}{m^3}$$

$$C = 0.92\frac{mg}{m^3}$$

14 Appendix F: First Aid

14.1 Topical Burns

Proper gloves should always be worn when handling sodium, never with bare skin. The burns from alkali (base) metals are worse than burns from acid. The burns are both chemical from the alkalinity and thermal from the heat generated when the sodium reacts with water. Damage to the skin starts before it begins to hurt. This reaction is called liquefication necrosis. The liquefication is caused by the alkali breaking weak protein bonds (denaturing) and the conversion of fats or lipids into soap and alcohol (saponification). This turns the skin into what a veteran of EBR-ll coined as a "caustic soup" (See Pat's story at the end of this section). The severity of scars left by sodium burns depends on where the burn is located and can range from light to grave.

The standard practice for treating exposure to sodium requires quick decontamination by first brushing any particles off skin or removing chunks with tweezers. Continuing damage occurs the longer that skin is in contact with sodium. After the sodium is removed the affected area is flushed with extreme amounts of water for at least 30 minutes. Individuals who have had working sodium experience have successfully used this flushing method. However, there is some debate in medical journals as to whether irrigating with oil instead of water might be a better solution as water might set off a reaction causing further damage. In the Annals of Emergency Medicine, volume 30, issue 5, the following advice is given; "In alkali metal burns (sodium, lithium, potassium, and so on), decontamination with water is specifically contraindicated. These metals react with water in a violent fashion releasing heat, hydroxide ion, and hydrogen gas. Proper treatment of alkali metal burns involves clothing removal and covering the affected area with mineral or cooking oil, followed by removal of any metal with dry forceps. Only then can the wound be irrigated with water and treated like other alkali burns." [107]

Individuals interviewed for this report said the only way they had treated exposure to sodium was flushing the skin with copious amounts of water and that they weren't entirely sure the oil method would work. However, there is a third alternative that merits more research. A report published in PubMed.gov, *The Treatment of Alkaline Burns of the Skin by Neutralization*, offers compelling evidence that alkaline burns on the skin could be neutralized with a weak (5%)

acetic acid such as basic household vinegar. The study experimented with alkali burns on rats and showed significant benefits to irrigating the wound with vinegar as opposed to water. [108]

Burns caused by sodium metal are not common which means images of these burns are hard to find. However, lithium burns give similar damage as sodium due to it also being an alkaline metal. Figure 142 and Figure 143 depict burns from the explosion of lithium-ion batteries contained in E-cigarettes. Figure 144 depicts a burn to the leg after a lithium ion cell phone battery burst in someone's pocket. From these images it can be seen that these burns can be dangerous and classified as third degree which require immediate medical attention.

Figure 142. Burns caused from lithium-ion E-cigarette explosion [109].

Figure 143. Alkaline burns to hand caused by explosion of lithium-ion battery from an E-cigarette [110].

Figure 144. Burns caused by cell phone lithium-ion battery after breaking in pocket [111].

Pat's Story

Patrick Kern worked with sodium in the EBR-ll test reactor and shares some of his experiences working with sodium and the injuries that can occur. "Most of the plant maintenance involving sodium involved the removal/replacement of components. In an ideal world, the sodium would drain out of the components, and you could cut them out and weld new ones in with minimal effort. However, this was the real world and the components typically stayed full of sodium. The simple process of sawing out the old component, digging out the bulk sodium and wiping the inside of the pipe with water and alcohol resulted in a steady stream of minor injuries. For the work, we had tools we built. We used a wood auger with a T-handle to remove the majority of the sodium, then we used screwdrivers with spoon-type ends welded to them to scrape the insides of the pipes. We had to clean the sodium back about 6 inches from the end of the pipes (on small pipes) so that the sodium would not melt into welds. Later in my career I found that we probably worried too much about removing the sodium back that far.

The injuries we suffered were mostly chemical burns from the caustic. Working in the clumsy position's endemic to industrial plant construction and with fire retardant suits, leather gloves and face shields we built up a lot of sweat. We would tape our gloves tightly to our wrists to prevent small sodium particles from getting in our gloves. Turned out this was not the best choice for some people (including me). Sweat would build up on your cuffs, small sodium particles would land on the cuffs (they may or may not have sparked), the sodium reacted with the moisture and before you even realized you had a problem, you had a caustic soup on your wrists. It is the kind of burn that sneaks up on you: by the time you realize what is going on, you just try to work through it."- Patrick Kern, 2021

14.2 Inhalation

Elemental sodium is usually not the concern with regards to inhalation. However, when sodium burns it releases toxic smoke containing sodium-hydroxide. Sodium-hydroxide causes irritation to the respiratory tract immediately when inhaled. Upper-airway obstruction can be caused by the swelling that this irritant produces and can cause asphyxia in severe cases. The lungs can also suffer inflammation and fill with fluid (non-cardiogenic pulmonary edema). Inhalation can cause permanent damage in the form of a chemical/irritant induced type of asthma called RADS (Reactive Airways Dysfunction Syndrome). The treatment of inhalation of sodium-hydroxide can only be treated through respiratory support methods as there is no antidote. This includes 100% humidified supplemental oxygen if required, or in serious cases, endotracheal intubation or the surgical creation of an airway will be needed. Children and people with respiratory issues are more susceptible to injury.

Laboratory Accidents

Sodium is easy to obtain for anyone over the age of 18 in the United States. A quick internet search will provide numerous videos depicting the classic sodium/water reaction performed by scientists and amateurs. This evidence would point the casual observer to believe that sodium metal is a source of amusement. The lack of respect for chemical properties inherent in sodium has caused many injuries. If too large a piece of sodium is used in an experiment, it could produce enough heat to ignite the hydrogen gas produced and release sodium-hydroxide. In 2012, Portland Fire and Rescue was called to David Douglas High School in Portland Oregon in response to an explosion. According to PF&R Public Information Officer Tommy Schroeder, "…the explosion had been caused by some type of sodium metal in the sink. When a student tried to use the drinking fountain, also in that sink, it reacted, and the result was a small explosion." This explosion exposed 25 students and one teacher to the toxic fumes, sending 12 of them and the teacher to the hospital with respiratory issues.

Considerably more accidents involving sodium occur in school and university labs than in industry labs. Figure 145 and the following story are an account given by Dr. Ed Henderson in which he demonstrated the properties of sodium metal to his students.

About 15 years ago, I wanted to show my students how soft a metal sodium is, and of course I planned to subsequently demonstrate its classic, fiery reaction with water. Luckily, I was wise enough to use the two-way fume hood setup. I cut the block, exposing its lustrous interior–the surface slowly oxidizes with time even when it is kept under oil. But I had made the mistake of not taking tongs with me. I had actually used my pocketknife to pull it out of its bottle, and after cutting it, I poked my knife into one of the halves and placed the knife and sodium into a beaker of water.

Any time an exothermic reaction is carried out, the vessel should be checked for cracks. I only noticed the dark line in the glass after I dropped in the knife and sodium. At the time I was also unaware of the precautionary trick of placing sand at the bottom of a beaker. It helps prevent overheated Pyrex from cracking. My last error was my worst one: sticking a knife into too large a piece of sodium is a bad idea because it causes the chunk to sink into water. Without the added weight, sodium, with a density of 0.97 g/cm^3, would not have sunk and not all of its surface would have come into contact with water; the reaction would have been slower and more controlled. The hydrogen would have ignited, but the reaction would not have generated as much pressure as when sodium is submerged.

To complete the disaster, our technician had recently left methanol in an open beaker in the fume hood. There was an immense explosion heard across our small school. The observing students gaped in astonishment but were unharmed since the protective pane on their side could not be opened. The fume hood glass on my side did not break, but all the glassware within it did. I had never totally lowered my window, and sodium hydroxide (NaOH) produced by the reaction along with bits of glass projected towards my belly. A couple of pieces actually got stuck in my shirt. When I unbuttoned it, I saw no blood but found NaOH reacting with my belly. [112]

Figure 145. Dr. Ed Henderson's lab space after the mishap [112].

Near Miss Reporting

According to the Near Miss Reporting Systems fact sheet from OSHA, a near miss is defined as "an unplanned event that did not result in injury, illness or damage–but had the potential to do so." Ample data reveals that near miss reporting prevents future accidents. OSHA and the National Safety Council Alliance states, "History has shown repeatedly that most loss producing events, both serious and catastrophic, were proceeded by near miss incidents."

The most controversial of near misses within the field of sodium reactors is Fermi 1. On October 5th, 1966, there was a partial meltdown when the flow of sodium was partially blocked by a piece of a zirconium flow guide. This led to around one percent of the fuel being damaged. There were no injuries or release of radiation. Some claimed the incident proved that the safety features of the reactor worked while others pushed the idea that the death of thousands was narrowly avoided [113]. Since the accident, several books have been written for both sides of the argument; *We Almost Lost Detroit* was written in 1975 by John G. Fuller which prompted Detroit Edison to write a rebuttal in 1976 titled *We Did Not Almost Lose Detroit*. Anti-nuclear activists still draw

attention to the event on its anniversary every year. Why? The answer lies in the minimizing of the dangers and the subsequent cover-ups that lead people to distrust an industry.

It is important for an organization, be it a lab or business, to have a system in place for reporting and following through on all near miss incidents. Without a system in place and encouragement to use it, personnel will be reluctant to report. This is due to a variety of valid reasons such as fear of additional work (forms to fill out, investigations to be done), loss of respect from employees or supervisors for being an 'informer,' and no follow up from the organization to fix the issue. The benefits of reporting outweigh the inconvenience and will save time, money, and lives.

Near Miss Investigation Form

When?

What?

Where?

Impact to organization:

Did it cause delays in time, production, or delivery?

Potential release to environment?

Caused by steps not being followed in order?

Follow up plan of action.

Emergency Action Plans

There are many types of emergencies that should be planned for. There are natural disasters, chemical spills/releases, fires, explosions, power outages and active shooters or terrorism. These

unfortunate incidents can be exasperated when there are potentially hazardous materials on site such as sodium. Emergency action plans need to be well thought out and practiced regularly to avoid injury to personnel and equipment. The plan must include an unobstructed exit route from all areas of the building. Evacuation maps of these routes should be clearly posted. Outdoor assembly points need to be known by all employees and a system to account for each person needs to be ready. Shelter in place plans need to be practiced for emergencies not requiring evacuation.

Emergency preparation can be hard to achieve. Leadership may not want to pay for it or make time to practice. Personnel might find it arduous or there could be language barriers to overcome. The cost and inconvenience might not seem worth it until there is an actual emergency. Identification of the most common types of emergencies and their subsequent response plans are essential to businesses in the long term. Money, lives, and reputations can be saved.

Common workplace dangers include chemical spills and fire. There are five different classes of fires. Class A involves combustible material such as trash or wood. Class B contains flammable liquids such as gasoline. Class C deals with electrical equipment. Class D is reserved for combustible metals which includes sodium. The final class is K, which involves cooking oil. Any one of these classes of fires is possible in a building and it is important to use the right type of fire extinguisher for the class of fire involved.

If the fire is related to sodium, a class D fire extinguisher must be used and there must be someone on shift who is trained to use it. Safety training is needed to help them be able to assess the situation and know if they can safely put out the fire themselves. A fire extinguisher should not be used until a fire alarm system has been activated. Factors that will need to be included in the assessment are size of the fire, amount of smoke, the proximity of other hazardous materials, and access to a clear escape route all need to be considered. The chance of injury increases under stressful conditions and inadequate safety training.

Part of the plan should include a relationship with first responders. According to fire chief Paul Radford of the Idaho Falls fire department they appreciate any information about the fire hazards that might be on site. The information sheet below was influenced by their input and would be good information to share to other first responders as a way of opening communication [114].

The need for planning and providing first responders good information before an accident was made apparent in a fire that started in an industrial warehouse in Morris, Illinois on June 29, 2021. This fire caused the evacuation of around three thousand residents due to the two hundred thousand pounds of lithium batteries stored in the building. Lithium and sodium are both alkali metals, with sodium being more reactive than lithium. The residents were evacuated for health and safety reasons as inhalation of the smoke can be deadly.

Besides the toxic smoke, there were other dangers. Fire chief Tracey Steffes gave a televised update on June 30, 2021, where he says, “This fire, because it involves lithium batteries, normal conventional firefighting such as water or firefighting foam, will not extinguish this fire. In fact, it will make this fire more violent…” [115] He also says that originally, his firefighters were not aware of the hazard and had tried to put out the fire with water. State and federal agencies were consulted, and the conclusion was to let the fire burn itself out overnight and then try to smother it.

The department originally planned on extinguishing the fire with road salt once they could get close enough to find the source of the blaze. After further assessment, the firemen first tried to extinguish the fire using a dry chemical, Purple-K, which did not work. Chief Steffes said, “The lithium fire laughed at the Purple-K- didn’t put a dent in it.” [116] 28 tons of Portland cement was finally used to smother the fire but as the lithium does not need oxygen to burn, some small hot spots remained.

Two days later on July 2nd, 2021 ABC7 Chicago News reported the blaze still had three small parts that were still burning but the majority was put out. The community is now facing a potentially large environmental hazard besides the inconvenience of being forced from their homes. While the tragedy might not have been avoidable, the degree of impact could have been lessened by having an emergency plan that included communication with first responders and a fire protection plan in place for the batteries.

Sodium

Emergency Responder

Quick Reference Fact Sheet

Protective Equipment

Coveralls:
Turn out gear or flash protection
Gloves:
Nitrile (>8-hour breakthrough for Kerosene and Naphtha)
Respirator:
Full face-piece APR with high efficiency filters **(SCBA)**

Health Effects

Toxic gasses are produced in fire
Inhalation will cause irritation to nose, throat, and lungs
Caustic: causes irritation to the skin

Site Decontamination

Refrain from washing into confined places such as a sewer
Cleanup must be done under supervision and direction of a specialist

Fire Fighting Hazard Data

- **DO NOT USE** water, Co2, or halogenated extinguishing agents on a class D fire
- **Sodium is a flammable solid and will ignite spontaneously when exposed to air**
- Produces violent reaction when exposed to water—**explosive hydrogen gas**
- **Do use powdered agents** such as powdered graphite or granular sodium chloride

First Aid

Exposure to skin/eyes

- Requires immediate decontamination
- Brush off skin/hair/eye
- Remove affected clothing
- Wash affected body part with a large amount of water for at least 30 minutes
- Requires immediate medical attention

Inhalation

- Keep victim in a position comfortable for breathing
- Administer oxygen if breathing is difficult
- If breathing has stopped, using universal precautions, start rescue breathing and CPR if necessary.
- Transfer to a medical facility
- Medical observation is needed for 24-48 hours on all suspected